**NATIONAL AND KAPODISTRIAN UNIVERSITY OF ATHENS**

Faculty of Pharmacy

Doctoral Dissertation

# Mechanistic studies of gold-catalyzed reactions between aromatic nitrogen heterocycles and alkynes using Density Functional Theory calculations.

Stylianakis G. Ioannis

**Athens February 2023**

**ΕΘΝΙΚΟ ΚΑΙ ΚΑΠΟΔΙΣΤΡΙΑΚΟ ΠΑΝΕΠΙΣΤΗΜΙΟ ΑΘΗΝΩΝ**

Τμήμα Φαρμακευτικής

Διδακτορική Διατριβή

# Μελέτες του μηχανισμού κατάλυσης από χρυσό αντιδράσεων μεταξύ αρωματικών αζωτούχων ετεροκυκλικών μορίων και αλκυνίων με υπολογισμούς Θεωρίας Συναρτησιακών Πυκνότητας.

Στυλιανάκης Γ. Ιωάννης

**Αθήνα Φεβρουάριος 2023**

**PhD THESIS**

**Stylianakis G. Ioannis**

**THREE-MEMBER ADVISORY COMMITTEE:**

**Professor A. Kolocouris (supervisor)**, Department of Pharmacy, National and Kapodistrian University of Athens

**Professor C.S. Lopez (co-supervisor)**, Faculty of Chemistry, University of Vigo, Spain

**Professor A. Tsotinis**, Department of Pharmacy, National and Kapodistrian University of Athens

**SEVEN-MEMBER EXAMINATION COMMITTEE**

**Professor A. Kolocouris**, Department of Pharmacy, National and Kapodistrian University of Athens

**Professor C.S. Lopez**, Faculty of Chemistry, University of Vigo, Spain

**Professor A. Tsotinis**, Department of Pharmacy, National and Kapodistrian University of Athens

**Assoc. Prof. D. Tzeli**, Department of Chemistry, National and Kapodistrian University of Athens

**Assoc. Prof. V. Sarli**, Department of Chemistry, Aristotle University of Thessaloniki

**Professor O. N. Faza**, Faculty of Chemistry, University of Vigo, Spain

**Assoc. Prof. G. C. Vougioukalakis**, Department of Chemistry, National and Kapodistrian University of Athens

Examination Date 21/2/2023

**ΔΙΔΑΚΤΟΡΙΚΗ ΔΙΑΤΡΙΒΗ**

**Στυλιανάκης Γ. Ιωάννης**

**ΤΡΙΜΕΛΗΣ ΕΠΙΤΡΟΠΗ ΠΑΡΑΚΟΛΟΥΘΗΣΗ:**

**Καθηγητής Α. Κολοκούρης (Επιβλέπων)**, Τμήμα Φαρμακευτικής, ΕΚΠΑ

**Καθηγητής C.S. Lopez (Συνεπιβλέπων)**, Faculty of Chemistry, University of Vigo, Spain

**Καθηγητής Α. Τσοτίνης**, Τμήμα Φαρμακευτικής, ΕΚΠΑ

**ΕΠΤΑΜΕΛΗΣ ΕΞΕΤΑΣΤΙΚΗ ΕΠΙΤΡΟΠΗ**

**Καθηγητής Α. Κολοκούρης**, Τμήμα Φαρμακευτικής, ΕΚΠΑ

**Καθηγητής C.S. Lopez**, Faculty of Chemistry, University of Vigo, Spain

**Καθηγητής Α. Τσοτίνης**, Τμήμα Φαρμακευτικής, ΕΚΠΑ

**Αναπλ. Καθηγήτρια Δ. Τζέλη**, Τμήμα Χημείας, ΕΚΠΑ

**Αναπλ. Καθηγήτρια Β. Σαρλή**, Τμήμα Χημείας, Αριστοτέλειο Πανεπιστήμιο Θεσσαλονίκης

**Καθηγήτρια O. N. Faza**, Faculty of Chemistry, University of Vigo, Spain

**Αναπλ. Καθηγητής Γ. Χ. Βουγιουκαλάκης**, Τμήμα Χημείας, ΕΚΠΑ

Examination Date 21/2/2023

# Acknowledgements

I would like to acknowledge the following people whose contribution was crucial for the successful completion of my PhD thesis:

My thanks to Professor Antonios Kolocouris for his scientific guidance and discussions he offered me, as well for his help on publication strategy, editing my thesis and accomplishing my PhD research work. But mainly, my thanks for his persistent efforts to persuade me that I could cope with a so demanding endeavor as a PhD project, keeping the door of his laboratory open to me for years.

My special thanks also to my co-supervisor Professor Carlos Silva Lopez for the training he offered me, for advancing the methods level applied in the thesis and for his contribution and help in solving calculations problems.

Thanks to Dr Iraklis Litinas for his contribution in looking for alternative reaction pathways in my mechanistic studies.

I would like to thank the researchers accepting to participate in the 7-member examination committee.

Generous allocation of supercomputer resources by the Galician Supercomputing Center (CESGA) is also acknowledged.

# Εκτενής περίληψη

Στην παρούσα διδακτορική διατριβή επιχειρείται η μελέτη αντιδράσεων καταλυόμενων από καταλύτες χρυσού με τη χρήση υπολογισμών DFT (Θεωρίας Πυκνότητας Συναρτησιοειδούς). Ο σκοπός της μελέτης είναι η εξαγωγή συμπερασμάτων για τον μηχανισμό και άλλων κρίσιμων χαρακτηριστικών των αντιδράσεων.

Στο πρώτο μέρος επιχειρείται μια σύνοψη των καταλυόμενων αντιδράσεων από χρυσό που περιλαμβάνουν π-συστήματα, μέσω παραδειγμάτων, τα οποία ταξινομούνται με χαλαρά κριτήρια.

Στο δεύτερο κεφάλαιο εξετάζουμε τον ρόλο της οξειδωτικής κατάστασης του χρυσού στην καταλυτική του δράση. Πιο συγκεκριμένα, τα σύμπλοκα του χρυσού του τύπου χρυσός – καρβένιο, π-αλκένιο, π-αλκίνιο και τα ιδιαίτερα χαρακτηριστικά κάθε ενός. Η διαφορετική οξειδωτική κατάσταση του χρυσού (I) ή (III) αντανακλά στη συγγένεια του καταλύτη για το π-σύστημα. Όλα τα παραπάνω παρουσιάζονται με τη μορφή παραδειγμάτων αποκλίνουσας κατάλυσης εξαιτίας της οξειδωτικής κατάστασης του χρυσού.

Στο τρίτο κεφάλαιο παρουσιάζονται οι ιδιαίτερες ιδιότητες του χρυσού που τον καθιστούν άριστο καταλύτη σε σχέση με τους καταλύτες των άλλων μετάλλων.

Στο τέταρτο κεφάλαιο, εξετάζουμε μια ποικιλία παραμέτρων όπως οι υποκαταστάτες του χρυσού, πρόσθετα και διαλύτης, καθώς και τον ρόλο τους στη ρύθμιση των εναλλακτικών μονοπατιών του μηχανισμού της αντίδρασης. Συνεπώς, η αποκλίνουσα κατάλυση είναι εφικτή λόγω των ανωτέρω παραγόντων.

Το πέμπτο κεφάλαιο είναι εισαγωγή στις μεθόδους που εφαρμόστηκαν στο πειραματικό μέρος. Γίνεται μια σύντομη περιγραφή των υπολογιστικών μεθόδων που χρησιμοποιήθηκαν στο πειραματικό μέρος.

Στο έκτο κεφάλαιο παρατίθενται οι καταλυόμενες από χρυσό αντιδράσεις που επιλέξαμε να μελετήσουμε, οι παρόμοιες με αυτές συνθετικές μέθοδοι που έχουν δημοσιευτεί, καθώς και οι λόγοι που επιλέξαμε να εστιάσουμε σε αυτές.

Στα κεφάλαια επτά έως εννέα περιέχονται τα πειραματικά αποτελέσματα και ο σχολιασμός τους για κάθε αντίδραση που επιλέξαμε να μελετήσουμε.

Στο κεφάλαιο επτά μελετήσαμε την καταλυόμενη από χρυσό (I) αντίδραση σύνθεσης του 4,7-δι-υποκατεστημένου ινδολίου/καρβαζολίου. Η επιλογή της

αντίδρασης βασίστηκε στο γεγονός ότι το ινδόλιο είναι πολύ συνηθισμένη δομή στα αλκαλοειδή και κάποια από αυτά παρουσιάζουν βιολογική δράση. Λόγω του σχετικού του ρόλου στη φαρμακευτική χημεία και τη βιομηχανία φαρμάκων, πολλές μέθοδοι σύνθεσης του ινδολίου έχουν αναπτυχθεί, αλλά μόνο λίγες από αυτές εκμεταλλεύονται μια προσέγγιση του τύπου [4+2]. Προσφάτως, μια επιτυχημένη προσπάθεια για τη σύνθεση ινδολίων και καρβαζολίων με διαμεσολάβηση χρυσού [4+2] προσθήκης διινίου σε πυρόλιο ή ινδόλιο αναφέρθηκε από τον Ohno. Ένα σύνολο από ενδιαφέροντα χαρακτηριστικά παρατηρήθηκαν στην αντίδραση που έμενε να μελετηθούν. Μελετούμε τον μηχανισμό της καταλυόμενης από χρυσό αντίδρασης του 1,3-διινίου με δακτυλίους πυρολίου και ινδολίου που οδηγούν σε υποκατεστημένα ινδόλια και καρβαζόλια αντίστοιχα. Τα μονοπάτια της αντίδρασης βρέθηκαν περισσότερο περίπλοκα από ότι είχαμε υποθέσει, για παράδειγμα, στον σχηματισμό των καρβαζολίων, ένα ανταγωνιστικό μονοπάτι που περιλαμβάνει τον σχηματισμό ενός απρόσμενου σπειρανικού ενδιαμέσου που προχωρά μέσω μετάθεσης 1,2-αλκινίου. Ανεξάρτητα από την παραπάνω περιπλοκή, η παρούσα μελέτη εξυπηρετεί στο να δώσει έμφαση στη σημασία που έχουν τα στοιχειώδη βήματα ενός μηχανισμού, που συχνά παραβλέπονται ως άσχετα με την κινητική, όπως η απόσπαση πρωτονίου/κατιόντος χρυσού από τα ενδιάμεσα τα αντίδρασης.

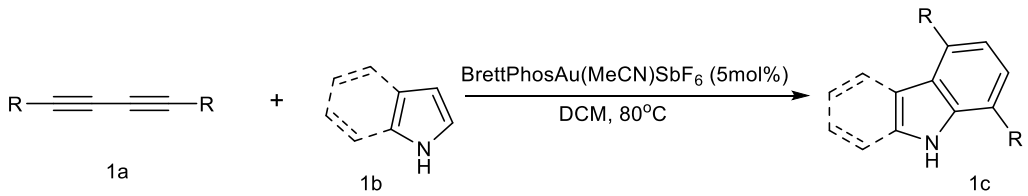


Σχήμα 1. Καταλυόμενη από χρυσό τυπική αντίδραση [4+2] μεταξύ 1,3-διινίου και πυρολίου (Ohno 2015)

Το όγδοο κεφάλαιο της διατριβής αποτελείται από τη μελέτη της καταλυόμενης από χρυσό (I) αντίδρασης σύνθεσης υποκατεστημένων ινδολίων ξανά, αλλά με μηχανισμό με ιδιαίτερα χαρακτηριστικά, δηλαδή με ένα ενδιάμεσο χρυσού-καρβενίου. Αποφασίσαμε να εστιάσουμε στη μελέτη μεθόδων σύνθεσης του ινδολίου, εξαιτίας της ύπαρξης του ινδολικού δακτυλίου στα αλκαλοειδή και στην αξιοσημείωτη ιστορία του στη φαρμακευτική βιομηχανία. Στη συνεχή αναζήτηση για πιο άμεση και αποδοτική πρόσβαση σε αυτές τις πολύτιμές δομές, μια νέα και αρκετά κομψή προσέγγιση βρέθηκε από τους Jin και τους συνεργάτες, στην οποία περιλαμβάνεται μια επαγόμενη από χρυσό (I) προσθήκη αλκινίου στο ανθρανύλιο. Η προσέγγιση αυτή οδηγεί στον σχηματισμό 7-ακυλο-ινδολίου με ένα αρκετα

γρήγορο τρόπο, που έχει αποδειχθεί ότι είναι συμβατός με μεγάλο εύρος αντιδρώντων, και από την πλευρά των αλκινίων αλλά και από την πλευρά των ανθρανυλίων. Μελετήσαμε τον μηχανισμό της αντίδρασης σε ένα σύνολο διαφορετικών αλκινίων, περιλαμβανομένων και των δι-υποκατεστημένων, για να βρούμε τις μεταξύ τους ομοιότητες και διαφορές και να βοηθήσουμε στον εντοπισμό των κομβικών βημάτων στο μονοπάτι της αντίδρασης. Η παρατηρούμενη τόπο-εκλεκτικότητα φαίνεται να συνδέεται με τον μη αντιστρεπτό σχηματισμό του κομβικής σημασίας ενδιαμέσου α-ιμινο-χρυσού καρβενίου, μέσω της αρχικής τόπο-εκλεκτικής πυρηνόφιλης προσβολής του ατόμου του N του ανθρανυλίου στο τμήμα του αλκινίου.

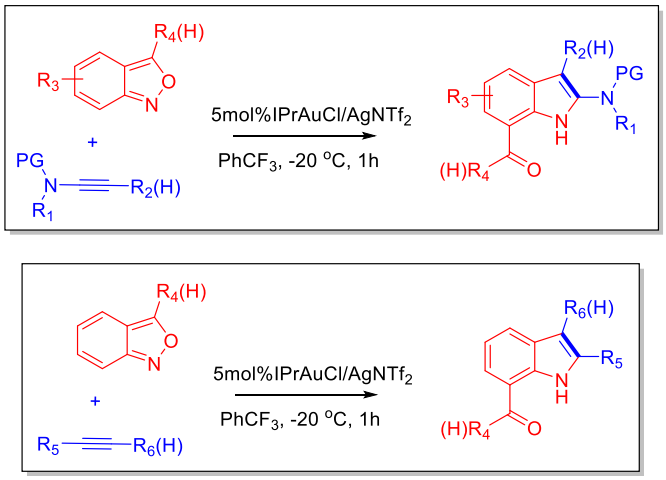


Σχήμα 2. Καταλυόμενη από χρυσό (I) C-H κυκλοποίηση των ανθρανυλίων με ακραία αλκίνια, ιναμίδια με βενζύλ και μέθυλο-σουλφονύλ υποκαταστάτες (Hashmi 2016).

Στο ένατο κεφάλαιο, το ενδιαφέρον μας μετατοπίζεται στα α-ιμινο-χρυσού καρβένια. Τα α-ιμινο-χρυσού καρβένια έχουν αναγνωριστεί ως κομβικής σημασίας ενδιάμεσα σε πληθώρα διαδικασιών, περιλαμβανομένης και της ενεργοποίησης των αλκινίων από χρυσό. Στην παρούσα εργασία, μελετήσαμε τα μονοπάτια της καταλυόμενης από χρυσό (I) [3+2] αντίδρασης μεταξύ των ήπιων πυρηνόφιλων ανθρανυλίου, 1,2,4-οξαδιαζολίου ή 4,5-διυδρο-1,2,4-οξαδιαζολίου και του ιναμιδίου PhC≡C-N(Ts)Me, που προχωρά μέσω του σχηματισμού του προαναφερθέντος α-ιμινο-χρυσού καρβενίου, το οποίο μετά από ενδομοριακή κύκλοποίηση, παράγει τόπο-εκλεκτικά 2-αμινο-3-φαίνυλο-7-ακυλο ινδόλια, N-ακυλο-5-αμινο-ιμιδαζόλια ή N-άλκυλο-4-αμινο-ιμιδαζόλια, αντίστοιχα. Σε όλες τις περιπτώσεις, η τόπο-εκλεκτικότητα των υποκαταστατών στις θέσεις 2,3 στο 7-ακυλο-ινδόλιο και στις

θέσεις 4,5 στον υποκατεστημένο δακτύλιο του ιμιδαζολίου καθορίζεται στο πρώτο μεταβατικό στάδιο, περιλαμβανομένης της προσβολής του αζώτου στον C1 ή C2 άνθρακα του ενεργοποιημένου ιναμιδίου. Η ακόλουθη απότομη πτώση της ενέργειας σχηματίζει το κομβικής σημασίας καρβένιο του α-ιμινο-χρυσού. Αυτά τα χαρακτηριστικά είναι πιο έντονα στις περιπτώσεις των αντιδράσεων του ανθρανυλίου και του 4,5-διύδρο-1,2,4-οξαδιαζολίου. Εντυπωσιακά, στην αντίδραση του 4,5-διύδρο-1,2,4-οξαδιαζόλιου η σημαντική πτώση της ενέργειας οφείλεται στον σχηματισμό ενός ασταθούς α-ιμινο-χρυσού καρβενίου το οποίο μετά από αυθόρμητη απόσπαση βενζαλδεϋδης μετατρέπεται σε ένα σταθερό. Συγκρινόμενο με το ανθρανύλιο, τα μονοπάτια των αντιδράσεων για το 1,2,4-οξαδιαζόλιο ή το 4,5-διύδρο-1,2,4-οξαδιαζόλιο βρέθηκαν να είναι σημαντικά πιο περίπλοκα από ότι είχαμε θεωρήσει στην αρχική έρευνα. Για παράδειγμα, σε σύγκριση με το σχηματισμό ενός πενταμελούς δακτυλίου από το καρβένιο του α-ιμινο-χρυσού, βρέθηκε ένα ανταγωνιστικό μονοπάτι που περιλαμβάνει τον σχηματισμό ενδιαμέσων αποτελούμενων από ένα τετραμελή δακτύλιο συμπυκνωμένο με έναν τριμελή, το οποίο μετά από μετάθεση και διάνοιξη του δακτυλίου οδήγησε στον ιμιδαζολικό δακτύλιο.

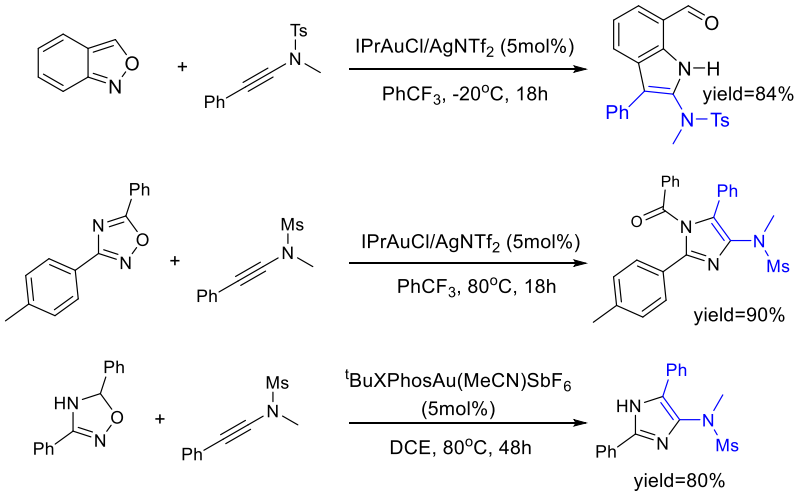


Σχήμα 3. Καταλυόμενη από χρυσό (I) αντίδραση του ανθρανυλίου, 1,2,4-οξαδιαζολίου ή του 4,5-διυδρο-1,2,4-οξαδιαζολίου με ιναμίδια που σχηματίζουν 2-αμινο-3-φαινυλο-7-ακυλο-ινδόλια, N-ακυλο-5-αμινο-ιμιδαζόλια ή N-αλκυλο-4-αμινο-ιμιδαζόλια, αντίστοιχα (Hashmi 2017 - Liu 2017).

# Extended Abstract

In this thesis we study, with the help of Density Functional Theory computation, series of gold catalyzed reactions. The aim of the study is to elucidate the mechanism of the reaction and other crucial traits.

In the first chapter it is attempted an overview on gold catalyzed reactions with π-systems via examples in which a loose classification is carried out.

In the second chapter we examine the role of oxidation state of gold on its catalytic activity. To be more precise, gold complexes of the type gold-carbene, π-alkene or π-alkyne exist and each one has special traits. The difference of oxidation state (I) or (III) of gold reflects on the affinity of the catalyst for π-systems. All the above are presented via examples of divergent catalysis due to the oxidation state of gold.

In the third chapter, gold and its special traits that render gold as an excellent catalyst comparing with other metal catalysts are presented.

In the fourth chapter, we examine a variety of parameters, like gold ligands, counterions, additives and solvent and its role on regulation of the alternative paths of the mechanism of a reaction. As a result, divergent catalysis due to the above factors is feasible.

The fifth chapter is an introduction to the methods applying on the experimental part. It is a brief presentation of the computational methods that were applied on the experimental part.

In the sixth chapter are presented the gold catalyzed reactions that we chose to study, similar synthetic methods that have been published and the reasons we decided to focus on them.

Chapters seven to nine contain the experimental results and discussion on them for each reaction we have study.

In chapter seven we studied the gold(I) catalyzed reaction of the synthesis of 4,7-disubstituted indoles/carbazoles. The choice of the reaction was based on the fact that indole is a very common structural motif in alkaloids, and a number of them feature remarkable bioactive properties. Due to its relevant role in medicinal chemistry and the pharma-industry, many methods for indole synthesis have been developed, but only a few of them exploit the [4 + 2] approach. Recently a successful attempt at indole and carbazole formation via a formal gold mediated [4 + 2] addition of a diyne

to pyrrole and indole rings has been reported by Ohno. A number of intriguing features observed in this reaction are however left to be resolved. We study herein the mechanism of the Au-catalyzed reaction of 1,3-diynes with pyrrole and indole rings leading to substituted indoles and carbazoles, respectively. The reaction pathways are found to be significantly more complex than we had anticipated; for example, in the case of carbazoles formation, one competitive route involves the generation of an unexpected spirane intermediate evolving via a 1,2-alkenyl migration. Beyond this complexity, the current study also serves to highlight the importance of fundamental steps that are often disregarded as kinetically irrelevant, such as the protodeauration of reaction intermediates.

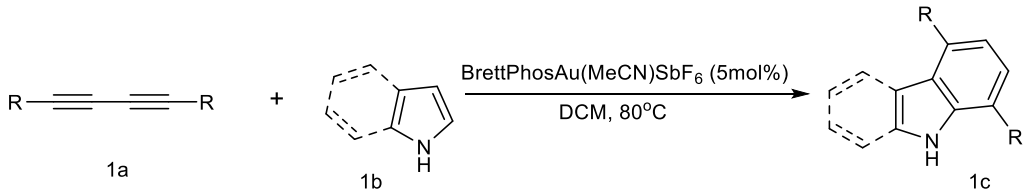


Scheme 1. Gold catalyzed formal [4+2] reaction between 1,3-diynes and pyrrole(Ohno 2015)

Chapter eight deals with the study of a gold(I) catalyzed reaction for the synthesis of substituted indoles again, but with a mechanism with special traits, that is, a gold carbene intermediate. We decided to focus on the study of synthetic methods of indole, due to the presence of the indole structural motif in alkaloids, with a remarkable history in pharma industry. In the continuous search for more direct and efficient access to these valuable structures, a new and rather elegant approach was found by Jin and coworkers, involving a gold(I)-mediated addition of alkynes onto anthranils. This approach selectively furnishes 7-acylindoles in a rather expeditious way, and it has been shown to be compatible with a large range of decorated reactants, both at the alkyne side and at the anthranil side. We studied the mechanism of this reaction with a set of different alkynes, including disubstituted ones, to establish similarities and differences between them and to aid in the elucidation of key steps in the reaction pathway. The observed regioselectivity seems to be connected to the irreversible formation of a key α-imino gold carbene intermediate, common to all reaction profiles, through the initial regioselective nucleophilic attack of the anthranil N atom onto the alkyne fragment.

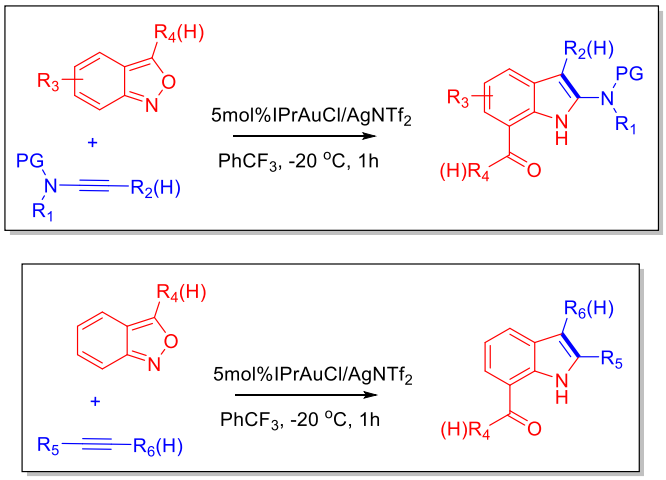


Scheme 2. Gold(I)-catalyzed C-H annulation of anthranils with terminal alkynes, ynamides with a benzyl and mesylate substituents (Hashmi 2016).

In chapter nine, our interest is displaced to α-imino gold carbenoid species. α-imino gold carbenoid species are recognized as key intermediates in a plethora of processes, involving gold activated alkynes. Here, we explored the pathways of the Au(I) catalyzed [3+2] reaction between the mild nucleophiles anthranil, 1,2,4-oxadiazole or 4,5-dihydro-1,2,4-oxadiazole and an ynamide, PhC≡C-N(Ts)Me, proceeding via the formation of the aforementioned α-imino gold carbene intermediate which, after intramolecular capture, produces regioselectively 2-amino-3-phenyl-7-acyl indoles, N-acyl-5-aminoimidazoles or N-alkyl-4-aminoimidazoles, respectively. In all cases, the regioselectivity of the substituents at 2, 3 in the 7-acyl-indole ring and 4, 5 in the substituted imidazole ring is decided at the first transition state, involving the attack of nitrogen onto the C1 or C2 carbon of the activated ynamide. A subsequent and steep energy drop furnishes the key α-imino gold carbene. These features are more pronounced for anthranil and 4,5-dihydro-1,2,4-oxadiazole reactions. Strikingly, in 4,5-dihydro-1,2,4-oxadiazole reaction the significant drop of energy is due to the formation of an unstable α-imino gold carbene which after a spontaneous benzaldehyde elimination is converted to a stabilized one. Compared to anthranil, the reaction pathways for 1,2,4-oxadiazoles or 4,5-dihydro-1,2,4-oxadiazoles are found to be significantly more complex than anticipated in the original research. For instance, compared to the formation of a five-member ring from the α-imino gold carbene, one competitive route involves the formation of intermediates consisting of a four-member ring condensed with a three-member ring which after a metathesis and ring expansion led to the imidazole ring.

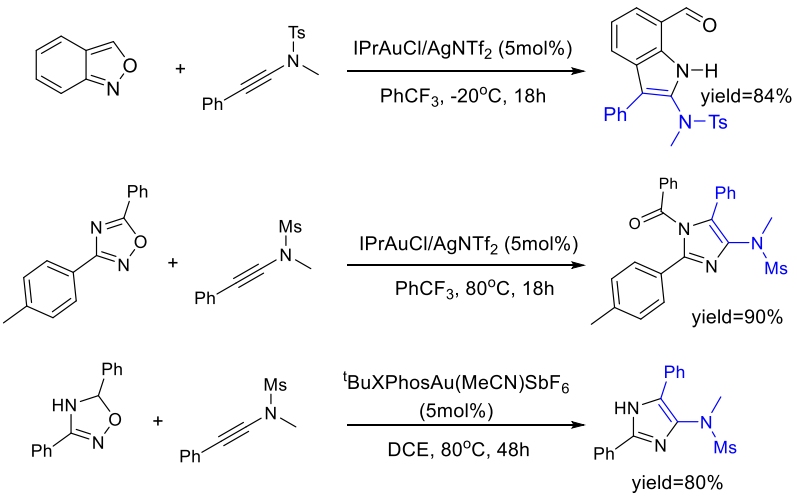


Scheme 3. Au(I)-catalyzed reaction of anthranil, 1,2,4-oxadiazoles or 4,5-dihydro-1,2,4-oxadiazoles with ynamides forming 2-amino-3-phenyl-7-acyl indoles, N-acyl-5-aminoimidazoles or N-alkyl-4-aminoimidazoles, respectively (Hashmi 2017 - Liu 2017).

# CONTENTS

# Chapter 1

## An overview on gold-catalyzed reactions with π-systems

### 1.1 Reactivity of gold with π-systems

Homogenous gold-catalysis blossoms year after year because of its beneficial traits like the mild reaction conditions and easiness of use. Thus, it is a powerful tool on the hands of synthetic chemists who work on organic and bioorganic synthesis or material science. A major part of homogenous gold catalysis is related to activated alkynes, allenes and alkenes. Gold complexes with the carbon π-system (double or triple C-C bond) are exposed to the attack of nucleophilic moieties. In the cases that an asymmetric and polarized substituted π-system is involved in a gold-catalysed reaction, the transformation reveals regio-, stereo- and chemoselectivity.

Regio-, stereo- and chemoselectivity are related to the nature of the substituents and orientation of the carbon π-system. Substituents can be divided to electron donating groups (EDGs) and electron withdrawing groups (EWGs).

In the case of an activated alkyne, under gold(I) catalysis, there are two carbons α and β (Scheme 1.1) where a nucleophile could attack. Due to EDGs and EWGs gold-alkyne complex is polarized and nucleophile prefers the more electron deficient center. [1]

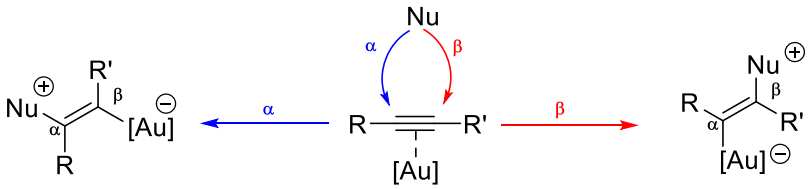


Scheme 1.1 Nucleophilic functionalization of alkyne under gold catalysis.

## 1.2 Gold-catalyzed functionalization of activated π-systems with electron donating group

### 1.2.1 Functionalization of ynamides

#### A. General reactivity profile of ynamides

Ynamides are classified as particularly activated alkynes bearing an electron donating group. The activation process of the ynamides follows a first step of activation by gold that forms a keteniminium intermediate. In contrast to ynamide that is a nucleophile, the keteniminium intermediate is a polarized and electrophilic species. At the second step, variable nucleophiles can approach and attack regioselectively at α carbon (Scheme 1.2).

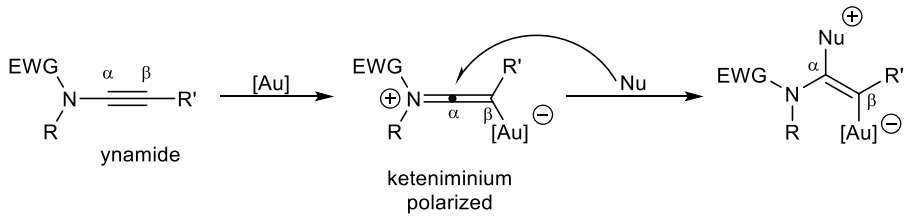


Scheme 1.2 General mechanism of a nucleophilic attack to an activated alkyne bearing an electron donating group (EDG) e.g. an ynamide.

Examples of the reaction of ynamides, allenamides with nucleophiles are included.

#### B. Functionalization with N-based nucleophiles

Some examples of the reaction of ynamides with N-, O- and C-based nucleophiles are commented. The mechanism of the reaction between an oxazole and ynamide is shown in Scheme 1.3. [2]

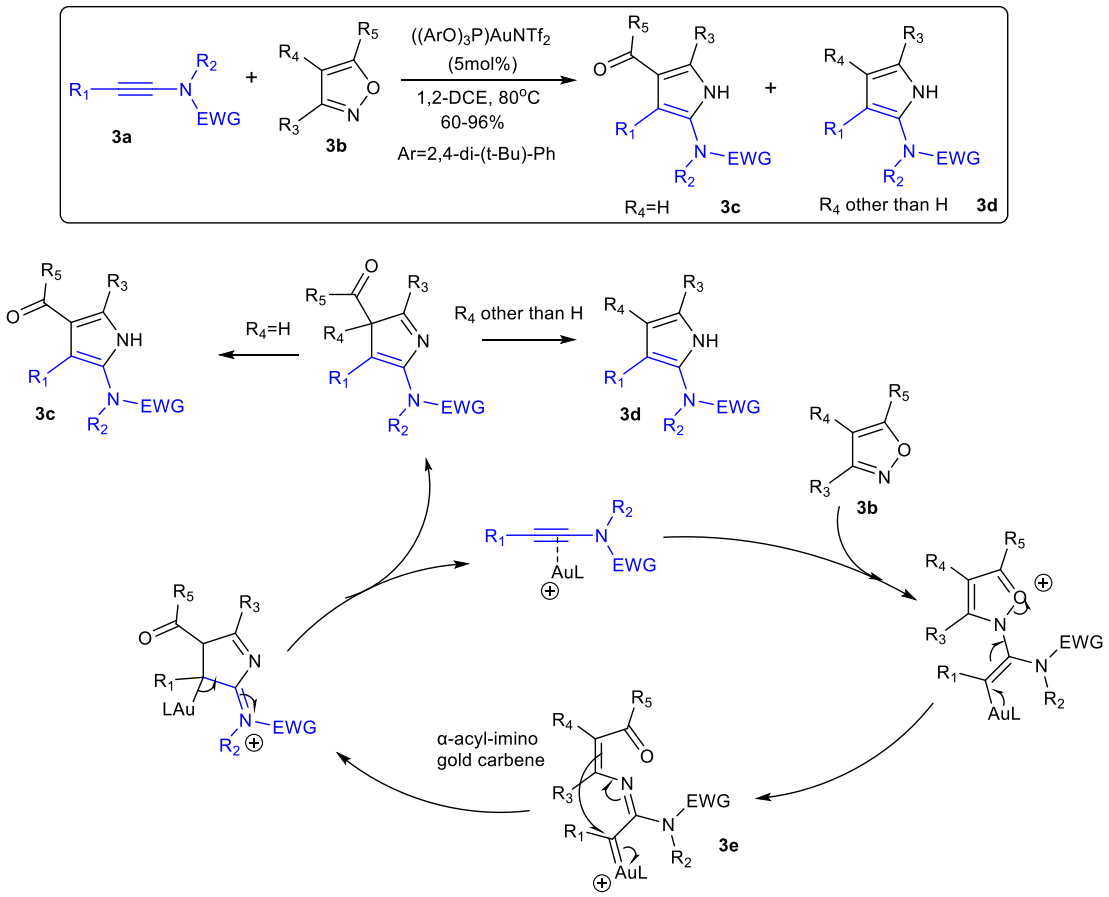


Scheme 1.3 Formal [3+2] cycloaddition between ynamides and isoxazoles (Ye 2015). [2]

The first step of the mechanism of the reaction is the activation of ynamide **3a** by gold(I) catalyst. Accordingly, isoxazole's **3b** nitrogen attacks to the α-carbon of the activated complex, forming α-imino gold carbene intermediate. Cyclization of α-imino gold intermediate **3e** and protodeauration leads to 2-amino pyrroles **3c**/**3d**.

Isoxazoles can be replaced by various nucleophiles including anthranils, [3] imines, [4] sulfoximines [5] etc. These reactions are shown in Schemes 1.4-1.6.

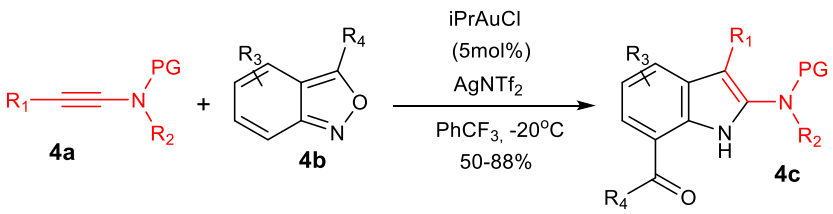


Scheme 1.4 Formal [3+2] Cycloaddition between ynamides and anthranils catalyzed by IPrAuCl/$AgNTf_2$ (Hashmi 2016). [3]

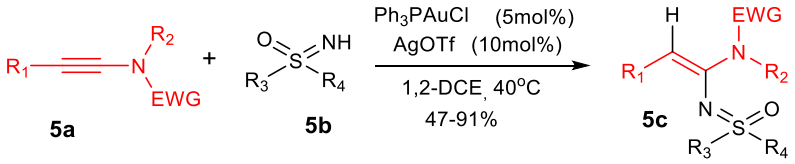


Scheme 1.5 Synthesis of vinyl sulfoximidoyl derivatives by hydrosulfoximination of ynamides with sulfoximines catalyzed by $Ph_3PAuCl/AgOTf$ (Wang and Chen 2016). [5]

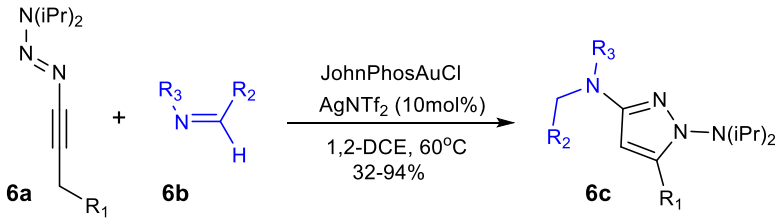


Scheme 1.6 Synthesis of 1,3-diaminopyrazoles from 1-alkynyltriazenes and imines catalyzed by JohnPhosAuCl/$AgNTf_2$ ( (Severin 2017). [4]

## C. Functionalization with O-based nucleophiles

Activated ynamides can react with O-based nucleophiles such as pyridine N-oxide and derivatives and sulfoxides forming an intermediate α-oxo gold carbene intermediate after the cleavage of the bond between oxygen and leaving group X. [1]

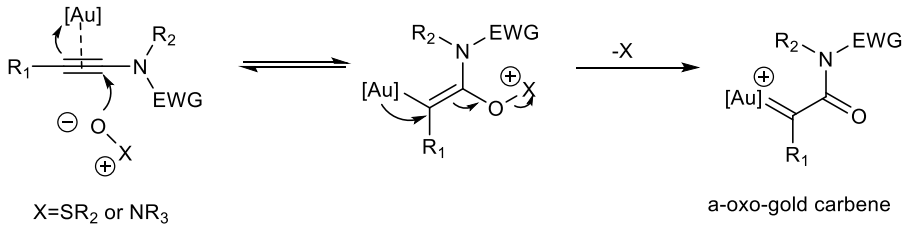


Scheme 1.7 α-Oxo gold carbenes from ynamide substrates. [1]

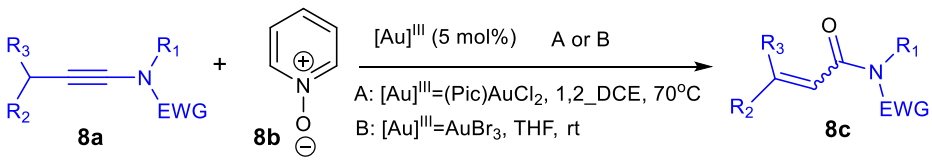


Scheme 1.8 Au(III)-catalyzed synthesis of α,β-unsaturated carbonyl derivatives by oxidation of ynamides (Martin 2011). [6]

In Scheme 1.8 is shown the synthesis of α,β-unsaturated carbonyl derivatives from the reaction of pyridine N-oxide and ynamides catalyzed by Au(III) .

Ynamides react with alcohols and ethers either intramolecularly or intermolecularly, forming fused imidazole heterocycles or diaminofurans according to Scheme 1.9. It is noteworthy that the reaction of Scheme 1.9 follows an opposite regio- selectivity. The formation of the six member ring, versus five member ring, is favored possibly due to the easier approach of OH group to the β-carbon of alkyne giving a 6-endo-dig attack. [7]

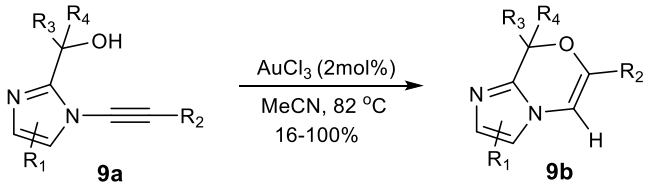


Scheme 1.9 Au(III)-catalyzed synthesis of O-heterocycles from ynamides via hydroalkoxylation (Kerwin 2009). [7]

2,5-Diaminofurans can be formed by the reaction of water with diynamides catalyzed by $Ph_3PAuNTf_2$. [8]

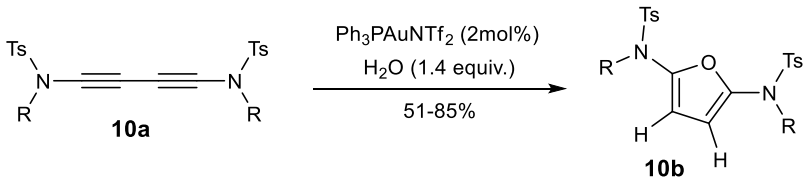


Scheme 1.10 Gold(I)-catalyzed synthesis of 2,5-diamino furan from diynes and water (Skrydstrup 2010). [8]

In the synthesis of dihydrobenzoxepines **11c** by the formal [4+3] cycloaddition between ynamides **11a** and epoxides **11b** catalyzed by $iPrAuNTf_2$, a retention of stereochemistry is observed (Scheme 1.11). [9]

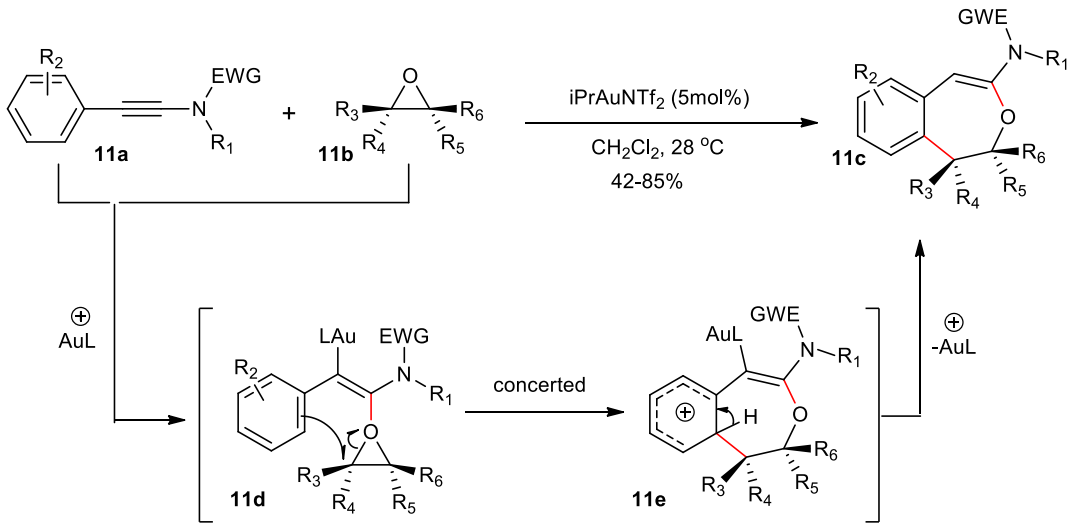


Scheme 1.11 Au(I)-catalyzed synthesis of dihydrobenzoxepines by the formal [4+3] cycloaddition between ynamides and epoxides (Liu 2012). [9]

Moreover, the reaction proceeds under a wide variety of substituents not only on ynamide **11a** but also on epoxide **11b**. The proposed mechanism of the reaction is that an initial nucleophilic attack of the epoxide **11b** onto the activated ynamide leads to oxonium intermediate **11d**. Possibly, the orientation of the attack is very strict due to the conformation constraint that aryl group induces to the oxiranyl ring orientation. In addition, a synchronous breaking of the bond C-O in the oxirane **11d** and the formation of the bond C-C between aryl group and oxirane contributes to the conservation of the stereochemical conformation. [9]

### D. Functionalization with C-based nucleophiles

In gold(I)-catalyzed reactions an activated ynamide can participate to cycloisomerizations, formal cycloadditions or hydro/hetero arylations with aryl or alkene groups. These reactions can be either intramolecular or intermolecular.

An example of gold(I)-catalyzed cycloisomerization is the reaction of the ynamide in Scheme 1.12. For the activation of ynamide either $(ArO)_3P)AuCl/AgOTf$ or $[(JohnPhos)Au(NCMe)]SbF_6$ is used as gold(I) catalyst. The nucleophilic attack by C2 indole carbon at α-carbon of the activated ynamide forms regioselectively a fused six member ring with indole. At the second step, a 5-exo-dig or 6-endo-dig cyclization leads to the formation of the two types of fused indole N-heterocycles. The role of the

$R_3$ alkyl group is crucial. A sizeable $R_3$ group favors 5-exo-dig attack while a small one urges the 6-endo-dig path.

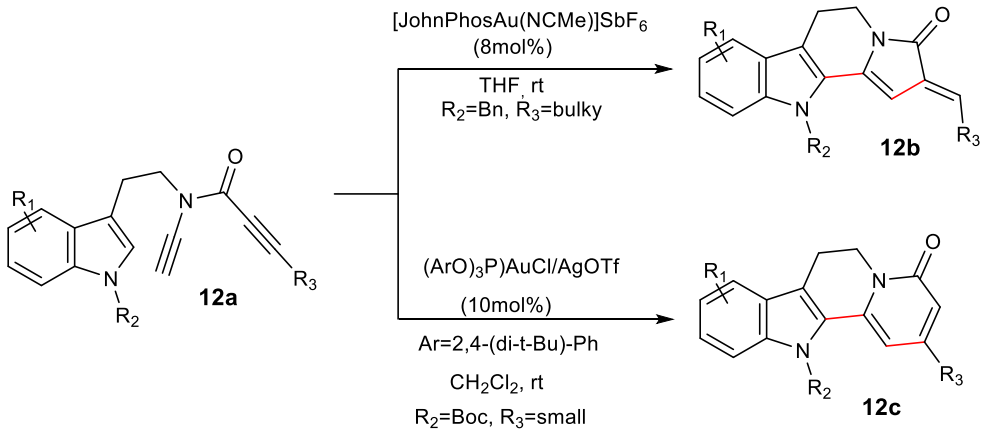


Scheme 1.12 Gold(I)-catalyzed cycloisomerization of tryptamine-derived ynamides (Liu 2019). [10]

A variation of the previous reaction is the synthesis of pyrrolo[2,1-a]isoquinolines **13d** from diynamides **13a** using iPrAuNTf$_2$. [11] The nucleophilic attack to the activated ynamide group is succeeded not only by benzene (Scheme 1.13) but also by heterocyclic arenes, e.g. an indole ring. An electron donating group on the phenyl ring (Scheme 1.13) or otherwise an heterocyclic arene increases the yield of the reaction. At the first step of the reaction, the activated ynamide **13b** is attacked at the α-carbon by the benzene ring forming a C-C bond. At the second step, the activated second alkyne moiety reacts intramolecularly through a 5-endo-dig cyclization with the nucleophilic N. Mechanistic studies, including DFT calculations, support that the path to the formation of pyrrolo[2,1-a]isoquinolines **13d** passes through a two-step [1,2]sulfonyl shift. [11]

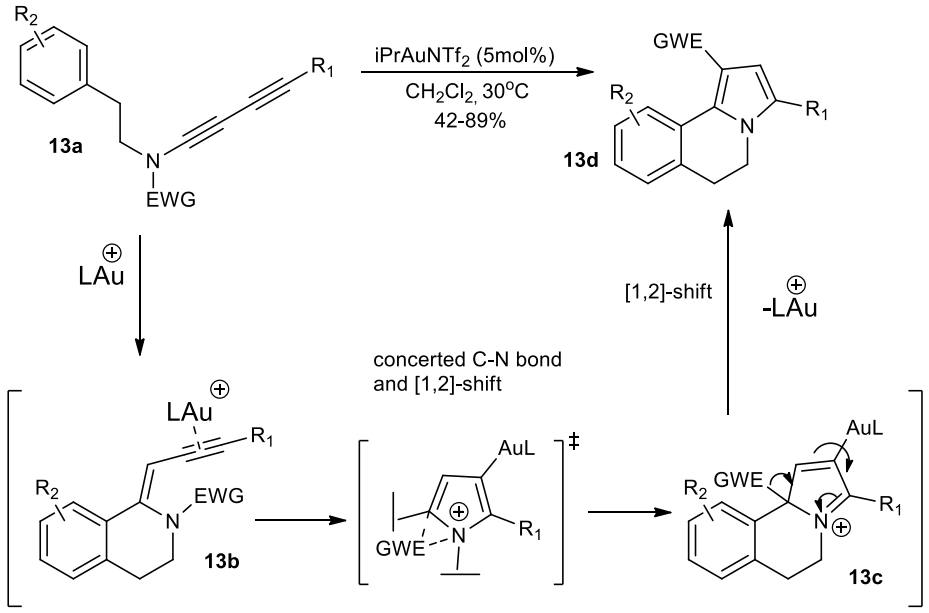


Scheme 1.13 Synthesis of pyrrolo[2,1-a]isoquinolines from diynamides (Huang 2019). [11]

**E. Intramolecular hydride shifts of keteniminium intermediates**

Functionalization of ynamides by an electrophilic gold(I) complex may be used for the formation of polycyclic compounds via an allene intermediate or can lead directly to an allenamide in the case that cyclization is not feasible.

In case that an allenamide is the final product, as is shown for the reaction in Scheme 1.14 catalyzed by [(JohnPhos)Au(NCMe)]$SbF_6$, [12] the presence of a benzyloxy group is necessary to act as a hydride donor. Transformation proceeds through a [1,5]-hydride shift from the benzylic group to the keteniminium. An unstable intermediate intervenes between allenamide and keteniminium. A concerted elimination of a molecule of benzaldehyde and catalyst forms the allenamide product. [12]

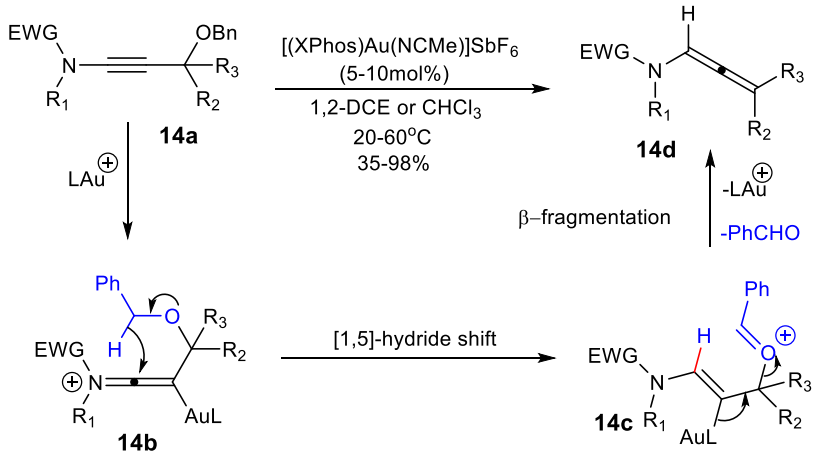


Scheme 1.14 Gold(I)-catalyzed formation of allenamide via intramolecular [1,5]-hydride shift (Gagosz 2017). [12]

### 1.2.2 Functionalization of ynol derivatives

Although ynols are sensitive to nucleophilic attack at α-carbon (Scheme 1.15), similarly to ynamides, there are fewer methods in the literature compared ynamides. Often, most of examples include ynols derivatives, like alkynyl-silyl-ynol ethers or alkynyl-aryl ethers. Functionalization of ynols can be succeeded with C-, N- and O-based nucleophiles according to Scheme 1.15.

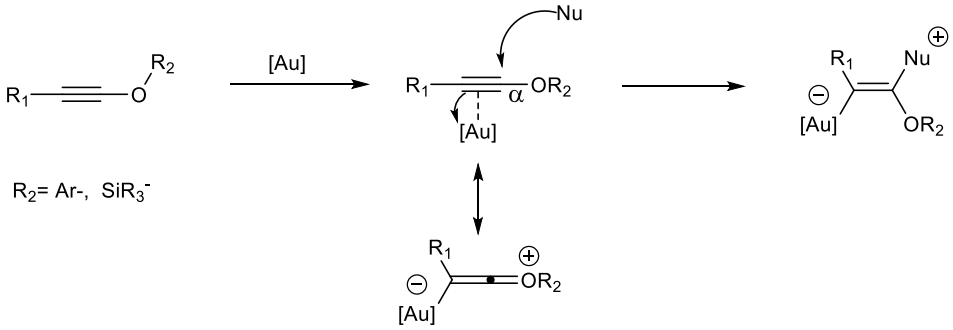


Scheme 1.15 Ynol derivatives employed in gold catalysis and their generic reactivity. [1]

Phenol derivatives can be formed by the gold(I)-catalyzed reaction of terminal arylalkynyl ethers (ynols) **16a** with 2,5-substituted furans **16b** (Scheme 1.16) catalyzed by iPrAuCl/NaBArF (BArF is a non-coordinating anion, i.e. the tetrakis[3,5-bis(trifluoromethyl)phenyl]borate). [13] This reaction is sensitive to steric

and electronic effects associated with the ynol adduct. Also, in the case of aliphatic ynol ethers the reaction proceeds in low yield. [13]

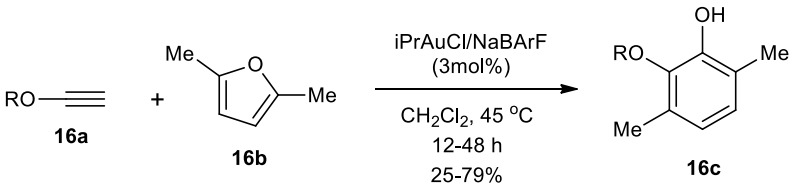


Scheme 1.16 Gold(I)-catalyzed reaction of alkynes with furans to phenols (Hashmi 2015). [13]

The synthesis of the benzo-furano-quinoline **17c** was carried out by the reaction of aryl-ethynyl ether **17a**, an ynol with an electron donating group, and anthranil **17b** using JohnPhosAuCl/AgSbF6 as catalyst (Scheme 1.17). [14] The reaction proceeds via an α-amino gold carbene intermediate **17d** which is then subjected to an intramolecular nucleophilic attack from aryloxy group to carbene. Next, an intramolecular condensation leads to the benzo-furano-quinoline **17c**.

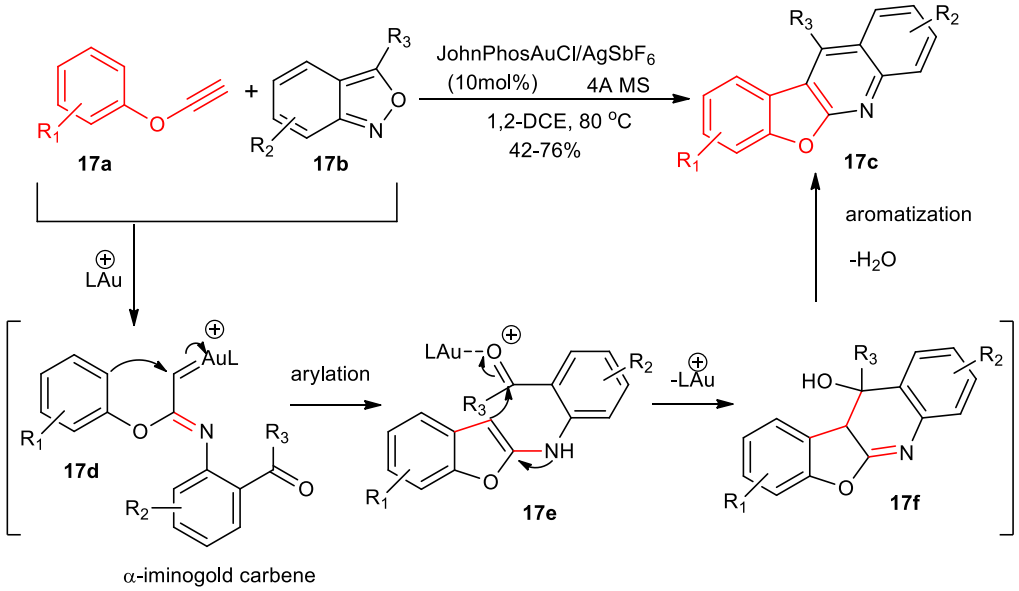


Scheme 1.17 Annulation of the anthranils with aryl-ethynyl ethers (Liu 2019). [14]

### 1.2.3 Functionalization of allenamides and allenyl ethers

#### A. General reactivity profile

Synthetic methods using allenyl derivatives are less abundant than methods using alkyl-derivatives because of the unstable nature of the former and the difficulties of manipulation. However, allenyl derivatives offer interesting chemical characteristics when are used as substrates for gold(I)-catalyzed reactions. There are two available positions on allenes, a central and a terminal one (α and γ) for the formation of a new C-C, C-N or C-O bond. A generic approach of the reactivity of the allenes with gold(I) catalyst is based on the presence of a N-, O-, S-, electron donating ligand that transforms the allene to an aurated alkenyl-indermediate. The latter is sensitive enough to intermolecular or intramolecular nucleophilic attack on positions α or γ (Scheme 1.18).

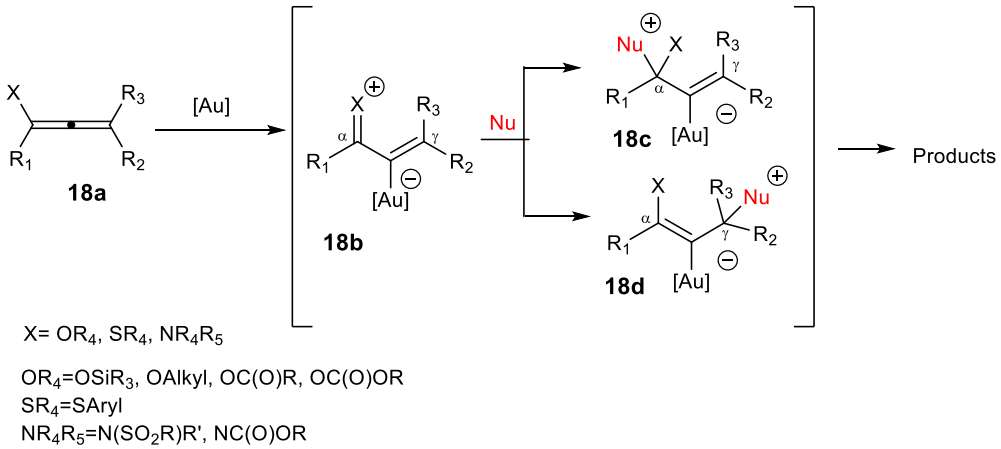


Scheme 1.18 Mode of reactivity of allenes substituted by a O-,S-,N-based electron donating group (Krause 2011). [15]

#### B. Functionalization with C-based nucleophiles

Benzyloxy group can be part of an allene following an Au(I)-catalyzed intramolecular cyclization. In Scheme 1.19 the activation of allene **19a** by AuCl leads to a cyclopropyl intermediate **19b**. Next, C-C bond rearrangement and deauration leads to the cyclohexadiene derivative **19c** which is easily aromatized to the benzyloxybenezene derivatives **19d** by means of the leaving group $R_2OCO$. [16]

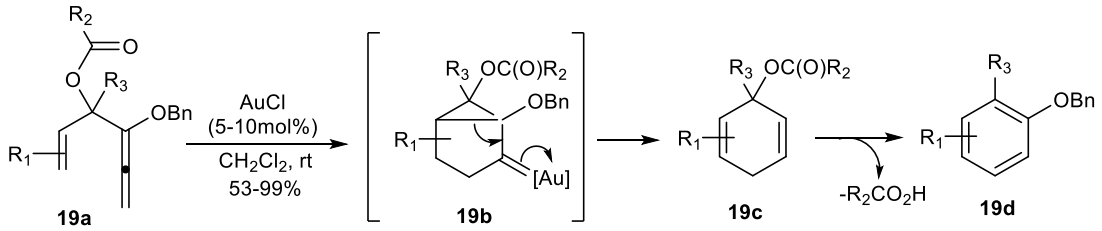


Scheme 1.19 Gold catalyzed synthesis of benzyloxybenzenes (Zhang 2007). [16]

Another example of Au(I)-catalyzed functionalization with C-based nucleophile is the formal [4+2] cycloaddition between an allene **20b** and 2-alkenylindoles **20a** leading to the formation of tetrahydrocarbazole derivatives **20f-20g** (Scheme 1.20). A suggested mechanism starts with the nucleophilic attack by the electron rich C-3 carbon of the indole ring at the terminal position γ-carbon of allene **20b**, that is activated by JohnPhosAuNTf$_2$ catalyst. The second step is the nucleophilic attack between the alkenyl side chain group and the β-carbon of the allene which leads to the cyclization product **20d**.

Both experimental conditions and Au(I) catalyst are crucial factors for the direction of the reaction and subsequently for the kind of its product. For instance, usage of $AuCl_3$ at low temperature (-70 to -50 $^oC$) with substoichiometric amount of allenamide produces indole **20g** as the main product. On the contrary, higher temperature (-20 $^oC$) and JohnPhosAuNTf$_2$ urge the reaction to the formation of the isomer **20f**. Excess of allenamide gives the disubstituted product **20f** due to one more nucleophilic addition at γ position of another gold(I)-activated allenamide. [17]

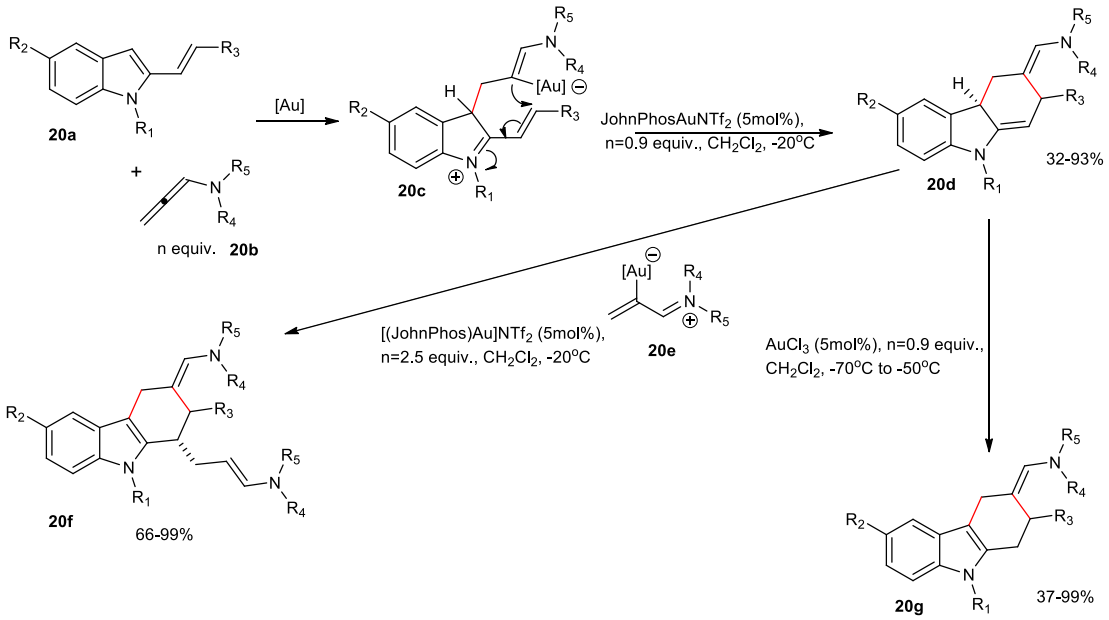


Scheme 1.20 Alkenylindoles as gold-catalyzed reaction partners in formal [4+2] cycloadditions with allenamide (Vicente 2013). [17]

### C. Functionalization with O-, N-based nucleophiles

Most common Au(I)-catalyzed functionalizations with O- and N- nucleophiles are the intramolecular ones. Typical examples are the formation of the dihydro-furan **21c** or compound **22c** in which a pyrrole ring has been constructed starting from allenes **21a** [18] or **22a** [19] with a vicinal hydroxyl or amino group, respectively. The first steps of both reactions probably are similar.

In the first case (Scheme 1.21) a nucleophilic attack of the hydroxyl group to the α-carbon of the activated allene with $Ph_3PAuCl/AgBF_4$ forms the intermediate **21b**. After protodeauration, the dihydrofuran **21c** is formed in good yields within a short reaction time (e.g. 5 min).

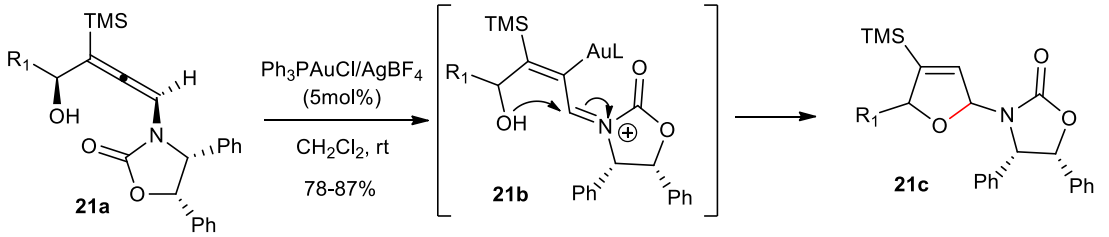


Scheme 1.21. Synthesis of dihydrofuran derivatives (Hegedus 2006). [18]

The second $Ph_3PAuNTf_2$-catalyzed reaction (Scheme 1.22) follows a differentiated path after protodeauration. Thus, after the nucleophilic attack of the amino group to the α-carbon of allene **22a**, and protodeauration, concerted steps of elimination of phosphate group and aromatization lead to the formation of pyrrole derivatives **22c**.

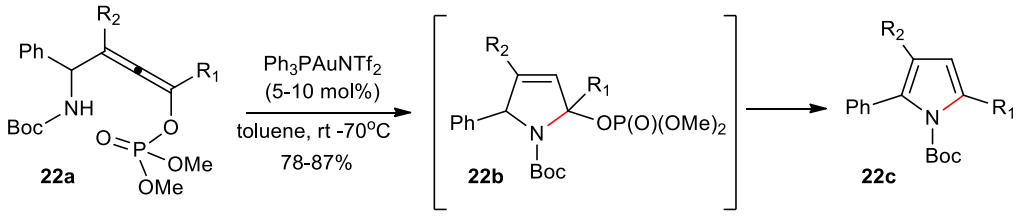


Scheme 1.22 Synthesis of pyrrole derivatives (Terada 2018). [19]

Example of intermolecular N-, O- and S- functionalization reactions by N-, O-, S-based nucleophiles are not very common. For example, a reaction can proceed with the regioselective addition of pyrazole, triazole or benzotriazole to allene under heating and microwave irradiation and catalyzed by $Ph_3PAuNTf_2$. The presence of co-catalyst $PtCl_2$ and the excess of the N-base nucleophile lead to double hydroamination products as it is depicted in Scheme 1.23.

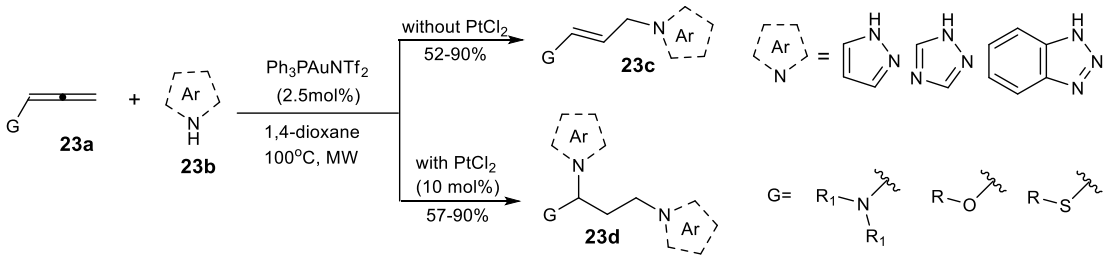


Scheme 1.23 Hydroamination of N-,O- and S- allenyl derivatives (Muñoz 2019). [20]

## 1.3 Gold-catalyzed functionalization of activated π-systems with a withdrawing group

### 1.3.1 Activated π-systems

Compared to the π-systems with EDGs discussed in the previous Section, the π-systems connected with electron withdrawing groups (EWGs) – see examples for alkynes, allenes and alkenes in Scheme 1.24 - show different chemistry. For example,

for alkynes, an EWG can be a carbonyl group directly connected to α-carbon. Thus, the alkyne derivative can be a ketone, a carboxylic acid, an ester or an amide. Alternatively, if the EWG is an imine group, instead of a carbonyl, the substrate should be an imine, an hydrazone or an oxime. The EWG can be a halogen, a boronate, a sulfoxide-sulfone or a fluorine group. Polarized π-systems, activated by electrophilic gold(I) catalyst present regioselectivity on the reaction with nucleophiles. Alkynes, allenes and alkenes bearing EWGs are rendered susceptible to nucleophilic attack at β-position of the π-system. [1]

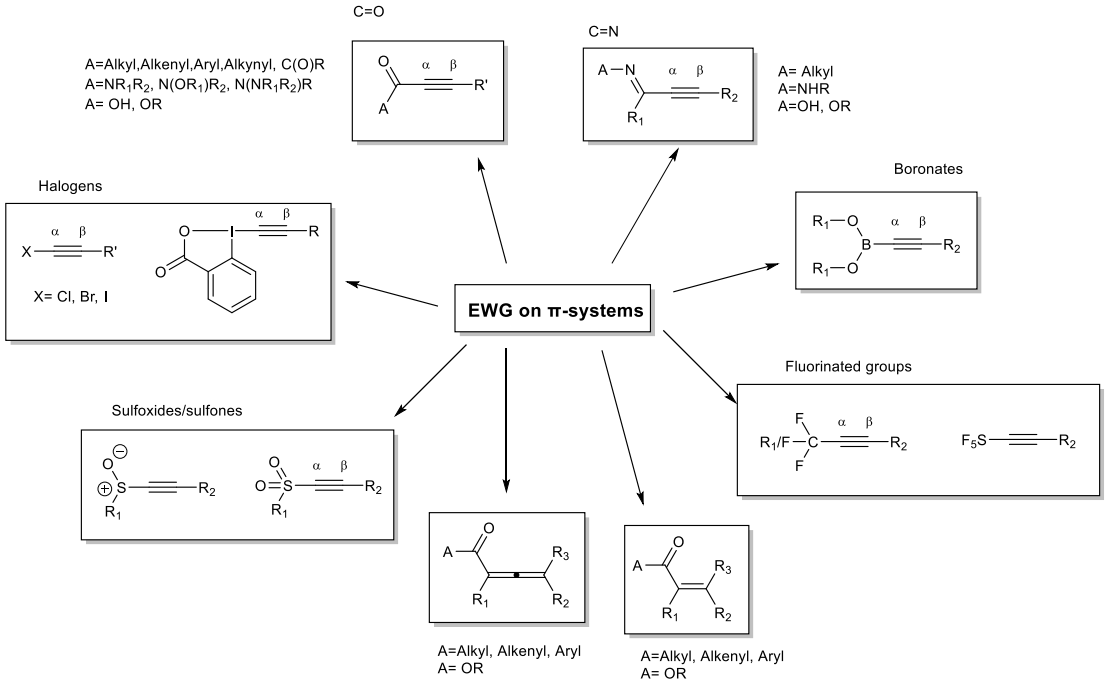


Scheme 1.24 Alkyne, allene and alkene derivatives with electron withdrawing substituents.

### 1.3.2 Alkynyl-carbonyl derivatives

### A. Generic reactivity profile

Alkynyl-carbonyl derivatives are susceptible to Au-catalyzed nucleophilic attack at the β-position of the π-system. The carbonyl EWG renders alkyne β-carbon electron poor so as a nucleophile may attack easily furnishing a large variety of products. C-, N- and O- based nucleophiles can be applied to regioselective reactions with alkynyl-carbonyl derivatives (Scheme 1.25).

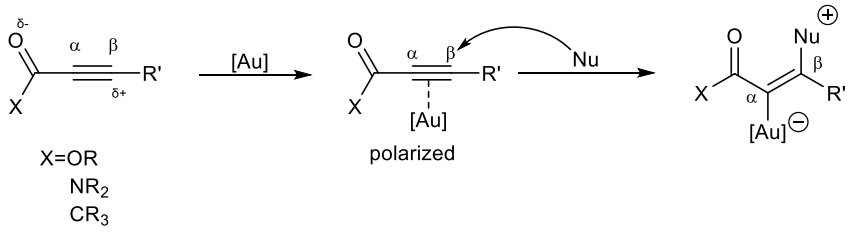


Scheme 1.25 Generic mechanism of a nucleophilic attack to an activated alkyne group of an alkynyl-ester derivative. [1]

**B. Functionalization with C-based nucleophiles**

Alkene or alkyne groups are used as C-based nucleophiles to electron deficient activated alkynes. There are several intramolecular or intermolecular cyclizations, cycloisomerizations and cycloadditions. Few examples are shown below.

The Au(I)-catalyzed cyclization of 1,6-enyne **26a** that bears as an EWG an ester or amide group tethered to the alkyne is presented (Scheme 1.26). First, the activated by $Ph_3PAuSbF_6$ alkyne is subjected to a nucleophilic attack by the adjacent alkene to the electron deficient β-carbon. After a 6-endo-dig cyclization and the formation of the intermediate **26b**, 1,2-carbon shift leads to the cyclobutane condensed bicyclic compound **26d**.

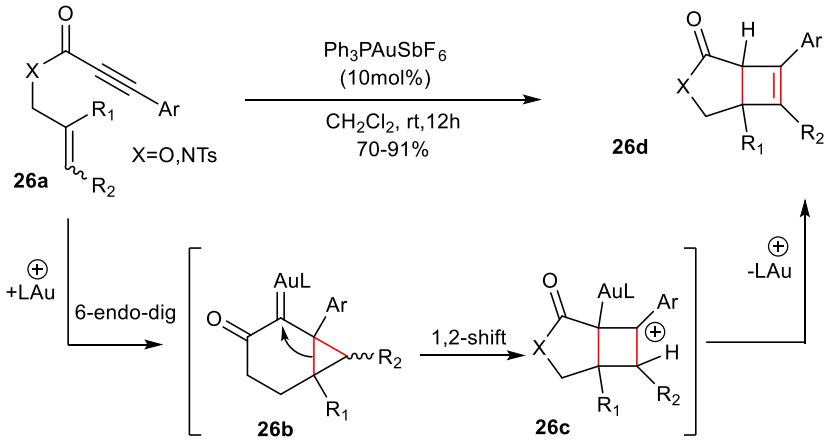


Scheme 1.26 Cyclization of 1,6-enynes (Kang and Chung 2009). [21]

On the other hand, an intermolecular nucleophilic attack to the Au(I)-activated electron deficient alkyne is shown in Scheme 1.27 between a propiolic acid **27b** and an alkene **27a** leading to the unsaturated δ-lactones **27d**. This is a [4+2] annulation

reaction that proceeds with a step of nucleophilic attack to the β-carbon of activated JohnPhosAuCl/$AgSbF_6$-alkyne forming a cyclopropyl gold carbene **27c**. Then the nucleophilic carbonyl oxygen of the intermediate **27c** attacks cyclopropyl ring which opens forming the unsaturated δ-lactone **27d**.

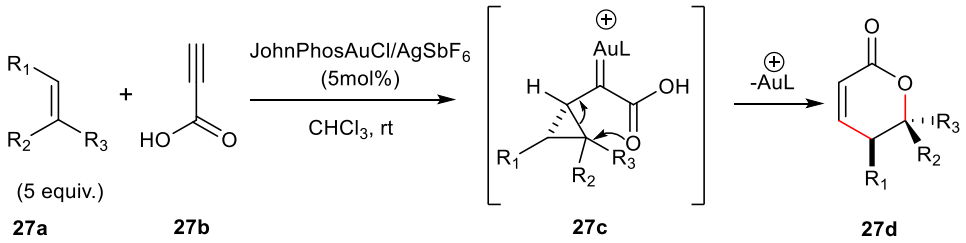


Scheme 1.27 Gold(I)-catalyzed reaction between propiolic acids and alkenes (Shin 2012). [22]

Gold(I)-catalyzed functionalization of alkynes with carbonyl group as EWG can be succeeded via the formation of enols or enol derivatives; enol group is acting as EWG as a tautomeric form of ketone group. Enol or enol derivative can be composed *in situ* unless it exists in a native form when is more stable than the ketone tautomer. One method to synthesize an enol or enol ester is the attack of an oxygen group to the gold(I)-activated terminal alkyne. In Scheme 1.28 is shown the synthesis of α-pyrones **28e** as an example of functionalization of an alkyne bearing an enol group as EWG in **28c**. [23] Gold(I) catalyst $Ph_3PAuCl/AgOTf$ activates the alkyne that accepts at C2 carbon the nucleophilic attack of the carboxylic group of the propiolic acid forming the enol **28c**. An intramolecular nucleophilic attack of the enol carbon to the activated β-carbon of the alkyne moiety and protodeauration of the intermediate **28d** leads to α-pyrone **28e**. [23]

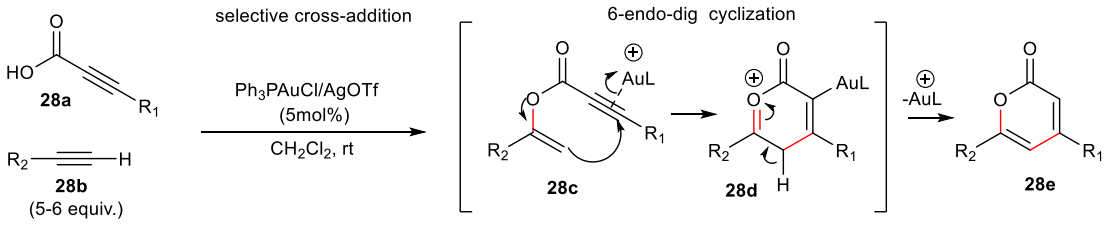


Scheme 1.28 Synthesis of α-Pyrones from enol esters (Schreiber 2011). [23]

A variation of the previous method is based on the replacement of enol ester with allenol ester moiety. [24,25] The first step of the mechanism of this reaction is a gold(I)-catalyzed [3,3]-rearrangement to form the allenyl ester **29b** from **29a** using $Ph_3PAuCl/AgSbF_6$. In the next step, gold(I) catalyst activates the triple bond of the alkyne while the β-carbon of the allenyl group carries out a nucleophilic attack to the β-carbon of alkyne moiety. After the formation of the cyclic product **29c**, reaction may follow different paths depending on the conditions. The presence of an alcohol in the reaction mixture urges the reaction to the formation of esters **29d**. If alcohol is substituted by aromatic system, arylation takes place instead of esterification, forming the compound **29e**. In the absence of a nucleophile, the alkenyl-α-pyrone **29f** is formed due to the redistribution of the π-electrons and deauration of intermediate **29c**.

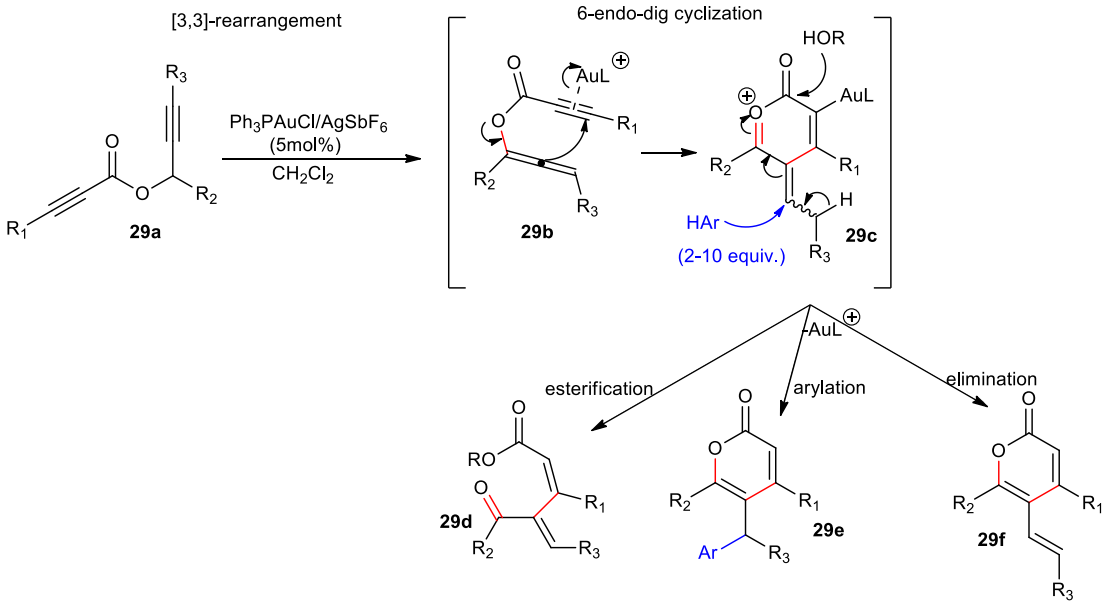


Scheme 1.29 Synthesis of α-pyrones from allenol esters (Schreiber 2007, 2011). [24,25]

## C. Functionalization with O-based nucleophiles

Many applications have been developed using O-based nucleophiles, like alcohols, ketones and aldehydes for the functionalization of alkynyl-carbonyl derivatives. These transformations can be hydrofunctionalizations, cyclizations, isomerizations, cascade reactions and oxidations. Typical example of intramolecular cyclization through a O-based nucleophile to the gold(I)-activated alkyne moiety of an alkynyl carbonyl

derivative is the reaction of hydroalkoxylation of alkynyl ester or alkynones for the formation of oxygen containing heterocycles as depicted in Scheme 1.30. Thus, the formation of oxazepinone **30b** proceeds via the activation of alkynone **30a** by the gold(I) catalyst ($Ph_3PAuCl/AgOTf$) following an 7-endo-dig nucleophilic attack of the hydroxyl group to the β-carbon of the bond. The combination of gold(I) catalyst $Ph_3PAuCl$ with AgOTf gives excellent yields. However, $Ph_3PAuCl$ alone can catalyze the reaction. [26]

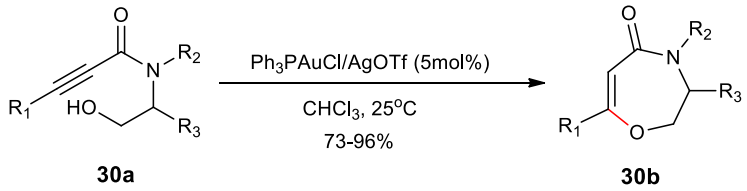


**30a** **30b**

Scheme 1.30 Synthesis of oxazepinones by intramolecular hydroalkoxylation (Van der Eycken 2015). [26]

Similar to the above method is the Au(III)-catalyzed synthesis of 5-, 6- and 7-member ring cyclic acetals **31e** and exocyclic enol ethers **31b-31d** [27] (Scheme 1.31). Despite the E-isomer is favored, a mixture of E- and Z-isomers is received. According to the proposed mechanism, after the nucleophilic attack of the hydroxyl group to the Au(I)-activated alkyne, the Z-enol ether **31b** is formed. Isomerization of the Z-enol ether **31b** to the intermediate oxocarbenium **31c** is the path that leads to the formation of E-isomer **31d**, while isomers **31b**, **31c** are in equilibrium. Both of the two structures are the substrate for the nucleophilic attack of an alcohol furnishing the acetal **31e**. [27] When the alcohol is absent the cyclic acetals bearing enol ester groups **32b** are obtained (Scheme 1.32).

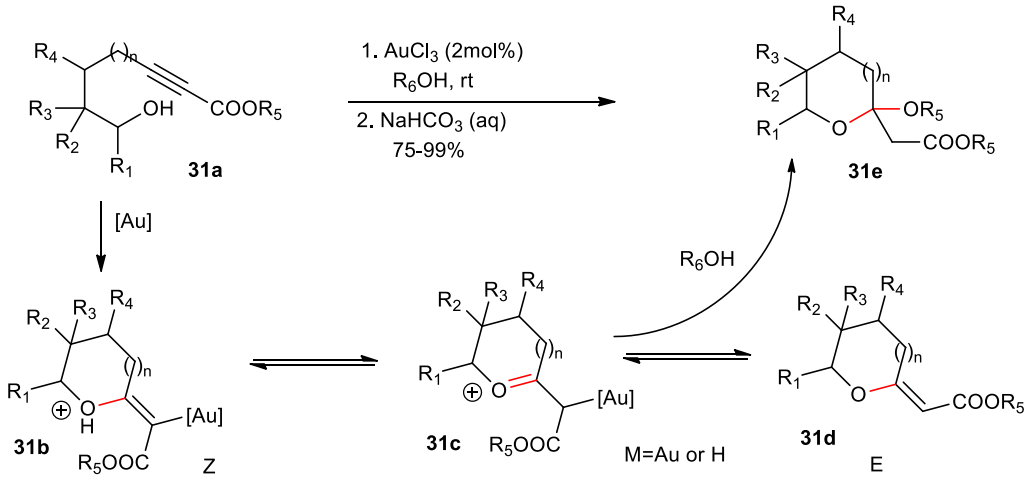


Scheme 1.31 Gold(III)-catalyzed synthesis of cyclic acetals and exocyclic enol ethers via an intramolecular hydroalkoxylation of alkynyl esters (Ley 2009). [27]

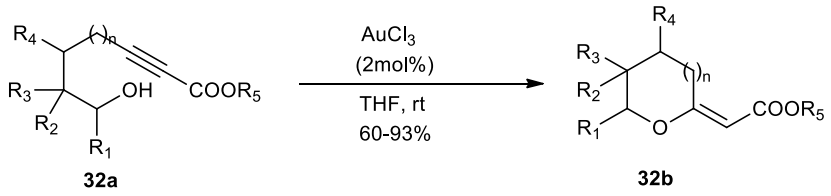


Scheme 1.32 Gold(III)-catalyzed synthesis of cyclic acetals **32b** bearing enolester groups via an intramolecular hydroalkoxylation of alkynyl esters (Ley 2009). [27]

Some O-based nucleophiles like pyridine N-oxide, quinoline N-oxide, nitro and sulfoxide groups (see $^{-}$O-LG$^{+}$ in Scheme 1.33) can oxidize the alkynyl-carbonyl substrate **33a** deriving the reactive intermediate **33b**, since they can attack from O-nucleophilic atom at the β-carbon of the activated alkyne moiety of the alkynyl-carbonyl derivative **33a**. According to the proposed mechanism the intermediate has two alternative paths. The first one is the cleavage of the bond O-LG forming an α,α´-dioxo gold carbene **33c**. The alternative path is that of a synchronus nucleophilic attack at α-carbon of the alkyne with O-LG bond cleavage, forming the 1,3-diketo compound **33d**. A very interesting point of the reaction is that the nature of the catalyst favors one path or the other. That is, the first path is favored by electron rich gold(I) catalysts. The second path is feasible with gold(III) catalysts.

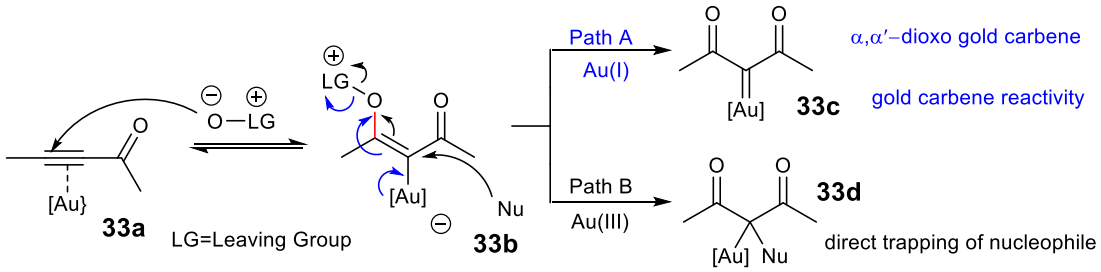


Scheme 1.33 Prevailing mechanism in gold-catalyzed oxidative functionalization of alkynyl-carbonyl derivatives. [1]

Extension of the above mechanism is the intramolecular C-H functionalization of aryl groups. According to the method, N-alkynoyl anilines **34a** under the action of 2-bromopyridine N-oxide are transformed to 3-acyloxindoles **34d** (Scheme 1.34). The mechanism consisted of a first oxidation step to a α,α′- dioxo gold carbene, followed by an electrophilic aromatic substitution to the adjacent aromatic ring of aniline. Finally, protodeauration and aromatization of the condensed rings lead to 3-acyloxindole **34d**. The method is tolerant to a variety of substituted anilines and several alkynamides.

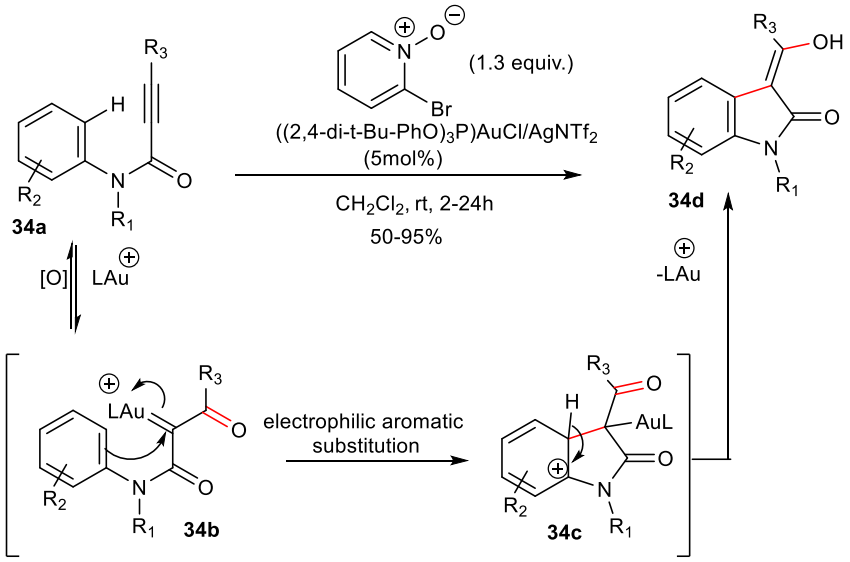


Scheme 1.34 Gold(I)-catalyzed intramolecular C-H functionalization of aryl groups (Zhang 2012). [28]

## D. Functionalization with N-based nucleophiles

Many synthetic methods have been developed with a variety of N-based nucleophiles functionalizing the alkynyl-carbonyl derivatives. The utility of these methods is owed to its application on compounds with industrial interest and synthesis of natural products.

An example of Au(I)-intermolecular functionalization of alkynyl esters or alkynones **35b** by N-based nucleophiles (e.g. aliphatic amines) in the presence of a aldehyde **35a** is the synthesis of 1,4-dihydropyridines **35f**. The proposed mechanism consists of the following steps. Methylamine carries out an 1,4-addition to alkynyl ester (or alkynone) **35b** forming the enamine **35c.** Enamine **35c** reacts with one more molecule of alkynyl ester (or alkynone) **35b** with the aid of $Ph_3PAuCl/AgOTf$ catalyst to afford dienamine **35d** which reacts with aldehyde **35a** to afford **35e** which after redistribution of π-electrons furnishes dihydropyridine **35f** (Scheme 1.35).

The pros of the method are the plurality of the substrates that can be used. Aldehyde can bear an alkyl, alkenyl or aryl group. Additionally, the reaction is feasible either with alkynones or alkynyl esters.

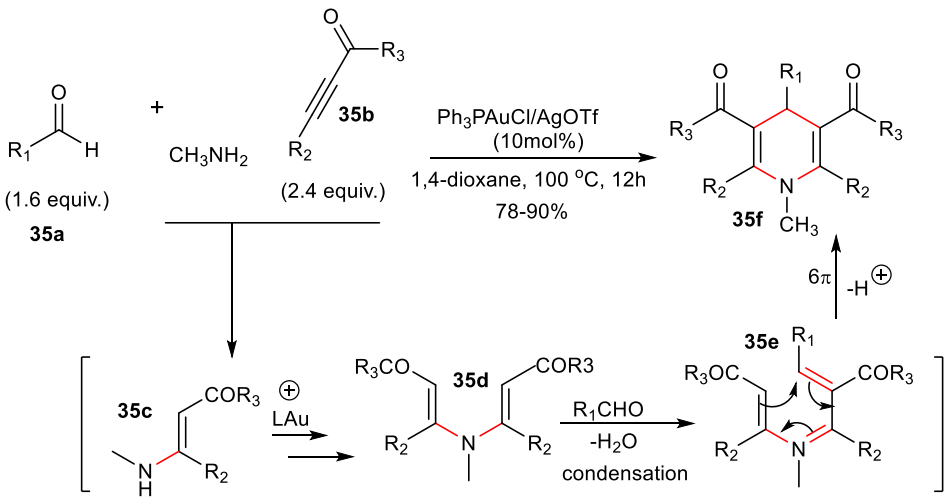


Scheme 1.35 Gold(I)-catalyzed synthesis of 1,4-dihydropyridines (Liu 2013). [29]

Anilines provide another case of a N-based nucleophile that can functionalize both alkynones or alkynyl esters or alkynyl amides. [30] The method allows the use of a large variety of anilines including α-keto anilines **36a** (see Scheme 1.36) that provide a

carbonyl group instead of the aldehyde molecule in Scheme 1.35. In the variation of the method, $Ph_3PAuCl/AgOTf$-catalyzed reaction of α-keto anilines **36a** with alkynones **36b**, the 3-acyl-kinolines **36c** are produced in good yields [30] (Scheme 1.36).

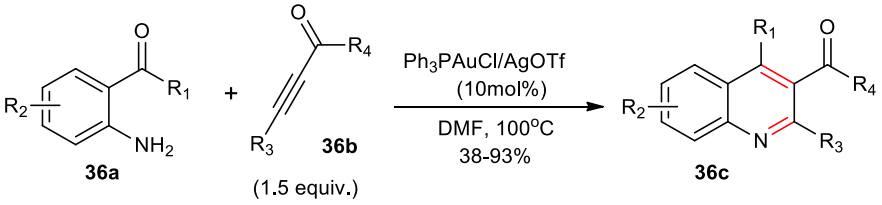


Scheme 1.36 Gold(I)-intermolecular condensation of ortho-acyl anilines with alkynones (Liu 2012). [30]

### 1.3.3 Allenyl carbonyl derivatives

#### A. Functionalization with O-based nucleophiles

Allenyl-carbonyl derivatives are very useful adducts for the formation of furans **37d** and butenolides **37e**. The gold-catalyzed cycloisomerization of allenones **37a** ($R_1$=alkyl group) forms **37b** which after deauration produces furans **37d**, while the gold-catalyzed cycloisomerization of allenoates **37a** ($R_1$=alkoxy group) forms butenolides **37e** after fragmentation and deauration (Scheme 1.37).

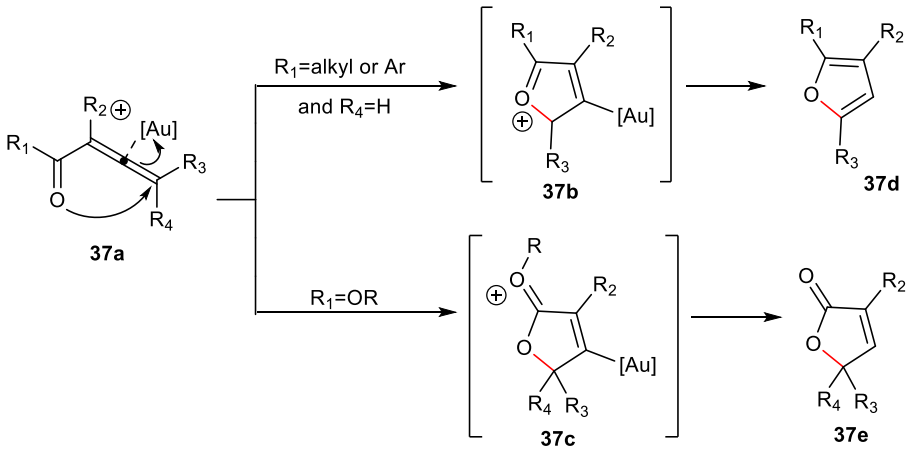


Scheme 1.37 General gold-catalyzed activation models of allenyl-carbonyl derivatives **37a** (Krause 2011). [15]

Gold(III)-catalyzed furan synthesis from allenones **38a** starts with the activation of allenyl group by $AuCl_3$ (Scheme 1.38). The carbonyl oxygen of allenone **38a** acts as nucleophile and realizes a 5-endo-trig cyclization to form an oxonium intermediate **38b**. After an aromatization step followed by a protodeauration step 2-alkyl furan **38c** is formed. However, the main disadvantage of the method is that the reaction can go further with an 1,4-addition step from furan **38c** as nucleophile resulting to an α,β-unsaturated ketone **38d**. [31] The mechanism of the reaction was studied with the use of DFT calculations not only for a variety of allyl-ketones [32,33] but also for gold(I) catalyst. [34]

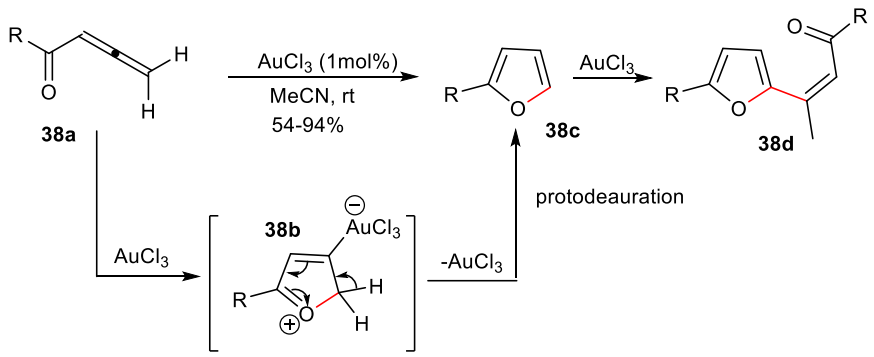


Scheme 1.38 Gold(III)-catalyzed furan synthesis from allenones (Hashmi 2000). [31]

More sophisticated methods have been developed that avoid by-products. A method for synthesis of the multifunctionalized 3-alkynylfurans **39d** from allenones **39a** and a hypervalent iodine reagent (TIPS-EBX) is based on a possible Au(I)/Au(III) redox cycle (Scheme 1.39). [35,36] According to DFT calculations, [36] at the first step of the proposed mechanism allenone **39a** Au(I)-cyclization takes place using AuCl and 2-pyridine carboxylic acid forming the intermediate **39b**. Accordingly, gold is oxidized from (I) to (III) state by the oxidizing reagent TIPS-EBX forming the intermediate **39c** where an alkynyl-TIPS moiety is connected to gold(III). Finally, a reductive elimination step leads to the transfer of alkynyl-TIPS moiety on the furan ring forming the 3-alkynylfuran **39d** (Scheme 1.39). [35,36]

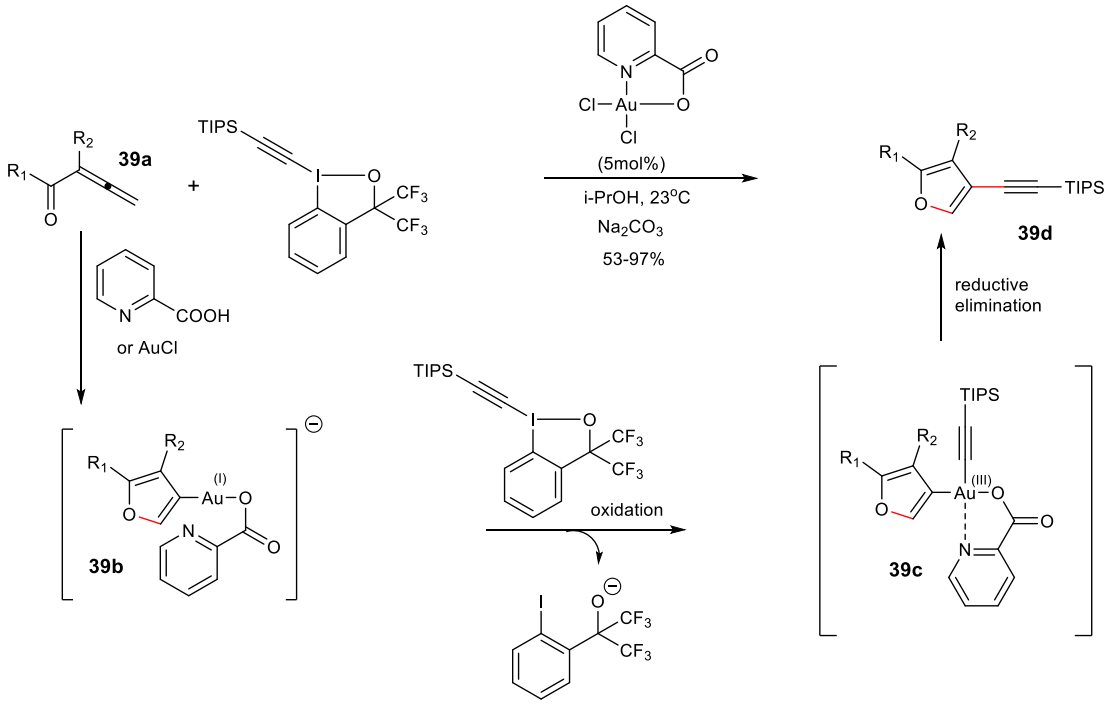


Scheme 1.39 Gold-catalyzed furan synthesis via gold(I)/gold(III) redox cycle (Waser 2013, Ariafard 2017). [35,36]

The synthesis of γ-butyrolactones derivatives can be performed via the action of various reagents on the intermediates of gold(I)-butenolides **40c**. The latter is formed by the cyclization of allenoates **40a** through intermediate **40b** in the presence of transition metals or electrophilic reagents, e.g. the gold(I) phosphine complex with AgOTf mixture in stoichiometric amounts (Scheme 1.40). The $R_3PAuCl/AgOTf$ catalyst renders the reaction feasible at room temperature. DFT calculations support the proposed mechanism. [37]

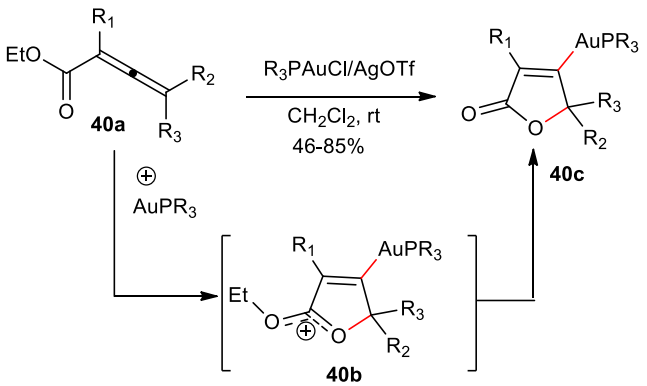


Scheme 1.40 Formation of gold(I)-butenolides and their reactivity (Hammond 2008, 2009). [38,37]

Gold(I)-butenolides are valuable substrates because the gold(I) complex can be substituted with various ligands leading to many different products as is shown in Scheme 1.41. Not only iodination and protodeauration can be applied but also dimerization via a redox process with the use of SelectFluor. [39,40]

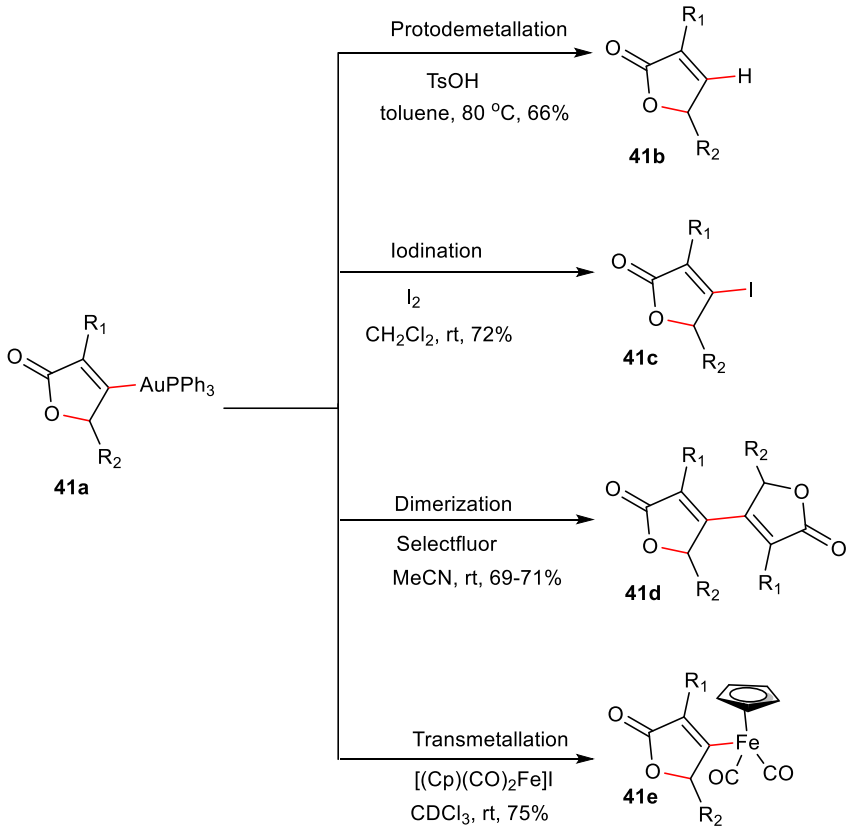


Scheme 1.41 Reactivity of gold(I)-butenolides (Graf 2010, Molinari 2011). [39,40]

Moreover, transmetallation is another useful feature of gold (I)-butenolides **42a** either with palladium(II) complexes, e.g. dppfPdCl$_2$ ((dppf=1,1′-bis(diphenyl-phosphino)ferrocene). The palladium(II) complex intermediates, e.g. **42b**, provide the mean of cross coupling reactions introducing a variety of aryl, alkenyl, allyl and benzyl groups to the position of gold, either via an intramolecular or to an intermolecular reaction leading to **42c**.

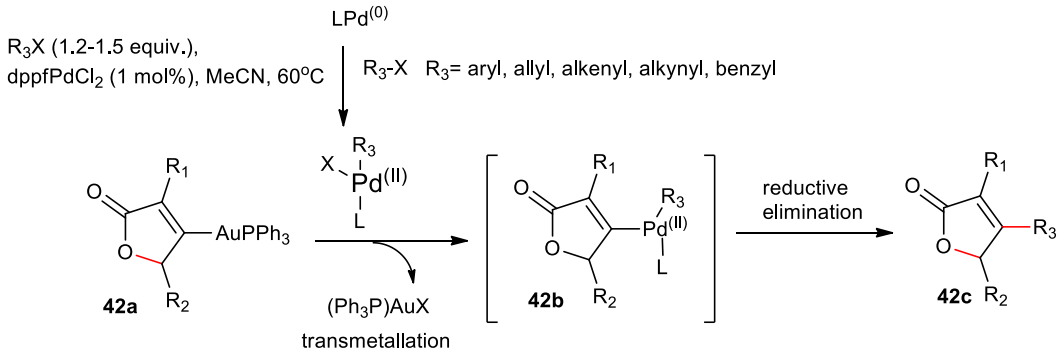


Scheme 1.42 Palladium(II)-transmetallation studies of gold (I)-butenolides (Rominger 2009, 2010, 2012). [41–43]

**B. Functionalization with other nucleophiles**

Compared to the typical cyclization of allenyl butenoates **40a** to lactone derivatives, e.g. **41b-c**, **42c**, allenoate esters with a second functional group which can be nucleophilic, e.g. **43a** could give an alternative gold(I)-catalyzed intramolecular nucleophilic addition (Scheme 1.43). Nucleophilic addition can proceed to α- or β-position of the allene moiety depending on the nature of the nucleophilic group and the size of the formed ring. As shown in Scheme 1.43, the reaction can furnish dihydrofurans **43c**, pyrroles **43d** or tetrahydropyridines **43e** using $Ph_3PAuCl/AgOTf$, $Ph_3PAuNTf2$, $Cy_3PAuNTf_2$, respectively, facilitating the intramolecular nucleophilic attack in the allenoate ester molecule **43a**. Methyl or ethyl esters are commonly used. [44–48]

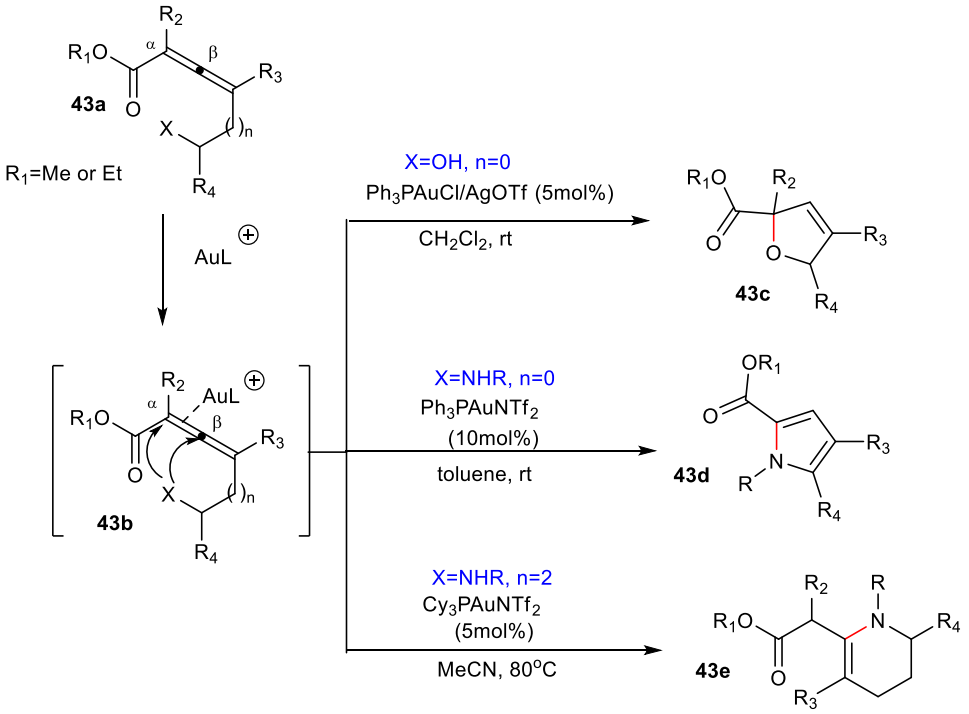


Scheme 1.43 Gold(I)-catalyzed intramolecular additions of O- and N- based nucleophilic group present into allenoates (List 2016, Raven 2013, Xu 2015, Terada 2019, Sun 2015). [44–48]

Haloalkynes are a category of alkynes with unique features due to the highly polarized carbon-halogen bond which implies stronger regioselectivity, compared with other alkyne substrates, for the gold(I)-catalyzed reactions of haloalkynes. Additionally, redox reactions and [1,2]–X rearrangements are very rare on all other types of alkynes. Haloalkynes give inter- and intramolecular functionalization with C, N- and O-based nucleophiles as has been thoroughly studied. Special emphasis is must be given for the case of alkynyl iodoniums that operate as excellent alkynyl transfer agents. In Scheme 1.44 is shown the alkynyl iodonium complex reagent TIPS-EBX and its relevance to the functionalization via gold(I)-catalyzed C-H reactions. [49–56]

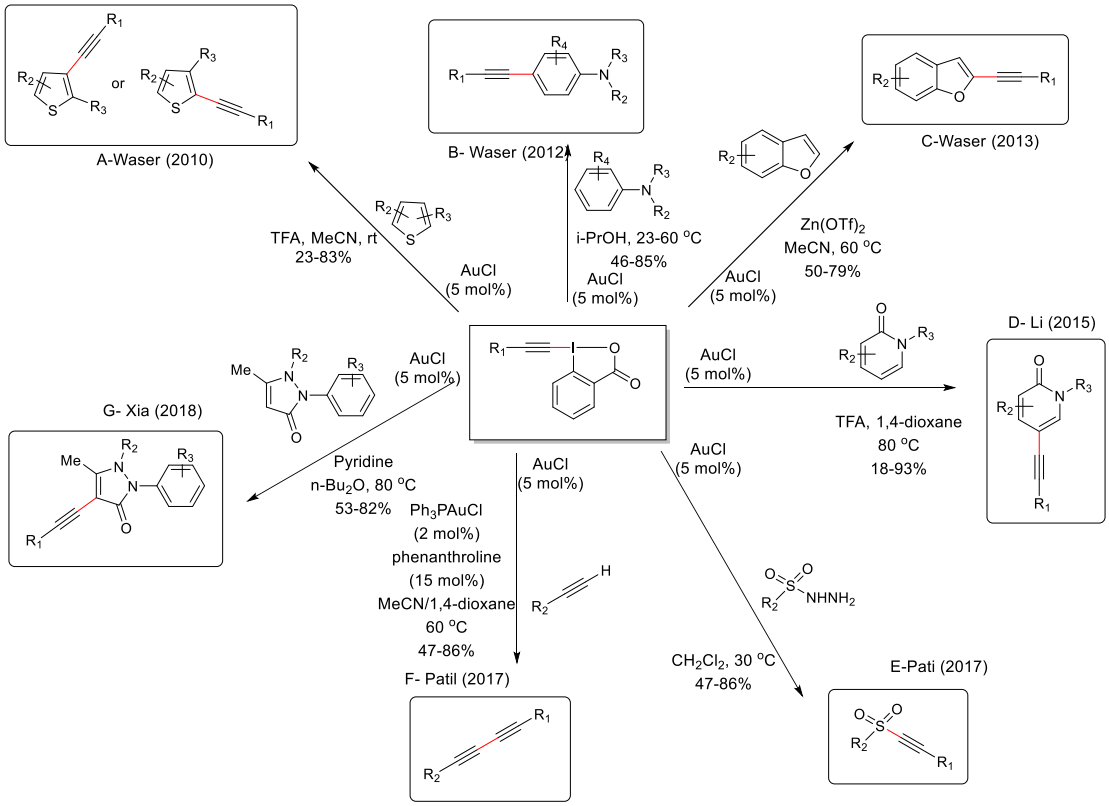


Scheme 1.44 Gold(I)-catalyzed C-H functionalization with TIPS-EBX (Waser 2010, 2012, 2013, Li 2016, Patil 2017, Xia 2018). [49–56]

## 1.4 Bibliography


(1) Dominic Campeau, David F. León Rayo, Ali Mansour, Karim Muratov, and F. G. Gold-Catalyzed Reactions of Specially Activated Alkynes, Allenes, and Alkenes. *Chem. Rev.* **2021**, *121* (14), 8756−8867.

(2) . Zhou, A.-H.; He, Q.; Shu, C.; Yu, Y.-F.; Liu, S.; Zhao, T. .; Zhang, W.; Lu, X.; Ye, L.-W. Atom-Economic Generation of Gold Carbenes: Gold-Catalyzed Formal [3 + 2] Cycloaddition Between Ynamides and Isoxazoles. *Chem. Sci.* **2015**, *6*, 1265−1271.

(3) Jin, H.; Huang, L.; Xie, J.; Rudolph, M.; Rominger, F. . H.; K., A. S. Gold-Catalyzed C-H Annulation of Anthranils with Alkynes: A Facile, Flexible, and Atom-Economical Synthesis of Unprotected 7- Acylindoles. *Angew. Chem., Int. Ed.* **2016**, *55* (2), 794–797.

(4) Jeanbourquin, L. N.; Scopelliti, R.; Fadaei-Tirani, F.; Severin, K. Gold-Catalyzed Synthesis of 1,3-Diaminopyrazoles from 1-Alkynyltriazenes and Imines. *Helv. Chim. Acta* **2017**, *100* (10), e1700186.

(5) Chen, Z.; Huang, J.; Wang, Z. Transition-Metal-Catalyzed Hydrosulfoximination and Oxidation Reaction for the Synthesis of Sulfoximine Derivatives. *J. Org. Chem.* **2016**, *81* (19), 9308−9314.

(6) Davies, P. W.; Cremonesi, A.; Martin, N. Site-Specific Introduction of Gold-Carbenoids by Intermolecular Oxidation of Ynamides or Ynol Ethers. *Chem. Commun.* **2011**, *47*, 379−381.

(7) Laroche, C.; Kerwin, S. M. Efficient, Regioselective Access to Bicyclic

Imidazo[1,2-x]- Heterocycles via Gold- and Base-Promoted Cyclization of 1-Alkynylimidazoles. *J. Org. Chem.* **2009**, *74* (23), 9229− 9232.

(8) Kramer, S.; Madsen, J. L. H.; Rottländer, M.; Skrydstrup, T. Access to 2,5-Diamidopyrroles and 2,5-Diamidofurans by Au(I)- Catalyzed Double Hydroamination or Hydration of 1,3-Diynes. *Org. Lett.* **2010**, *12* (12), 2758−2761.

(9) Karad, S. N.; Bhunia, S.; Liu, R.-S. Retention of Stereochemistry in Gold-Catalyzed Formal [4 + 3] Cycloaddition of Epoxides with Arenynamides. *Angew. Chem., Int. Ed.* **2012**, *51* (35), 8722− 8726.

(10) Liu, C.; Sun, Z.; Xie, F.; Liang, G.; Yang, L.; Li, Y.; Cheng, M. .; Lin, B.; Liu, Y. Gold(I)-Catalyzed Pathway-Switchable Tandem Cycloisomerizations to Indolizino[8,7-b] Indole and Indolo[2,3-a] Quinolizine Derivatives. *Chem. Commun.* **2019**, *55*, 14418−14421.

(11) Liu, J.; Chakraborty, P.; Zhang, H.; Zhong, L.; Wang, Z.-X. .; Huang, X. Gold-Catalyzed Atom-Economic Synthesis of Sulfone- Containing Pyrrolo[2,1-a]Isoquinolines from Diynamides: Evidence for Consecutive Sulfonyl Migration. *ACS Catal.* **2019**, *9* (3), 2610−2617.

(12) Zhao, Q.; Gagosz, F. Synthesis of Allenamides and Structurally Related Compounds by a Gold-Catalyzed Hydride Shift Process. *Adv. Synth. Catal.* **2017**, *359* (18), 3108–3113.

(13) Zeiler, A.; Ziegler, M. J.; Rudolph, M.; Rominger, F. . H.; K., A. S. Scope and Limitations of the Intermolecular Furan-Yne Cyclization. *Adv. Synth. Catal.* **2015**, *357* (7), 1507−1514.

(14) Patil, M. D.; Liu, R. S. Direct Access to Benzofuro[2,3- b]Quinoline and 6H-Chromeno[3,4-b]Quinoline Cores Through Gold-Catalyzed Annulation of Anthranils with Arenoxyethynes and Aryl Propargyl Ethers. *Org. Biomol. Chem.* **2019**, *17*, 4452−4455.

(15) Krause, N.; Winter, C. Gold-Catalyzed Nucleophilic Cyclization of Functionalized Allenes: A Powerful Access to Carboand Heterocycles. *Chem. Rev.* **2011**, *111* (3), 1994−2009.

(16) Huang, X.; Zhang, L. AuCl-Catalyzed Synthesis of Benzyl- Protected Substituted Phenols: A Formal [3 + 3] Approach. *Org. Lett.* **2007**, *9* (22), 4627−4630.

(17) Pirovano, V.; Decataldo, L.; Rossi, E.; Vicente, R. Gold- Catalyzed Synthesis of Tetrahydrocarbazole Derivatives through an Intermolecular Cycloaddition of Vinyl Indoles and N-Allenamides. *Chem. Commun.* **2013**, *49*, 3594−3596.

(18) Hyland, C. J. T.; Hegedus, L. S. Gold-Catalyzed and NIodosuccinimide-Mediated Cyclization of γ-Substituted Allenamides. *J. Org. Chem.* **2006**, *71* (22), 8658−8660.

(19) Kondoh, A.; Iino, A.; Ishikawa, S.; Aoki, T.; Terada, M. Efficient Synthesis of Polysubstituted Pyrroles Based on [3 + 2] Cycloaddition Strategy Utilizing [1,2]-Phospha-Brook Rearrangement under Brønsted Base Catalysis. *Chem. - Eur. J.* **2018**, *24* (57), 15246−15253.

(20) Alonso, J. M.; Muñoz, M. P. Platinum and Gold Catalysis: Àla Carte Hydroamination of Terminal Activated Allenes with Azoles. *Org. Lett.* **2019**, *21* (18), 7639−7644.

(21) Lee, Y. T.; Kang, Y. K.; Chung, Y. K. Au(I)-Catalyzed Cycloisomerization Reaction of Amide- or Ester-Tethered 1,6-Enynes to Bicyclo[3.2.0]Hept-6-En-2-Ones. *J. Org. Chem.* **2009**, *74* (20), 7922− 7934.

(22) Yeom, H.-S.; Koo, J.; Park, H.-S.; Wang, Y.; Liang, Y.; Yu, Z.-; X.; Shin, S.

Gold-Catalyzed Intermolecular Reactions of Propiolic Acids with Alkenes: [4 + 2] Annulation and Enyne Cross Metathesis. *J. Am. Chem. Soc.* **2012**, *134* (1), 208−211.

(23) Luo, T.; Dai, M.; Zheng, S.-L.; Schreiber, S. L. Syntheses of α- Pyrones Using Gold-Catalyzed Coupling Reactions. *Org. Lett.* **2011**, *13* (11), 2834−2836.

(24) Luo, T.; Schreiber, S. L. Complex α-Pyrones Synthesized by a Gold-Catalyzed Coupling Reaction. *Angew. Chem., Int. Ed.* **2007**, *46* (43), 8250−8253.

(25) Luo, T.; Schreiber, S. L. Gold(I)-Catalyzed Coupling Reactions for the Synthesis of Diverse Small Molecules Using the Build/Couple/Pair Strategy. *J. Am. Chem. Soc.* **2009**, *131* (15), 5667−5674.

(26) Peshkov, A. A.; Nechaev, A. A.; Pereshivko, O. P.; Goeman, J.; L.; Van der Eycken, J.; Peshkov, V. A.; Van der Eycken, E. V. Gold and Silver-Catalyzed 7-Endo-Dig Cyclizations for the Synthesis of Oxazepines. *Eur. J. Org. Chem.* **2015**, *19*, 4190−4197.

(27) Diéguez-Vázquez, A.; Tzschucke, C. C.; Crecente-Campo, J. .; McGrath, S.; Ley, S. V. AuCl3-Catalyzed Hydroalkoxylation of Conjugated Alkynoates: Synthesis of Five- and Six-Membered Cyclic Acetals. *Eur. J. Org. Chem.* **2009**, *2009* (11), 1698−1706.

(28) Qian, D.; Zhang, J. Catalytic Oxidation/C−H Functionalization of N-Arylpropiolamides by Means of Gold Carbenoids: Concise Route to 3-Acyloxindoles. *Chem. Commun.* **2012**, *48*, 7082−7084.

(29) Wang, S.; Chen, H.; Zhao, H.; Cao, H.; Li, Y.; Liu, Q. Gold- Catalyzed Multicomponent Reaction: Facile Strategy for the Synthesis of N-Substituted 1,4-Dihydropyridines by Using Activated Alkynes, Aldehydes, and Methanamine. *Eur. J. Org. Chem.* **2013**, 7300− 7304.

(30) Cai, S.; Zeng, J.; Bai, Y.; Liu, X.-W. Access to Quinolines through Gold-Catalyzed Intermolecular Cycloaddition of 2-Aminoaryl Carbonyls and Internal Alkynes. *J. Org. Chem.* **2012**, *77* (1), 801−807.

(31) Hashmi, A. S. K.; Schwarz, L.; Choi, J.-H.; Frost, T. M. A New Gold-Catalyzed C−C Bond Formation. *Angew. Chem., Int. Ed.* **2000**, *39* (13), 2285−2288.

(32) Ran Fang, L. Y. and Y. W. A DFT Study on the Mechanism of Gold(Iii)-Catalyzed Synthesis of Highly Substituted Furansvia [3, 3]-Sigmatropic Rearrangements and/or [1, 2]-Acyloxy Migration Based on Propargyl Ketones. *Org. Biomol. Chem.* **2011**, *9*, 2760–2770.

(33) Lizi Yang, Ran Fang, Y. W. On the Mechanism of AuCl3-Catalyzed Synthesis of Highly Substituted Furans from 2-(1-Alkynyl)-2-Alken-1-Ones with Nucleophiles: A DFT Study. *Comput. Theor. Chem.* **2011**, *965* (1), 180–185.

(34) Jinsheng Zhang, Wei Shen, Longqin Li, and M. L. Gold(I)-Catalyzed Cycloaddition of 1-(1-Alkynyl)Cyclopropyl Ketones with Nucleophiles To Yield Substituted Furans: A DFT Study. *Organometallics* **2009**, *28* (11), 3129–3139.

(35) Li, Y.; Brand, J. P.; Waser, J. Gold-Catalyzed Regioselective Synthesis of 2- and 3-Alkynyl Furans. *Angew. Chem., Int. Ed.* **2013**, *52* (26), 6743−6747.

(36) Ghari, H.; Li, Y.; Roohzadeh, R.; Caramenti, P.; Waser, J. .; Ariafard, A. Gold-Catalyzed Domino Cyclization-Alkynylation Reactions with EBX Reagents: New Insights into the Reaction Mechanism. *Dalt. Trans.* **2017**, *46*, 12257−12262.

(37) Liu, L.-P.; Hammond, G. B. Reactions of Cationic Gold(I) with Allenoates: Synthesis of Stable Organogold(I) Complexes and Mechanistic Investigations

on Gold-Catalyzed Cyclizations. *Chem. - Asian J.* **2009**, *4* (8), 1230−1236.
(38) Liu, L.-P.; Xu, B.; Mashuta, M. S.; Hammond, G. B. Synthesis and Structural Characterization of Stable Organogold(I) Compounds. Evidence for the Mechanism of Gold-Catalyzed Cyclizations. *J. Am. Chem. Soc.* **2008**, *130* (52), 17642−17643.
(39) Hashmi, A. S. K.; Ramamurthi, T. D.; Todd, M. H.; Tsang, A.; S. K.; Graf, K. Gold-Catalysis: Reactions of Organogold Compounds with Electrophiles. *Aust. J. Chem.* **2010**, *63* (12), 1619−1626.
(40) Hashmi, A. S. K.; Molinari, L. Effective Transmetalation from Gold to Iron or Ruthenium. *Organometallics* **2011**, *30* (13), 3457−3460.
(41) Hashmi, A. S. K.; Lothschütz, C.; Döpp, R.; Rudolph, M. .; Ramamurthi, T. D.; Rominger, F. Gold and Palladium Combined for Cross-Coupling. *Angew. Chem., Int. Ed.* **2009**, *48* (44), 8243−8246.
(42) Hashmi, A. S. K.; Döpp, R.; Lothschütz, C.; Rudolph, M. .; Riedel, D.; Rominger, F. Scope and Limitations of Palladium- Catalyzed Cross-Coupling Reactions with Organogold Compounds. *Adv. Synth. Catal.* **2010**, *352* (8), 1307−1314.
(43) Hashmi, A. S. K.; Lothschütz, C.; Döpp, R.; Ackermann, M. .; De Buck Becker, J.; Rudolph, M.; Scholz, C.; Rominger, F. On Homogeneous Gold/Palladium Catalytic Systems. *Adv. Synth. Catal.* **2012**, *354* (1), 133−147.
(44) Tap, A.; Blond, A.; Wakchaure, V. N.; List, B. Chiral Allenes via Alkynylogous Mukaiyama Aldol Reaction. *Angew. Chem., Int. Ed.* **2016**, *55*, 8962−8965.
(45) Selig, P.; Turočkin, A.; Raven, W. Guanidine-Catalyzed γ- Selective Morita−Baylis−Hillman Reactions on α,γ-Dialkyl-Allenoates: Access to Densely Substituted Heterocycles. *Synlett* **2013**, *24* (19), 2535−2539.
(46) Lu, Z.; Han, J.; Hammond, G. B.; Xu, B. Revisiting the Influence of Silver in Cationic Gold Catalysis: A Practical Guide. *Org. Lett.* **2015**, *17* (18), 4534−4537.
(47) Kondoh, A.; Ozawa, R.; Terada, M. Synthesis of Trisubstituted Allenamides Utilizing 1,2-Rearrangement of Dialkoxyphosphoryl Moiety under Brønsted Base Catalysis. *Chem. Lett.* **2019**, *48*, 1164−1167.
(48) Liu, K.; Zhu, C.; Min, J.; Peng, S.; Xu, G.; Sun, J. Stereodivergent Synthesis of N-Heterocycles by Catalyst-Controlled, Activity-Directed Tandem Annulation of Diazo Compounds with Amino Alkynes. *Angew. Chem., Int. Ed.* **2015**, *54* (44), 12962−12967.
(49) Brand, J. P.; Waser, J. Direct Alkynylation of Thiophenes: Cooperative Activation of TIPS-EBX with Gold and Bronsted Acids. *Angew. Chem., Int. Ed.* **2010**, *49* (40), 7304−7307.
(50) Brand, J. P.; Chevalley, C.; Scopelliti, R.; Waser, J. Ethynyl Benziodoxolones for the Direct Alkynylation of Heterocycles: Structural Requirement, Improved Procedure for Pyrroles, and Insights into the Mechanism. *Chem. - Eur. J.* **2012**, *18*, 5655−5666.
(51) Brand, J. P.; Waser, J. Para-Selective Gold-Catalyzed Direct Alkynylation of Anilines. *Org. Lett.* **2012**, *14* (3), 744−747.
(52) Li, Y.; Waser, J. Zinc-Gold Cooperative Catalysis for the Direct Alkynylation of Benzofurans. *Beilstein J. Org. Chem.* **2013**, *9*, 1763−1767.
(53) Li, Y.; Xie, F.; Li, X. Formal Gold- and Rhodium-Catalyzed Regiodivergent C-H Alkynylation of 2-Pyridones. *J. Org. Chem.* **2016**, *81* (2), 715−722.
(54) Shinde, P. S.; Patil, N. T. Gold-Catalyzed Dehydrazinative C(Sp)-S Coupling

Reactions of Arylsulfonyl Hydrazides with Ethynylbenziodoxolones for Accessing Alkynyl Sulfones. *Eur. J. Org. Chem.* **2017**, *2017* (24), 3512−3515.

(55) Banerjee, S.; Patil, N. T. Exploiting the Dual Role of Ethynylbenziodoxolones in Gold-Catalyzed C(Sp)-C(Sp) Cross- Coupling Reactions. *Chem. Commun.* **2017**, *53*, 7937−7940.

(56) Wang, X.; Li, X.; Zhang, Y.; Xia, L. Gold(I)- and Rhodium(III)-Catalyzed Formal Regiodivergent C-H Alkynylation of 1-Arylpyrazolones. *Org. Biomol. Chem.* **2018**, *16*, 2860−2864.

# Chapter 2

## Gold–carbene or –π-alkene or –π-alkyne complexes in gold (I) or (III) oxidation form in catalysis

### 2.1 Gold-carbon bond in gold(I)- and gold(III)-carbene complexes

Year after year, the number of publications on the homogenous gold catalysis increases. [1–5] Different types of gold catalysts are invented. Both oxidation states of gold, gold(I) and gold(III) are catalytically active. As regards the case of gold(III) many uncertainties exist regarding the structure and the oxidation state of actual catalytic species. [2,6] For example, experimental data have showed the reduction of gold(III) to gold(I) during catalytic cycle. [6] In some cases, more suspicious for catalytic activity remains gold(I) than gold(III), [6] while in other cases the opposite. [7] In the case of gold(I), other species that are present in the reaction mixture with catalyst, like counterions can interfere to the mechanism [8] of the reaction or finally the cofactors can provide the hidden catalyst. [9]

Comparing the electron distribution, gold(I) behaves like a main group element while gold(III) displays all of the characteristics of a transition metal. Thus, gold(I) forms linear, two-coordinate complexes because of the filled 5d-shell, while gold(III) adopts almost exclusively the square-planar coordination geometry because of the $d^8$ electron distribution. Moreover, the intensive relativistic effects on gold(I) that are diminished on gold(III), contract the bonds' length of the gold(I) complexes. The experimental proof is the comparison of bond length metal-ligand of the pairs Ag(I)/Au(I) pair versus Ag(III)/Au(III). The relativistic Au-L bond length contraction is much diminished for gold(III) so as Ag(III) and Au(III) have closely similar covalent radii. [10,11] The covalent radius of Au(III) bonded to alkyl or aryl ligands is about 1.27 – 1.30 Å, while the ionic radius is taken as 0.85 Å, which enables accommodation in the plane of porphyrins. [12]

Additionally, gold(I) shows a tendency to form multi-metallic aggregations, even with other gold(I) ions, a phenomenon known as aurophilicity. [2, 13]

Many experimental data on catalysed reactions by both oxidation states of gold exist where in many cases the same reactant leads to different products depending on oxidation state of the gold. The divergent catalysis between gold(I) and gold(III) and the mechanistic explanation is a topic of interest. [13,14] According to the suggested mechanisms on gold-catalysed reactions, carbene transfer reactions are very common. Regarding this, we intent to compare the stability and the traits of carbenes formed by gold(I) and gold(III). The bonding in these $AuL^+$ species is resulted (a) from the lone pair of the carbon ligand forming a strong σ bond with an orbital of appropriate symmetry of gold to form a carbocation like structure (b) from the π-back donation of the metal d-orbital to an empty p-orbital of carbon to form a singlet carbene like structure. Thus, the stabilization of the carbene-like structure is related to the π-backdonation from gold(I). [15,16,5] Consequently, in a gold carbene intermediate, the σ- and π-bonding ranges from a gold stabilized singlet carbene to a gold-coordinated carbocation depending the substituents in the carbene as is described in Scheme 2.1. Thus, the ancillary ligand has a critical role on the stability of the carbene regulating the reactivity profile of the catalyst via the control on the π-backbonding. Strongly σ-donating and weakly π-acidic ligands are expected to improve the carbene-like reactivity. Ligands like N-heterocyclic carbene (NHC) [17,18] or cyclic(alkyl)(amino)carbenes (CAAC) [19] reveal an enhanced σ-donor character of gold-carbon bond . The bulky 1,3-bis(2,6-diisopropylphenyl)imidazol-2-ylidene (IPr) [20,21] represents the most important NHC ligand throughout the field of homogeneous catalysis. The replacement of one of the electronegative amino substituents of NHCs by a strong σ-donor alkyl group makes the CAAC ligands even more electron-rich. [19] In contrast, phosphines which are weak σ-donating and π-acidic ligands enhance the carbocation-like character of the intermediates. [5] Experimental evidence was sought for the transition from the HOMO character in the carbene to the LUMO character in the carbene. The first directs an anti-bonding σ interaction of the fully occupied $sp^2$ orbitals in the singlet carbene with an empty gold(I) 5d orbitals while the latter directs the interaction of the empty p orbital of the carbene with a doubly occupied gold(I) 5d orbital.

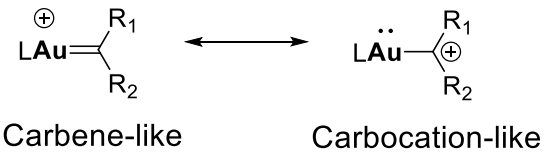


Scheme 2.1. Resonance forms of a gold-carbene complex.

An experimental evidence on the nature of the gold(I)-carbon bond, i.e. a strong Au-C σ bond vs a significant Au=C backbonding, was provided by Straub, [22] in which the gold(I) carbene complex in Scheme 2.2 was synthesized. The strong Au-C σ bond and the significant Au=C back-bonding is consistent with a major impact of relativistic effects on gold′s valence shell, that is, higher energy for gold′s 5d orbitals and a lower energy for gold′s 6s orbitals. This gold(I)–carbene complex, with the IPr as NHC ligand, was the first metal complex without heteroatom donor substituents linked to the metal and with high carbenoid (Au=C) character, in contrast to other complexes with predominant ammonium ylide or oxonium ylide ligand character.

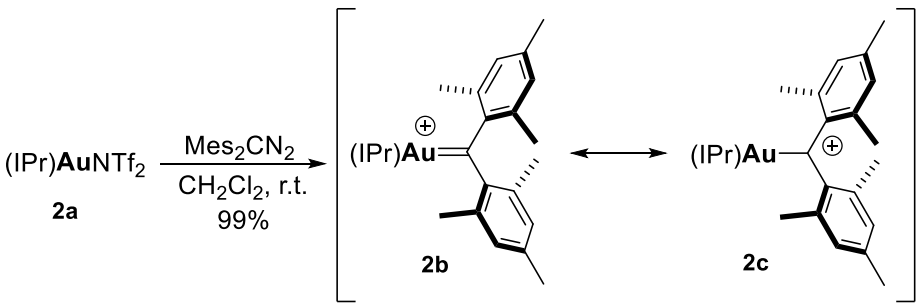


Scheme 2.2. Synthesis of the first gold carbene derivative without heteroatom donor substituents connected with the metal (Straub 2015). [22]

On the contrary, a gold(III)–carbene has not only different reactivity compared with a gold(I)–carbene, but also is synthesized differently as depicted in Scheme 2.3. [23,24] According to DFT calculations on the gold(III)–carbene complex in Scheme 2.3, the Au-C bond has a single bond character and the carbene carbon has a nucleophilic character. That is, it can react with electrophiles such as $CS_2$ and PhNCS. [23,24]

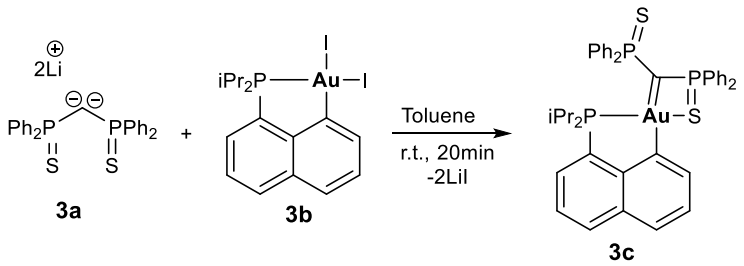


Scheme 2.3. Synthesis of a gold(III)-carbene derivative(Mézailles 2006- Bourissou 2017). [23,24]

## 2.2 Gold(I)– and gold(III)–π-alkene and –π-alkyne complexes

Gold activates π-bonds either in the form of gold(I) or gold(III). The ability of gold(I) to activate alkenes was demonstrated with the isolation of gold(I)-alkene complexes. IPrAu(I) pre-catalyst forms complexes with alkenes like norbornadiene and styrene have been isolated and characterized. [25,26] Afterwards, many alkyl phosphine–gold(I)–π-alkene complexes were synthesized, composed by various alkenes (Scheme 2.4). [25,26,27,28] Shortly after the first gold(III)–π-alkene complexes were synthesized (Scheme 2.4). [29,30,31] However, on the contrary to gold(I) complexes, the gold(III)-π-alkene complexes were not such stable and abundant. For some of them, the efforts to be crystallized were proved to be successful, e.g. for Tilset's complex [29] (Scheme 2.4), both X-rays and calculations revealed a weak metal d→π*(C=C) backbonding but significant enough to stabilize the Au(III) bis(alkene) complex. More recently, the isolation and characterization of the Bourissou's complex [31] (Scheme 2.4) confirmed previous mechanistic proposals for its existence in various works where that complex was formed. [5,29–32]

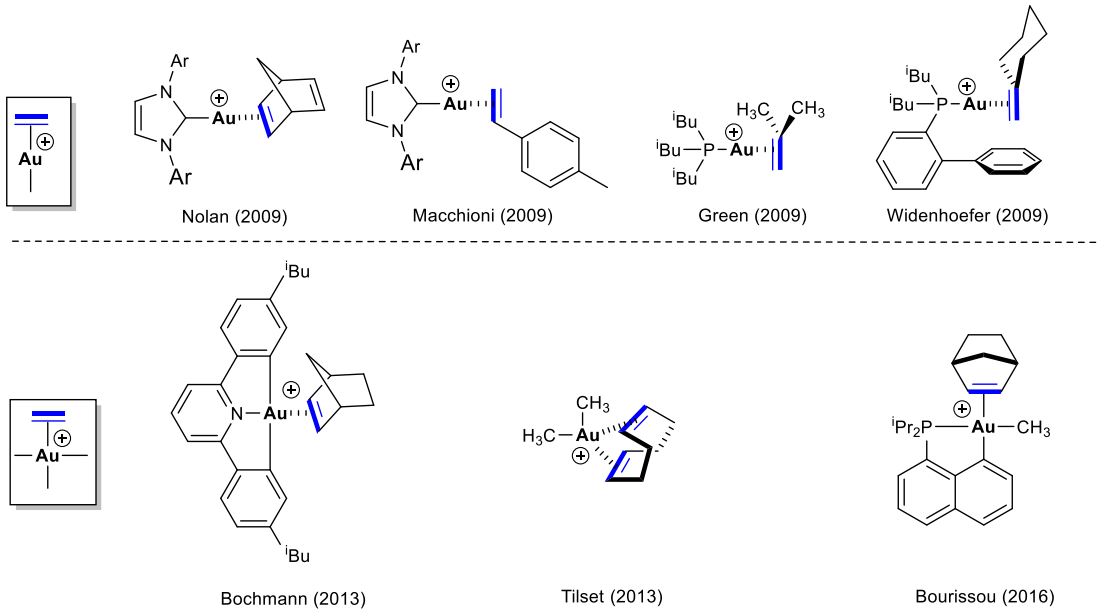


Scheme 2.4. Gold(I) [25,26,27,28] – and gold(III) [30,29,31] –π-alkene complexes.

Alkynes form with gold(I) also π-complexes similarly to alkenes. Not only stable NHC-gold(I) complexes with alkynes are formed but also phosphine-type ligands with gold(I). Some of the stable π-alkyne–gold(I) complexes structures are depicted at Scheme 2.5. [33–36]

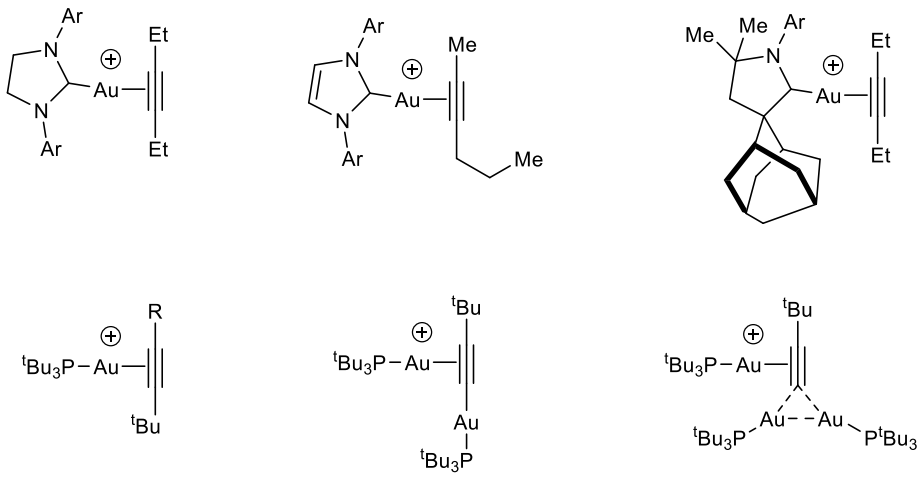

Scheme 2.5. Cationic gold(I)–π-alkyne complexes containing either a NHC-ligand [33,34] or an alkyl phosphine ligand. [35,36]

Comparison of the activation of alkynes by gold(I) and gold(III) led to the conclusion that back-donation is very weak in gold(III) complexes. Since the stability of a gold(III)-π-alkyne complex depends on π-donation from the triple bond, due to the reduced back-bonding capacity of gold(III), one of the alkyne-C atoms is charged positive, so as it renders more susceptible to nucleophilic attack. The resulting polarization of the C≡C bond is much larger for gold(III) than for gold(I) alkyne complexes. [37,38] Thus, the attempts for the isolation of similar to gold(I)-π-alkyne complexes (Scheme 2.5) were unsuccessful since gold(III) can't form a stable complex and is reduced to gold(I) or gold(0) spontaneously. Synthesis of gold(III) alkyne complexes succeeded with the use of C^N and C^C donor ligands as depicted in Scheme 2.6. [37,39]

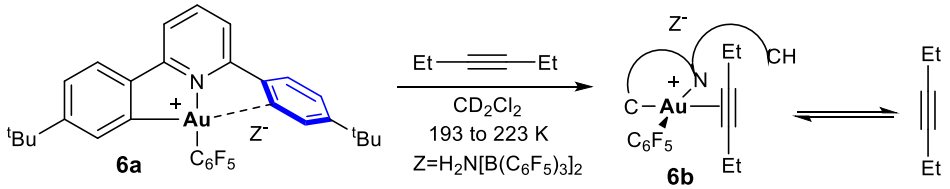


Scheme 2.6. Generation of a C^N chelated alkyne complex (Rocchigiani, 2017,2018). [37,39]

## 2.3 Divergent catalysis for gold(I) and gold(III) catalysts

Cycloisomerization of indole–tethered alkynes is example of a gold-catalyzed regiodivergent reaction. [40] The transformation proceeds on a first step with the triple bond activation either by gold(I) or gold(III) catalyst. However, gold(I) JohnPhosAu(MeCN)$SbF_6$ catalyst, favours the 6-exo-dig cyclization while gold(III) $AuCl_3$ catalyst favours the 7-endo-dig cyclization via a nucleophilic attack by indole C3 in both cases (Scheme 2.7). The spiro intermediates **7b**/**7d** undergo a 1,2-alkyl shift followed by a re-aromatization and protodeauration step, forming the azepino[4,5-b]indole **7c** derivatives and the eight-member ring derivative **7e**, respectively [40] (Scheme 2.7).

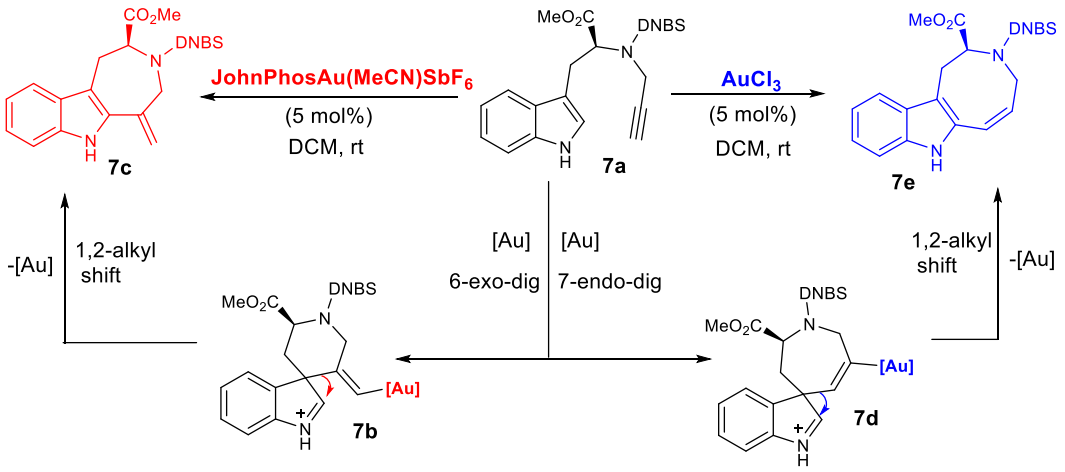


Scheme 2.7. Regiodivergent cycloisomerization of alkyne-tethered indoles (Echavarren 2006). [40]

Cycloisomerization of allenic hydroxylamines is another divergent catalytic reaction, in which the choice of catalyst gold(I) or gold(III) urge the reaction to the formation of a five member or six member ring, respectively. [41] Phosphine ligand–gold(I) catalysts promote the 5-endo-dig cyclization to form dihydroisoxazoles **8b** while the 6-endo-trig cyclization is favoured by the use of $AuCl_3$ catalyst to furnish 3,6-dihydro-1,2-oxazine **8c** as the major product. [41] The alternative pathways of the divergent catalysis were investigated by DFT calculations. [42]

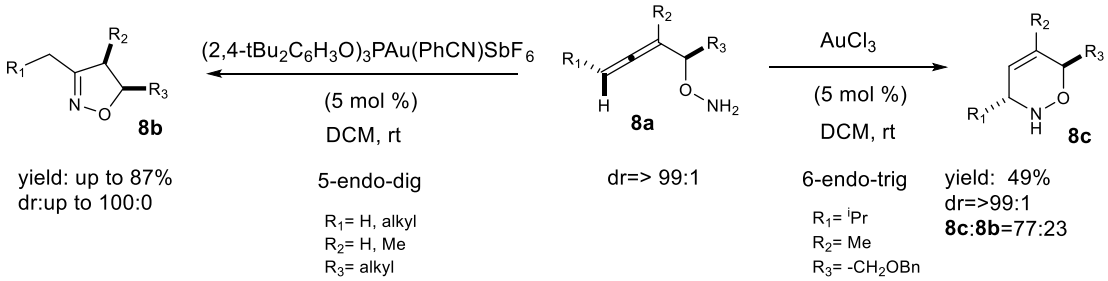


Scheme 2.8. Divergent catalysis in the cycloisomerization of allenic hydroxylamine ethers with gold(I) or gold(III) complexes (Krause 2009). [41]

Gold–catalyzed cycloisomerization of 1,6-diyne esters **9a** can lead either to 1H-cyclopenta[b]naphthalene **9b** after treatment with $IPrAu(PhCN)SbF_6$ catalyst or to cyclopentenyl diketone **9c** after treatment with $PicAuCl_2$ catalyst; [43] possibly due to the different Lewis acidity between gold(I) and gold(III) catalysts (Scheme 2.9).

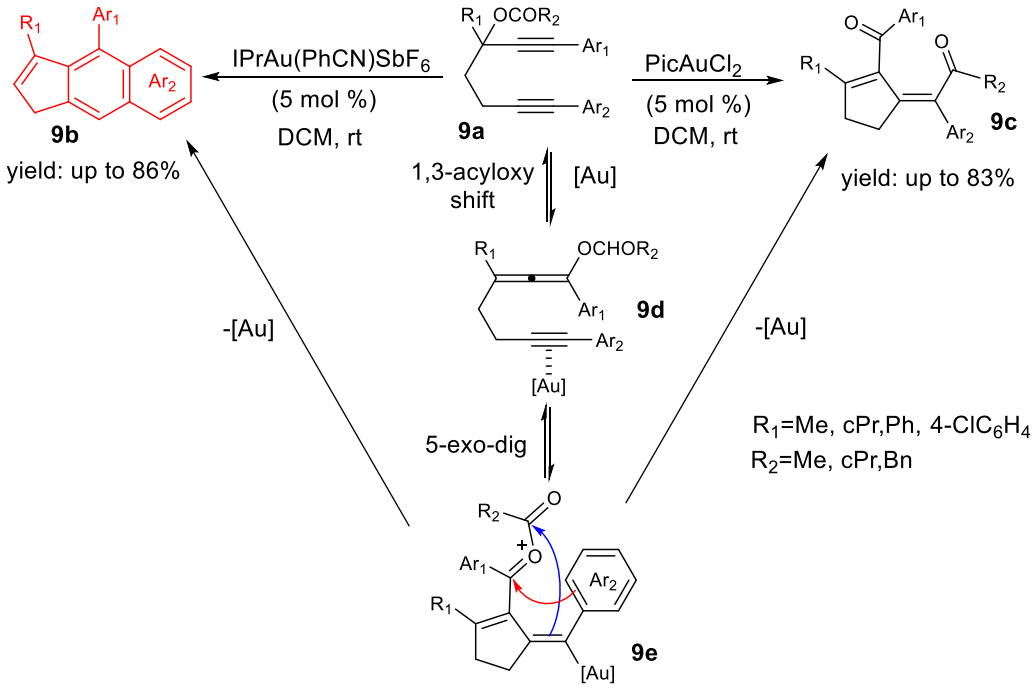


Scheme 2.9. Divergent cycloisomerization of 1,6-diyne esters (Chan 2014). [43]

According to the proposed mechanism supported by DFT calculations, [44] the gold-activated alkyne **9a** undergoes a 1,3-acyloxy shift to **9d** which after a 5-exo-dig cyclization furnishes the intermediate **9e**. From that point divergent catalysis begins. Gold(I) catalyst urges the intermediate to an intramolecular Friedel-Crafts cyclization [44] to furnish 1H-cyclopenta[b]naphthalene **9b** [43,44] while gold(III) catalyst induces a 1,5-acyloxy shift [44], producing the cis-cyclopenten-2-yl δ-diketone **9c** without by-products. [43,44]

In Scheme 2.10 both gold(I) and gold(III) catalysts bear NHC ligands and the same counterions. Starting from ketene acetal **10a** and cinnamaldehyde **10b**, the NHC-gold(I) catalyst IPrAuCl **10e**, which **is** activated by AgOTf, promotes the formation of Mukaiyama aldol product **10c** by a 1,2-addition. In contrast gold(III) complex **10f** leads to the products of 1,4-addition **10d**, in a Mukaiyama-Michael reaction. [45]

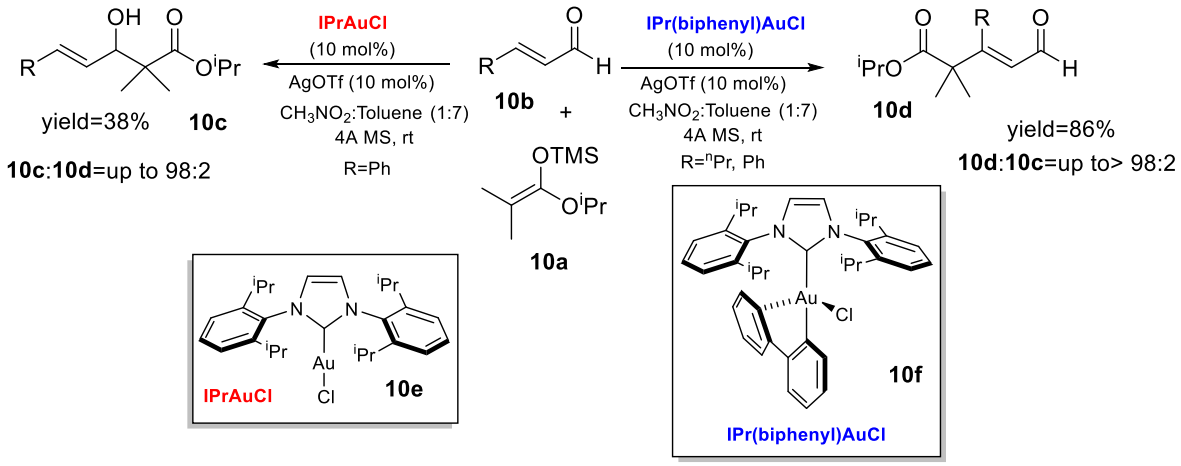


Scheme 2.10. Different reactivity with NHC gold(I) and gold(III) catalysts for the reaction between a cinnamaldehyde and a ketene acetal (Toste 2015). [45]

## 2.4 Bibliography


(1) Mato, M.; Franchino, A.; García-Morales, C.; Echavarren, A. M. Gold-Catalyzed Synthesis of Small Rings. *Chem. Rev.* **2021**, *121* (14), 8613–8684. https://doi.org/10.1021/acs.chemrev.0c00697.

(2) Rocchigiani, L.; Bochmann, M. Recent Advances in Gold(III) Chemistry: Structure, Bonding, Reactivity, and Role in Homogeneous Catalysis. *Chem. Rev.* **2021**. https://doi.org/10.1021/acs.chemrev.0c00552.

(3) Dominic Campeau, David F. León Rayo, Ali Mansour, Karim Muratov, and F. G. Gold-Catalyzed Reactions of Specially Activated Alkynes, Allenes, and Alkenes. *Chem. Rev.* **2021**, *121* (14), 8756–8867.

(4) Reyes, R. L.; Iwai, T.; Sawamura, M. Construction of Medium-Sized Rings by Gold Catalysis. *Chem. Rev.* **2021**, *121* (14), 8926–8947. https://doi.org/10.1021/acs.chemrev.0c00793.

(5) Gimeno, R. P. H. and M. C. Main Avenues in Gold Coordination Chemistry. *Chem. Rev.* **2021**, *121* (14), 8311–8363. https://doi.org/10.1021/acs.chemrev.0c00930.

(6) Caiyun Zhang, Gendi Wang, Licheng Zhan, Xueyan Yang, Jiwei Wang, Yin Wei, Sheng Xu*, Min Shi, and J. Z. Gold(I) or Gold(III) as Real Intermediate Species in Gold-Catalyzed Cycloaddition Reactions of Enynal/Enynone? *ACS Catal.* **2020**, *10* (12), 6682–6690.

(7) Marta Castiñeira Reis, Marta Marín-Luna, Nenad Janković, Olalla Nieto Faza, C. S. L. Au(III) Catalyzes the Cross-Coupling between Activated Methylenes and Alkene Derivatives. *J. Catal.* **2020**, *392*, 159–164.

(8) Lu, Z.; Li, T.; Mudshinge, S. R.; Xu, B.; Hammond, G. B. Optimization of Catalysts and Conditions in Gold(I) Catalysis - Counterion and Additive Effects. *Chem. Rev.* **2021**, *121* (14), 8452–8477. https://doi.org/10.1021/acs.chemrev.0c00713.

(9) Tuan Thanh Dang, Florian Boeck, and L. H. Hidden Brønsted Acid Catalysis: Pathways of Accidental or Deliberate Generation of Triflic Acid from Metal Triflates. *J. Org. Chem.* **2011**, *76* (22), 9353–9361. https://doi.org/10.1021/jo201631x.

(10) Pérez-Bitrián, A.; Baya, M.; Casas, J. M.; Martín, A.; Menjón, B.; Orduna, J. An Organogold(III) Difluoride with a Trans Arrangement. *Angew. Chemie - Int. Ed.* **2018**. https://doi.org/10.1002/anie.201802379.

(11) Schwerdtfeger, P.; Boyd, P. D. W.; Brienne, S.; Burrell, A. K. Relativistic Effects in Gold Chemistry. 4. Gold(III) and Gold(V) Compounds. *Inorg. Chem.* **1992**. https://doi.org/10.1021/ic00042a016.

(12) Harrach, G.; Valicsek, Z.; Horváth, O. Water-Soluble Silver(II) and Gold(III) Porphyrins: The Effect of Structural Distortion on the Photophysical and Photochemical Behavior. *Inorg. Chem. Commun.* **2011**. https://doi.org/10.1016/j.inoche.2011.08.003.

(13) Faza, O.N., López, C. S. Computational Approaches to Homogeneous Gold Catalysis. In *Homogeneous Gold Catalysis. Topics in Current Chemistry*; Springer, 2014; pp 213–285. https://doi.org/https://doi.org/10.1007/128_2014_591.

(14) Faza, O.N., Rodríguez, R.Á. & López, C. S. Performance of Density Functional Theory on Homogeneous Gold Catalysis. *Theor Chem Acc* **2011**, *128*, 647–661.

(15) Benitez, D.; Shapiro, N. D.; Tkatchouk, E.; Wang, Y.; Goddard, W. A.; Toste, F. D. A Bonding Model for Gold(I) Carbene Complexes. *Nat. Chem.* **2009**. https://doi.org/10.1038/nchem.331.

(16) Echavarren, A. Carbene or Cation? *Nat. Chem* **2009**, *1*, 431–433. https://doi.org/https://doi.org/10.1038/nchem.344.

(17) Littke, A. F.; Fu, G. C. Palladium-Catalyzed Coupling Reactions of Aryl Chlorides. *Angewandte Chemie - International Edition*. 2002. https://doi.org/10.1002/1521-3773(20021115)41:22<4176::AID-ANIE4176>3.0.CO;2-U.

(18) Herrmann, W. A. N-Heterocyclic Carbenes: A New Concept in Organometallic Catalysis. *Angewandte Chemie - International Edition*. 2002. https://doi.org/10.1002/1521-3773(20020415)41:8<1290::AID-ANIE1290>3.0.CO;2-Y.

(19) Lavallo, V.; Canac, Y.; Präsang, C.; Donnadieu, B.; Bertrand, G. Stable Cyclic (Alkyl)(Amino)Carbenes as Rigid or Flexible, Bulky, Electron-Rich Ligands for Transition-Metal Catalysts: A Quaternary Carbon Atom Makes the Difference. *Angew. Chemie - Int. Ed.* **2005**. https://doi.org/10.1002/anie.200501841.

(20) Huang, J.; Stevens, E. D.; Nolan, S. P.; Petersen, J. L. Olefin Metathesis-Active Ruthenium Complexes Bearing a Nucleophilic Carbene Ligand. *J. Am. Chem. Soc.* **1999**. https://doi.org/10.1021/ja9831352.

(21) Arduengo, A. J. Looking for Stable Carbenes: The Difficulty in Starting Anew. *Accounts of Chemical Research*. 1999. https://doi.org/10.1021/ar980126p.

(22) Hussong, M.W., Hoffmeister, W.T., Rominger, F. and Straub, B. F. Copper and Silver Carbene Complexes without Heteroatom-Stabilization: Structure, Spectroscopy, and Relativistic Effects. *Angew. Chem. Int. Ed.* **2015**, *54*, 10331–10335. https://doi.org/https://doi.org/10.1002/anie.201504117.

(23) Thibault Cantat, Louis Ricard, Pascal Le Floch, and N. M. Phosphorus-Stabilized Geminal Dianions. *Organometallics* **2006**, *25* (21), 4965–4976. https://doi.org/10.1021/om060450l.

(24) A. Pujol, M. Lafage, F. Rekhroukh, N. Saffon-Merceron, A. Amgoune, D. Bourissou, N. Nebra, M. Fustier-Boutignon, N. M. A Nucleophilic Gold(III) Carbene Complex. *Angew. Chem. Int. Ed.* **2017**, *56*, 12264.

(25) Pierre de Frémont, Nicolas Marion, Steven P. Nolan. Cationic NHC–Gold(I) Complexes: Synthesis, Isolation, and Catalytic Activity. *J. Organomet. Chem.* **2009**, *694* (4), 551–560. https://doi.org/https://doi.org/10.1016/j.jorganchem.2008.10.047.

(26) Daniele Zuccaccia, Leonardo Belpassi, Francesco Tarantelli, and A. M. Ion Pairing in Cationic Olefin−Gold(I) Complexes. *J. Am. Chem. Soc.* **2009**, *131* (9), 3170–3171.

(27) Thomas N. Hooper, Michael Green, John E. McGrady, J. R. P. and C. A. R. Synthesis and Structural Characterisation of Stable Cationic Gold(i) Alkene Complexes. *Chem. Commun.* **2009**, 3877–3879.

(28) Timothy J. Brown, M. G. D. and R. A. W. Syntheses and X-Ray Crystal Structures of Cationic, Two-Coordinate Gold(i) π-Alkene Complexes That Contain a Sterically Hindered o-Biphenylphosphine Ligand. *Chem. Commun.* **2009**, 6451–6453.

(29) Eirin Langseth, Margaret L. Scheuermann, Dr. David Balcells, Prof. Werner Kaminsky, Prof. Karen I.

Goldberg, Prof. Odile Eisenstein, Dr. Richard H. Heyn, P. M. T. Generation and Structural Characterization of a Gold(III) Alkene Complex. *Angew. Chem. Int. Ed.*, **2013**, *125* (6), 1704–1707.

(30) Dr. Nicky Savjani, Dragoş-Adrian Roşca, Dr. Mark Schormann, P. D. M. B. Gold(III) Olefin Complexes. *Angew. Chem. Int. Ed.*, **2013**, *52*, 874–877. https://doi.org/10.1002/anie.201208356.

(31) Feriel Rekhroukh, Laura Estevez, Christian Bijani, Karinne Miqueu, Abderrahmane Amgoune, and D. B. Coordination–Insertion of Norbornene at Gold: A Mechanistic Study. *Organometallics* **2016**, *35* (7), 995–1001. https://doi.org/10.1021/acs.organomet.6b00040.

(32) David Balcells, Odile Eisenstein, M. T. and A. N. Coordination and Insertion of Alkenes and Alkynes in AuIII Complexes: Nature of the Intermediates from a Computational Perspective. *Dalt. Trans.*, **2016**, *45*, 5504–5513. https://doi.org/10.1039/C5DT05014F.

(33) Jennifer A. Akana, Koyel X. Bhattacharyya, Peter Müller, and J. P. S. Reversible C−F Bond Formation and the Au-Catalyzed Hydrofluorination of Alkynes. *J. Am. Chem. Soc.* **2007**, *129* (25), 7736–7737. https://doi.org/10.1021/ja0723784.

(34) Vincent Lavallo, Guido D. Frey Dr., Bruno Donnadieu, Michele Soleilhavoup Dr., G. B. P. Homogeneous Catalytic Hydroamination of Alkynes and Allenes with Ammonia. *Angew. Chem. Int. Ed.* **2008**, *47*, 5224–5228. https://doi.org/https://doi.org/10.1002/anie.200801136.

(35) Timothy J. Brown, Ross A. Widenhoefer. Synthesis and Equilibrium Binding Studies of Cationic, Two-Coordinate Gold(I) π-Alkyne Complexes. *J. Organomet. Chem.* **2011**, *696* (6), 1216–1220. https://doi.org/https://doi.org/10.1016/j.jorganchem.2010.09.055.

(36) Thomas N. Hooper, M. G. and C. A. R. Cationic Au(i) Alkyne Complexes: Synthesis, Structure and Reactivity. *Chem. Commun.*, **2010**, *46*, 2313–2315. https://doi.org/https://doi.org/10.1039/B923900F.

(37) L. Rocchigiani, J. Fernandez-Cestau, G. Agonigi, I. Chambrier, P. H. M. Budzelaar, M. B. Gold(III) Alkyne Complexes: Bonding and Reaction Pathways. *Angew. Chem. Int. Ed.* **2017**, *56* (44), 13861–13865.

(38) Luca Gregori, Diego Sorbelli, Leonardo Belpassi, Francesco Tarantelli, and P. B. Alkyne Activation with Gold(III) Complexes: A Quantitative Assessment of the Ligand Effect by Charge-Displacement Analysis. *Inorg. Chem.* **2019**, *58* (5), 3115–3129. https://doi.org/10.1021/acs.inorgchem.8b03172.

(39) I. Chambrier, L. Rocchigiani, D. L. Hughes, P. M. H. Budzelaar, M. Bochmann. Thermally Stable Gold(III) Alkene and Alkyne Complexes: Synthesis, Structures, and Assessment of the Trans-Influence on Gold–Ligand Bond Enthalpies. *Chem. Eur. J.* **2018**, *24* (44), 11467–11474. https://doi.org/https://doi.org/10.1002/chem.201802160.

(40) Ferrer, C.; Echavarren, A. M. Gold-Catalyzed Intramolecular Reaction of Indoles with Alkynes: Facile Formation of Eight-Membered Rings and an Unexpected Allenylation. *Angew. Chem., Int. Ed.* **2006**, *45* (7), 1105−1109.

(41) Winter, C. and Krause, N. Structural Diversity through Gold Catalysis: Stereoselective Synthesis of N-Hydroxypyrrolines, Dihydroisoxazoles, and Dihydro-1,2-Oxazines. *Angew. Chem. Int. Ed.* **2009**, *48* (34), 6339–6342. https://doi.org/https://doi.org/10.1002/anie.200902355.

(42) Kiriakidi, S.; Nieto Faza, O.; Kolocouris, A.; López, C. S. Governing Effects in the Mechanism of the Gold-Catalyzed Cycloisomerization of Allenic Hydroxylamine Derivatives. *Org. Biomol. Chem.* **2017**, *15* (28), 5920–5926. https://doi.org/10.1039/c7ob01275f.

(43) Dan Li, Weidong Rao, Guan Liang Tay, Benjamin James Ayers, and P. W. H. C. Gold-Catalyzed Cycloisomerization of 1,6-Diyne Esters to 1H-Cyclopenta[b]Naphthalenes, Cis-Cyclopenten-2-Yl δ-Diketones, and Bicyclo[3.2.0]Hepta-1,5-Dienes. *J. Org. Chem.* **2014**, *79* (23), 11301–11315. https://doi.org/10.1021/jo5020195.

(44) Yunhe Li, Peng-Cheng Tu, Lin Zhou, Alexander M. Kirillov, Ran Fang, and L. Y. How Does the Catalyst Affect the Reaction Pathway? DFT Analysis of the Mechanism and Selectivity in the 1,6-Diyne Ester Cycloisomerization. *Organometallics* **2018**, *37* (2), 261–270.

(45) Chung-Yeh Wu, Takahiro Horibe, C. B. J. & F. D. T. Stable Gold(III) Catalysts by Oxidative Addition of a Carbon–Carbon Bond. *Nature* **2015**, *517*, 449–454. https://doi.org/https://doi.org/10.1038/nature14104.

# Chapter 3

## Traits of gold(I) as catalyst versus other metal catalysts

### 3.1 Differences between the electronic structure of gold and other metals

Gold has remarkable properties that set it apart from other metals. The noble metals are best known for their inert character and resistance to oxidation and chemical attack and have therefore long been regarded as unpromising for catalytic applications. Being the most electronegative of metallic elements (2.54 on the Pauling scale), almost identical to carbon, gold forms highly covalent, hydrolytically stable, Au–C bonds. This is also the reason why the exploration of its organometallic chemistry has so long lagged behind work on other noble metals. [1] This situation has now drastically changed.

Although many transition metals are commonly used as catalysts, gold reveals divergent chemical properties. The unique catalytic properties of gold originate from its electron structure and the relativistic effects that accompany electron distribution. More than any other element gold is subject to relativistic effects. Relativistic effects are present when particles move with velocity close to the velocity of light *c*. Then, the mass of the moving particle, e.g. of an electron, increases. Moreover, the relation between electron mass and electron orbit is inversely proportional. Consequently, due to relativistic effect 1s orbital contracts, and so do all s and p atomic orbitals, reducing atomic radius and increasing ionization energies. [2] However, for most of the elements the contraction of the atomic radius is not as significant as it is for the elements with filled 4f and 5d orbitals. Thus, for the elements like platinum, gold and mercury with electron structure $[Xe]4f^{14}5d^{9}6s^{1}$, $[Xe]4f^{14}5d^{10}6s^{1}$ and $[Xe]4f^{14}5d^{10}6s^{2}$, respectively, relativistic effects have high impact on atomic radius due to contraction of 6s atomic orbital. [3]

In addition, the contraction of s and p atomic orbitals implies a better shielding for the electrons of d and f orbitals. So, the nuclear attraction on the electrons of d and f orbitals is decreased. Consequently, the d and f orbitals expand while s and p orbitals contract. In the case of gold with electron structure $[Xe]4f^{14}5d^{10}6s^{1}$, 6s orbital contraction and 5d orbital expansion explain its catalytic properties.

The position of gold in the Periodic Table is unique and gold exists as catalyst both in gold(I) or gold(III) forms. In the oxidation state I, with a filled d shell, gold behaves rather like a main group element and forms linear, two-coordinate complexes which show a marked reluctance to interact with donor ligands perpendicular to the molecular axis. Gold in the oxidation state III, on the other hand, displays all the characteristics of a transition metal, adopts almost exclusively the square-planar coordination geometry that is so familiar from other heavy metal cations with $d^8$ electronic structure and is distinctly different in terms of structure and reactivity from gold(I) compounds.

Catalytic activity of gold(I) is related with its Lewis acidity. The contraction of valence s and p orbitals of gold(I) affect LUMO energy that decreases rendering gold a stronger Lewis acid with higher electronegativity compared with copper or silver.

Gold(I) catalyst is abundant either as inorganic gold (AuCl) or in complex with organic ligands. The ligand of gold controls its Lewis acidity. The contraction of 6s orbital strengthens the Au-ligand bond. [4] According to NBO (natural bond orbital) [5] calculations, a comparative study between gold(I) and silver(I) with phosphine ligand revealed that the covalent character of the bond is stronger in Au(I) complex. [6,7] Consequently, according to HSAB concept ("hard and soft (Lewis) acids and bases"), [8,9] Au(I) catalysts are soft acids due to its extended radius and diffused charge and form bonds with more covalent character. Thus, these catalysts prefer reacting with soft bases like π-systems, e.g alkynes, alkenes, allenes, and “soft” atoms like P and S. Whereas gold(I) species [LAu]+ are known as a carbophilic electrophiles and bind preferentially also to “soft” bases, gold(III) is a “hard” Lewis acid. This is reflected in the stability of their OH and F compounds: whereas the first isolable gold(I) hydroxide and fluoride complexes LAuX (X = OH, F; L = N-heterocyclic carbene NHC) [10] were only reported since 2005, examples of structurally characterized hydroxo [11] and fluoro [12,13] complexes of gold(III) have been known for several decades.

While gold(I) prefers reacting with alkynes and alkenes the formation of Au(I)-alkyne is favored versus Au(I)-alkene complexes and consequently a variety of alkyne catalyzed versus alkene catalyzed reactions exists. That trait of Au(I) is referred in bibliography as “alkynophylicity”. A possible explanation of “alkynophylicity” of Au(I) is that due to the lower energy of LUMO of Au(I)-alkyne complex compared to the energy of LUMO of Au(I)-alkene, the addition of a nucleophile to the activated complex is easier in the first case. [2]

Of course, in the field of gold (I) catalysis, the type of ligand is a factor that affects the selectivity of the catalyst not only due to the drift of Lewis acidity of catalyst but also to its geometry. In the next chapter we will examine the impact of ligand on gold(I) catalysis.

The reactivity of metal complexes is directed by the trend in metal-ligand bond energies. For gold, depending on the nature of the O-ligand, the sequence is Au-H > Au-O > Au-C or Au-H > Au-C > Au-O, whereas for other metals including its neighbor in the Periodic Table, platinum(II), the trend Pt-O > Pt-H > Pt-C is observed. [14] Oxygen and fluoride ligands tend to act as good leaving groups and are utilized with good effect in ligand substitution and catalytic reactions. The bond dissociation energies of gold(I) compounds tend to be larger than those of gold(III) but follow the same trend.

Thus, due to the relativistic effect that is intense in gold(I), unique catalytic properties are present in comparison with other transition metal catalysis. Thus, reactions using the same starting material but a different metal catalyst can afford different products, since each catalyst can activate selectively different functional groups leading the system to discrete pathways. However, the prediction of divergent catalysis, due to different metal catalyst, is still not feasible and remains empirical. [15–17]

There has been a spectacular rise in the application of soluble gold(I) catalysts in synthesis. Their development has been the subject of numerous reviews. [21,22,23–30,31] Examples of divergent gold(I) catalysis [29] are next presented with a mechanism suggested often from quantum chemistry calculations.

## 3.2 Divergent gold catalysis – gold(I) vs other metal catalysts

### 3.2.1 Au vs Pt

The work of Lu and Ye [30–32] is an example of divergent catalysis between gold and platinum. The reaction between isoxazoles **1a** and ynamides **1b** leads either to 2-aminopyrroles **1g** at the presence of gold(I) catalyst $[(2,4\text{-}tBu_2C_6H_3O)_3PAuNTf_2)]$ or to 1,3-oxazepine **1i´** at the presence of platinum(II) ($PtCl_2$) respectively. According to DFT calculations and experimental data the first steps of the proposed mechanism of the reaction are common. [32] Thus, after the activation of ynamide **1b** by the catalyst, is following the nucleophilic attack of isoxazole **1a** and the N-O bond cleavage, and then the α-imino metal carbene intermediate **1d/1d´** is formed (Scheme 3.1). From that step,

divergent steps are observed through nucleophilic attack at the metal-coordinated carbocation of **1d/1d´** favoring a 1,5-cyclization forming 2-aminopyrrole **1g** for the gold catalyst while platinum prefers 1,7-cyclization forming 1,3-oxazepine **1i´**(Scheme 3.1).

It was proposed that the observed regioselectivity of the reaction is controlled by steric factor in nucleophilic attack at the metal-coordinated carbocation of intermediate **1d/1d´**. The linear structure of gold(I) catalyst renders the intermediate **1d** less sterically hindered so as the nucleophilic attack by the carbon-carbon double bond is favored. On the contrary, metal-coordinated carbocation in intermediate **1d´** is more sterically hindered due to the bigger size of platinum making feasible only the nucleophilic attack from the more sterically exposed oxygen. Although platinum(II) catalyst is harder Lewis acid than gold(I), the steric factor plays here a dominant role.

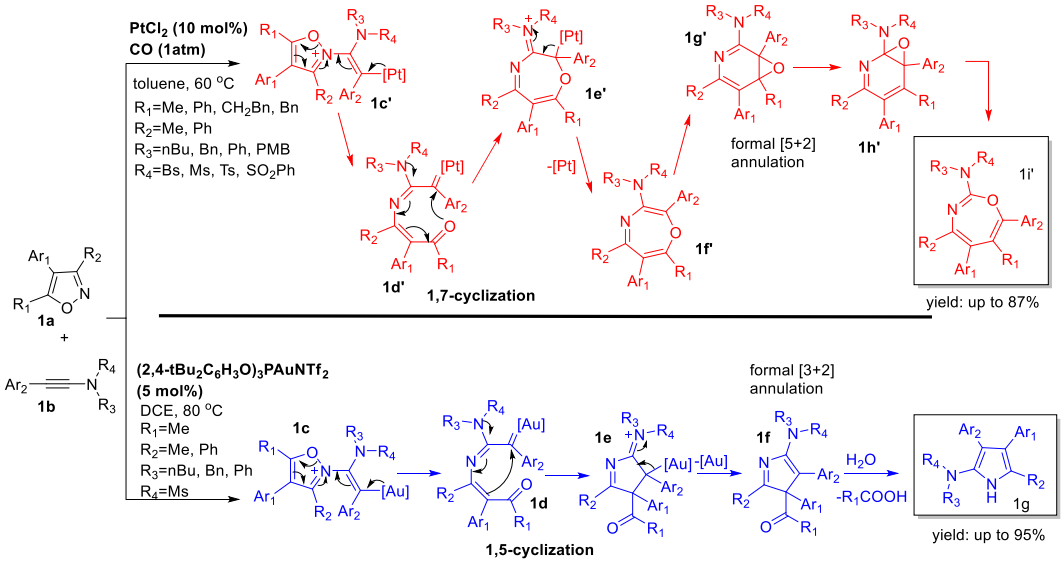


Scheme 3.1 Formal [3+2] vs [5+2] annulation in the gold(I) vs Pt(II) catalyzed reaction between an isoxazole and ynamide (Lu & Ye 2015, 2017). [30–32]

### 3.2.2 Au vs Ag

The cycloisomerization reaction of indolyl ynones **2a** catalyzed by gold (I) or silver(I) catalyst studied by Taylor and Unsworth is another example. [33] Gold (I) catalyst ($Ph_3PAuNTf_2$) furnishes the carbazole **2e** while silver catalyst (AgOTf) furnished the spyrocyclic product **2c´** (Scheme 3.2). According to the proposed mechanism, both catalysts, $Ph_3PAuNTf_2$ and AgOTf, activate alkyne group urging the system to a 5-endo-dig cyclization to form spirocyclic intermediate **2b/2b´**. In the case of silver catalysis the

path is over with the desilveration and formation of the spyrocyclic product **2c´**. However, in the case of gold(I) catalysis the activation of the alkyne follows a cascade of ring expansion, aromatization and deauration that leads to the formation of carbazole **2e** (Scheme 3.2).

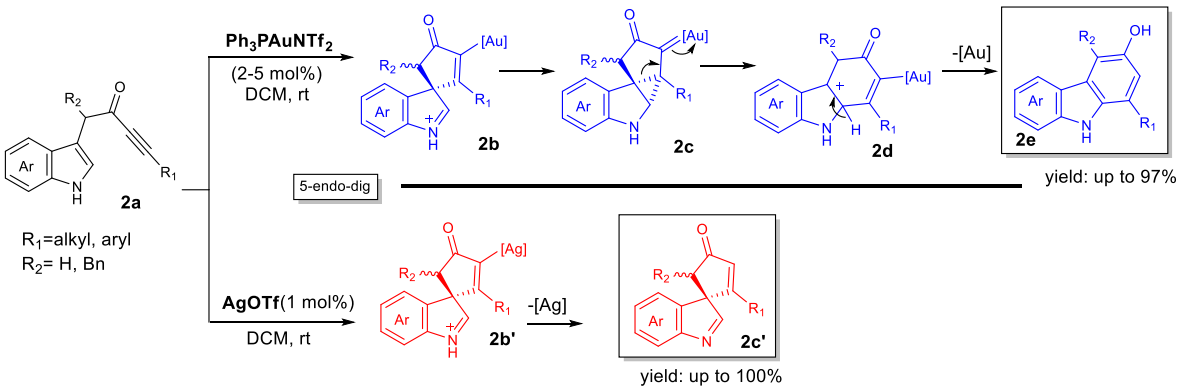


Scheme 3.2 Regiodivergent cycloisomerization of indolyl ynones (Taylor & Unsworth 2016). [33]

### 3.2.3 Au vs Pd

The Au(I) (MeDalPhosAuCl)-catalysed reaction of N-phenylpyrrole **3a** with iodobenzene **3b** leads selectively to the C3 – substituted pyrrole **3c** studied by Bourissou in 2017. [34] The Pd(II) ($PdCl_2$)-catalysed version of the same reaction, studied by Yamaguchi in 2014, [35] furnishes selectively the C2 – substituted pyrrole **3d** (Scheme 3.3). Noteworthy is the role of the MeDalPhos ligand in gold complex that enables gold catalyst to oscillate during catalytic cycle between oxidation states I and III [34] (Scheme 3.4), adding to the reaction traits of high reactivity and selectivity using variant aryl halides as substrates as revealed in the works of Bourissou in 2019,[36] 2020,[37] and Patil in 2020. [38]

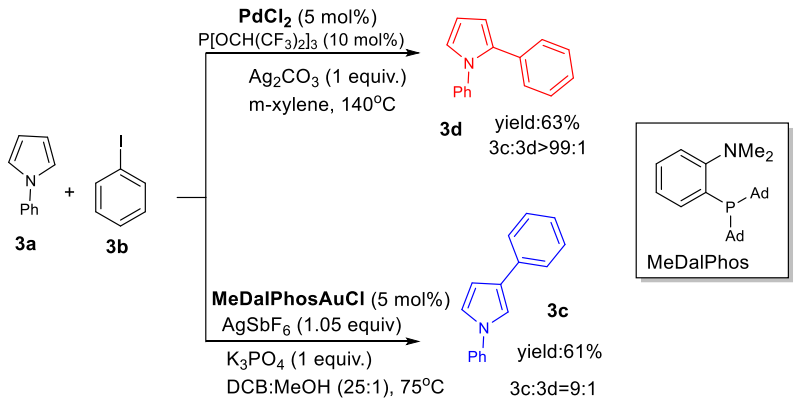


Scheme 3.3 C2- vs C3- arylation of N-phenyl substituted pyrrole in the presence of palladium(II) vs gold(I) catalyst, respectively (Bourissou 2017, [34] Yamaguchi 2014 [35]).

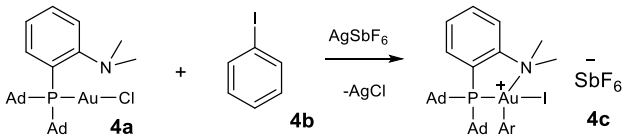


Scheme 3.4 Activation of phenyliodide by MeDalPhos gold(I) catalyst. MeDalPhos ligand induces oscillation of oxidation state between Au(I) and Au(III) during catalytic cycle.

### 3.2.4 Au vs Rh

The alkynylation of isoquinolones **5a** catalyzed by gold(I) or rhodium(II)studied by Patil in 2016 [39] is another representative divergent gold(I) catalytic reaction due to the chemoselectivity observed depending the metal catalyst applied. The reaction reveals a regiodivergent to C4 or C8 C-H alkyne insertion when gold(I) or rhodium(II), respectively, is used. [39] In the reaction between isoquinolone **5a** and 1-[(triisopropylsilyl)ethynyl]-1,2-benziodoxol-3(1H)-one (TIPS-EBX) **5b**, the latter undergoes selectively carbophilic activation of alkyne group when gold(I) catalyst is present. Then, a C-H insertion at C4 is favoured, and the α,β-elimination of gold is the last step furnishing product **5e**.

On the contrary, rhodium (II) catalyst promotes C-H activation of the C8 position of isoquinolones **5a**. The activated complex undergoes the insertion of TIPS-EBX to form the intermediate **5d´.** Product **5e´** is obtained after the reductive elimination of rhodium.

Theoretical studies on the mechanism and regioselectivity of the reaction, as well on the role of TIPS-EBX were carried out by Liu and co-workers. [40]

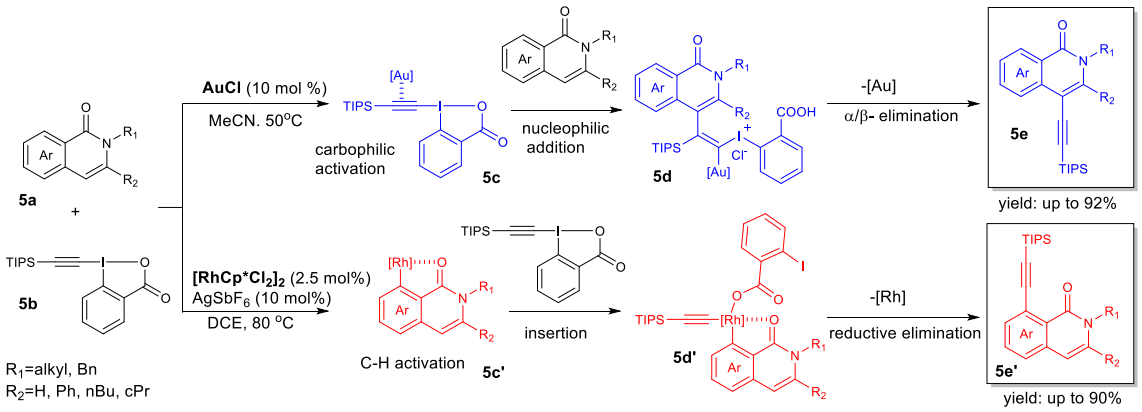


Scheme 3.5 Regioselective C-H alkynylation of isoquinolones in the presence of gold(I) or rhodium(II) catalyst (Patil 2016). [39]

### 3.2.5 Au vs Sc

The reaction between 1-(1-alkynyl)-cyclo-propyl-ketones **6a** and nitrones **6b** furnishes either [4+3] cycloaddition products **6e** or [3+3] cycloaddition products **6e´** depending whether the applied catalyst is Au(I) or Sc(III) (Scheme 3.6) as studied by Zhang in 2010. [41] The $Sc(OTf)_3$/Phen catalyst activates chemoselectively the carbonyl group of ketone **6a** facilitating the nucleophilic attack of nitrone **6b** onto cyclopropyl ring. Then, the intermediate **6d´** undergoes a formal [3+3] cycloaddition to furnish a tetrahydro-1,2-oxazine derivative **6e´**.

On the contrary, $Ph_3PAuOTf$ catalyst activates selectively the alkyne group in ketone **6a**, altering the mechanism of the reaction to a step of 5-endo-dig nucleophilic attack of carbonyl oxygen on the activated alkyne group. Then a nucleophilic attack of nitrone **6b** on the cyclopropyl ring and finally a formal [4+3] cycloaddition furnishes a 5,7-fused bicyclic furo [3,4-d][1,2]-oxazepine **6e** (Scheme 3.6).

Noteworthy, according to the proposed mechanisms, both pathways, either [3+3] or [3+4] cycloaddition steps proceed via a chair like transition state (Scheme 3.6). [41] Mechanistic studies are available on the gold (I) catalyzed scale of the reaction. Experimental work on the kinetics of the reaction shed light on the stereo selectivity [42] while DFT calculations supported a mechanism via the formation of an oxonium ion. [43]

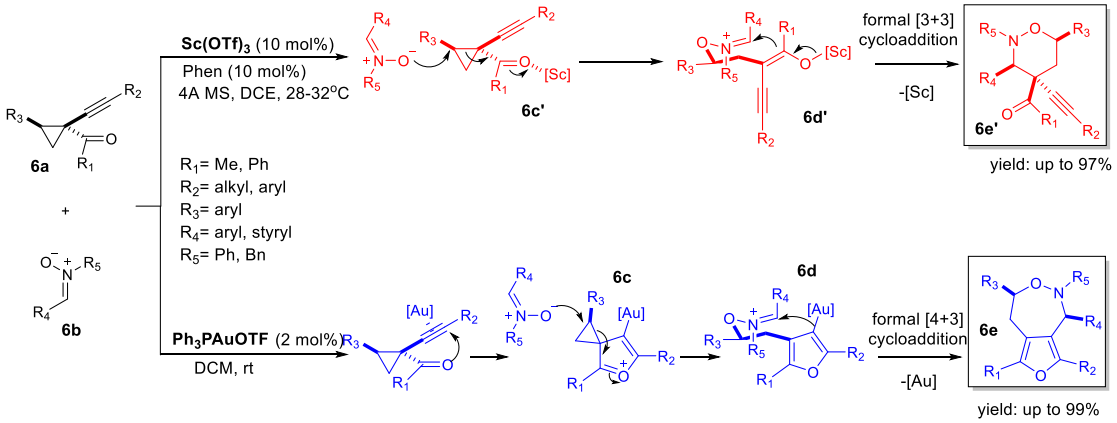


Scheme 3.6 Regioselective Control in the Diastereoselective 1,3-Dipolar Cycloaddition Reactions of 1-(1- Alkynyl)cyclopropyl Ketones with Nitrones (Zhang 2010). [41]

### 3.2.6 Au vs Cu

Nakamura in 2013 [44] and 2015 [45] studied the reaction of O-propargylic oximes **7b** with maleimides **7a** in the presence of gold(I) ($Ph_3PAuNTf_2$) and copper(II) $[CuCl(cod)]_2$ catalysts, respectively (Scheme 3.7). The reaction begins with the activation of the alkyne group of O-propargylic oxime **7b**, similarly by both catalysts which follow the nucleophilic attack of nitrogen to the activated alkyne group to produce via a 5-endo-dig cyclization the common intermediate **7c/7c´**. The intermediate **7c/7c´** follows a different path regarding the applied catalyst. Copper(II) catalyst lowers the activation energy for the cleavage of C-O bond to form N-allenyl-nitrone **7d´**. N-allenyl-nitrone **7d´** reacts with maleimide **7a** through a [3+2] cycloaddition forming N-allenylisoxazolidone **7e´** which undergoes a 1,3-oxygen shift to the oxazepine derivative **7f´**. [45]

On the contrary, gold(I) catalyst maintains the energy barrier for the bond C-O cleavage high. The reaction prefers an intermolecular methylene transfer to form diene **7d** which reacts with maleimide **7a** through to form isoxazole **7e**.

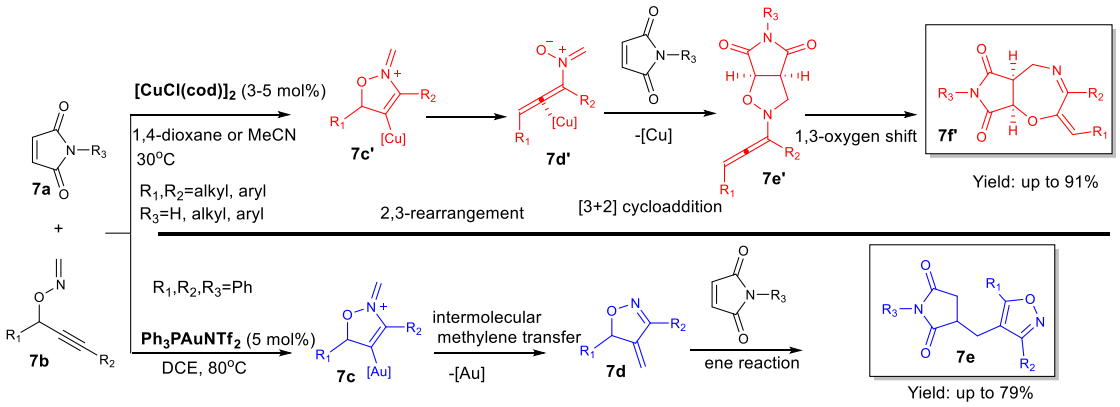


Scheme 3.7 Reactions between O-Propargylic-Oximes and Dipolarophiles catalyzed by Au(I) or Cu(I) (Nakamura 2013, 2015). [44, 45]

## 3.3 Bibliography


(1) Raubenheimer, H. G.; Schmidbaur, H. The Late Start and Amazing Upswing in Gold Chemistry. *J. Chem. Educ.* **2014**. https://doi.org/10.1021/ed400782p.

(2) Gorin, D., Toste, F. Relativistic Effects in Homogeneous Gold Catalysis. *Nature* **2007**, No. 446, 395–403.

(3) Desclaux, J. P. Relativistic Dirac–Fock Expectation Values for Atoms with Z=1 to Z=120. *At. Data Nucl. Data Tables* **1973**, *12* (4), 311–406.

(4) J.P.DesclauxP.Pyykkö. Dirac–Fock One-Center Calculations—Molecules CuH, AgH and AuH Including P-Type Symmetry Functions. *Chem. Phys. Lett.* **1976**, *39* (2), 300–303.

(5) Weinhold, F. The Path to Natural Bond Orbitals. *Isr. J. Chem.* **2022**, *62* (1–2). https://doi.org/10.1002/ijch.202100026.

(6) Schwerdtfeger, P., Hermann, H. L. & Schmidbaur, H. Stability of the Gold(I)–Phosphine Bond. A Comparison with Other Group 11 Elements. *Inorg. Chem.* **2003**, *42* (4), 1334–1342.

(7) . Schwerdtfeger, P., Boyd, P. D. W., Burrell, A. K., Robinson, W. T. & Taylor, M. J. Relativistic Effects in Gold Chemistry. 3. Gold(I) Complexes. *Inorg. Chem.* **1990**, *29* (18), 3593–3607.

(8) Pearson, R. G. Hard and Soft Acids and Bases. *J. Am. Chem. Soc.* **1963**, *85* (22), 3533–3539. https://doi.org/10.1021/ja00905a001.

(9) Pearson, R. G. Hard and Soft Acids and Bases, HSAB, Part 1: Fundamental Principles. *J. Chem. Educ.* **1968**. https://doi.org/10.1021/ed045p581.

(10) Nelson, D. J.; Nolan, S. P. Hydroxide Complexes of the Late Transition Metals: Organometallic Chemistry and Catalysis. *Coordination Chemistry Reviews*. 2017. https://doi.org/10.1016/j.ccr.2017.10.012.

(11) Jones, P. G.; Schelbach, R.; Schwarzmann, E. Hydroxy Complexes of Gold 2. Calcium Aurates [1]. *Zeitschrift fur Naturforsch. - Sect. B J. Chem. Sci.* **1987**. https://doi.org/10.1515/znb-1987-0502.

(12) Einstein, F. W. B.; Rao, P. R.; Trotter, J.; Bartlett, N. The Crystal Structure of Gold Trifluoride. *J. Chem. Soc. A Inorganic, Phys. Theor. Chem.* **1967**. https://doi.org/10.1039/J19670000478.

(13) Réffy, B.; Kolonits, M.; Schulz, A.; Klapötke, T. M.; Hargittai, M. Intriguing Gold Trifluoride-Molecular Structure of Monomers and Dimers: An Electron Diffraction and Quantum Chemical Study. *J. Am. Chem. Soc.* **2000**. https://doi.org/10.1021/ja992638k.

(14) Roşca, D. A.; Wright, J. A.; Bochmann, M. An Element through the Looking Glass: Exploring the Au-C, Au-H and Au-O Energy Landscape. *Dalton Transactions*. 2015. https://doi.org/10.1039/c5dt03930d.

(15) Trost, B. M. Selectivity: A Key to Synthetic Efficiency. *Science (80-. ).* **1983**, *219* (4582), 245–250.

(16) Kumar, R. R.; Kagan, H. B. Regioselective Reactions on a Chiral Substrate Controlled by the Configuration of a Chiral Catalyst. *Adv. Synth. Catal.Synth. Catal.* **2010**, *352* (2–3), 231–242.

(17) Mahatthananchai, J.; Dumas, A. M.; Bode, J. W. Catalytic Selective Synthesis. *Angew. Chem., Int. Ed.* **2012**, *51* (44), 10954−10990.

(18) Asiri, A. M.; Hashmi, A. S. K. Gold-Catalysed Reactions of Diynes. *Chem. Soc. Rev.* **2016**, *45* (16), 4471–4503. https://doi.org/10.1039/c6cs00023a.

(19) Yang, W.; Hashmi, A. S. K. Chem Soc Rev Mechanistic Insights into the Gold Chemistry of Allenes. **2014**, No. 2, 2941–2955. https://doi.org/10.1039/c3cs60441a.

(20) Echavarren, A. M.; Hashmi, A. S. K.; Toste, F. D. Gold Catalysis - Steadily Increasing in Importance. *Advanced Synthesis and Catalysis*. 2016. https://doi.org/10.1002/adsc.201600381.

(21) Krause, N.; Winter, C. Gold-Catalyzed Nucleophilic Cyclization of Functionalized Allenes : A Powerful Access to Carbo- and Heterocycles. **2011**.

(22) Halliday, C. J. V; Lynam, J. M. Gold–Alkynyls in Catalysis: Alkyne Activation, Gold Cumulenes and Nuclearity. **2016**, *44* (0). https://doi.org/10.1039/c6dt01641c.

(23) Gagosz, F. Gold Vinylidenes as Useful Intermediates in Synthetic Organic Chemistry. *Synthesis (Germany)*. 2019. https://doi.org/10.1055/s-0037-1611647.

(24) Hashmi, A. S. K.; Rudolph, M. Gold Catalysis in Total Synthesis. *Chem. Soc. Rev.* **2008**. https://doi.org/10.1039/b615629k.

(25) Wang, Y. M.; Lackner, A. D.; Toste, F. D. Development of Catalysts and Ligands for Enantioselective Gold Catalysis. *Acc. Chem. Res.* **2014**. https://doi.org/10.1021/ar400188g.

(26) Fensterbank, L.; Malacria, M. Molecular Complexity from Polyunsaturated Substrates: The Gold Catalysis Approach. *Acc. Chem. Res.* **2014**. https://doi.org/10.1021/ar4002334.

(27) Zi, W.; Dean Toste, F. Recent Advances in Enantioselective Gold Catalysis. *Chemical Society Reviews*. 2016. https://doi.org/10.1039/c5cs00929d.

(28) Harris, R. J.; Widenhoefer, R. A. Gold Carbenes, Gold-Stabilized Carbocations, and Cationic Intermediates Relevant to Gold-Catalysed Enyne Cycloaddition. *Chemical Society Reviews*. 2016. https://doi.org/10.1039/c6cs00171h.

(29) Chetan C. Chintawar, Amit K. Yadav, Anil Kumar, Shashank P. Sancheti, and N. T. P. Divergent Gold Catalysis: Unlocking Molecular Diversity through Catalyst Control. *Chem. Rev.* **2021**, *121* (14), 8478−8558.

(30) Zhou, A.-H.; He, Q.; Shu, C.; Yu, Y.-F.; Liu, S.; Zhao, T.; Zhang, W.; Lu, X.; Ye, L.-W. Atom-Economic Generation of Gold Carbenes: Gold-Catalyzed Formal [3 + 2] Cycloaddition between Ynamides and Isoxazoles. *Chem. Sci.* **2015**, No. 6, 1265−1271.

(31) Xiao, X.-Y.; Zhou, A.-H.; Shu, C.; Pan, F.; Li, T.; Ye, L.-W. Atom- Economic Synthesis of Fully Substituted 2-Aminopyrroles via Gold- Catalyzed Formal [3 + 2] Cycloaddition between Ynamides and Isoxazoles. *Chem. - Asian J.* **2015**, *10* (9), 1854−1858.

(32) Shen, W.-B.; Xiao, X.-Y.; Sun, Q.; Zhou, B.; Zhu, X.-Q.; Yan, J.- Z.; Lu, X.; Ye, L.-W. Highly Site Selective Formal [5 + 2] and [4 + 2] Annulations of Isoxazoles with Heterosubstituted Alkynes by Platinum Catalysis: Rapid Access to Functionalized 1,3-Oxazepines and 2,5- Dihydropyridines. *Angew. Chem., Int. Ed.* **2017**, *56* (2), 605–609.

(33) Liddon, J. T. R.; James, M. J.; Clarke, A. K.; O'Brien, P. . T.; R. J. K.; Unsworth, W. P. Catalyst -Driven Scaffold Diversity: Selective Synthesis of Spirocycles, Carbazoles and Quinolines from Indolyl Ynones. *Chem. - Eur. J.* **2016**, *22* (26), 8777−8780.

(34) Zeineddine, A.; Estévez, L.; Mallet-Ladeira, S.; Miqueu, K.; Amgoune, A.; Bourissou, D. Rational Development of Catalytic Au(I)/Au(III) Arylation Involving Mild Oxidative Addition of Aryl Halides. *Nat.*

*Commun.* **2017**, No. 8, 565–572.

(35) Ueda, K.; Amaike, K.; Maceiczyk, R. M.; Itami, K.; Yamaguchi, J. β-Selective CSH Arylation of Pyrroles Leading to Concise Syntheses of Lamellarins C and I. *J. Am. Chem. Soc.* **2014**, *136* (38), 13226–13232.

(36) Rodriguez, J.; Zeineddine, A.; Sosa Carrizo, E. D.; Miqueu, K.;Saffon-Merceron, N.; Amgoune, A.; Bourissou, D. . . Catalytic Au(I)/ Au(III) Arylation with the Hemilabile MeDalphos Ligand: Unusual Selectivity for Electron-Rich Iodoarenes and Efficient Application to Indoles. *Chem. Sci.* **2019**, No. 10, 7183–7192.

(37) Rodriguez, J.; Adet, N.; Saffon-Merceron, N.; Bourissou, D. Au(I)/Au(III)-Catalyzed C-N Coupling. . *Chem. Commun.* **2020**, No. 56, 94–97.

(38) Akram, M. O.; Das, A.; Chakrabarty, I.; Patil, N. T. Ligand- Enabled Gold-Catalyzed C(Sp2))N Cross-Coupling Reactions of Aryl Iodides with Amines. *Org. Lett.* **2019**, *21* (19), 8101–8105.

(39) Shaikh, A. C.; Shinde, D. R.; Patil, N. T. Gold vs Rhodium Catalysis: Tuning Reactivity through Catalyst Control in the C-H Alkynylation of Isoquinolones. *Org. Lett.* **2016**, *18* (5), 1056–1059.

(40) Fengyue Zhao, Benzhen Xu, Dongcheng Ren, Lingli Han, Zhangyu Yu, and T. L. C–H Alkynylation of N-Methylisoquinolone by Rhodium or Gold Catalysis: Theoretical Studies on the Mechanism, Regioselectivity, and Role of TIPS-EBX. *Organometallics* **2018**, *37* (6), 1026–1033.

(41) Zhang, Y.; Liu, F.; Zhang, J. Catalytic Regioselective Control in the Diastereoselective 1,3-Dipolar Cycloaddition Reactions of 1-(1- Alkynyl)Cyclopropyl Ketones with Nitrones. *Chem. - Eur. J.* **2010**, *16* (21), 6146–6150.

(42) YunFeng Yan, ZhiYuan Geng, Y. W. & S. L. Reaction Mechanism and Chemoselectivity of Gold(I)-Catalyzed Cycloaddition of 1-(1-Alkynyl) Cyclopropyl Ketones with Nucleophiles to Yield Substituted Furans. *Sci. China Chem.* **2012**, *55*, 1413–1420.

(43) Kinetic Resolution of 1-(1-Alkynyl)Cyclopropyl Ketones by Gold(i)-Catalyzed Asymmetric [4+3]Cycloaddition with Nitrones: Scope, Mechanism and Applications. *Chem. Commun.*, **2012**, *48* (Yanqing Zhang and Junliang Zhang), 4710–4712.

(44) Nakamura, I.; Kudo, Y.; Terada, M. Oxazepine Synthesis by Copper-Catalyzed Intermolecular Cascade Reactions between OPropargylic Oximes and Dipolarophiles. *Angew. Chem., Int. Ed.* **2013**, *52* (29), 7536–7539.

(45) Nakamura, I.; Gima, S.; Kudo, Y.; Terada, M. Skeletal Rearrangement of O-Propargylic Formaldoximes by a Gold-Catalyzed Cyclization/Intermolecular Methylene Transfer Sequence. *Angew. Chem., Int. Ed.* **2015**, *54* (24), 7154–7157.

# Chapter 4

## The effect of ligands and counterions in gold(I) complexes and of solvent in gold(I) catalysis

### 4.1 The role of the ligand in gold(I) catalyst complex

Gold(I)-catalyzed reactions present sensitivity to various factors that can affect the products formation. Factors like counterions and ligands in the gold(I) complex can affect the reaction mechanism and consequently the type and yield of the products. We will present few examples of divergent gold catalyzed reactions due to different structure of ligands and counterions, accompanied by an attempt to provide explanations of each factor role.

A reaction that showed the key role of the ligand in gold(I) catalyst complex is the hydration-oxacyclization of skipped diynones. [1] Depending the reaction conditions and the ligand in gold(I) complex, a five or a six member heterocyclic ring can be formed. The two pathways of the reaction are depicted to Scheme 4.1. According to the first path, 5 mol % of $Ph_3PAuCl/AgSbF_6$ catalyst in dioxane/water at 100 °C, leads to the formation of 3(2H)-furanones **1b** as a major product. Ceteris paribus, a change of the ligand of the gold(I) catalyst from $Ph_3PAuCl/AgSbF_6$ to $IPrAuNTf_2$ urges the reaction to the formation of the 4-pyrones **1c** as a major product. It is proposed that the observed regioselectivity resulted as a combination of both, ligand and counteranion type.

The suggested mechanism is consisting by two steps. [1] The first step is the hydration of the one of two alkyne groups in diynone, and the second step is the intramolecular endo-oxacyclization followed by protodeauration. The regioselectivity of the reaction is controlled by the hydration step of diyne. Thus, using the $IPrAuNTf_2$ catalyst after a Michael addition of water at the terminal carbon of the activated alkyne group, a 6-endo-dig cyclization leads to the formation of 4-pyrones **1c**. On the contrary using the $Ph_3PAuCl/AgSbF_6$ catalyst, a Michael addition of water at the other carbon of the activated alkyne group, which is in α-position to carbonyl, urges the transformation to the 3(2H)-furanone **1b**.

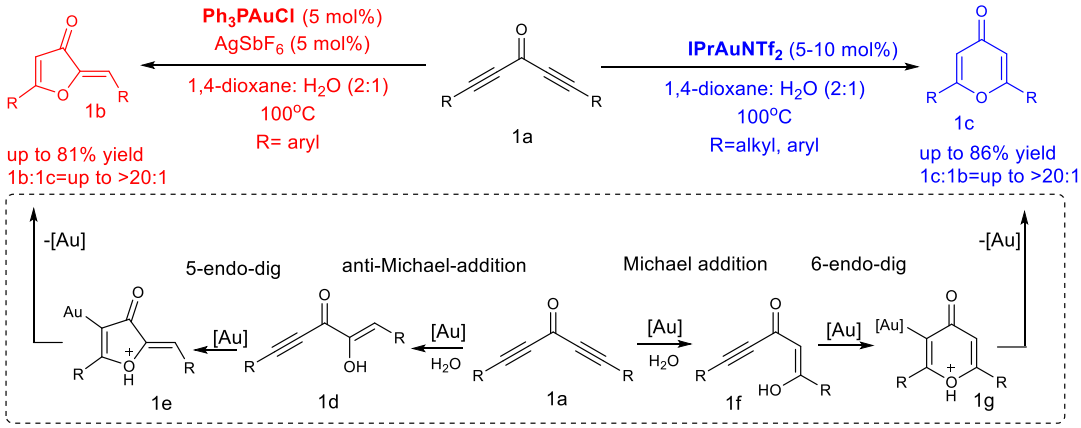


Scheme 4.1 Gold catalyzed regiodivergent hydration-cyclization of diynones (Sanz 2020). [1]

An example that reveals the key role of electron density of the ligand in gold(I) complex is the cyclization reaction of N-(3-iodoprop-2-ynyl)-N-tosylanilines **2a** (Scheme 4.2). [2]

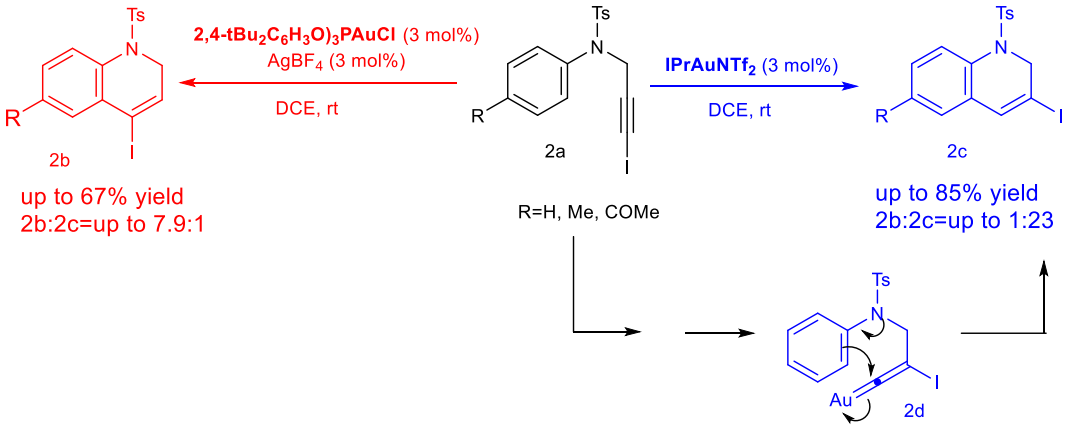


Scheme 4.2 Ligand controlled gold(I) catalyzed regioselective intramolecular hydroarylation of N-(3-iodoprop-2-ynyl)-N-tosylanilines; in the case of (2,4-$tBu_2C_6H_3O)_3PAuCl$ the $AgBF_4$ is used as $Cl^-$ scavenger (González 2011). [2]

Applying the electron deficient catalyst (2,4-$tBu_2C_6H_3O)_3PAuCl$ in the cyclization reaction of N-(3-iodoprop-2-ynyl)-N-tosylanilines **2a** the expected product of hydroarylation **2b** is received as the major product. However, ceteris paribus, substitution of (2,4-$tBu_2C_6H_3O)_3PAuCl$ with the electron rich $IPrAuNTf_2$ catalyst turns the balance to the formation of 3-iodide quinoline **2c** derivatives instead of 4-iodide quinoline derivatives **2b**. That is, an isomerization step of 1,2-iodide shift interferes before cyclization step. The reaction proceeds via the formation of a gold(I)-vinylidine indermediate **2d**. Moreover, the role of substituent in the R group

attached with phenyl group is similar with the ligands in gold(I) complexes. Electron rich substituents favor the formation of 4-iodide-derivatives **2b**. On the other hand, if R group is an electron-withdrawing substituent, the iodide migration path is favored.

The cycloisomerization of alkynones **3a** (Scheme 4.3) is a case of a chemoselective catalyzed reaction regarding the ligand of the gold(I) catalyst complex. [3] If IPrAu+ catalyst is applied, then benzofuran **3c** is formed. Otherwise, the use of $Ph_3PAu^+$ leads to the transformation of alkynones to 6,7-dihydrobenzofunan-4(5H)-ones **3b**. The difference between the two cases is the electronic properties of the ligand in the gold(I) complex that affects the electrophilicity of gold. In general, electron rich ligands like IPr favor the transformation of alkynones **3a** to benzofurans **3c** and electron deficient ligands like $Ph_3P$ favor the transformation of alkynones to 6,7-dihydrobenzofunan-4(5H)-ones **3b**.

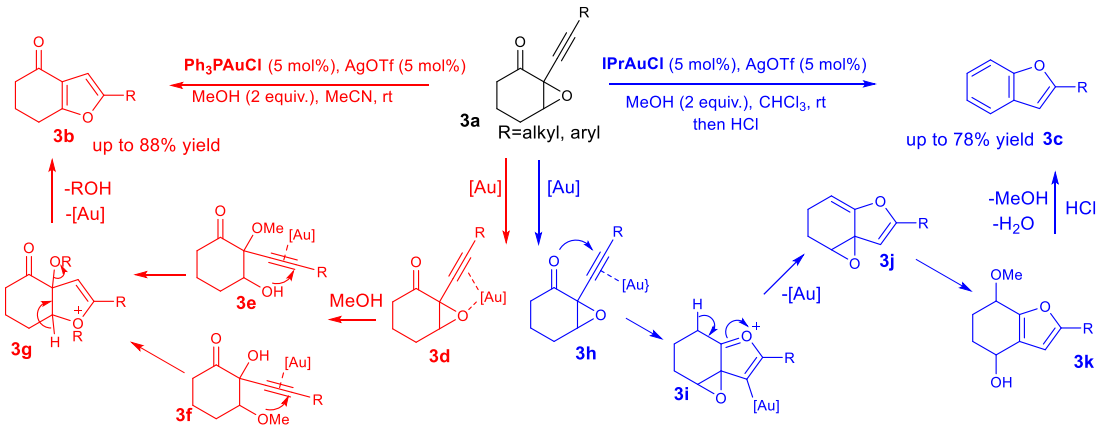


Scheme 4.3 Chemoselectivity control in gold-catalyzed transformation of 1-(alkynyl)-7-oxabicyclo[4,1,0]heptan-2-ones (Hashmi 2013). [3]

For the first step of the divergent reaction, it is proposed that IPr ligand as an electron rich group suppresses electrophilicity of gold center and transforms it to a soft Lewis acid. Thus, only the alkyne moiety is activated by gold catalyst and becomes susceptible to a nucleophilic attack by the adjacent carbonyl oxygen. After deprotonation and protodeauration the intermediate **3j** is obtained. A methanol molecule contributes to the epoxide ring opening forming the intermediate **3k** that undergoes aromatization in the presence of HCl to benzofuran.

On the other hand, $Ph_3P$ group is not as electron rich ligand as IPr. Thus, $Ph_3PAu^+$ catalyst is a harder Lewis acid than $IPrAu^+$. Consequently, gold(I) catalyst activates

both alkyne and epoxy moiety. The nucleophilic attack of methanol to both carbons of the epoxide ring leads to two isomers **3e/3f**. Both of them after a 5-endo-dig cyclization reaction, undergo elimination of water or methanol and protodeauration furnishing 6,7-dihydrobenzofunan-4(5H)-ones **3b**.

Normally, activation of alkyne moiety via π-complex formation is succeeded. However, an alternative way of dual σ,π-activation has been reported and supported not only by experimental data, but also by mechanistic studies with NMR. [4] Thus, in the gold(I)-catalyzed heterocyclization of 1-(orthoethynylaryl) urea **4a** is a case that ligand in gold's complex determines also the activation mode of the alkynyl moiety (Scheme 4.4). [4] The use of $IPrAu^+$ catalyst leads to the transformation of 1-(orthoethynylaryl) urea **4a** to quinazolin-2-one **4b**. Steric crowding is the dominant factor for which IPr ligand induces a π-mode activation of alkyne group. Thus, steric hindrance between the bulky ligand of gold(I) complex and substrate, activates alkyne group unsymmetrically rendering benzylic carbon more electrophilic and consequently more susceptible to the nucleophilic attack of N-3 via a 6-exo-dig cyclization furnishing quinazolin-2-one **4b**. [4]

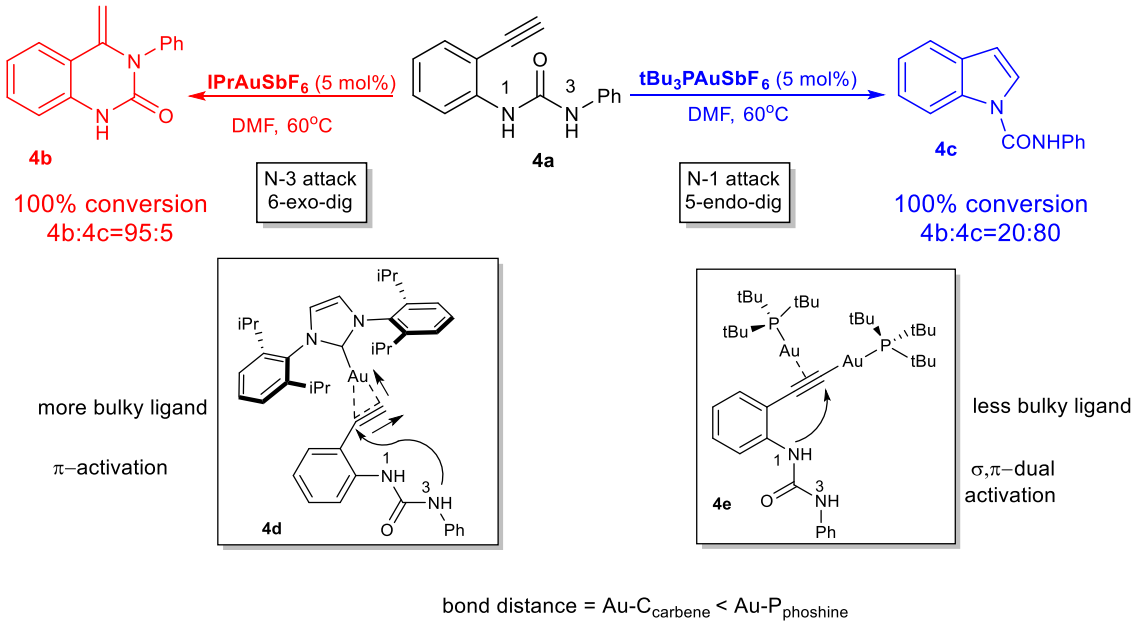


Scheme 4.4 Ligand-dependent competitive activation modes of terminal alkyne (Medio-Simón 2014). [4]

The alternative path of this reaction is the transformation of 1-(orthoethynylaryl) urea **4a** to N-substituted indoles **4c**. [4] The reaction proceeds via a dual σ,π-activation of triple bond. Due to the less sizeable ligand $(tBu)_3P$ the activation of alkyne moiety is symmetrical. The acidic proton is substituted by a molecule of the catalyst. Finally, the dual activated intermediate furnishes via 5-endo-dig cyclization indole **4c**. Experimental data confirmed this mechanism. [4]

Ligands in gold(I) complexes may regulate the ability of the catalyst to activate π-systems. [5] A case of regulation of the activity of gold(I) catalyst is the divergent cycloisomerization of ortho-(propargyloxy)aryl methylenecyclopropanes **5a**. According to Scheme 4.5, ortho-(propargyloxy)aryl methylenecyclopropanes **5a** can be transformed to methylenecyclopropane 2H-chromene **5c** derivatives using the catalyst $(4\text{-}CF_3C_6H_4)_3PAuSbF_6$ or to cyclobutene-substituted 2H-chromenes **5b** using the catalyst $IPrAuSbF_6$. Despite at a first glance it seems to be a dual path reaction, in fact it is a one way reaction with an additional step of expansion of the cyclopropane ring to cyclobutene. First, gold(I) catalyst activates alkyne group that accepts the intramolecular nucleophilic attack of the tethered aryl group. Methylenecyclopropane-2H-chromene **5c** is formed after protodeauration of the intermediate **5e**. After the formation of 2H-chromene **5c** derivative the regulatory role of the ligand of gold(I) complex begins. If the ligand is electron deficient, like $(4\text{-}CF_3C_6H_4)_3P$, the reaction stops at this step. But in the case that the ligand is electron rich, like IPr, the electron rich complex $IPrAuSbF_6$ activates effectively the double bond of methylenecyclopropane **5c**. Due to activation of the double bond, a carbocation **5f** is formed that leads to tandem alkyl swift and 1,2-H swift furnishing finally a cyclobutene-substituted 2H-chromene **5b**. [5] The suggested reaction mechanism was confirmed experimentally. The methylenecyclopropane-2H-chromene **5c** transformed to cyclobutene-substituted 2H-chromene **5b** under the action of $IPrAuSbF_6$ catalyst. [5]

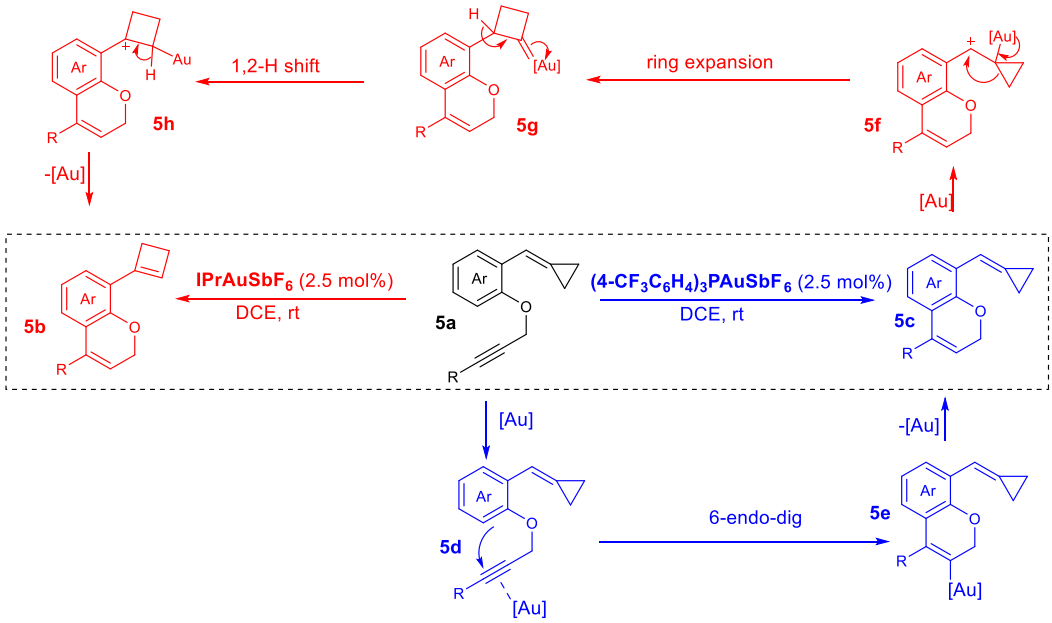


Scheme 4.5 Gold(I)-catalyzed transformation of ortho-(propargyloxy)aryl methylenecyclopropanes (Shi 2016). [5]

A divergent reaction in which not only ligands, but also a combination of factors like solvent, temperature and counterion affect the balance of products is presented in Scheme 4.6. The 3-propargylindoles **6a** can be converted according to Nazarov or iso-Nazarov cyclization. [6,7] After a first common step of 1,2-indole shift, 3-propargylindole is converted to the gold(I)-carbene intermediate **6e**. The transformation can be carried out either using $Ph_3PAuNTf_2$ in dichloromethane at room temperature or with $(2,4\text{-}tBu_2C_6H_3O)_3PAuCl/AgOTf$ in toluene at 0 $^oC$. The second step of the transformation is differentiated according to factors of the reaction, like the nature of the ligand, solvent, counterion and temperature. $Ph_3PAuNTf_2$/DCM/rt turns the balance to the iso-Nazarov reaction and to 3-(inden-2-yl)indoles **6c** formation. On the contrast, the mix of $(2,4\text{-}tBu_2C_6H_3O)_3PAuCl/AgOTf$ /toluene/ 0 $^oC$ favors Nazarov cyclization that furnish product **6b**. [6,7] The divergent nature of the reaction attracted the attention of chemists who investigated the mechanism not only experimentally but with DFT calculations also.[7,8,9]

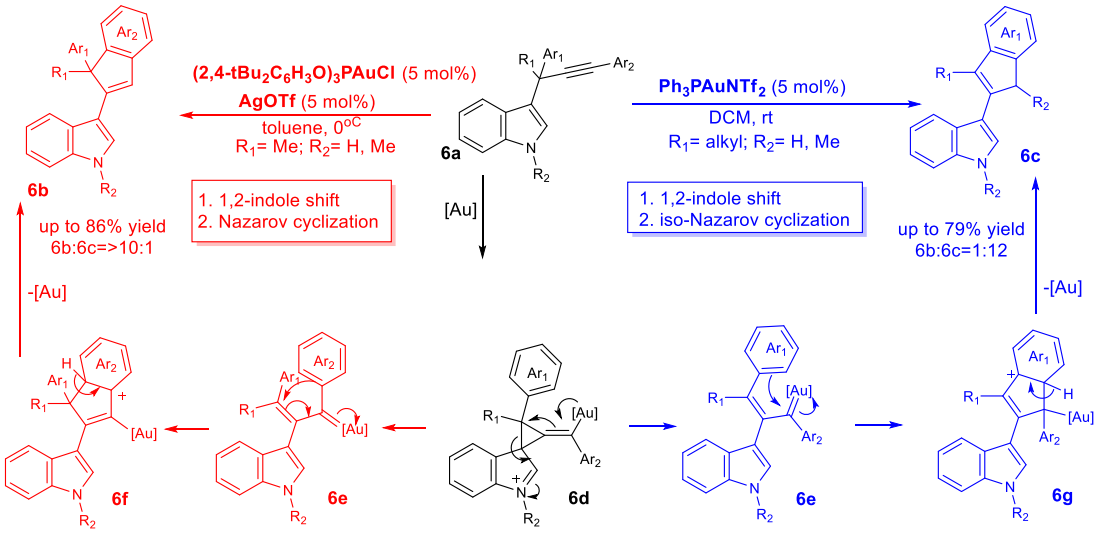


Scheme 4.6 Gold (I)-catalyzed tandem reaction of 3-propargylindole initiated by 1,2-indole migration (Sanz 2011). [6,7]

The regulating role of ligand is presented in the [5+2] and [5+1] annulation reactions between 1,2-benzoisoxazoles **7b** and ynamides **7a** (Scheme 4.7). The [5+2] annulation reaction is favored when IPrAuCl/$AgNTf_2$ catalyst is used. On the contrary, JohnPhosAuCl/$AgNTf_2$ turns the balance to the [5+1] annulation. Thus, the reaction between 1,2-benzoisoxazoles **7b** and ynamides **7a** is rendered chemodivergent due to the ligands of the gold(I). [10] Reaction initiates with a nucleophilic attack of the N of 1,2-benzoisoxazole onto the activated alkyne moiety of ynamide. Intermediate **7e** may follow the path to **7c** or **7d** regarding the applied catalyst. IPr ligand is more electron-rich than phosphine ligand in complex JohnPhosAuCl. Thus, the first catalyst favors the path to **7c** due to its better ability to stabilize the gold(I)-carbene intermediate **7f**. The alternative path of the reaction starts from the less sterically hindered conformation **7e´** and includes a 1,2-alkene swift and N-O bond cleavage, followed by a 1,2-sulfonamide swift. After deauration the product **7d** is formed. [10] DFT calculations also support the assumed mechanism and rationalize the product stereoselectivity.[11]

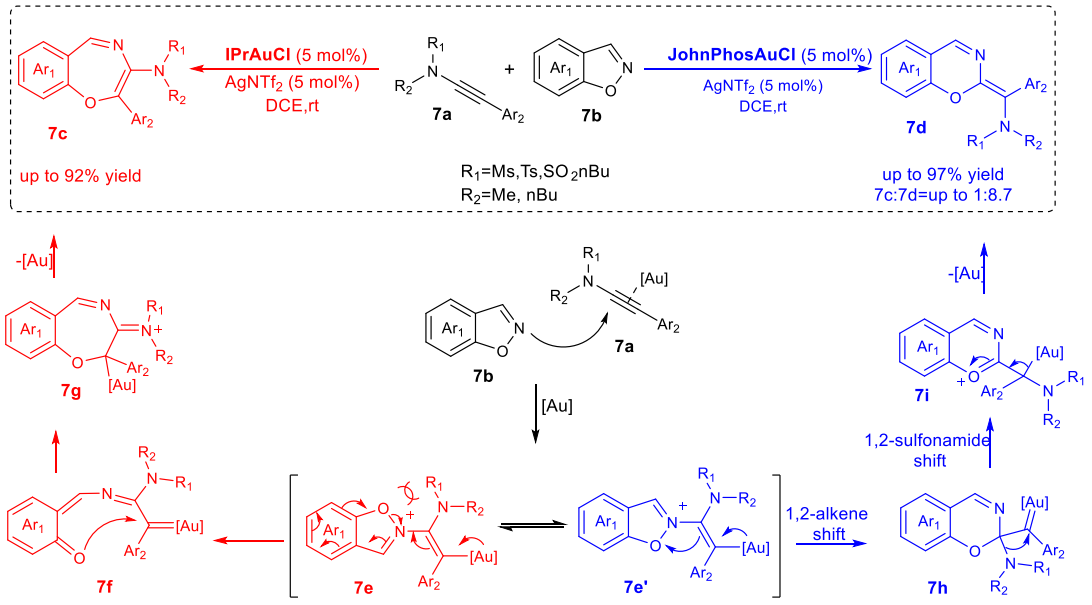


Scheme 4.7 Ligand-dependent [5+2] vs [5+1] annulations between ynamides and 1,2-benzoisoxazoles (Liu 2018). [10,11]

The gold(I)-catalyzed divergent reaction of cycloaddition of allene-dienes reveals interesting findings about their mechanism using DFT calculations. Electronic properties of gold(I) complex catalyst are regulated by its ligand. As a result, the cycloaddition reaction of allene-dienes is related to the electronic properties of catalyst and the products may alter related to this. Thus, [4+3] cycloaddition is the result of the action of JohnPhosAuCl/$AgSbF_6$ catalyst on allene-dienes **8a**. Allene's activation by gold(I) promotes the formation of cycloheptene gold(I)-carbene intermediate **8e**. Accordingly, 1,2-hydryd shift furnishes cycloheptadiene **8c** (Scheme 4.8).

Changing the electron properties of gold(I) using $(2,4\text{-}tBu_2C_6H_3O)_3PAuCl$/ $AgSbF_6$, catalyst is rendered electron deficient and [4+2] cycloaddition is favored. [12] The initial assumption that due to the lack of back-bonding ability of gold(I) center, the formation of carbocation **8d** is favored directly from the activated allene-diene **8a**, did not assured by DFT calculations. According to the DFT calculations, the potential energy surface of the reaction to **8c** is featured by low energy barriers for both of catalysts. Then, a question arises on why different catalysts alter the products of the reaction. The solution of the riddle is the ability of the electron deficient catalyst to convert intermediate **8e** to intermediate **8d** via a 1,2-alkyl shift (ring contraction) while JohnPhosAuCl favors the 1,2-hydrid shift to form **8c**. [13]

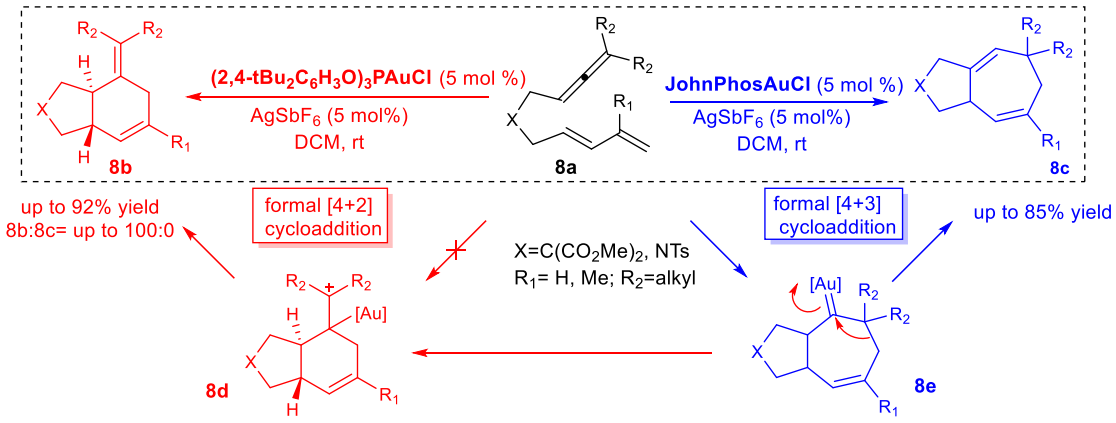


Scheme 4.8 Gold(I)-catalyzed [4+2] vs [4+3] cycloaddition of allene-dienes (Toste 2009). [13]

One year later, the regulating role of ligands was studied in a similar work on gold(I)-catalyzed cycloisomerization reaction of allene-ene **9a** [14] (Scheme 4.9). Formal [3+2] cycloisomerization is dominant when L2 ligand is present. On the contrary, formal [2+2] cycloisomerization is favored by L1 ligand. After a first common step of cyclization, the intermediate **9e** is formed. Then, two divergent paths are available. The first one is the 5-endo-trig cyclization to **9g** intermediate which is converted to **9h** due to 1,2-Me-shift and finally to **9c** / **9d** after deauration. Alternatively, cyclization of **9e** to **9f** intermediate and deauration leads to **9b**.

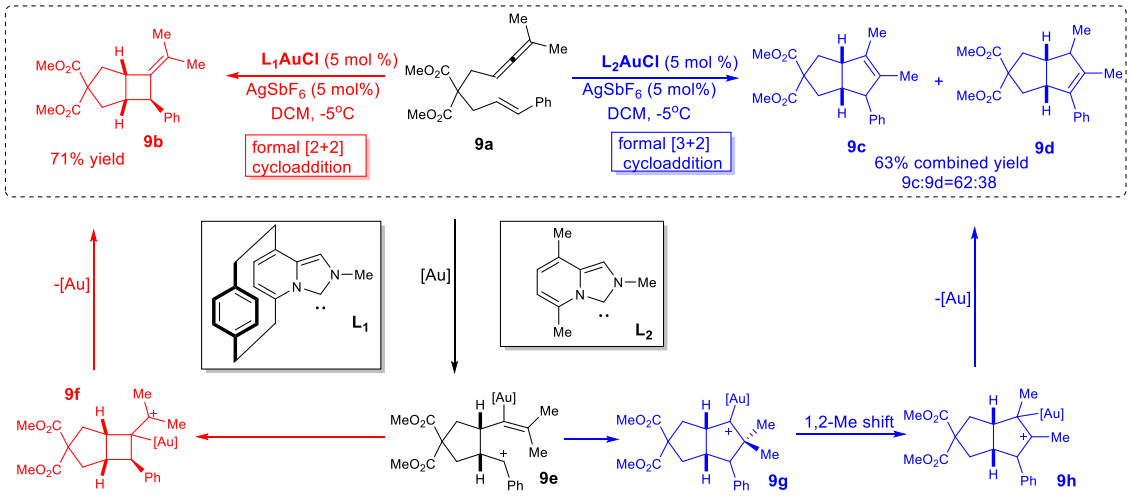


Scheme 4.9 Tuning π-acceptor ability of NHC ligands to control the reaction outcome (Fürster 2010). [14]

The key role of the ligands L1 and L2 to the mechanism of the reaction is possibly related to the π-acceptor ability of NHC (N-heterocyclic carbene). [14] Although both

ligands (L1 and L2) featured by similar σ-donor ability, L1 have higher π-acceptor ability due to its lower LUMO energy. Consequently, Au(I)-L2 complex is electron rich compared with the electron deficient Au(I)-L1 system. Thus, L2 favors [3+2] cycloaddition and L1 [2+2]. [14]

### 4.2 The role of solvent, counterions and additives

Gold(I) catalysts are commercially available at an inactive form and afterwards get activated *in situ*. The former are less stable but could be stabilized by the appropriate counterions. Nowadays, a large variety of counterions are available such as halogen anions ($Cl^-$, $Br^-$, $I^-$), oxygen based ions ($OTs^-$, $OMs^-$), nitrogen based ions ($NTf_2^-$), carbon based ions ($CN^-$), boron based ions ($BF_4^-$) and fluorinated ions ($SbF_6^-$, $PF_6^-$). [15]

During a catalytic cycle the gold(I) complex dissociates to gold(I) cation and counterion, and a complex with the substrate associates again with the counterion:

$$LAu^+X^- + S \leftrightarrow LAu^+S^- + X^-$$

Consequently, the role of gold(I) affinity to counterion/substrate and the polarity of the solvent are crucial. Solvents with low dielectric constant (benzene, toluene, dichloromethane or dichloroethane) urge the system of catalyst/counterion to exist as a contact ion pair. Then, counterion remains close to the reaction center and possibly participates to the mechanism of the reaction. On the other hand, polar solvents with high dielectric constant (alcohols, nitromethane, acetonitrile) dissociate the system of catalyst/counterion, solvate the ions and keep the counterion away from the catalytic center. As a result, the contribution of the counterion to the mechanism or the reaction is minor. [16]

It is almost clear that in the case of polar solvent the role of counterion is out of interest. However, for the case of non-polar solvents the examination of the role of counterion could be presented through a case study. The gold(I)-catalyzed addition to triple bond for an alkyne is divided to four steps: (1) catalyst activation; (2) alkyne activation by gold(I) (3) nucleophilic attack to the activated triple bond and (4) protodeauration.

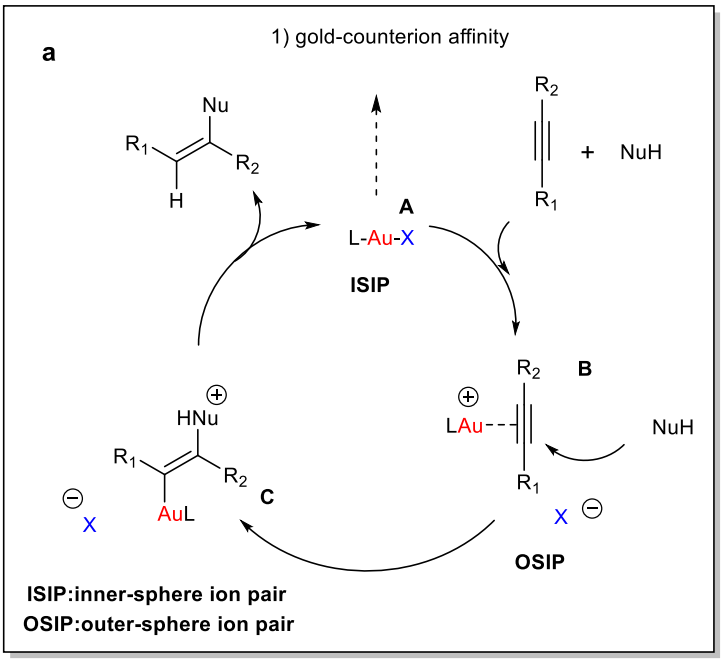


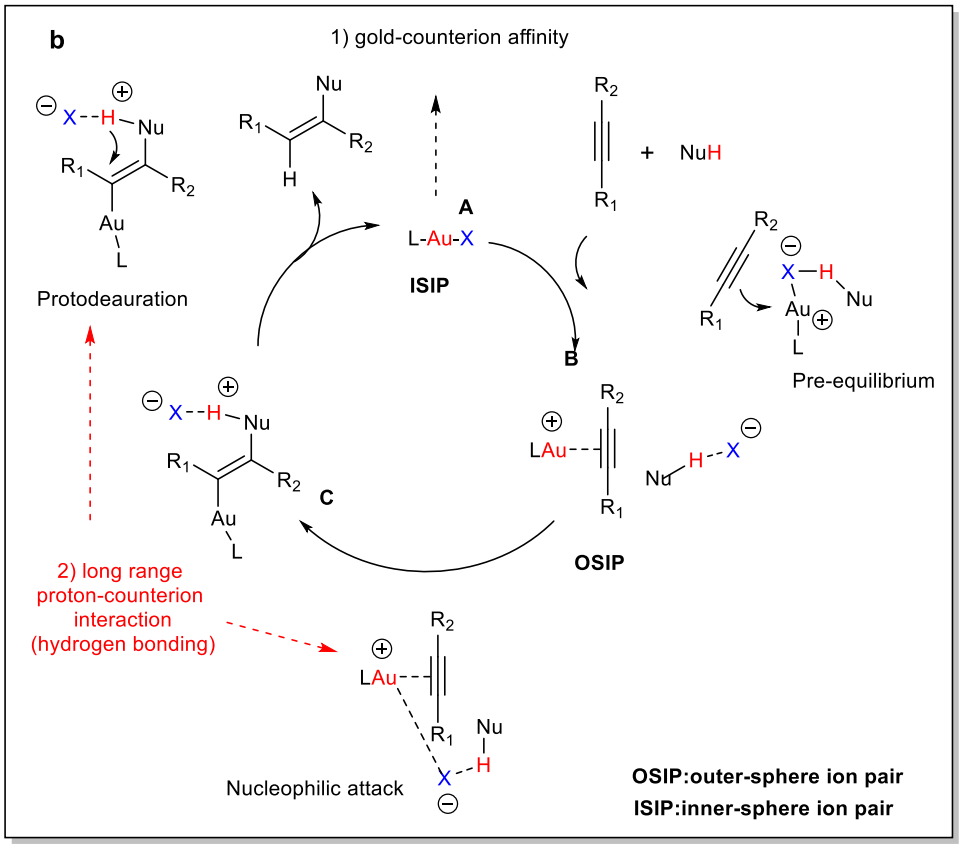


Scheme 4.10 Counterion effect in cationic gold(I) catalytic cycle; (a) no active proton is involved (e.g. NuH=alkene); (b) an active proton is involved (e.g. NuH=RO-H, $R_2N$-H). [17]

During the catalytic cycle (Scheme 4.10.a) the counterion is displaced from a region close to gold(I) (inner sphere ion pair ISIP) to a region far away from gold(I)

(outer sphere ion pair OSIP). The sooner the counterion passes from ISIP to OSIP the higher is the catalyst activity. The energy barrier between the two states is related with the affinity of the counterion to gold(I) cation. Counterions like $Cl^-$ which bind strongly with gold(I) reduce catalytic activity, impeding the formation of the complex gold(I)/alkyne. Thus, the counterion affinity is inversely proportional to the catalyst activity. [17]

The model becomes more complicated if an active proton is involved. The kind and the intensity of interaction between counterion and the active proton (-OH, $-NH_2$) of the nucleophile may change the reaction rate. If the counterion could act as acceptor to a hydrogen bond, then the nucleophilicity of the attacking nucleophile increases. The interacting counterion with the active proton could orientate properly (Scheme 4.10b) the nucleophile at the outer sphere for the nucleophilic attack.

At the last step of a catalytic cycle, that of protodeauration, gold(I) must dissociate from the substrate to be regenerated. A proton must replace it. The counterion can get involved in breaking a bond X-H and transfer the proton. However, sometimes counterions play an undefined role to the stability of gold catalyst.

To predict the chemical traits of counterions, the dissociation energy of counterions from gold(I) catalyst have been calculated (gold affinity index). Moreover, a model of hydrogen bond formation of counterion with phenol corresponds to the hydrogen bond basicity index. Using these two indexes (Table 4.1), it is possible to predict how the counterion could affect a gold(I) catalyzed reaction.

Table 4.1 Gold(I) affinity related counterion effect on cycloisomerization of 1,6-enyne. [18]

| $X^-$ | Gold affinity index | Relative initial rate |
|---|---|---|
| $AcO^-$ | 6.1 | 0.0 |
| $TfO^-$ | 2.4 | 1.0 |
| $BF_4^-$ | 0.5 | 7.1 |
| $SbF_6^-$ | 0 | 21 |
| $CTf_3^-$ | 0.2 | 32 |
| $Al[OC(CF_3)_3]_4^-$ | ~0 | 42 |

For example, in the case of a reaction without active hydrogen (Scheme 4.11), a counterion with low gold affinity index could be related with a high reactivity catalyst. That is, the low affinity of counterion leads to the easier formation of gold(I) – substrate complex and consequently to faster kinetics. [18]


Scheme 4.11 Gold (I)-catalyzed cycloisomerization reaction of 1,6-enyne. [18]

On the other hand, the presence of an active proton makes the situation more complicated (Scheme 4.12).

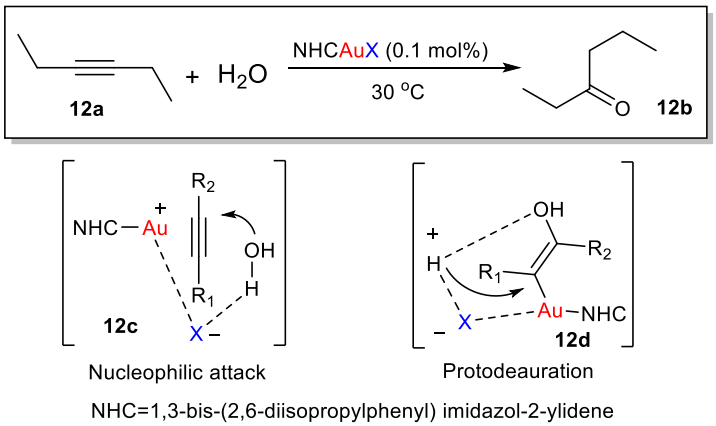


Scheme 4.12 Gold(I)-catalyzed hydration reaction of alkyne (investigation on counterion effect) (Zuccaccia 2016). [19]

Then, high gold(I) affinity index values are accompanied by low gold(I) activity but high gold(I) affinity index values correspond to strong hydrogen bond ability of the counterion. However, strong hydrogen bond ability is necessary for counterions that participate to a reaction with active proton. The balance between these two contrasting features is not so clear. A good yield is received as a result of a good balance between basicity and gold coordination ability of the counterion (Table 4.2). [19]

Table 4.2 Experimental data of counterion effect on the gold(I)-catalyzed hydration reaction of alkyne. [19]

| X | $BF_4$ | $SbF_6$ | BArF | OTf | $NTf_2$ | OTs | TFA |
|---|---|---|---|---|---|---|---|
| Ketone yield/ % | **< 1** | **< 1** | **< 1** | **> 99** | **> 99** | **< 1** | **< 1** |

The exact mechanism of counterions participation in asymmetric synthesis is not well defined. However, from the existing data on the field, the researchers converge that a chiral counterion (Scheme 4.13) can induce the asymmetric synthesis (Scheme 4.14).

The reactions follow a mechanism including a dinuclear gold complex. Chiral counterions could orientate the substrate at the right orientation to induce enantioselectivity. Moreover, chiral ligands combined with chiral counterion can give better results. [20]

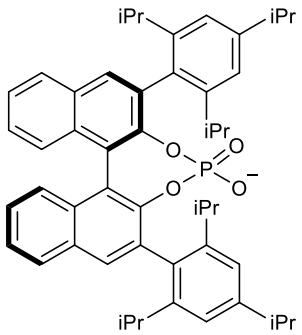


(R)-TRIP

Scheme 4.13 Chiral counterion (R)-TRIP induce enantioselectivity. [20]

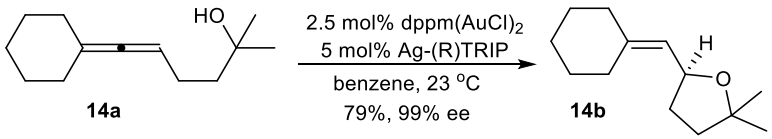


Scheme 4.14 Chiral counterion strategy for enantioselective functionalization of allenes ee=enantiomeric excess. [20]

In the previous section we referred to the role of ligands as a factor for divergent reactions. In fact, counterions can play a similar role. Counterions can differentiate the mechanism of the Au(I)-catalyzed reaction. There are several examples showing the role of counterions.

A divergent cycloisomerization of homopropargylic ketones due to counterions $SbF_6^-$ and $OTf^-$ has been reported (Scheme 4.15). [21] Noteworthy, the solvent also may play a crucial role on the mechanism of this reaction affecting the activity of the gold(I) catalyst.

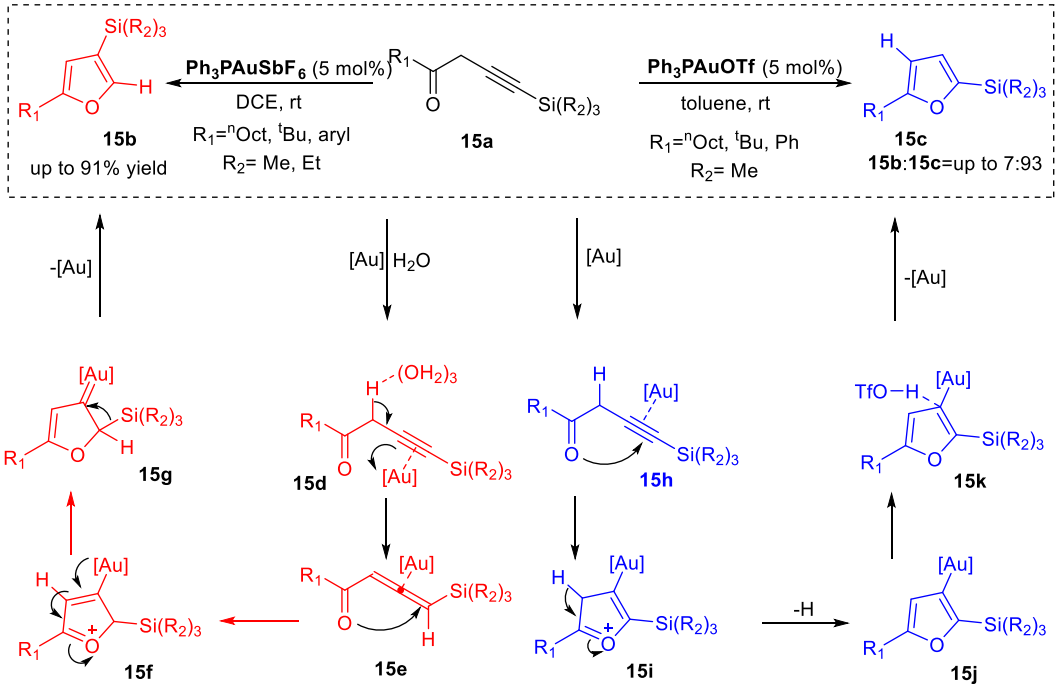


Scheme 4.15 Counterion directed divergent cycloisomerization of homopropargyl ketones (Li and Gevorgyan 2010). [21]

In the case of $TfO^-$ counterion, the reaction starts with a first step of alkyne activation by the gold(I) catalyst, followed by a 5-endo-dig cyclization. Carbonyl oxygen nucleophilic attack to triple bond forms the intermediate **15i**. Next, 1,2-hydride shift leads to the product **15c**. The 1,2-hydride shift consists of two steps; a deprotonation and protodeauration step that both catalyzed by $TfO^-$. [21]

The second path of the reaction where $SbF_6^-$ counterion is present, it is dominated by 1,2-Si shift. Similarly, the reaction starts with the activation of triple bond by gold(I) catalyst. However, an isomerisation step to form propargyl-allenyl intermediate **15e** is preceded to cyclization step. Possibly, due to $SbF_6^-$ counterion and water molecules this isomerization takes place. Next, a cyclization step leads to the intermediate **15f** and then to **15g**. Finally, 1,2-Si shift and deauration lead to the formation of the 3-silyl-substituted furan **15b**. The 1,2-Si shift was suggested by DFT calculations as the more favourable step kinetically. [21]

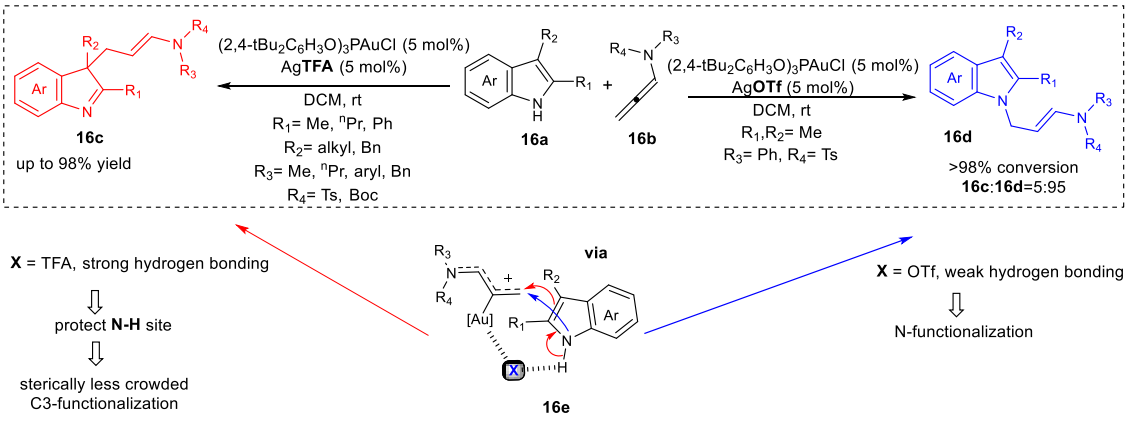


Scheme 4.16 Counterion directed divergent dearomatization of indoles with allenamides (Bandini 2014). [22,23]

Another example of the critical role of counterions on the mechanism of the reaction is the reaction of C3-alkyl indoles with allenamides. [22,23] According to Scheme 4.16, 2,3-disubstituted indoles **16a** react with allenamides **16b** to form either C3-alkylation product **16c** or N-alkylation product **16d**. The reaction proceeds with the catalyst $(2,4\text{-}tBu_2C_6H_3O)_3PAuCl$ and an ion chloride scavenger, either AgOTf or AgTFA. N-alkylation product **16d** is favored by $TfO^-$ counterion, while C3-alkylation product **16c** and dearomatization of indole is favored by $TFA^-$ counterion.

$TFA^-$ counterion's trait has much stronger hydrogen bonding ability than $TfO^-$ counterion. Consequently, these two counterions present different coordinating tendency, changing the mechanism of the reaction. The intermediate **16e** is the structure in which counterion reveals its regulating role. $TFA^-$ counterion forms a strong hydrogen bond with N-H, and by weakening the nucleophilicity of N the reaction proceeds with the nucleophilic attack to the allene by C3 carbon of indole forming the product **16c**. On the contrast, $TfO^-$ with low ability for hydrogen bonding, facility the nucleophilic attack to activated allenamide by the N of the intermediate **16e** to form the N-alkylation product **16d**. [22,23]

Additives are compounds that accompany catalysts and increase its activity. The role of the additives is not clear enough. It has been proposed that an additive can act as:

a. hydrogen bond acceptor

b. gold(I) catalyst activator

c. acidic co-catalyst. [15]

d. hydrogen bond acceptor.

### 4.2.1 Additive as a hydrogen bond acceptor

Hydrogen bonding acceptors additives could act according to two possible models. Thus, an additive, like pyridine N-oxide, can assist to the formation of a positive charged intermediate due to its basicity. Afterwards, the intermediate undergoes protodeauration as shown in Scheme 4.17. [15]

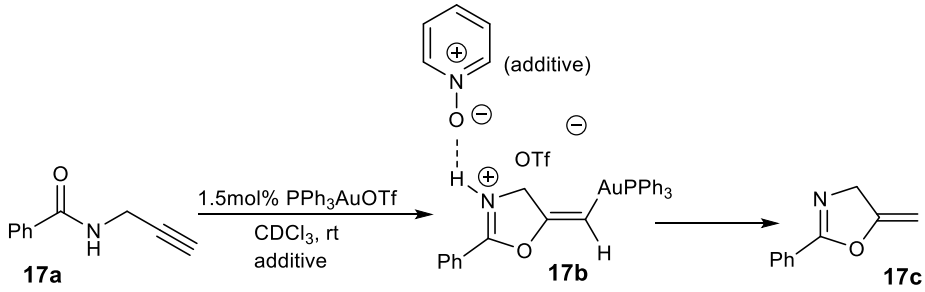


Scheme 4.17 Hydrogen bonding acceptor (pyridine N-oxide) in gold(I) catalyzed cyclization of propargyl amide (Hammond 2021). [15]

Another possible contribution of a hydrogen bond acceptor additive is revealed with triazole additives (Scheme 4.18). Triazole coordinates with $Ph_3PAu^+$, stabilizes gold(I) cation and retards catalyst decomposition. [24]

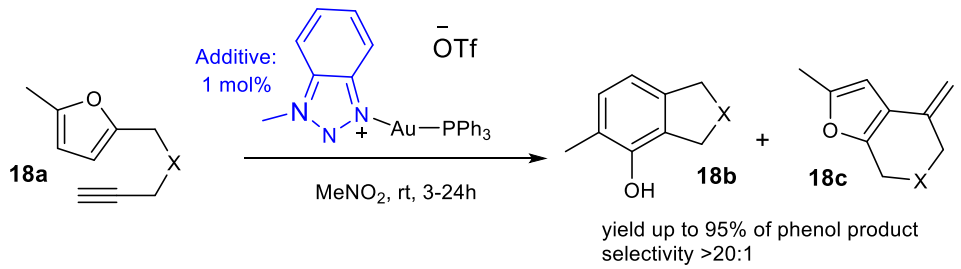


Scheme 4.18 Triazole-gold(I) complex catalyzed phenol synthesis (Shi 2010). [24]

### 4.2.2 Additive as a gold(I) catalyst activator

In many cases, inactive gold(I) catalyst is used in its chloride form. Silver salts work as chloride scavengers, releasing gold(I) cationic catalyst according to the following reaction

$$LAuCl + AgOTf \rightarrow LAuOTf + AgCl \downarrow$$

Excess of silver salt increases the efficiency of catalysis. [25]

Another category of catalyst activator are metals triflates like $Yb(OTf)_3$. $Yb(OTf)_3$ is a Lewis acid that complexes with chloride anion of the catalyst, e.g. $(PMe_3)AuCl$, and releases the active gold(I) form of it. It is remarkable that the catalyst is more efficient when it is activated by the additive than in its active form $(PMe_3)AuOTf$ . [26]

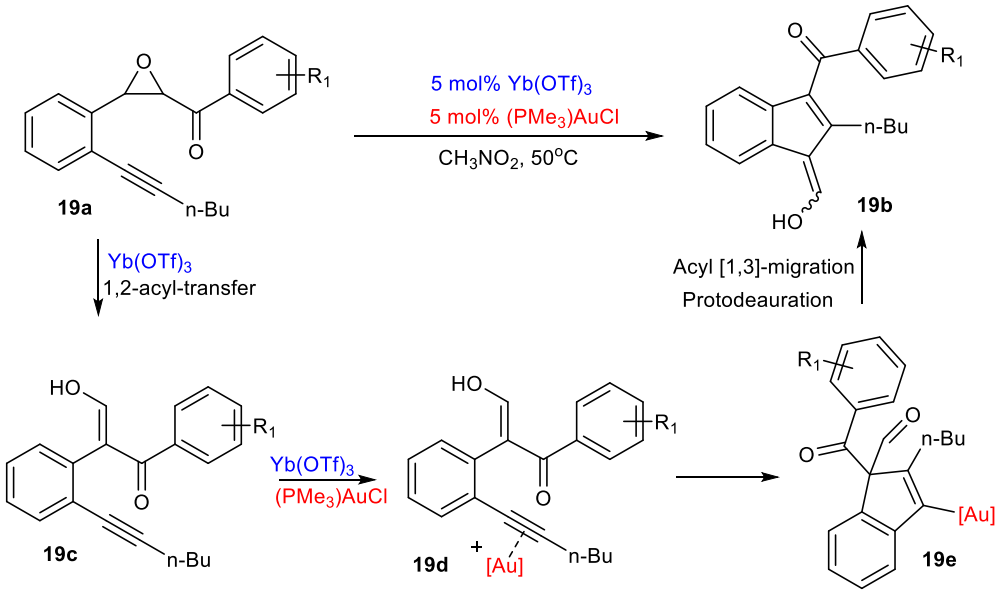


Scheme 4.19 Yb(III) activation of gold(I) in the rearrangement reaction of epoxy alkynes (Shi 2010). [26]

### 4.2.3 Additive as acidic co-catalyst

Acidic co-catalysts could have a synergistic effect in gold(I) catalyzed reactions, assisting gold (I) at a still not defined mechanism.

An acidic co-catalyst can act as a Lewis acid or a Brönsted-Lowry acid to increase cationic gold (I) acidity (Scheme 4.20).

Another way that an acidic co-catalyst can act as Lewis acid is revealed through gallium salts that have a synergistic effect on the gold(I)-catalyzed reaction of diketone with activated alkyne. A suggested explanation is that gallium cations stabilize the enolic form of diketone via chealation and increase the nucleophilicity of

diketone (Scheme 4.21). According to DFT calculations that verify the previous assumption the energy difference between HOMO and LUMO reduces due to the synergy of gallium with gold catalyst. [27]

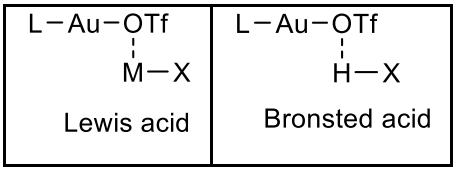


Scheme 4.20 Two possible ways of action of acidic co-catalyst as a Lewis acid or Brönsted-Lowry acid. [15]

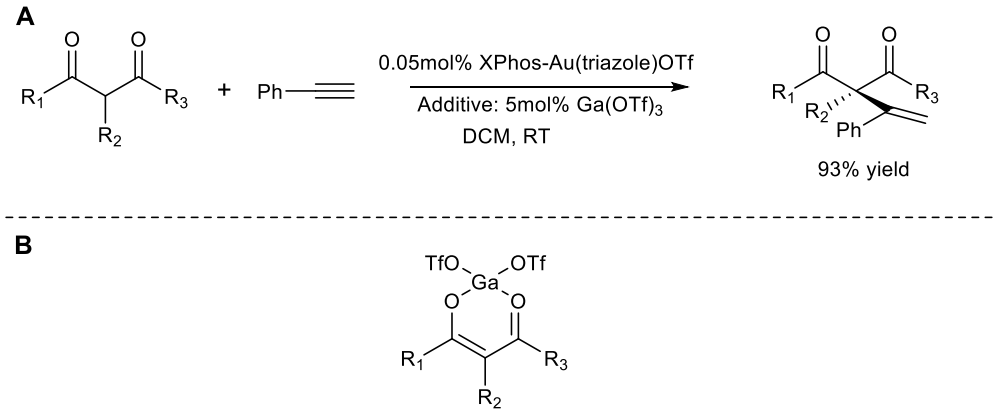


Scheme 4.21 A. Au(I)/Ga(III) catalytic system in ambient Nakamura reaction. B. Ga(III) diketone complex as active intermediate formed during the catalytic cycle (Petersen 2014). [28]

### 4.2.4 Additive as a hydrogen bond donor

An acid can facilitate a gold(I)-catalyzed reaction through hydrogen bonding donor effect. [29] The action of the acids is related to the protodeauration step of the gold(I)-catalyzed reaction (Scheme 4.22).

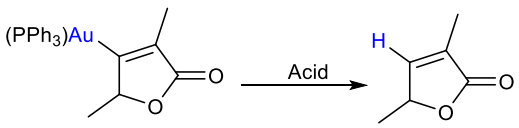


Scheme 4.22 Study of protodeauration using acids of different strengths.

As the acid gets stronger the conversion gets faster. The relation between the strength of acid and reaction rate is shown in Table 4.3.

Table 4.3 pKa values of various acids in relation to their catalytic ability on the reaction of Scheme 4.22. [29]

| Acid | pKa | Conversion |
|---|---|---|
| TfOH | -14 | 100% in 5 min |
| TsOH | -2 | 80% in 1h |
| $CF_3COOH$ | -0.25 | 70% in 1h |
| $CH_3COOH$ | 4.76 | 0% in 12h |

**4.3 Bibliography**

(1) Solas, M.; Muñoz, M. A.; Suárez-Pantiga, S.; Sanz, R. Regiodivergent Hydration-Cyclization of Diynones under Gold Catalysis. *Org. Lett.* **2020**, *22* (19), 7681−7687.

(2) Morán-Poladura, P.; Suárez-Pantiga, S.; Piedrafita, M. . R.; E.; González, J. M. Regiocontrolled Gold(I)-Catalyzed Cyclization Reactions of N-(3-Iodoprop-2-Ynyl)-N-Tosylanilines. *J. Organomet. Chem.* **2011**, *696* (1), 12−15.

(3) Wang, T.; Shi, S.; Vilhelmsen, H. M.; Zhang, T.; Rudolph, M. .; Rominger, F.; Hashmi, A. S. K. Chemoselectivity Control: Goldcatalyzed Synthesis of 6,7-Dihydrobenzofuran-4(5H)-Ones and Benzofurans from 1-(Alkynyl)-7-Oxabycyclo[4.1.0]Heptan-2-Ones. *Chem. - Eur. J.* **2013**, *19* (37), 12512−12516.

(4) Gimeno, A.; Cuenca, A. B.; Suárez-Pantiga, S.; de Arellano, C.; R.; Medio-Simón, M.; Asensio, G. Competitive Gold-Activation Modes in Terminal Alkynes: An Experimental and Mechanistic Study. *Chem. - Eur. J.* **2014**, *20* (3), 683−688.

(5) Fang, W.; Tang, X.-Y.; Shi, M. Gold(I)-Catalyzed Intramolecular Hydroarylation and the Subsequent Ring Enlargement of Methylenecyclopropanes to Cyclobutenes. *RSC Adv.* **2016**, *6* (46), 40474−40479.

(6) Sanz, R.; Miguel, D.; Rodríguez, F. Gold(I)-Catalyzed Tandem Reactions Initiated by 1,2-Indole Migrations. *Angew. Chem., Int. Ed.* **2008**, *47* (38),

7354−7357.

(7) Álvarez, E.; Miguel, D.; García-García, P. . F.-; Rodríguez, M. A.; Rodríguez, F.; Sanz, R. Solvent and Ligand Induced Switch of Selectivity in Gold(I)-Catalyzed Tandem Reactions of 3- Propargylindoles. *Beilstein J. Org. Chem.* **2011**, *7*, 786−793.

(8) Estela Álvarez, Olalla Nieto Faza, Carlos Silva López, Manuel A. Fernández-Rodríguez, R. S. Brønsted Acid-Catalyzed Cascade Reactions Involving 1,2-Indole Migration. *Chem. – A Eur. J.* **2015**, *21*, 12889–12893.

(9) Sanz, R., Miguel, D., Gohain, M., García-García, P., Fernández-Rodríguez, M., González-Pérez, A., Nieto-Faza, O., de Lera, Á. and Rodríguez, F. Synthesis of Diverse Indole-Containing Scaffolds by Gold(I)-Catalyzed Tandem Reactions of 3-Propargylindoles Initiated by 1,2-Indole Migrations: Scope and Computational Studies. *Chem. – A Eur. J.* **2010**, *16* (32), 9818–9828.

(10) Prakash D. Jadhav, Xin Lu, and R.-S. L. Gold-Catalyzed [5+2]- and [5+1]-Annulations between Ynamides and 1,2-Benzisoxazoles with Ligand-Controlled Chemoselectivity. *ACS Catal.* **2018**, *8* (10), 9697–9701. https://doi.org/10.1021/acscatal.8b03011.

(11) R. Vanjari, S. Dutta, B. Prabagar, V. Gandon, A. K. S. Ring Expansion and 1,2-Migration Cascade of Benzisoxazoles with Ynamides: Experimental and Theoretical Studies. *Chem. - Asian J.* **2019**, *14* (24), 4828–4836.

(12) Mauleón, P.; Zeldin, R. M.; González, A. Z.; Toste, F. D. Ligand-Controlled Access to [4 + 2] and [4 + 3] Cycloadditions in Gold-Catalyzed Reactions of Allene-Dienes. *J. Am. Chem. Soc.* **2009**, *131* (18), 6348−6349.

(13) Alonso, I.; Trillo, B.; López, F.; Montserrat, S.; Ujaque, G. .; Castedo, L.; Lledós, A.; Mascareñas, J. L. Gold-Catalyzed [4C+2C] Cycloadditions of Allenedienes, Including an Enantioselective Version with New Phosphoramidite-Based Catalysts: Mechanistic Aspects of the Divergence between [4C+3C] and [4C+2C] Pathways. *J. Am. Chem. Soc.* **2009**, *131* (36), 13020−13030.

(14) Alcarazo, M.; Stork, T.; Anoop, A.; Thiel, W.; Fürstner, A. Steering the Surprisingly Modular π-Acceptor Properties of N-Heterocyclic Carbenes: Implications for Gold Catalysis. *Angew. Chem., Int. Ed.* **2010**, *49* (14), 2542−2546.

(15) Zhichao Lu, Tingting Li, Sagar R. Mudshinge, Bo Xu, and G. B. H. Optimization of Catalysts and Conditions in Gold(I) Catalysis—Counterion and Additive Effects. *Chem. Rev.* **2021**, *121* (14), 8452–8477.

(16) Macchioni, A. Ion Pairing in Transition-Metal Organometallic Chemistry. *Chem. Rev.* **2005**, *105* (6), 2039−2074.

(17) Ciancaleoni, G.; Belpassi, L.; Zuccaccia, D.; Tarantelli, F. .; Belanzoni, P. Counterion Effect in the Reaction Mechanism of NHC Gold(I)-Catalyzed Alkoxylation of Alkynes: Computational Insight into Experiment. *ACS Catal.* **2015**, *5* (2), 803–814.

(18) Lu, Z.; Han, J.; Okoromoba, O. E.; Shimizu, N.; Amii, H. .; Tormena, C. F.; Hammond, G. B.; Xu, B. Predicting Counterion Effects Using a Gold Affinity Index and a Hydrogen Bonding Basicity Index. *Org. Lett.* **2017**, *19* (21), 5848−5851.

(19) Gatto, M.; Belanzoni, P.; Belpassi, L.; Biasiolo, L.; Del Zotto, A. .; Tarantelli, F. . Z. Solvent-, Silver-, and Acid-Free NHC-Au-X Catalyzed Hydration of Alkynes. The Pivotal Role of the Counterion. *ACS Catal.* **2016**, *6* (11), 7363−7376.

(20) Hamilton, G. L.; Kang, E. J.; Mba, M.; Toste, F. D. A Powerful Chiral Counterion Strategy for Asymmetric Transition Metal Catalysis. *Science (80-. ).* **2007**, *317* (5837), 496−499.

(21) Dudnik, A. S.; Xia, Y.; Li, Y.; Gevorgyan, V. Computation- Guided Development of Au Catalyzed Cycloisomerizations Proceeding via 1,2-Si or 1,2-H Migrations: Regiodivergent Synthesis of Silylfurans. *J. Am. Chem. Soc.* **2010**, *132* (22), 7645−7655.

(22) Jia, M.; Cera, G.; Perrotta, D.; Monari, M.; Bandini, M. Taming Gold(I)-Counterion Interplay in the Dearomatization of Indoles with Allenamides. *Chem. - Eur. J.* **2014**, *20* (32), 9875−9878.

(23) Rocchigiani, L.; Jia, M.; Bandini, M.; Macchioni, A. Assessing the Role of Counterion in Gold-Catalyzed Dearomatization of Indoles with Allenamides by NMR Studies. *ACS Catal.* **2015**, *5* (7), 3911−3915.

(24) Chen, Y.; Yan, W.; Akhmedov, N. G.; Shi, X. 1,2,3-Triazole as a Special "X-Factor" in Promoting Hashmi Phenol Synthesis. *Org. Lett.* **2010**, *12* (2), 344–347.

(25) Weber, D.; Gagné, M. R. Dinuclear Gold-Silver Resting States May Explain Silver Effects in Gold(I)-Catalysis. *Org. Lett.* **2009**, *11* (21), 4962−4965.

(26) Dai, L.-Z.; Shi, M. Gold(I)- and Yb(OTf)3-Cocatalyzed Rearrangements of Epoxy Alkynes: Transfer of a Carbonyl Group in a Five-Membered Carbocycle. *Chem. - Eur. J.* **2010**, *16* (8), 2496−2502.

(27) Rameswar Bhattacharjee, A. N. and A. D. Mechanistic Insights into the Synergistic Catalysis by Au(i), Ga(Iii), and Counterions in the Nakamura Reaction. *Org. Biomol. Chem.* **2015**, *13*, 7412–7420.

(28) Xi, Y.; Wang, D.; Ye, X.; Akhmedov, N. G.; Petersen, J. L. . S.; X. Synergistic Au/Ga Catalysis in Ambient Nakamura Reaction. *Org. Lett.* **2014**, *16* (1), 306–309.

(29) Liu, L.-P.; Xu, B.; Mashuta, M. S.; Hammond, G. B. Synthesis and Structural Characterization of Stable Organogold(I) Compounds. Evidence for the Mechanism of Gold-Catalyzed Cyclizations. *J. Am. Chem. Soc.* **2008**, *130* (52), 17642−17643.

# Chapter 5

## Reaction Pathways Modeling Basics

### 5.1 Computational methods

Density functional theory is nowadays among the most widely employed electronic structure models for molecular simulations. DFT combines the benefits of the low computational cost of single determinant models with the recovery of electron correlation comparable to higher order and more costly ab-initio methods. Thus, throughout this work, the Kohn–Sham formulation of density functional theory was employed. [1,2]

### 5.2 Density Functional Theory - Kohn-Sham approximation

According to Kohn Hohenberg-Kohn theorems if we know the electron density we can describe the state of a system and the electron density on ground state matches to the minimum energy of the system. But there were not any manner to find them without the use of wave function Ψ until Kohn and Sham [2] introduced a functional with the type below.

$$F[\rho(r)]=T[\rho(r)]+\xi_{XC}[\rho(r)] \quad (5.1)$$

Where T[ρ(r)] is the functional of kinetic energy of the many electron system and $\xi_{XC}[\rho(r)]$ is the functional of exchange correlation.

So, the energy of a many electron system can be written as

$$E[\rho(r)]=T[\rho(r)]+V_{ne}[\rho(r)]+V_{ee}[\rho(r)]+E_{XC}[\rho(r)] \quad (5.2)$$

Where $V_{ne}[\rho(r)]$ is the functional of potential energy because of the interaction electron- nuclei

$V_{ee}[\rho(r)]$ is the functional of potential energy because of the interaction electron-electron

and $E_{XC}[\rho(r)]$ is the functional of exchange correlation energy. [3]

According to Kohn-Sham model, the kinetic energy term is divided in two parts. The first term is the kinetic energy of a fictitious model system of non-interacting electrons whose the kinetic energy is the sum of the individual electronic kinetic energies and is calculated exactly. The second term is the exchange-correlation energy that includes all the interactions that are not described in the previews terms. We set the total electron density in ground state $\rho_s$ equal to the demanding density $\rho_o$ of a

interactive many electron real system. In this way the kinetic energy of non-interacting electrons $T_s$ can be expressed on relation of one electron orbitals. Finally, the equation (5.2) transformed to

$$E[\rho(r)]=T_s[\rho(r)]+V_{ne}[\rho(r)]+V_{ee}[\rho(r)]+E_{XC}[\rho(r)] \quad (5.3)$$

The optimisation of the system can be succeeded by solving the one electron equation Kohn-Sham. There is one KS equation for every electron. The KS equations are similar to HF equations but KS include electron correlation effect. KS equations are of the below type. [4, 5]

$$h_i^{KS}\varphi_i^{KS}=\varepsilon_i^{KS}\varphi_i^{KS} \quad (5.4)$$

Finally, it can be proved that electron density is given by the equation 5.5

$$\rho(r)=\Sigma|\psi_i^{KS}(r)|^2 \quad (5.5)$$

### 5.3 DFT Methods

Variable DFT methods have been developed with gradient complication. These methods from the most simple to more complicated are the local density approximation (LDA), the generalized gradient approximation (GGA), meta-GGA (MGGA), hybrid GGA (HGGA) and double-hybrid density functionals (DH).

LDA

The main idea of LDA is that we suppose a homogenous electron density cloud. At such a simple model it is feasible the elucidation of the form of exchange-correlation energy functional.

$$E_{XC}^{LDA}[\rho] = \int \rho(\vec{r})\varepsilon_{xc}(\rho(\vec{r}))d\vec{r} \quad (5.6)$$

Where $\varepsilon_{XC}$ is the exchange-correlation energy for each particle in the homogenous electron cloud. The term $\varepsilon_{XC}$ can be split into the term of correlation and to the term of exchange.

$$\varepsilon_{XC}(\rho(\vec{r})) = \varepsilon_X(\rho(\vec{r})) + \varepsilon_C(\rho(\vec{r})) \quad (5.7)$$

The term of exchange is exact known and for the term of correlation there are some different expressions [6,7]

GGA

In fact, the assumption of homogenous electron density is not realistic. New functionals that contain derivatives of electron density to describe the heterogeneity of

electron density and the solution to the problem of the holes of functionals led to GGA functionals. GGA functionals are described as below

$$E_{XC}^{GGA}[\rho_\alpha,\rho_\beta] = \int f(\rho_\alpha,\rho_\beta,\nabla\rho_\alpha,\nabla\rho_\beta)d\vec{r} \quad (5.8)$$

The $E_{XC}^{GGA}$ can be split into functionals, one of exchange and another of correlation.

$$E_{XC}^{GGA} = E_X^{GGA} + E_C^{GGA} \quad (5.9)$$

The exchange functional can be expressed as below

$$E_X^{GGA} = E_X^{LDA} - \sum_\sigma \int F(s_\sigma)\rho_\sigma^{4/3}(\vec{r})d\vec{r} \quad (5.10)$$

The term $s_\sigma$ is a parameter of local heterogeneity. At a homogenous electron density cloud the value of $s_\sigma$ =0 at every point.

The factor F is crucial for the behavior of the exchange functional. The way that F is calculated classifies GGA exchange functional. Two groups of GGA exchange functional have been developed. At the first type of GGA exchange functional are FT97, PW91, CAM(A) and CAM(B). [8,9,3]

The second group of GGA exchange functionals consists of B86, P, LG, PBE and later the PW91 and LYP. [10,11,12,13,6,14]

Meta generalized gradient approximation (MGGA)

The MGGA functionals are functionals in which there is a term of Laplacian of electron density (the second derivative of electron density). MGGA functionals are the BB95, τ-HCTH, TPSS, M06-L, M11-L, MN12-L, VSXC [15,16,17,18,19,20]

Hybrid generalized gradient approximation (HGGA)

HGGA functionals are these functionals in which a part of the exchange energy is calculated by HF. The part of correlation energy is calculated by various types of functionals. The percentage of distribution of HF exchange energy as well the type of functionals they are used define the HGGA. At the first HGGA functional which was developed by Becke (1.29) the parameters α, b and c are semiempirical and their values after optimization are α=0.20, b=0.72 and c=0.81.

$$E_{XC}^{B3PW91} = (1-\alpha)E_X^{LSDA} + \alpha E_X^{HF} + b\Delta E_X^{B} + E_C^{LSDA} + c\Delta E_C^{PW91} \quad (5.11)$$

The HGGA functional B3LYP, that faces a widespread use, has the same values of the coefficients α, b and c. The B3LYP model is describes by the equation (5.12)

$$E_{XC}^{B3LYP}=(1-\alpha)E_X^{LSDA}+\alpha E_X^{HF}+b\Delta E_X^{B}+(1-c)E_C^{LSDA}+c\Delta E_C^{LYP} \quad (5.12)$$

For B3LYP the error for the energy bond calculated around 2kcal/mol.

Hybrid meta-generalized gradient approximation (HMGGA)

Following the same strategy with the production of HGGA functionals, the addition of HF exchange functional to MGGA produces HMGGA. MGGA functionals differ from GGA ones because they contain the Laplacian of electron density. Representative HMGGA functionals are the Minnesota functionals (M05, M05-2X, M06, M06-2X and M06-HF). [21,22,23]

Double hybrid density functional approximation (DHDFA)

Last, the most modern group of functionals are DHDFA. DHDFA introduced by Grimme in 2006. [24] The combination of exchange and correlation energies from wavefunctions and DFT is the main idea of DHDFA functionals. [25,26,27]

$$E_{DHDFA}=E_{HF}+\alpha_1 E_X^{DFT}+\alpha_2 E_X^{FOCK}+b_1 E_C^{DFT}+b_2 E_C^{postHF} \quad (5.13)$$

Where $E_X^{DFT}$ and $E_X^{FOCK}$ are the exchange energies from DFT and HF methods

$E_C^{DFT}$ and $E_C^{postHF}$ are the correlation energies from DFT and post-HF methods.

Representative DHDFA functionals are B2-PLYP, B2GP-PLYP and PWPB95.[24,28,29,30]

Throughout this work, the Kohn–Sham formulation of density functional theory was employed. The meta-hybrid density functional M06-2X has been used with the extended double-ζ quality Def2-SVPP basis set for all the static calculations.

### 5.3.1 Functional M06

The functional of choice is M06 because it is efficient enough to reproduce the effect of the donor properties of gold's ligand on the experimental barriers for bond rotation in gold carbenoids. On the contrary, other popular functionals like B3LYP or BP86 fail. [31,32] The meta-hybrid density functional M06 [33] has been used with the extended double-ζ quality Def2-SVPP basis set for all the static calculations. [34] This combination of density functional and basis set has been found to provide good performance in homogeneous gold catalysis. [32]

For M06, as a meta-hybrid fuctional, the hybrid exchange-correlation energy can be described by the relation

$$E_{XC}^{hyb} = \frac{X}{100} E_X^{HF} + \left(1 - \frac{X}{100}\right) E_X^{DFT} + E_C^{DFT} \quad (5.14)$$

where $E_X^{HF}$ is the nonlocal Hartree–Fock (HF) exchange energy,
$X$ is the percentage of Hartree–Fock exchange in the hybrid functional,
$E_X^{DFT}$ is the local DFT exchange energy,
and $E_C^{DFT}$ is the local DFT correlation energy.

All geometry optimizations have been carried out using tight convergence criteria and a pruned grid for numerical integration with 99 radial shells and 590 angular points per shell. In some challenging cases, this grid was enlarged to 175 radial shells and 974 points per shell for first row atoms and 250 shells and 974 points per shell for heavier elements. These challenging optimizations are usually associated with very soft vibrational modes (usually internal rotations). Analysis of the normal modes obtained via diagonalization of the Hessian matrix was used to confirm the topological nature of each stationary point.

### 5.3.2 Minimization algorithm [35, 4, 36]

For the optimization of structures Gaussian09 software was used. Accordingly, it is presented in brief the optimization algorithm either for the extraction of a minimum either for a transition state structure. At the beginning, Berny algorithm was released as “a modified conjugate gradient algorithm for geometry optimization is outlined for use with *ab* initio MO methods” but also is applied to DFT methods in our calculations on Gaussian09. At each step, a one-dimensional minimization using a quartic polynomial is carried out, followed by an n-dimensional search using the second derivative matrix. By suitably controlling the number of negative eigenvalues of the second derivative matrix, the algorithm can also be used to locate transition structures.

For minimum, maximum and saddle point the first order derivative of potential energy function is zero. To investigate if a point is maximum, minimum or saddle point it is necessary to calculate the force constant (Hessian) matrix or else a second order derivative criterion. Hessian matrix is the matrix whose elements are second order derivatives of potential energy at that point. Using the eigenvalues of the Hessian matrix we conclude about the nature of the structure. If all eigenvalues of the force constant matrix are positive, the point is a minimum. If all eigenvalues of the

force constant matrix are negative the point is a maximum and if there is only one negative (imaginary) eigenvalues of the force constant matrix then it is a saddle point.

The optimization converges when the root-mean-square gradient and the absolute value of the largest component of the gradient must fall below their respective thresholds.

For the elicitation of a transition structure the above minimization algorithm can be modified properly, forcing the second derivative matrix to contain a single negative eigenvalue.

The above algorithm designed for ab-initio methods, is applied also at DFT on Gaussian09 software. [36]

### 5.3.3 Wavefunction stability [37 ,36]

The wavefunction stability for each optimized structure has also been checked. A stability analysis can be applied to determine if the SCF solution found is stable with respect to variations which break spin and/or spatial symmetry. The total energy E of the system is given by $E=E_{N1}+E_{J1}+E_{XC}$. The variation of the KS energy $E$ can be written as $\delta E=\delta E_N+\delta E_1+\delta E_2$

### 5.3.4 Intrinsic Reaction Coordinate (IRC) [38, 4]

The IRC is the steepest descent path from the transition-state point to a stable equilibrium point where the vibrational and rotational movement are absent. Along this path the gradient of the potential energy is maximized. The IRC equation with internal motion is

$$\frac{\sum_{j=1}^{n} a_{1j}dq_j}{\frac{\partial V}{\partial q_1}} = \frac{\sum_{j=1}^{n} a_{2j}dq_j}{\frac{\partial V}{\partial q_2}} = \ldots = \frac{\sum_{j=1}^{n} a_{nj}dq_j}{\frac{\partial V}{\partial q_n}} \quad (5.15)$$

where

$$a_{ij} = \sum_{\alpha=1}^{N} M_\alpha \left( \frac{\partial X_\alpha}{\partial q_i}\frac{\partial X_\alpha}{\partial q_j} + \frac{\partial Y_\alpha}{\partial q_i}\frac{\partial Y_\alpha}{\partial q_j} + \frac{\partial Z_\alpha}{\partial q_i}\frac{\partial Z_\alpha}{\partial q_j} \right) \quad (5.16)$$

and

$$dX_\alpha = \sum_{i=1}^{n} \frac{\partial X_\alpha}{\partial q_i} dq_i, \; dY_\alpha = \sum_{i=1}^{n} \frac{\partial Y_\alpha}{\partial q_i} dq_i, \; dZ_\alpha = \sum_{i=1}^{n} \frac{\partial Z_\alpha}{\partial q_i} dq_i \quad (5.17)$$

The utility of the method is that we can extract details on the mechanism of a chemical reaction, focusing on the interactions of HOMO and LUMO orbitals on the obtained consecutive geometries along the reaction path. [39]

### 5.3.5 Solvation

Solvation effects have been taken into account variationally throughout the optimization procedures via the polarizable continuum model (PCM) [40] using parameters for dichloromethane and taking advantage of the smooth switching function developed by York and Karplus. [41]

### 5.3.6 Model catalyst

Concerning the structures involved in these simulations, we simplified the cationic gold complex employed in the experimental work using 1,3-bis-methyl-imidazol-2-ylidene gold as a simpler model of the catalyst IPrAuCl/$AgNTf_2$ and trimethyl-phosphine gold for tBuXPhosAu(MeCN)$SbF_6$ used in the experimental work [42,43] in order to find a balance between accuracy and computational efficiency. All the calculations performed in this work have been carried out with the Gaussian 09 program. [36]

## 5.4 Bibliography


(1) Hohenberg, P. and Kohn, W. Inhomogeneous Electron Gas. *Phys. Rev.* **1964**, *136* (3B), B864–B871.

(2) Kohn, W. and Sham, L. J. Self-Consistent Equations Including Exchange and Correlation Effects. *Phys. Rev.* **1965**, *140* (4A), A1133–A1138.

(3) Kolocouris, A. *Υπολογιστική Χημεία Μοριακών Συστημάτων-Βασικά Πρότυπα Και Εργαστηριακές Ασκήσεις*; 2011.

(4) Α.Κολοκουρης. *Υπολογιστική Χημεία-Μοριακές Προσομοιώσεις. Θεωρίες, Μέθοδοι Και Εφαρμογές.*; Επιστημονικές εκδόσεις Παρισιανού Α.Ε., 2021.

(5) Christopher J. Cramer. *Essentials of Computational Chemistry-Theories and Models*; John Wiley and Sons Ltd, 2004.

(6) John P. Perdew and Yue Wang. Accurate and Simple Analytic Representation of the Electron-Gas Correlation Energy. *Phys. Rev. B.* **1992**, *45* (23), 13244–13249.

(7) S. H. Vosko, , L. Wilk, and, M. N. Accurate Spin-Dependent Electron Liquid Correlation Energies for Local Spin Density Calculations: A Critical Analysis. *Can. J. Phys.* **1980**, *58* (8), 1200–1211.

(8) Filatov M., Thiel W. A New Gradient-Corrected Exchange-Correlation Density Functional. *Mol. Phys.* **1997**, *91* (5), 847–860.

(9) Gregory J. Laming, Volker Termath, and N. C. H. A General Purpose Exchange-correlation Energy Functional. *J. Chem. Phys.* **1993**, *99* (11), 8765–8773.

(10) A. D. Becke. Density Functional Calculations of Molecular Bond Energies. *J. Chem. Phys.* **1986**, *84* (8), 4524–4529.

(11) John P. Perdew. Density-Functional Approximation for the Correlation Energy of the

Inhomogeneous Electron Gas. *Phys. Rev. B* **1986**, *33* (12), 8822--8824.
(12) Lacks, Daniel J. and Gordon, R. G. Pair Interactions of Rare-Gas Atoms as a Test of Exchange-Energy-Density Functionals in Regions of Large Density Gradients. *Phys. Rev. A* **1993**, *47* (6), 4681–4690.
(13) Perdew, John P. and Burke, Kieron and Ernzerhof, M. Generalized Gradient Approximation Made Simple. *Phys. Rev. Lett.* **1996**, *77* (18), 3865–3868.
(14) Lee, Chengteh and Yang, Weitao and Parr, R. G. Development of the Colle-Salvetti Correlation-Energy Formula into a Functional of the Electron Density. *Phys. Rev. B* **1988**, *37* (2), 785–789.
(15) Becke, A. D. Density-functional Thermochemistry. IV. A New Dynamical Correlation Functional and Implications for Exact-exchange Mixing. *J. Chem. Phys.* **1996**, *104* (3), 1040–1046.
(16) Handy, A. D. B. and N. C. New Exchange-Correlation Density Functionals: The Role of the Kinetic-Energy Density. *J. Chem. Phys.* **2002**, *116* (22), 9559–9569.
(17) Tao, Jianmin and Perdew, John P. and Staroverov, Viktor N. and Scuseria, G. E. Climbing the Density Functional Ladder: Nonempirical Meta--Generalized Gradient Approximation Designed for Molecules and Solids. *Phys. Rev. Lett.* **2003**, *91* (14), 146401.
(18) Truhlar, Y. Z. and D. G. A New Local Density Functional for Main-Group Thermochemistry, Transition Metal Bonding, Thermochemical Kinetics, and Noncovalent Interactions. *J. Chem. Phys.* **2006**, *125* (19), 194101.
(19) Truhlar, R. P. and D. G. M11-L: A Local Density Functional That Provides Improved Accuracy for Electronic Structure Calculations in Chemistry and Physics. *J. Phys. Chem. Lett.* **2012**, *3* (1), 117–124.
(20) Scuseria, T. V. V. and G. E. A Novel Form for the Exchange-Correlation Energy Functional. *J. Chem. Phys.* **1998**, *109* (2), 400–410.
(21) Yan Zhao, Nathan E. Schultz, and D. G. T. Exchange-Correlation Functional with Broad Accuracy for Metallic and Nonmetallic Compounds, Kinetics, and Noncovalent Interactions. *J. Chem. Phys.* **2005**, *123* (16), 161103.
(22) Yan Zhao, Nathan E. Schultz, and D. G. T. Design of Density Functionals by Combining the Method of Constraint Satisfaction with Parametrization for Thermochemistry, Thermochemical Kinetics, and Noncovalent Interactions. *J. Chem. Theory Comput.* **2006**, *2* (2), 364–382.
(23) Zhao, Y., Truhlar, D. G. The M06 Suite of Density Functionals for Main Group Thermochemistry, Thermochemical Kinetics, Noncovalent Interactions, Excited States, and Transition Elements: Two New Functionals and Systematic Testing of Four M06-Class Functionals and 12 Other Function. *Theor Chem Acc.* **2008**, *120*, 215–241.
(24) Grimme, S. Semiempirical Hybrid Density Functional with Perturbative Second-Order Correlation. *J. Chem. Phys.* **2006**, *124* (034108).
(25) Igor Ying Zhang & Xin Xu. Doubly Hybrid Density Functional for Accurate Description of Thermochemistry, Thermochemical Kinetics and Nonbonded Interactions. *Int. Rev. Phys. Chem.* **2011**, *30* (1), 115–160.
(26) J. C. Sancho-García and C. Adamo. Double-Hybrid Density Functionals: Merging Wavefunction and Density Approaches to Get the Best of Both Worlds. *Phys. Chem. Chem. Phys.*, **2013**, *15*, 14581–14594.
(27) Goerigk, L.; Grimme, S. Double-hybrid Density Functionals. *Wiley Interdiscip. Rev. Comput. Mol. Sci.* **2014**, *4* (6), 576–600.
(28) Amir Karton, Alex Tarnopolsky, Jean-François Lamère, George C. Schatz, and J. M. L. M. Highly Accurate First-Principles Benchmark Data Sets for the Parametrization and Validation of Density Functional and Other Approximate Methods. Derivation of a Robust, Generally Applicable, Double-Hybrid Functional for Thermochemistry and Thermochemical . *J. Phys. Chem. A* **2008**, *112* (50), 12868–12886.
(29) Alex Tarnopolsky, Amir Karton, Rotem Sertchook, Dana Vuzman, and J. M. L. M. Double-Hybrid Functionals for Thermochemical Kinetics. *J. Phys. Chem. A* **2008**, *112*

(1), 3–8.
(30) Lars Goerigk and Stefan Grimme. Efficient and Accurate Double-Hybrid-Meta-GGA Density Functionals—Evaluation with the Extended GMTKN30 Database for General Main Group Thermochemistry, Kinetics, and Noncovalent Interactions. *J. Chem. Theory Comput.* **2011**, *7* (2), 291–309.
(31) Benitez, D., Shapiro, N., T. A Bonding Model for Gold(I) Carbene Complexes. *Nat. Chem* **2009**, *1*, 482–486.
(32) Faza, O.N., Rodríguez, R.Á. & López, C. S. Performance of Density Functional Theory on Homogeneous Gold Catalysis. *Theor Chem Acc* **2011**, *128*, 647–661.
(33) Zhao, Y.; Truhlar, D. G. The M06 Suite of Density Functionals for Main Group Thermochemistry, Thermochemical Kinetics, Noncovalent Interactions, Excited States, and Transition Elements: Two New Functionals and Systematic Testing of Four M06-Class Functionals and 12 Other Function. *Theor. Chem. Acc.* **2008**. https://doi.org/10.1007/s00214-007-0310-x.
(34) Bauernschmitt, R.; Ahlrichs, R. Stability Analysis for Solutions of the Closed Shell Kohn-Sham Equation. *J. Chem. Phys.* **1996**, *104* (22), 9047–9052. https://doi.org/10.1063/1.471637.
(35) Schlegel, H. B. Optimization of Equilibrium Geometries and Transition Structures. *J. Comput. Chem.*, **1982**, *3*, 214–218.
(36) Frisch, M. J. .; Trucks, G. W. .; Schlegel, H. B. .; Scuseria, G. E. .; Robb, M. A. .; Cheeseman, J. R.; Scalmani, G. .; Barone, V. .; Mennucci, B. .; Petersson, G. A.; Nakatsuji, H. .; Caricato, M. .; Li, X. .; Hratchian, H. P. .; Izmaylov, A. F. .; Bloi, D. J. Gaussian 09. Wallingford 2009.
(37) Rüdiger Bauernschmitt and Reinhart Ahlrichs. Stability Analysis for Solutions of the Closed Shell Kohn–Sham Equation. *J. Chem. Phys.* **1996**, *104*, 9047–9052.
(38) Kenichi Fukui. The Path of Chemical Reactions - the IRC Approach. *Acc. Chem. Res.* **1981**, *14* (12), 363–368. https://doi.org/10.1021/ar00072a001.
(39) Kenichi Fukui. Role of Frontier Orbital in Chemical Reaction. *Science (80-. ).* **1982**, *218*, 747–754.
(40) Tomasi, J.; Mennucci, B.; Cammi, R. Quantum Mechanical Continuum Solvation Models. *Chem. Rev*. **2005**. https://doi.org/10.1021/cr9904009.
(41) York, D. M.; Karplus, M. A Smooth Solvation Potential Based on the Conductor-like Screening Model. *J. Phys. Chem. A* **1999**, *103* (50), 11060–11079. https://doi.org/10.1021/jp992097l.
(42) Zhongyi Zeng, Hongming Jin, Jin Xie, Bing Tian, Matthias Rudolph, Frank Rominger, and A. S. K. H. α-Imino Gold Carbenes from 1,2,4-Oxadiazoles: Atom-Economical Access to Fully Substituted 4-Aminoimidazoles. *Org. Lett.* **2017**, *19* (5), 1020–1023.
(43) Xu, W.; Wang, G.; Sun, N.; Liu, Y. Gold-Catalyzed Formal [3 + 2] Cycloaddition of Ynamides with 4,5-Dihydro-1,2,4-Oxadiazoles: Synthesis of Functionalized 4-Aminoimidazoles. *Org. Lett.* **2017**, *19* (12), 3307–3310. https://doi.org/10.1021/acs.orglett.7b01469.

# Chapter 6

## Theoretical background

Among the plethora of organic reactions catalyzed by gold(I)/gold(III) [1,2,3,4,5,6,7,8] that are abundant in the literature, we chose to study those leading to products with a potential pharmacological interest. The activated alkyne-gold catalyst complex very often takes part in cyclization reaction to form heterocyclic compounds. Thus, heterocycles like indole, imidazole or carbazole can be synthesized by gold catalysis. [2] All these scaffolds are abundant not only on pharmaceutical compounds, but also on natural products. [9,10]

Due to the fact that indole is a common motif in biomolecules, many synthetic methods were developed for indole containing molecules or substituted indoles. [11] Nevertheless, indole derivatives still remain a desirable target for synthetic chemists and pharmacologists. In figure 1 are presented, in brief, some indole derivatives from the families of natural products and drugs. [12,13]

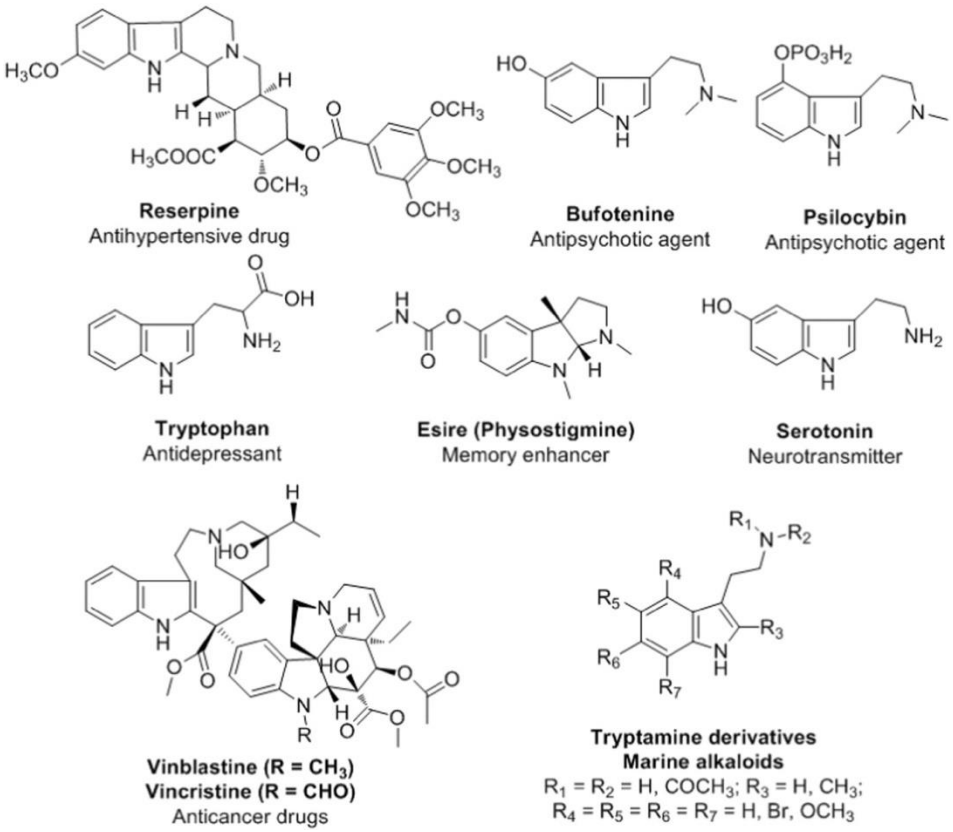


Figure 1. Bioactive natural alkaloids containing indole ring. [12]

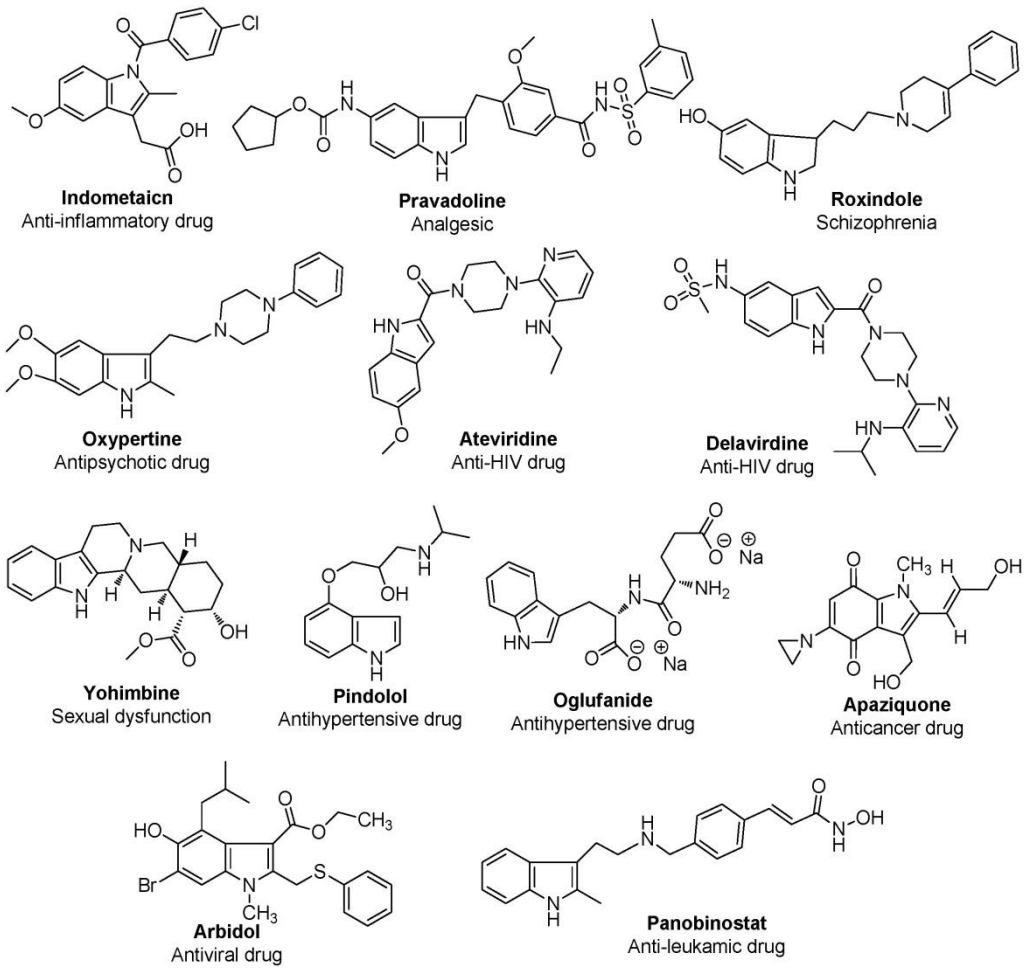


Figure 2. Few marketed drugs containing indole motif. [12]

Another molecule of interest, not such as indole but important enough to be ignored is carbazole. Synthetic methods for carbazoles are target for synthetic chemists since are biological active compounds exhibiting antimicrobial, antitumor, [14] antiepileptic, antihistaminic, antioxidative, anti-inflammatory, antidiarrhoeal, analgesic, neuroprotective and pancreatic lipase inhibition properties. [15] Moreover, they are frequently present at alkaloid natural products. [16,10] In figure 3 are presented some bioactive carbazoles found in natural products.

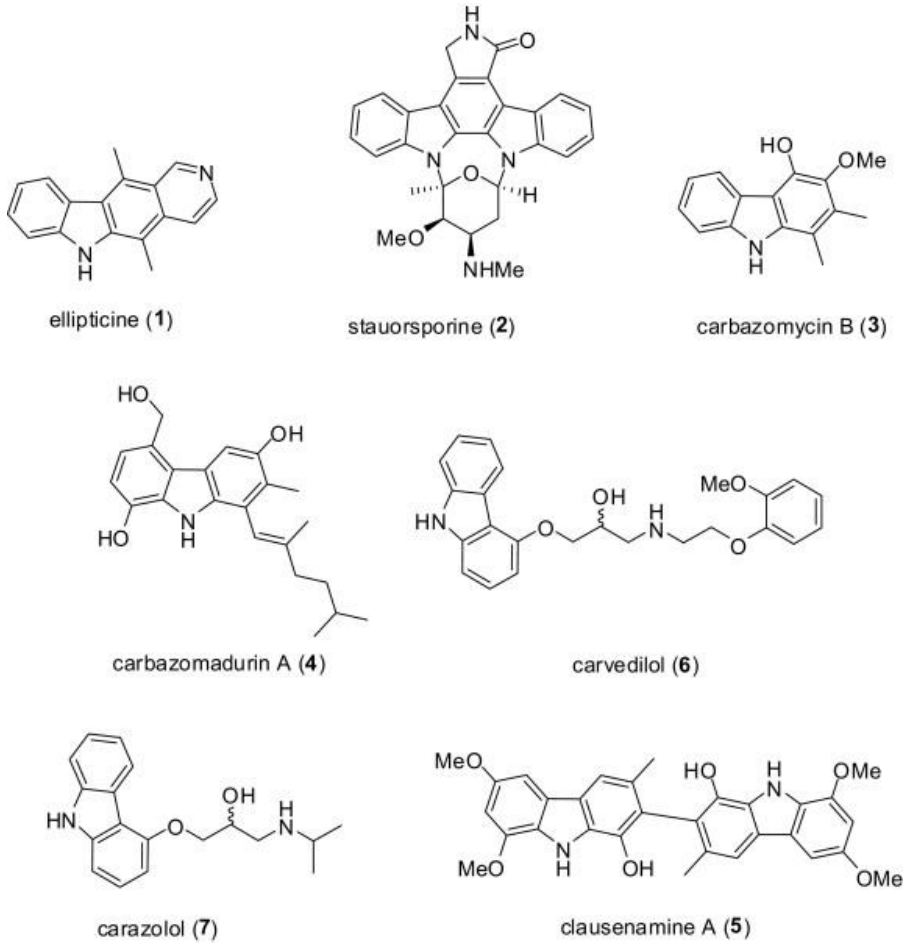


Figure 3. Bioactive carbazole natural products.[16]

Finally, the imidazole moiety is abundant in natural products [17] and drugs with a variety of biological activity. Imidazole derivatives reveal analgesic and anti-inflammatory activity, cardiovascular activity, anti-neoplastic activity, anti- fungal activity, anti- anthelmintic activity. [18]

| | | | |
|---|---|---|---|
| 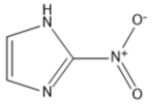 | 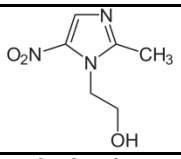 | 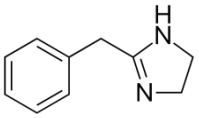 | 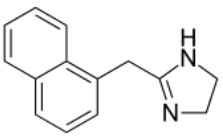 |
| 2-nitro imidazole | 1-(2-hydroxyethyl)-2-methyl-5-nitroimidazole | | naphazoline |
| (azomycin) | (metronidazole) | priscol | privine |
| anti-bacterial agent | anti-bacterial agent | vasodilating | vasoconstricting |

Figure 4. Various imidazole derivatives used as drugs. [18]

A small library of 4-aminoimidazole derivatives is already known for its activity as Src family kinase (SFK) inhibitors. [19], [20],[21]

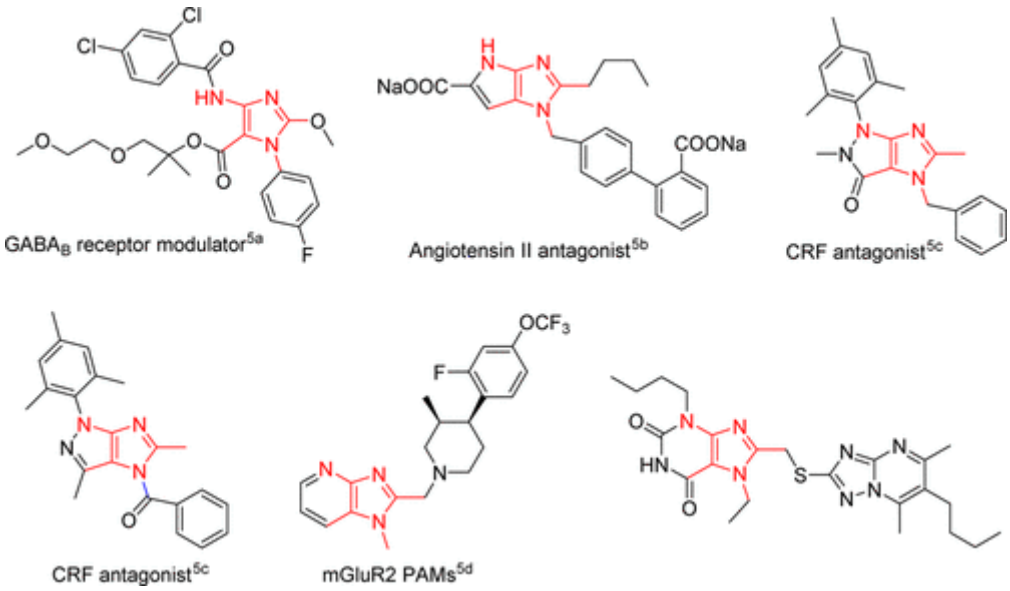


Figure 5. Representative bioactive compounds with fully substituted 4-aminoimidazole frameworks (in red). [22]

From the above three types of organic skeletons we decided to study the synthetic methods of the most rare ones, that is of 4,7-di-phenyl-indoles, 1,4-di-phenyl-carbazole, 7-acyl-indoles and 4-amino-1,3-imidazole derivatives. Below, we present for each product similar or relevant works on that are available in the literature.

## 6.1 The key role of protodeauration in the gold catalyzed reaction of 1,3-diynes with pyrrole and indole to form complex heterocycles.

In the first part of this thesis we studied the Au(I) catalyzed cyclization reaction of diynes. There are several methods of Au(I) catalyzed cyclization reaction of diynes in bibliography. [4] Most the methods are classified as intramolecular cyclizations. For the formation of medium size rings, an effective method was published that is based on the use of dienyne derivatives (Scheme 6.1).

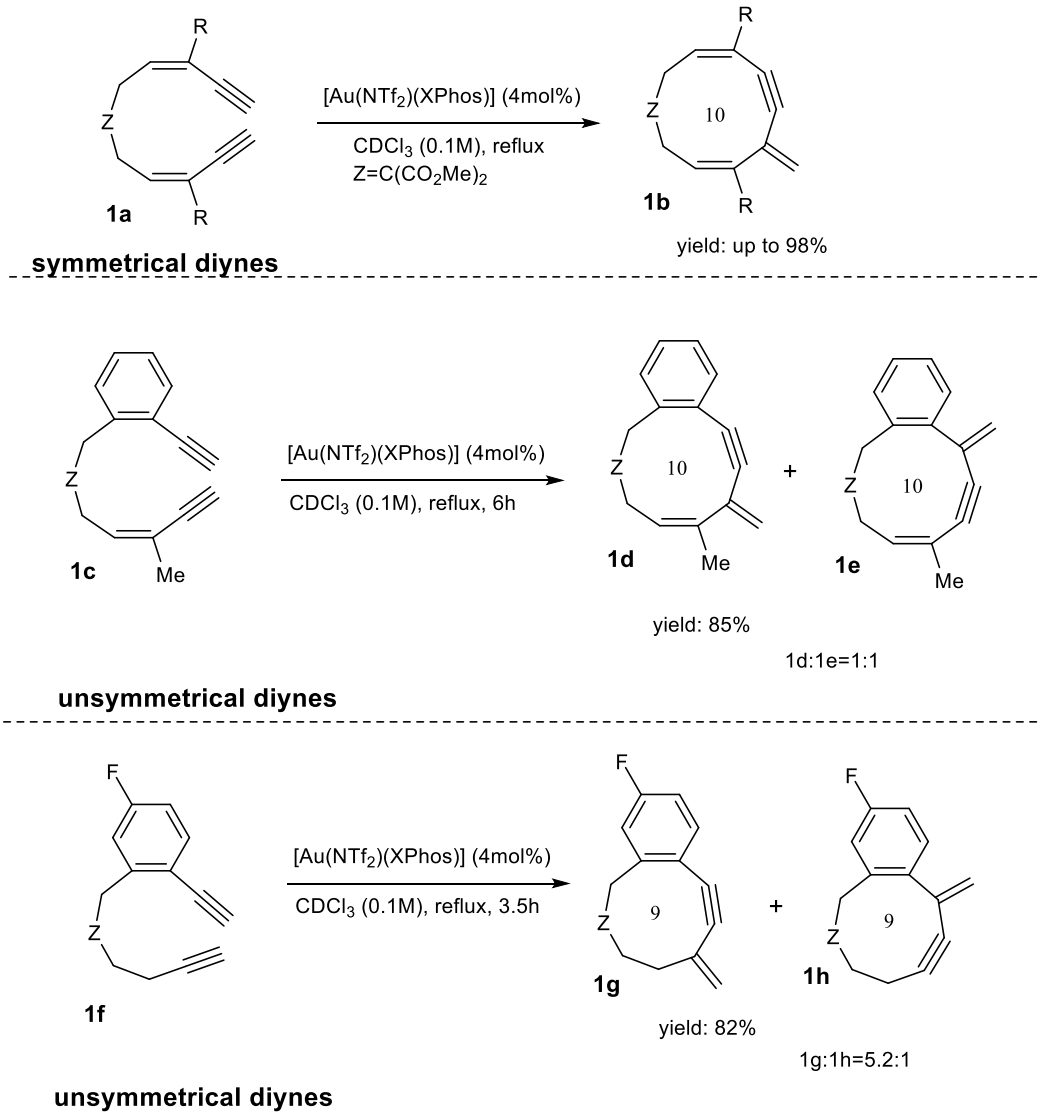


Scheme 6.1. synthesis of medium sized cycloalkynes by a gold(I)-catalysed cycloisomerisation of diynes (Gagosz 2009). [23]

In the case of symmetrical diynes **1a** the formation of a 10-membered cycloalkynes **1b** proceeds via a 10-exo-dig cycloisomerization. The reaction is catalyzed by Au(I)-XPhos presenting good to excellent yield. [23]

However, in the case of unsymmetrical diynes **1c,** 10-membered cycloalkynes **1d** and **1e** are produced with a ratio 1:1. The absence of the conjugated system in **1f** changes the ratio of the products **1g**:**1h** from 1:1 to 5.2:1. The proposed mechanism consists of a dual reactivity role for gold catalyst, as an electrophilic activator for one alkyne group and nucleophilic activator for the other. For the former, gold acts via π-coordination and for the latter via the formation of gold acetylide. [24]

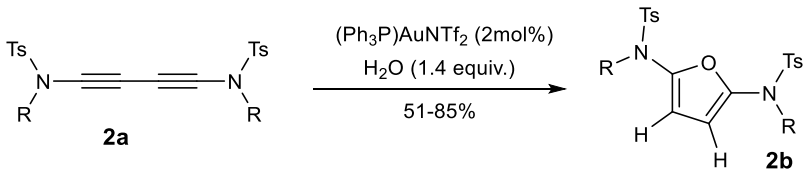


Scheme 6.2. Gold catalyzed synthesis of 2,5-diamino furan from diynes and water (Skrydstrup) [25]

A method for the synthesis of 2,5-diaminofuranes **2b** with medium to good yield was proposed by Skrydstrup. [25] According to the above intermolecular method, the formation of 2,5-diaminofuranes **2b** is based on the hydration of 1,3-diynamides **2a** with the use of $Ph_3PAuNTf_2$ catalyst.

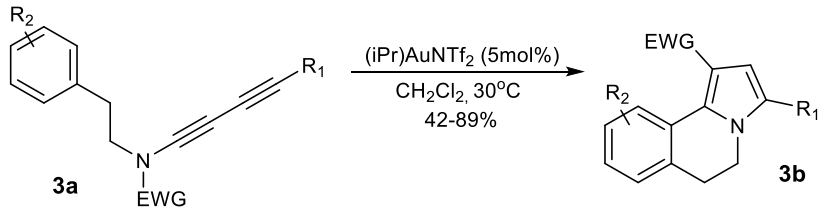


Scheme 6.3. Synthesis of pyrrolo[2,1-a]isoquinolines from diynamides (Huang 2019) [26]

A method for the synthesis of condensed pyrroles is based on the utility of intramolelular diynamides. [26] Thus, starting from diynamides **3a**, the synthesis of pyrrolo[2,1-a]isoquinolines **3b** proceeds via a step by step activation of the π-systems by $IPrAuNTf_2$ catalyst. First, a nucleophilic attack to the activated ynamide group can be succeeded by benzene or indole ring. An electron donating group on the aromatic ring increases the yield of the reaction. Activated heterocyclic arenes can be applied with good results. Then, a second step of activation of the second π-system leads to cyclization and the formation of pyrrole ring.

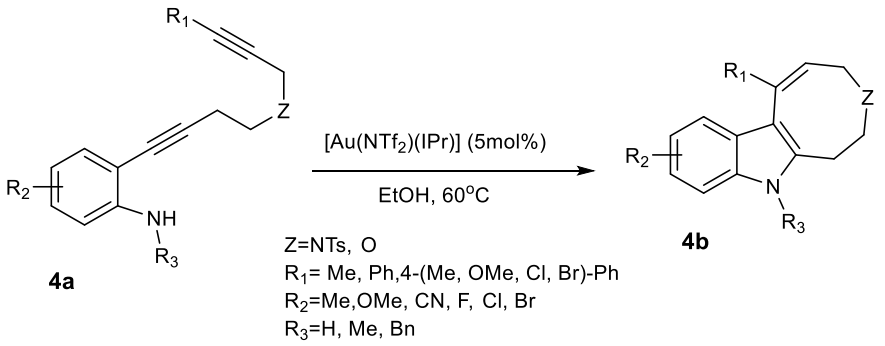


Scheme 6.4. Synthesis of eight-membered oxocine-fused indoles by Au-catalyzed cascade cyclizations (Ohno 2020). [27]

A similar mechanism was proposed for the intramolecular cyclization reaction of the N substituted anilines **4a**. The utility of the method is the synthesis of fused indole rings. [27,4] Comparing the method with the previous one, a few points of interest are obvious. In this case there is not a conjugated system consisted of two alkyne groups and one amine group. The Z group (NTs or O) interferes between two alkyne groups and amine-group is displaced on benzene ring. Thus, according to the proposed mechanism, [27,4] after the activation of the adjacent to phenyl ring alkyne, a cascade reaction begins. After a first cyclization step of 5-endo-dig hydroamination, a second 8-endo-dig cyclo-isomerization step follows with the participation of the terminal alkyl group. Finally, eight-member cyclized oxocine-fused indole derivatives **4b** are formed.

An alternative method for the synthesis of eight member ring fused indolizine derivatives presented by Liu. [28] Starting from N-substituted indoles **5a** that bears a tethered diyne moiety on the N-substituent, eight member ring fused indolizine derivatives **5b** are formed in good yield with the action of $AuCl(PAd_3)$ catalyst.

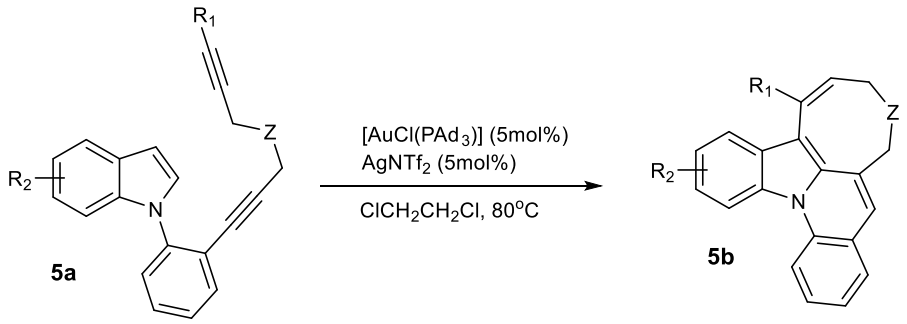


Scheme 6.5. Construction of indolizine derivatives via Au-catalyzed cycloisomerization of diynes (Liu 2018). [28]

A few years before Liu's publication, Ohno [29,30] had succeeded the synthesis of fused indoles either with a seven or a six member ring system. For both cases an intermolecular cyclization reaction between indole moiety and a diyne lead to condensed rings. Moreover, the method had been tested not only for indole as starting material but also for pyrrole leading to substituted indoles.

At his former work on one pot reaction for the synthesis of 4,7-disubstituted-indole, Ohno [29] tested the possibility of intermolecular formal [4+2] reaction between 1,3-diynes and pyrroles. It is an atom economical method that provides a variety of 4,7-disubstituted-indoles and carbazoles respectively from directly available 1,3-diynes.
The author provides a possible mechanism of the reaction relying on experimental data. Intermolecular hydroarylation of 1,3-diynes **6a** with pyrroles **6b** proceeds to an enyne type intermediate that is isolated. Subsequently, a second step of 6-endo-dig hydroarylation leads to the formation of 4,7-disubstituted indoles. Then, instead of pyrroles, indoles were tested with good results on the synthesis of disubstituted carbazoles.

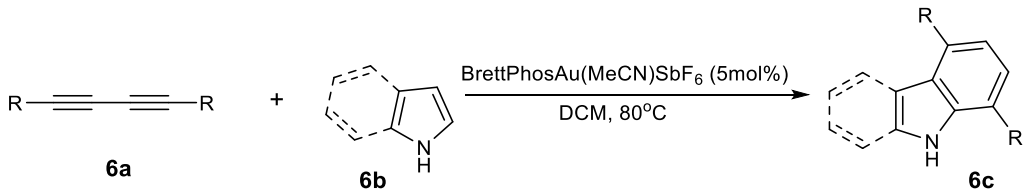


Scheme 6.6. Gold catalyzed formal [4+2] reaction between 1,3-diynes and pyrrole (Ohno 2015). [29]

The proposed gold catalyzed method diverges from other typical synthetic methods of indole due to the fact that the indole ring is built on pyrrole ring while at other methods benzene ring is the building block on which the pyrrole ring must be formed.

The extension of the above work is the publication that followed [30] on 2017. In this case, skipped diynes (1,4-diynes) react with pyrroles furnishing 1,6-dihydrocyclohepta[b]-pyrroles in good yields. The reaction proceeds via an initial step of hydroarylation of diyne with pyrrole, followed by a second step of a 7-endo-dig [31] cyclization. The main point of interest between this method and the previous one is the lack of resonance at skipped diynes. Similarities are more than the differences, that is, in both methods phosphine ligand catalyst is used BrettPhosAu(MeCN)$SbF_6$ vs JohnPhosAu(MeCN)$SbF_6$. In both methods not only pyrrole is used as nucleophile bul also indole with good yields. However, in the case of the formal [4+2] reaction between the conjugated 1,3-diynes and pyrrole, an enyne type intermediate isolated.

On the contrary, the [5+2] reaction between 1,4-diynes and pyrrole does not form a stable and isolated enyne type intermediate.

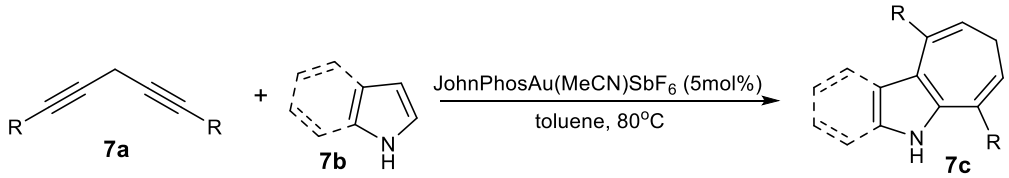


Scheme 6.7. Gold catalyzed formal [5+2] reaction between skipped 1,4-diynes and pyrrole (Ohno 2017). [30]

An attempt to establish a theoretical model for the mechanism of the above reaction was published by Fang [32]. The pathways for the four possible products were examined using DFT calculations. At the beginning, for the step of hydroarylation two paths **a** and **b** are possible. For path a, two feasible pathways of cycloisomerization exist, 7-endo-dig and 6-exo-dig. [31] Similarly, for path b, two alternative paths are 6-endo-dig or 5-exo-dig [31] cyclizations. After the calculation of the energy barriers of each step, the energy profile of the mechanism of the reaction that can shed light on the special traits of the reaction. Thus, the rate limiting step of the reaction is defined, as well the cause of high regioselectivity that the reaction exhibits. Additionally, the impact of proton transfer step on the reaction pathway is clarified. Finally, the influence of factors like solvent and ligand of the catalyst are examined.

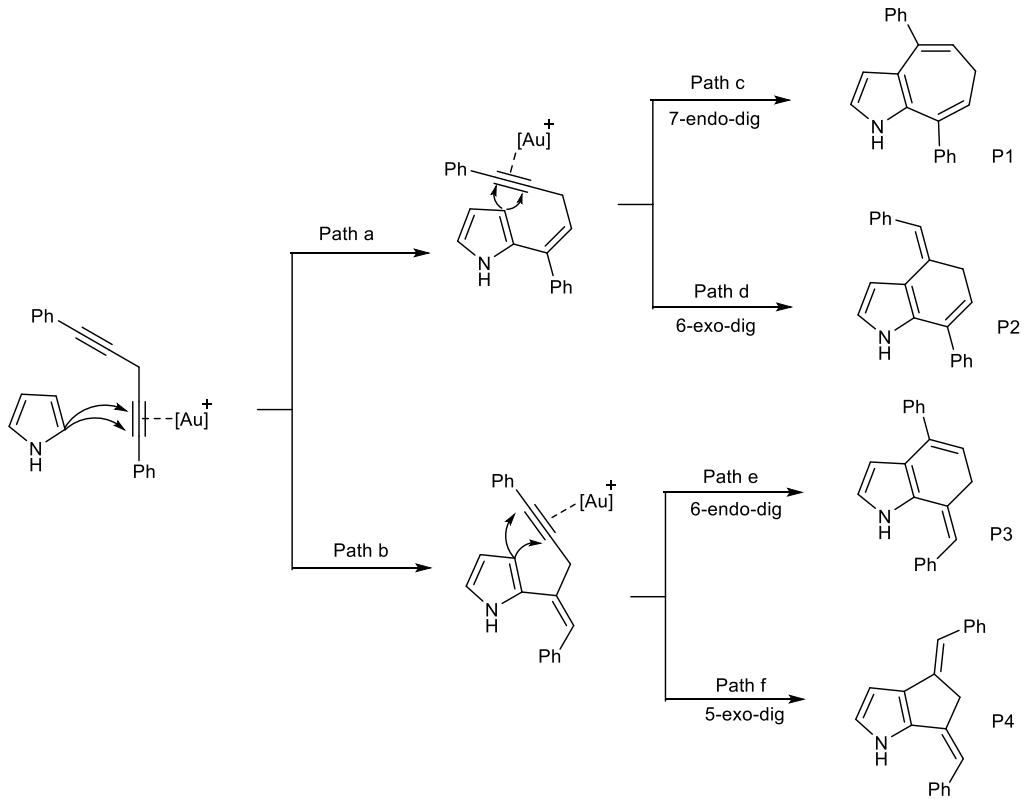


Scheme 6.8. Representation of Main Pathways in the Au(I)-Catalyzed Reaction between 1,4-Diyne and Pyrrole Proposed by Ohno et al [30]

So, regarding the above references, we decided to focus on gold catalyzed formal [4+2] reaction between 1,3-diynes and pyrrole (scheme 6.6) and indole, because it is a one pot reaction method, is atom economical with good yields and the products are valuable building blocks with significant biological activity [33] and interest for pharmaceutical purposes.

The indole motif is ubiquitous in biochemical systems, it is an integral part in tryptophane and its derivatives can be found in neurotransmitters and an ever increasing number of drugs. [12,13] Carbazole derivatives also possess a broad range of biological properties, including antibacterial, anti-inflammatory, and antitumor activities. [10,14,9] Additionally, carbazoles also exhibit interesting properties as organic materials, such as hole-transporting, photoconductive, and photorefractive effects.

To an attempt to explore the mechanism of the reaction, discreete points of interest arise. A similar approach to Fang's work [32] applied, splitting the reaction to all possible obvious paths. Thus, the first part of this work is the exploration of four different paths starting from 1,3-diyne and pyrrole to regioisomeric products **P1**-**P4**. Then, a comparative study between 1,3-dines and the skipped 1,4-diynes follows in

order to reveal the result of the methylene group that interferes between the alkyne groups. That is, how the interruption of resonance among alkyne groups influence the chemical profile of the reaction. Noteworthy, that in the case of 1,3-diynes an enyne intermediate is isolated while in the reaction with skipped diynes not. Next, we tried to correlate the kind of substituent of 1,3-diyne with the yield of the reaction, since there are experimental data of various substituents. Finally, based on the experimental data that the reaction proceeds not only with pyrrole but also with indole to form carbazole, we tried to certify or to change the proposed mechanism model.

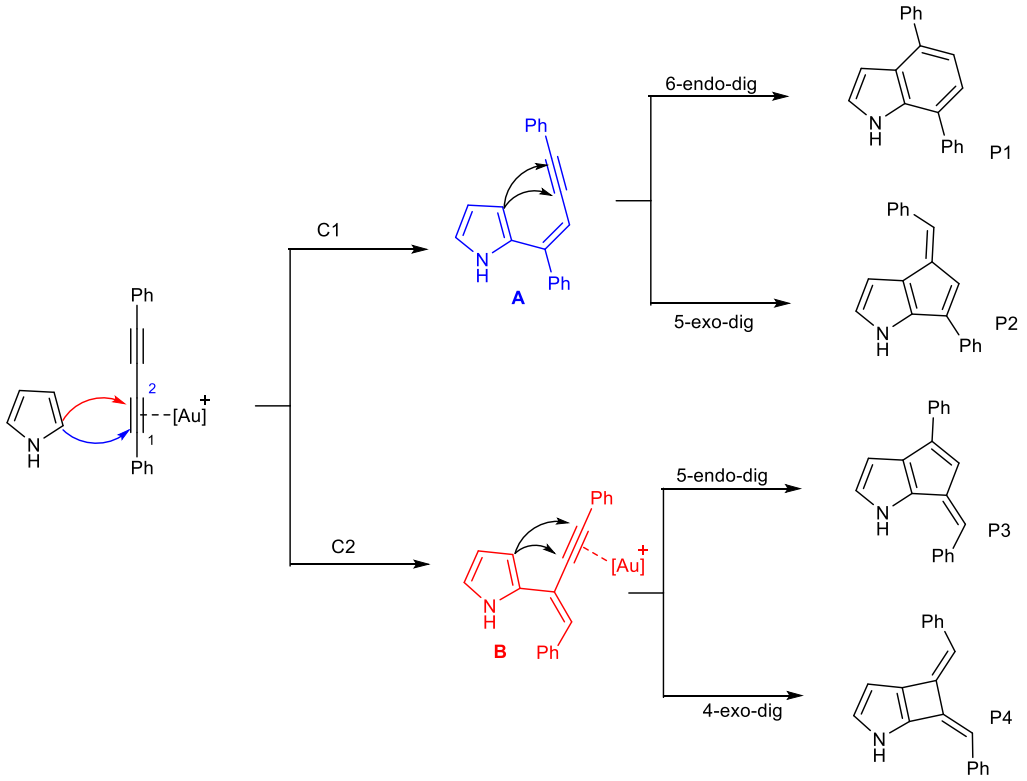


Scheme 6.9. Representation of Main Pathways in the Au(I)-Catalyzed Reaction between 1,3-Diyne and Pyrrole

The essential pattern of the mechanism of the reaction is devided to two parts, a first step of hydroarylation and a second step of cyclization. For the first step there are two possible pathways, the nucleophilic attack of C2 of pyrrole to C1 or C2 of the triple bond system of 1,3-diyne, leading to the enyne intermediates, **B** and the observable **A**. From that point, two different ways for cyclization are available for each enyne **A** and **B**. For enyne intermediate **A** either 6-endo-dig or 5-exo-dig cyclizations are feasible, leading to products P1 (1,4-disubstituted-indole) and **P2**

(cyclopenta[b]pyrrole) respectively. Similarly, for enyne intermediate **B** either 5-endo-dig or 4-exo-dig cyclizations are feasible. Products **P3** (cyclopenta[b]pyrrole) and P4 (cyclobuta[b]pyrrole) are formed respectively. The same model applied with indole, instead of pyrrole, in the role of nucleophile.

On the basis of the structures in scheme 6.9, DFT calculations realized, revealing the energy profile of the reaction as depicted at schemes 6.10a and 6.10b. The main steps of the mechanism are presented: i. the activation of triple bond of 1,3-diyne by gold catalyst, ii. nucleophilic attack by C2 of pyrrole to the activated alkyne iii migration of the gold catalyst to the unreacted distal alkyne and iv. formation of the second sigma bond by an intramolecular attack of the pyrrole ring that leads to the ring closure.

## 6.2. On the Mechanism of the Au(I)-Mediated Addition of Alkynes to Anthranils to Furnish 7-Acylindoles

In the second part of the thesis our interest is displaced to gold catalyzed synthetic methods of substituted indoles bearing functional groups. In the first part, the examined gold catalysed reactions was focused on the formation of 4,7 di-phenyl indoles. There are several methods for the synthesis of substituted indoles with aliphatic groups or phenyl ring at almost any position of the indole scaffold, position 2 [34,35,36,37,38,39], position 3 [40,41,42,43] or di-substituted at both positions 2 and 3. [44,45,46] Some of the above methods are based on a metal catalyst like Co, Cu, Ir, Ru, Au and some others are metal free [43]. Substitution at positions 4 to 7 is related to the initial synthons that are used.

However, the presence of a functional group on indole ring renders the molecule a building block on the hands of synthetic chemists. Thus, functional groups can be considered cyano, carboxy ester, amino, keto or formyl group. Some of the synthetic methods of substituted indoles with functional groups are presented below.

**Substituted indloles by cyano group**

The introduction of cyanide group in the indole ring can be achieved either by the use of catalyst or not. For the introduction of CN at 2-position of indole, catalyzed methods have been reported either by Pd catalyst [47] or Ir catalyst. [48]

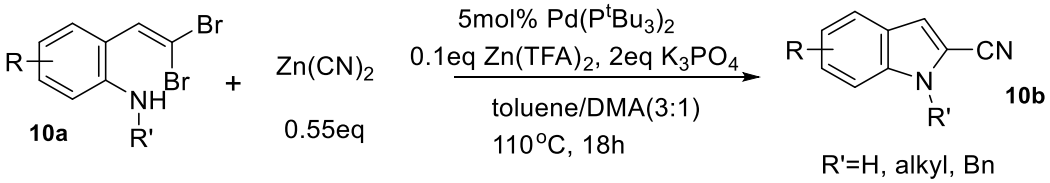


Scheme 6.10. Palladium-Catalyzed Synthesis of 2-Cyanoindoles from 2-*gem*-Dihalovinylanilines (Lautens 2017). [47]

Additionally, an electrochemical synthesis has been published. [49]

For the introduction of CN at 3-position of indole ring more synthetic methods are available. Catalytic methods using Mn(III), Zn(II) and Cu(I) have been reported. A Mn(III)-mediated radical cascade cyclization of *o*-alkenyl aromatic isocyanides with boronic acids under mild reaction conditions provides *N*-unprotected 2-aryl-3-cyanoindoles. [50]

A copper-catalyzed one-pot multicomponent cascade reaction of 1-bromo-2-(2,2-dibromovinyl)benzenes with aldehydes and aqueous ammonia enables a selective synthesis of various indole derivatives. 3-Cyano-1*H*-indoles. [51]

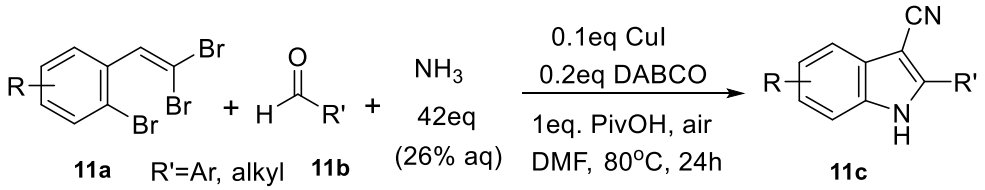


Scheme 6.11. Selective Access to 3-Cyano-1*H*-indoles through Copper-Catalyzed One-Pot Multicomponent Cascade Reactions (Fan 2015) [51]

The synthesis of *N*-arylindole-3-carbonitriles has been succeeded in two steps from starting material 2-aryl-3-arylamino-2-alkenenitriles. After a first step halogenation by NBS or NCS and a second step of intramolecular cyclization catalysed by $Zn(OAc)_2$. [52]

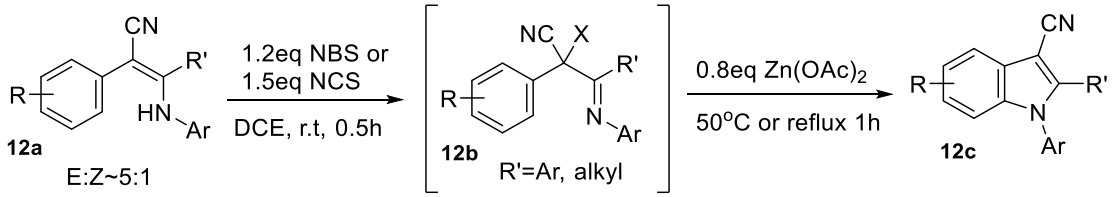


Scheme 6.12. Oxidative Cyclization of 2-Aryl-3-arylamino-2-alkenenitriles to *N*-Arylindole-3-carbonitriles Mediated by NXS/$Zn(OAc)_2$ ( Zhao 2011). [52]

**Substituted indoles by carboxy ester group**

Several methods for the introduction of an ester group at positions 2 and 3 of indole ring exist. Intramolecular cyclization methods of the appropriate substituted benzene synthons lead to 2-substituted indoles using iron(II) triflate as catalyst [53] or Rhodium(II) perfluorobutyrate. [54] On the contrary, bimolecular method of cyclization of 2-vinylanilines and alkynoates provides 2-substituted indoles, at the absence of metal catalyst is available in the literature. [55]

In the case of substituted indoles at 3-position by ester group there are more choices. The preparation of *N*-substituted indole-3-carboxylates can be achieved via metal free bimolecular reactions [56,57] in high yields.

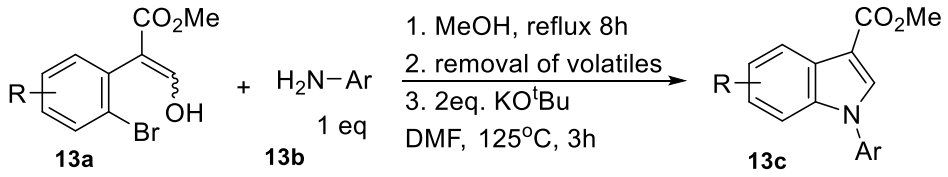


Scheme 6.13. Synthesis of Indoles via Electron-Catalyzed Intramolecular C–N Bond Formation (Karchava 2018). [56]

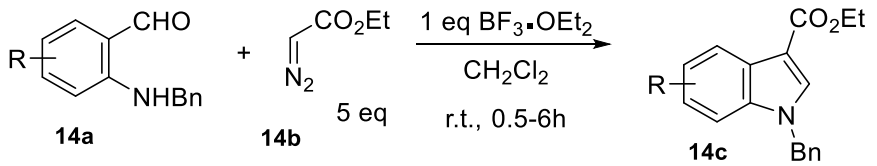


Scheme 6.14. Synthesis of Substituted Indole from 2-Aminobenzaldehyde through [1,2]-Aryl Shift (Fournier 2010). [57]

Additionally, bimolecular methods assisted by various metal catalysts like Pd, Rh, Cu

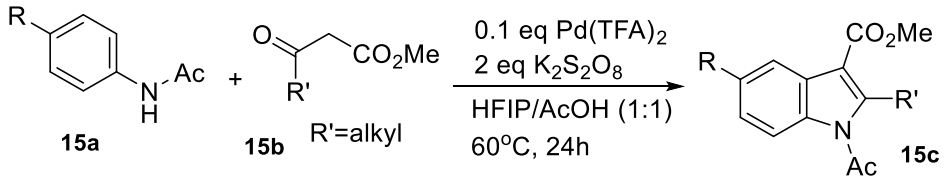


Scheme 6.15. Palladium-Catalyzed Direct Oxidative C–H Activation/Annulation for Regioselective Construction of *N*-Acylindoles (Y.R.Lee 2020). [58]

As depicted at the scheme 6.15, Pd(II) catalyzes coupling/annulation reaction of anilides and α-dicarbonyl compounds providing diverse *N*-acyl indoles with high functional group tolerance and excellent regioselectivity. [58]

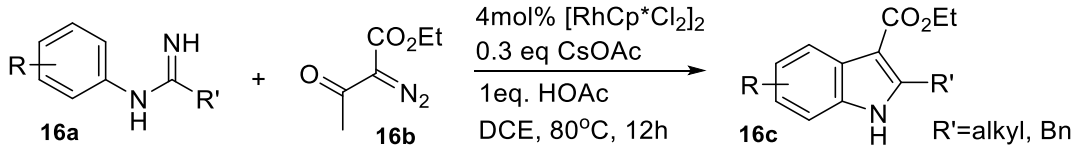


Scheme 6.16. Rh(III)-Catalyzed Synthesis of *N*-Unprotected Indoles from Imidamides and Diazo Ketoesters via C–H Activation and C–C/C–N Bond Cleavage (Li 2016). [59]

Starting from similar synthons, Rh(III) catalyst provides the same variety of indoles as above, with the difference of unprotected N. [59]

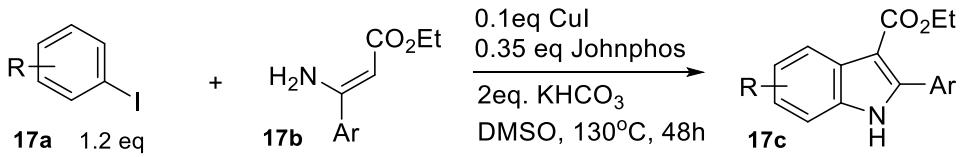


Scheme 6.17. Copper-Catalyzed Synthesis of Multisubstituted Indoles through Tandem Ullmann-Type C–N Formation and Cross-dehydrogenative Coupling Reactions (Chen 2018). [60]

The last presented bimolecular method for the synthesis of substituted imidazoles at 3-position by an ester group is a copper catalyzed reaction. Starting from aryl iodides and enamines copper catalyses an Ullmann-type C-N bond formation followed by intramolecular cross-dehydrogenative coupling. [60] Moreover, unimolecular catalysed methods are also available. Basically, intramolecular cyclization methods are available, which are catalyzed by metals like Ru, Pd, Zn.

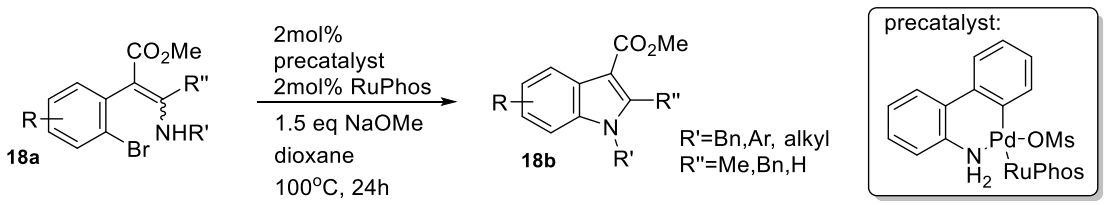


Scheme 6.18. A Practical Synthesis of Indoles via a Pd-Catalyzed C–N Ring Formation (Taylor 2014). [61]

At the first example, a cyclization step that consists of a Pd-catalyzed C-N bond coupling resembles the bimolecular reaction of CuI. [60] Halo-aryl enamines enables the synthesis of *N*-functionalized C2-/C3-substituted indoles bearing the ester group at 3-position. [61]

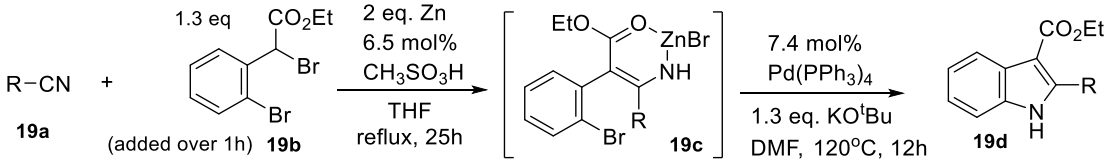


Scheme 6.19. Palladium-Catalyzed Intramolecular Trapping of the Blaise Reaction Intermediate for Tandem One-Pot Synthesis of Indole Derivatives (S.Lee 2011). [62]

The next synthetic method for 3-carboxy ester indoles is a combination of two catalyzed reaction which proceed in a tandem way. At the first step an α-halo-ester reacts with a nitrile under the catalytic action of Zn to form β-enamino ester (Blaise

reaction). The presence of Pd catalyst enables the C-N coupling to form the indole derivative. [62]

**Substituted indoles by amino/amido group**

For the synthesis of substituted animo-indoles, there are several methods of direct introduction of amino-group at the indole ring with the assist of metal catalyst Ir(III), Cu(I) or even electrochemically with Ni electrode. [63] Some of these methods are presented below.

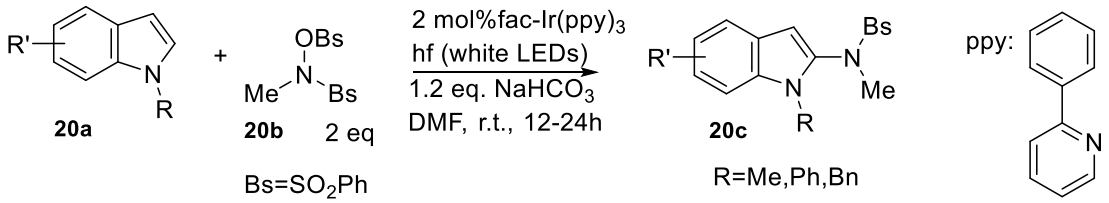


Scheme 6.20. Visible-Light-Promoted Redox Neutral C–H Amidation of Heteroarenes with Hydroxylamine Derivatives (Qin 2014). [64]

A method of direct insertion of amino group on the indole ring with high regioselectivity was published by Q.Qin. The method uses hydroxylamine derivatives as synthons of amine group and is quite tolerant not only to indole but also to pyrroles and furans achieving high yields. [64]

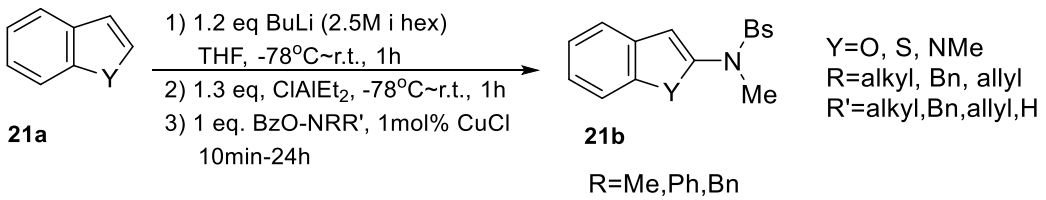


Scheme 6.21. Copper-Catalyzed Electrophilic Amination of Heteroarenes via C–H Alumination ( Y.Lee 2015). [65]

A variation of the above method is the CuCl catalyzed electrophilic amination reaction of heteroarenes with O-benzoyl hydroxylamines. The method is a one pot reaction while proceeds with very good yields. [65]

The alternative manner for the insertion of amino group in indole ring can be achieved via intramolecular catalyzed cyclization of precursor synthons. Thus, starting from *gem*-dibromo-vinyl-anilides and sulfonamides, 2-Amidoindoles are formed. [66]

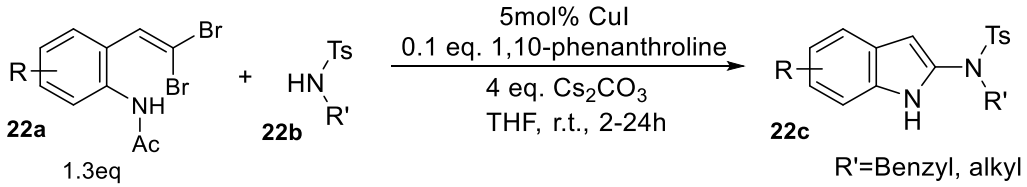


Scheme 6.22. CuI-Catalyzed Coupling of *gem*-Dibromovinylanilides and Sulfonamides: An Efficient Method for the Synthesis of 2-Amidoindoles and Indolo[1,2-*a*]quinazolines (Perumal 2014). [66]

A different approach to the problem of insertion of amino group at 2-position of indole is the method of Ye et al. Starting from ynamides and benzyl azides they succeeded to compose 2-aminoindoles using (IPr)AuNTf$_2$ as catalyst, in the presence of molecular sieves, at ambient temperature. The fascination issue on their method is that the addition of an oxidant such as AgOAc in combination with raised temperature turns the reaction to β-carboline formation. [67]

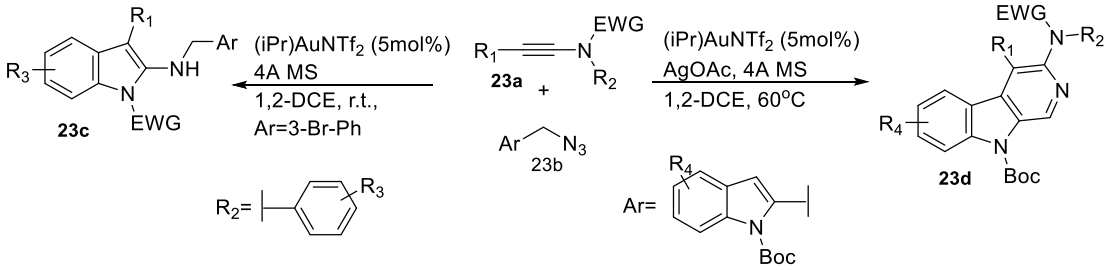


Scheme 6.23. Synthesis of Indoles and b-Carbolines by reaction of ynamides with benzyl azides (Ye 2015). [67]

A few years later, a method for the synthesis of 2-amino indoles based on the use of ynamides and sulfilimine ylides was published. Ylides are nitrene transfer reagents to alkynes which are activated by gold catalysts. The reaction is a formal [3+2] cycloaddition that is catalyzed by (Pic)AuCl$_2$. [68,69]

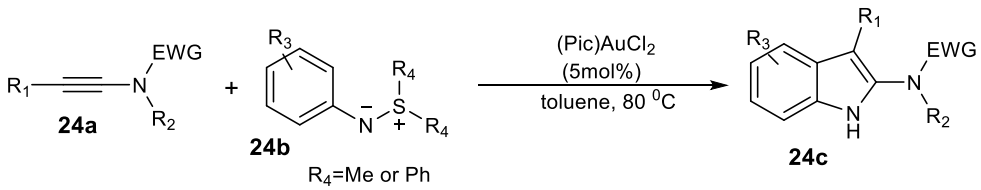


Scheme 6.24. Synthesis of 2-amino - indoles using sulfilimine ylides (Hashmi 2019). [68,69]

**Substituted indoles by formyl group**

For the insertion of a formyl group in the indole moiety, there are a few methods either of a direct insertion or indirect, that is, with the use of the appropriate precursor molecule. In any case, the presence of a catalyst is necessary. A couple of methods are presented below.

For the direct insertion of formyl group at 3-position of indole an efficient iron-catalyzed C3-selective formylation of free or N-substituted indoles provides 3-formylindoles in good yields. The reaction proceeds in the presence of formaldehyde and aqueous ammonia. The air is the oxidant reagent of the reaction. [70]

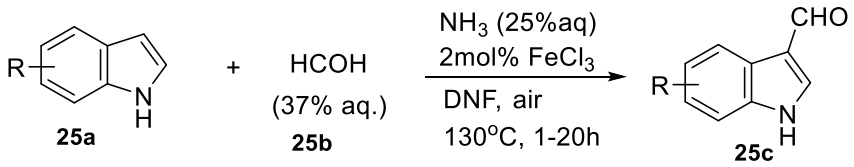


Scheme 6.25. Iron-Catalyzed C3-Formylation of Indoles with Formaldehyde and Aqueous Ammonia under Air (B.Zeng 2017). [70]

For the insertion of formyl group at 2-position of indole ring a method was presented by P. Kothandaraman at 2011. The method is based on a gold(I)-catalyzed cycloisomerization of 1-(2-(tosylamino)phenyl)prop-2-yn-1-ols. The reaction is tolerant to a variety of substrates and proceeds with good yields. [71]

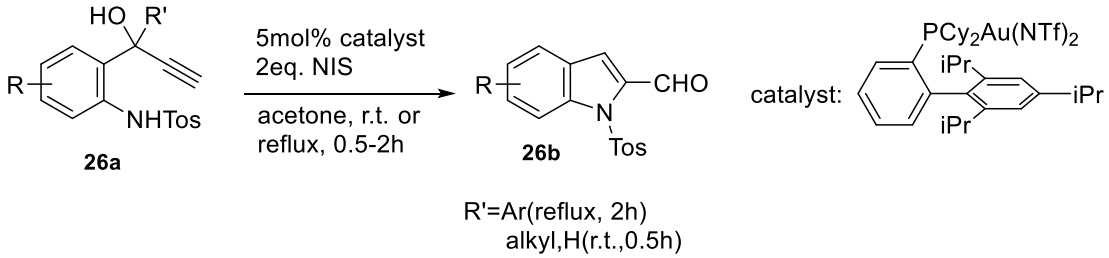


Scheme 6.26. Gold-Catalyzed Cycloisomerizations of 1-(2-(Tosylamino)phenyl)prop-2-yn-1-ols to 1*H*-Indole-2-carbaldehydes (Kothandaraman 2011). [71]

A very different approach to the synthesis of formyl indoles was presented by Hashmi et al. This method is a variation of the previous work of the same researcher on the synthesis of 2-aminoindoles from ynamides and sulfilimine ylides. Replacing sulfilimine ylides by anthranil, 7acyl-indoles are formed.

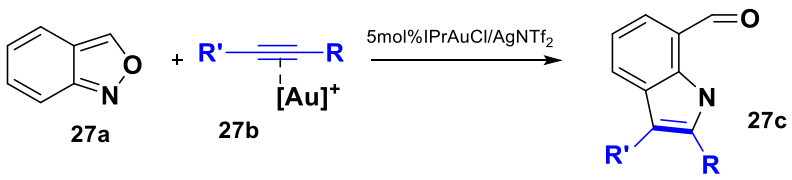


Scheme 6.27. Generic synthetic method of 7-acyl-indoles by anthranil. (Hashmi 2016) [72]

The method, as a tool for synthetic chemists, offers many benefits. The main pros are referred below. First, it is a novel, short, and atom-economical synthesis of 7-acyl indoles through gold-catalyzed C-H annulation of anthranils with alkynes.

Moreover, the substrate scope is remarkably broad and the mild reaction conditions tolerate a diverse set of functional groups, which further strengthens the synthetic impact of this method. [72]

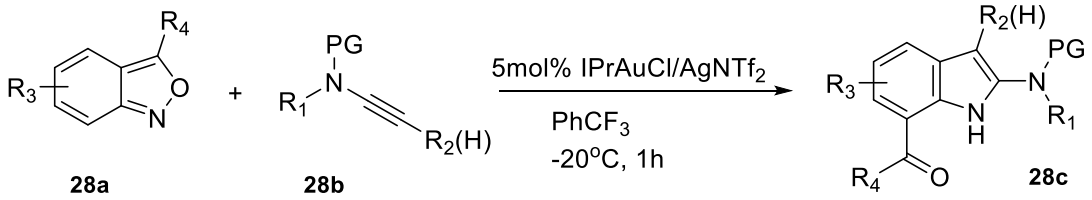


Scheme 6.28. Synthesis of 2-amino-7-acyl-indoles by anthranil and ynamides. (Hashmi 2015) [72]

At the first part of Hashmi's work was presented the reaction between anthranil and ynamides with a benzyl and mesylate substituents (e.g. BnN(Ms)≡CH). The reaction proceeds at short reaction time (1h) and low temperature -20°C. It is noteworthy that when R2 is phenyl or aliphatic group the yield goes down or is trivial respectively. [72]

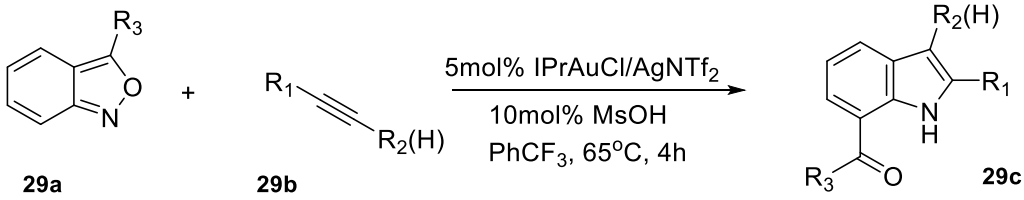


Scheme 6.29. Synthesis of 7-acyl-indoles by anthranil and alkynes (Hashmi 2015). [72]

Later non-polarized terminal alkynes or di-substituted alkynes were tested. Higher temperature and long reaction time were demanded to a good but in any case lower yield comparing with the reaction with ynamides. In general, the reaction proceeds smoothly with ynamides, non-polarized alkynes and non-terminal alkynes. [72]

From the aspect of the chemical traits of the method, according to the authors' aspect, the reaction proceeds via an intermediate a-imino gold carbene, generated by an intermolecular reaction. Due to the high electrophilicity of the a-imino gold carbenoid, an intramolecular ortho-aryl C-H insertion could afford the 7-formyl indoles. According to the authors, the reaction of anthranils with electron-donating groups usually proceeds with higher yields, which suggests an electrophilic aromatic substitution mechanism. [72]

Finally, an unsymmetrical alkyl/aryl-substituted alkyne was tested as a substrate. Instead of a mixture or 2-alkyl-3-aryl indole and 2-aryl-3-alkyl indole, only one product 2-alkyl-3-aryl indole is formed in low yield. According to the authors one of two paths leads to the formation of an unstable α-imino gold carbene that undergoes a hydride-shift by the adjacent alkyl group preventing the formation of 2-aryl-3-alkyl indole. [72]

Observing all these traits, we decided that it was worthy to investigate the mechanism of the reaction. Thus, the aim of this work is the exploration of the mechanism of the reaction between anthranils and alkynes, proposing a possible mechanism. Then, after studying a variety of alkynes we aim to establish similarities and differences between them. Next we would be able to explain the regioselectivity with ynamides and terminal alkynes, which selectively provide the 2-, compared to the 3-substituted 7-acyl-indole ring. Finally, we aim to elucidate key steps in the reaction pathway, to validate author's proposal for an α-imino gold carbene intermediate and to correlate its formation with regioselectivity.

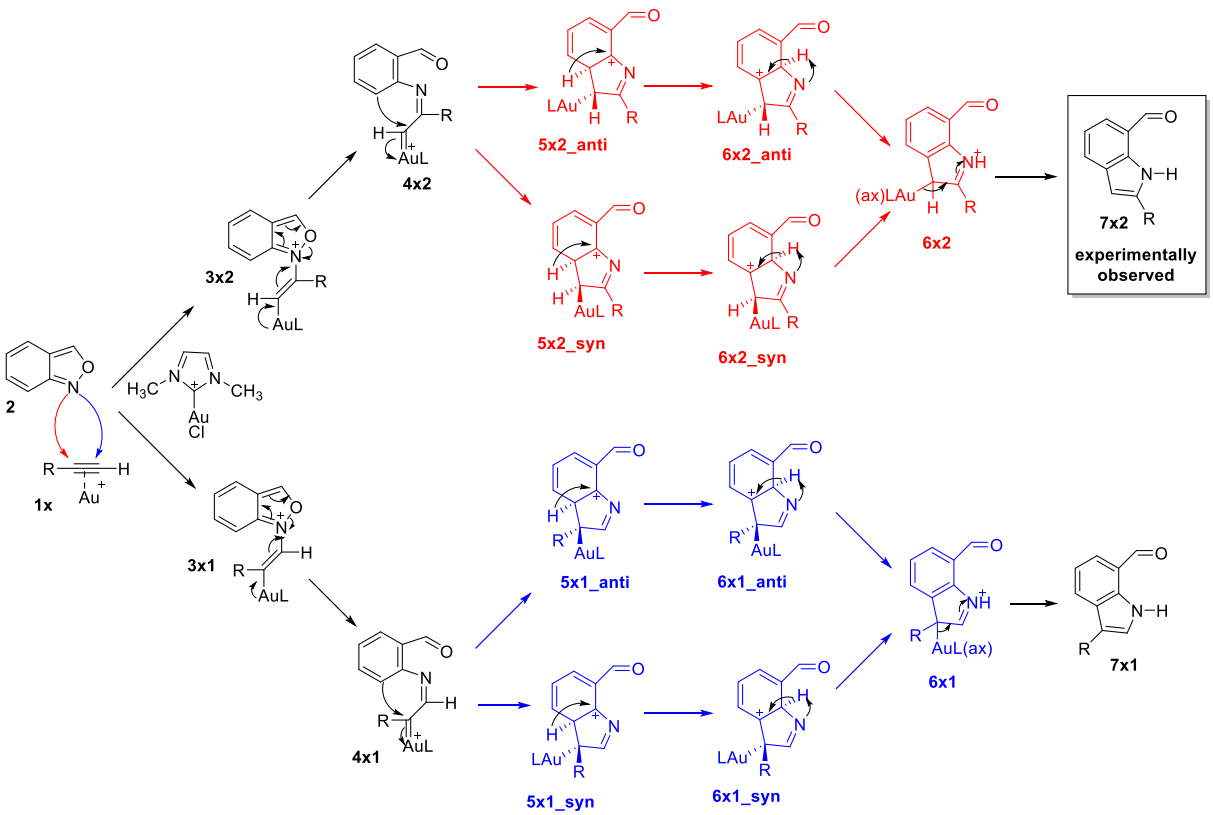


Scheme 6.30. Regioselectivity models description for the mechanism of the reaction of a terminal alkyne with anthranil.

To check the assumptions that we expressed above, we propose a mechanistic model with the below traits: i. it can explain the experimental data, ii. it is rational and simple iii. It covers as many aspects of the problem as possible and iii. It is consistent with the aims of our project.

Thus, for the reaction of anthranil with the gold-activated triple bond we anticipated a mechanism consisting of six steps. There are two alternatives for the initial nucleophilic attack onto the triple bond (Scheme 6.30), where regioselectivity is determined: the nitrogen atom of the oxazole ring can attack the gold-polarized triple bond at C-1 (path 1) or C-2 (path 2) to generate intermediates 3x2 or 3x1, respectively. The second step involves an interesting redistribution of $\pi$-electrons resulting in the cleavage of the N-O bond to form 4x2 (path 2) or 4x1 (path 1). Then, an electrophilic aromatic substitution reaction occurs between the electron deficient carbon of the $\alpha$-imino gold carbene and the phenyl fragment resulting in intermediates 5x2 or 5x1, which can have an anti or syn relative orientation of the hydrogen atoms attached to the bond forming carbons (Scheme 6.30). The fourth and fifth steps comprise proton migrations such that ring aromaticity is recovered at the

phenyl unit (6x2 or 6x1, respectively), and the sixth step includes the de-auration and concomitant aromatization of the pyrrole ring to form isomeric 7-acylindoles 7x2 or 7x1, respectively. The product obtained in the experiment is 7x2 with the substituent on the reacting alkyne installed at 2- instead of the 3-carbon of the 7-acyl-indole ring.

## 6.3. Formation and Intramolecular Capture of α-Imino Gold Carbenoids in the Au(I)-Catalyzed [3+2] Reaction of Anthranils, 1,2,4-Oxadiazoles and 4,5-Dihydro-1,2,4-Oxadiazoles with Ynamides

At the third part of the thesis we focused on reactions that proceed via the formation of the α-imino gold carbene that afterwards it is captured intramolecularly in formal [3+2] cycloadditions. In fact, threre are several publications in which the organic chemists insist that the gold catalysed reactions that present proceed via an α-imino-gold carbenoids.

The first reported example of a gold-catalyzed heterocyclic synthesis invoking the participation of α-imino gold carbene complexes can be attributed to Toste in the Au(I)-catalyzed acetylene Schmidt reaction of homopropargyl azides acting as nitrene transfer reagents to furnish substituted pyrroles in 2005. [73] For this intermediate, Goddard and Toste [74] suggested a three-centre four-electron σ-bond due to donation to the empty 6s orbital of gold from the occupied orbitals at the ligand and the carbene carbon atom, as well as two orthogonal π-electron density back-donations from filled gold 5d orbitals to π-acceptor orbitals in the carbene carbon atom and on the ligand. As a result, they suggested that *the reactivity in gold(I)-coordinated carbenes is best accounted for by a continuum ranging from a metal-stabilized singlet carbene to a metal-coordinated carbocation*. Additionally, the bond order in gold(I) carbene complexes is typically close to one (or even less), and therefore, the Au=C representation is not accurate, although it may be convenient mainly for mechanistic purposes. Ynamides, which are strongly polarized alkynes, [75] have been established as an extremely powerful tool for the rapid and versatile assembly of structurally complex N-containing molecules [76–79] with gold-catalyzed reactions. [80] In such reaction, the participation of α-imino gold carbene intermediates is carried out through their capture with diverse types of nucleophiles.

First, we examined the mechanism of the reaction between anthranils and ynamides as reported by Hashmi (2nd part). We analyzed the reaction pathway, we compared DFT calculations with experimental data and we tested different types of substates (ynamides, terminal alkynes, di-substituted alkynes) and we concluded that all the versions follow the same mechanistic pattern and experimental evidence are in accordance with calculations. However, not only Hashmi's group but also other synthetic groups have published synthetic methods on gold catalysis where they

propose the same pattern for a variety of different substrates. Moreover, a small drift on the reaction conditions change drastically the product. Above, we present a few examples for both cases, drift on substrates and reaction conditions. Anyway, the question that we are obliged to give response is if these reactions follow the same mechanistic pattern and proceed via an α-imino gold intermediate irrelevantly of the substrate.

A first trial to prove the existence of a mechanism via α-imino gold carbene was carried out by Hashmi's group. They applied the appropriate changes to the structure of the ynamide in two ways. First, they interfere a methylene group between β-carbon of ynamide and its terminal group, so as since the α-imino gold is formed a hydrid shift can be accomplished. Consequently the destruction of carbene is going to redirect the path of the reaction away of the cyclization with phenyl ring. Second, the introduction of a silyl ether on the ynamide scaffold urges further the reaction away from the path of α-imino gold intermediate leading to the formation of quinolines. [81]

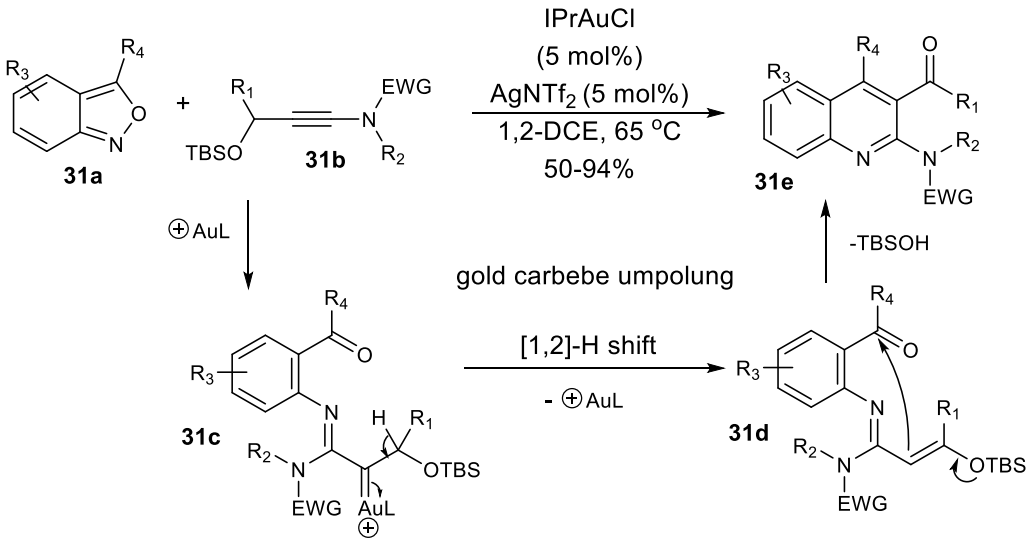


Scheme 6.31. Gold-Catalyzed Synthesis of Quinolines from Propargyl Silyl Ethers and Anthranils through the Umpolung of a Gold Carbene Carbon (Hashmi 2016). [81]

In a similar approach to the problem of capturing α-imino gold carbenoid was the gold (III) catalyzed reaction of anthranils with N-allyl-ynamides. The hypothesis that allyl group on N can react with α-imino gold intermediate redirecting the path of the reaction away from the indole formation is correct. Experimentally, the alternative path is dominant leading to the synthesis of [3.1.0]azabicycles product. [82]

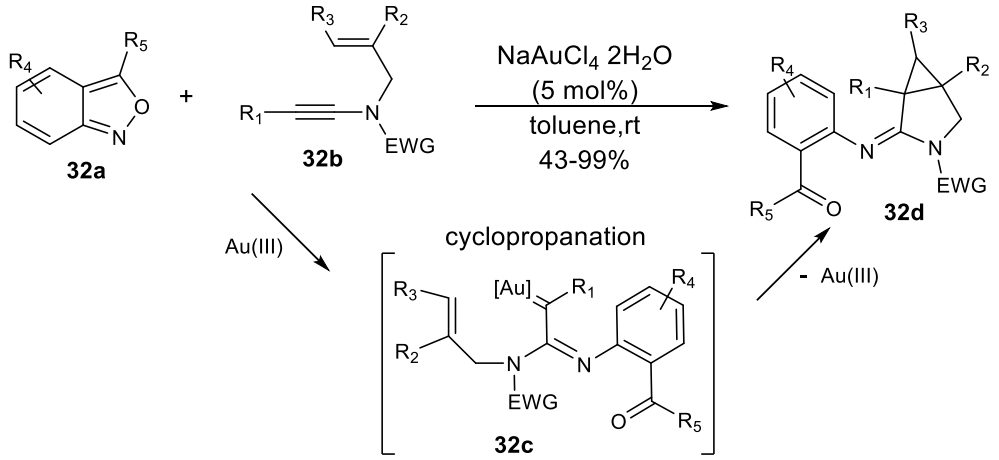


Scheme 6.32. Synthesis of cyclopropane-fused azaheterocycles by Au(III) catalysis (Hashmi 2019). [82]

Next, the interest is displaced to the anthranil moiety and the possible changes at its structure. First, the idea of using 1,2-benzisoxazoles, an isomer of anthranil (2,1-benzisoxazole) was applied by two groups; that of R.-S. Liu, Y. Liu, and the other one, that of Sahoo and Gandon. Depending on the nature of the gold catalyst the reaction leads to a formal [5 + 1] or [5 + 2] annulations. The [5 + 1] annulations afford 1,3-benzoxazines in either the Z or E geometry (with moderate selectivity) while [5 + 2] annulations give 1,4-benzoxazepines in good to excellent yields. The divergent catalysis of the reaction can be described as follow. The use of Au(I) or Au(III) catalysts led to [5 + 1] or [5 + 2] products, respectively. In general, the use NHC-Au(I) or phosphine-Au(I) catalysts led to [5 + 2] or [5 + 1] products, respectively. [83, 84]

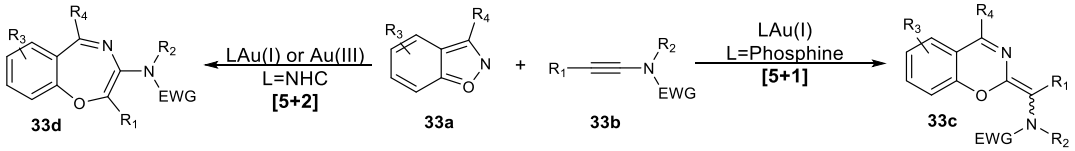


Scheme 6.33. [5+1] and [5+2] annulations of 1,2-benzisoxazoles and ynamides (R.S.Liu 2018 - Y.Liu 2018). [83,84]

A reaction that follows the previous pattern presented by two groups Liu and Bao independently one from the other. The ynamides react with benzofurazan N-oxide instead of benzisoxazoles to furnish 2-amido-7-nitro indoles. The reaction proceeds in the presence of gold(I) catalyst. The novelty of the method is that benzofurazan N-oxide function as nitrene transfer despite N-oxides function as oxygen transfer.

Possibly, this type of inversion on the chemical activity is owed to the gold catalyst. [85,86]

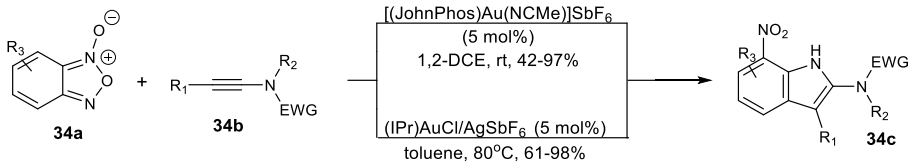


Scheme 6.34. Synthesis of indoles via C-H annulation (Y.Liu 2019 – Bao 2020). [85,86]

The next step to our navigation to the chemistry of α-imino-gold carbenoids is a drastically drift on the anthranil ring. Regarding that anthranil ring consists of two aromatic rings that co-exist as a fused moiety the question is what could happen if the phenyl ring was absent.

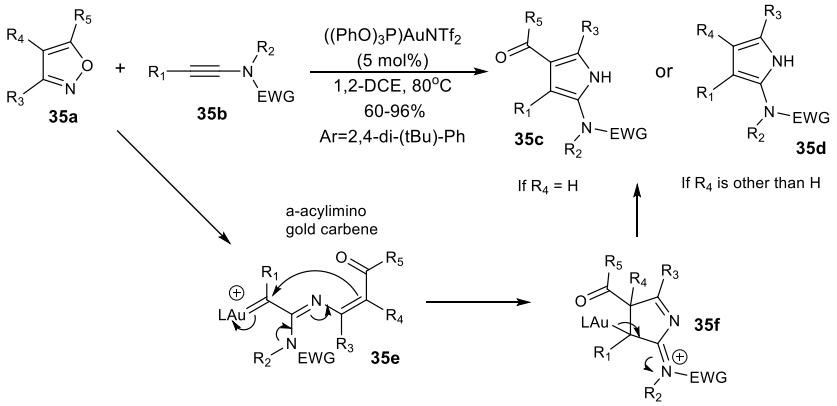


Scheme 6.35. Formal [3+2] cycloaddition between ynamides and isoxazoles (Ye 2015). [87]

Ynamides react with isoxazoles providing amino pyrroles. According to the proposed mechanism by authors, gold (I) activates triple bond, forms α-imino gold carbene and after an intramolecular cyclization and gold release, forms 3H-aminopyrroles. Then, 3H-aminopyrroles may follow alternative paths of isomerization to form 1H-aminopyrroles. [88]

The α-imino gold intermediate mechanism is tested at the next citation of the reaction between isoxazoles and 3-en-1-ynamides. The authors propose a key Au(I)-stabilized aza-heptatrienyl cation, which undergoes cyclization followed by isomerization to yield the final product. It is noteworthy that azepine formation is sensitive to the conformation of intermediate. Thus, factors that may change its

conformation, like substituents of vinyl group or the presence of Lewis acids redirect the reaction to the formation of pyridines. [89]

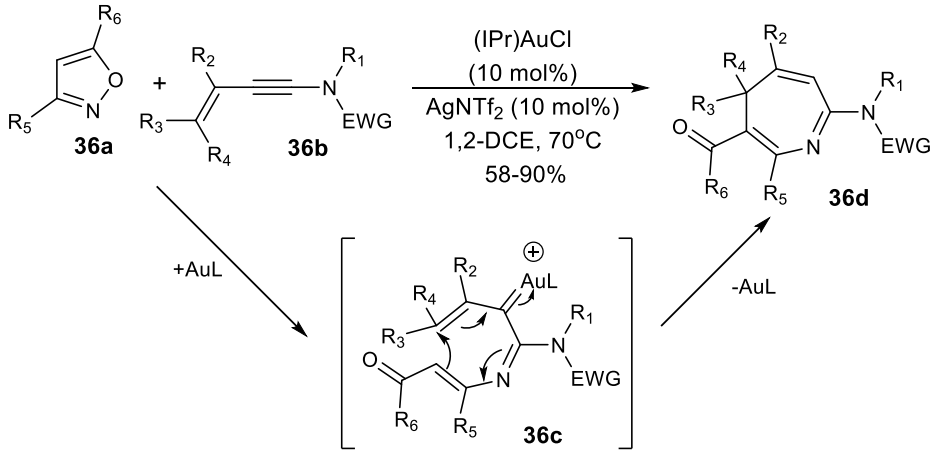


Scheme 6.36. Formal [4+3] annulation in the synthesis of azepines (R.S.Liu 2018). [89]

As a conclusion with up to now data we accept that the gold (I) catalysed reactions between ynamides and anthranil like scaffolds proceed via an α-imino-gold carbene intermediate. In the cases of lack of the fused phenyl ring, the mechanism sustains similar. The question that arises is how the mechanism may change or how the gold intermediate is stabilized if we introduce one more hetero atom on the isoxazole ring. Thus, dioxazoles were used as reactants to a similar reaction with ynamides forming the expected oxazoles derivatives, while the method is compatible with various alkyl and (hetero) aromatic groups. [90]

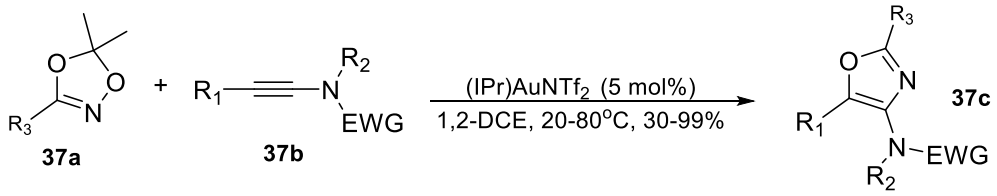


Scheme 6.37. Dioxazoles as nitrene equivalents (Y.Liu 2016). [90]

Then, two publications, one complementary to the other, were released. The first one was a follow up report by Liu described the efficient synthesis (40−94%) of amino imidazoles from ynamides and 4,5-dihydrooxadiazoles while the other by Hashmi. The latter showed that fully unsaturated oxadiazoles could also be used for the synthesis of amino imidazoles from ynamides. Both groups explain the results adopting a mechanism of an α-imino gold carbene.

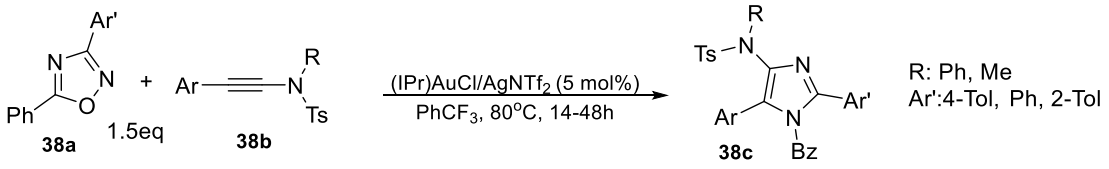


Scheme 6.38. Synthesis of fully substituted 4-aminoimidazoles α-imino gold carbenes from 1,2,4-Oxadiazoles (Hashmi 2017). [22]

A gold-catalyzed selective [3 + 2] annulation of 1,2,4-oxadiazoles with ynamides enables an atom-economical synthesis of fully substituted 4-aminoimidazoles. The reaction proceeds with 100% atom economy, exhibits good functional group tolerance, and can be conducted in gram scale. [22]

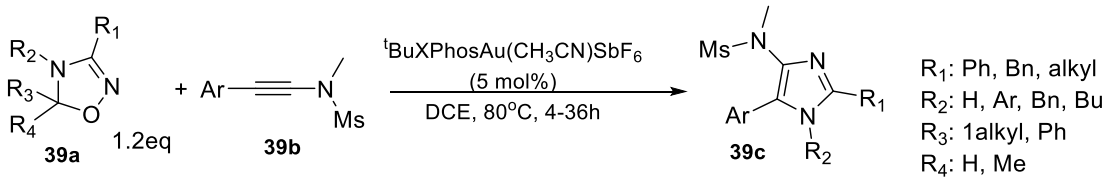


Scheme 6.39. Gold-catalyzed formal [3 + 2] cycloaddition of ynamides with 4,5-dihydro-1,2,4-oxadiazoles (Y.Liu 2017). [87]

A gold-catalyzed formal [3 + 2] cycloaddition of ynamides with 4,5-dihydro-1,2,4-oxadiazoles provides a concise and regioselective access to highly functionalized 4-aminoimidazoles likely via the formation of an α-imino gold carbene intermediate followed by cyclization. [91]

However, for the synthesis of 4-amino imidazoles catalysed methods with other metals, except gold, are available in literature. Some of them reveal similar features to the reactions we studied, while others seem to follow a similar mechanism irrelevant the starting point. Despite our goal is to investigate the traits and mechanism of reactions where an α-imino gold carbenoid is formed, we take a look at some different but not irrelevant reactions to our issue.

Starting with Novikov's group that published a Rh(II) catalyzed method of transannulation of 1,2,4-oxadiazoles (Scheme 6.40a) or 1,2,4-oxadiazol-5-ones (Scheme 6.40b) with N-sulfonyl-1,2,3-triazoles provides fully substituted amidoimidazoles. Possibly, N-sulfonyl-1,2,3-triazoles is the equivalent to the

activated ynamides. In which manner Rh catalyses the reaction is a question that is out of the interest and the goals of the thesis.

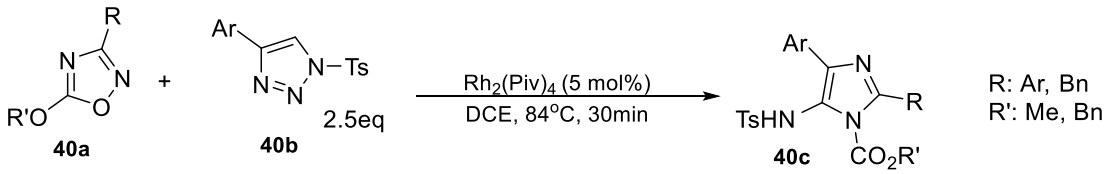


Scheme 6.40a

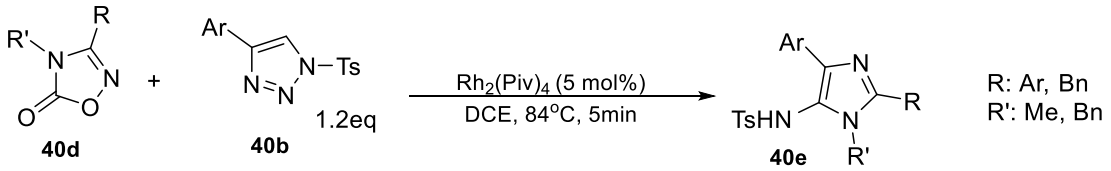


Scheme 6.40b. Rh(II)-Catalyzed Transannulation of 1,2,4-Oxadiazole Derivatives with 1-Sulfonyl-1,2,3-Triazoles: Regioselective Synthesis of 5-Sulfonamidoimidazoles. [92]

So on, a metal catalyzed method for the synthesis of amino imidazoles is the reaction between propargylamines with carbodiimides, in the presence of 5 mol% of the titanacarborane monoamide. The reaction is a [3+2] annulation that proceeds in good to excellent yields. [93]

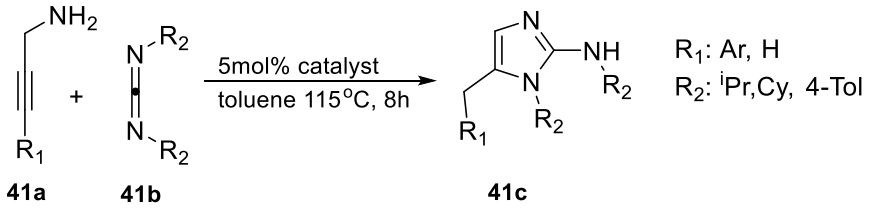


Scheme 6.41. Atom-Economical Synthesis of 2-Aminoimidazoles via [3+2] Annulation Catalyzed by Titanacarborane Monoamide(Xie 2011). [93]

Reactions of propargylamines with carbodiimides, in the presence of 5 mol% of the titanacarborane monoamide $[\sigma{:}\eta^1{:}\eta^5\text{-}(OCH_2)(Me_2NCH_2)C_2B_9H_9]Ti(NMe_2)$, afford a new class of substituted 2-aminoimidazoles via [3+2] annulation in good to excellent yields. A possible reaction mechanism is proposed.

Then a copper catalyzed method is suspicious for similar mechanism. The reaction is the synthesis of substituted imidazoles from terminal alkynes with amidines in the

presence of $Na_2CO_3$, pyridine, a catalytic amount of $CuCl_2 \cdot 2H_2O$, and oxygen (1 atm). [94]

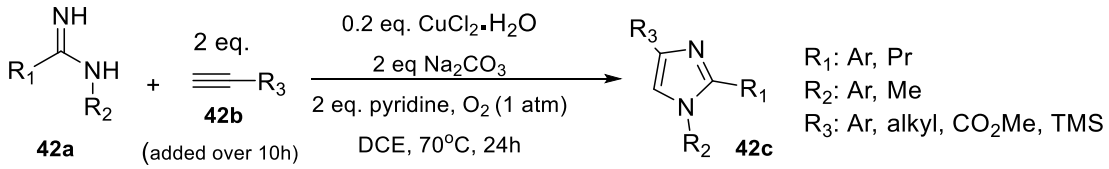


Scheme 6.42. Copper-Catalyzed Oxidative Diamination of Terminal Alkynes by Amidines: Synthesis of 1,2,4-Trisubstituted Imidazoles (Neuville 2013). [94]

Last, a sequential Staudinger/aza-Wittig/Ag(I)-catalyzed cyclization/isomerization reaction of easily accessible propargylazide derivatives with triphenylphosphine, isocyanates, and amines provided fully substituted imidazoles in good overall yields.[95]

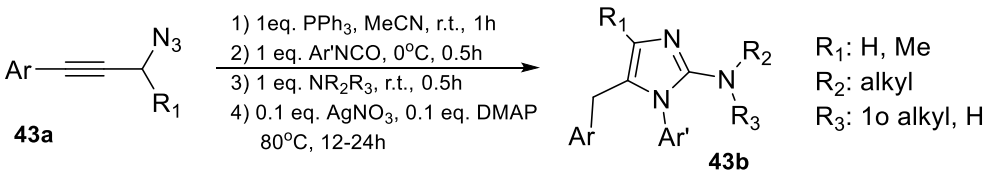


Scheme 6.43. One-Pot Synthesis of Polysubstituted Imidazoles (Ding 2017). [95]

As a continuation on our efforts to gain a deeper insight in the intricacies of gold mediated transformations [24,25,26–33,34–36] and particularly reaction mechanisms including gold carbenes, [80,8,22,91,106–109,110] we carried out here a thorough investigation on the reaction mechanism of the Au(I) catalyzed [3+2] reaction of mild nitrogen nucleophiles in the antranil, 1,2,4-oxadiazole or 4,5-dihydro-1,2,4-oxadiazole series with ynamides. We paid particular attention to the regioselectivity of these reactions which can afford 7-acylindoles substituted at 2-, or/and 3-position, and 5- or 4-aminoimidazoles, respectively, as well as to the formation of the α-imino gold carbene intermediate, and to the difference in reactivity between aromatic and non-aromatic substrates (oxadiazole vs dihydrooxadiazole).

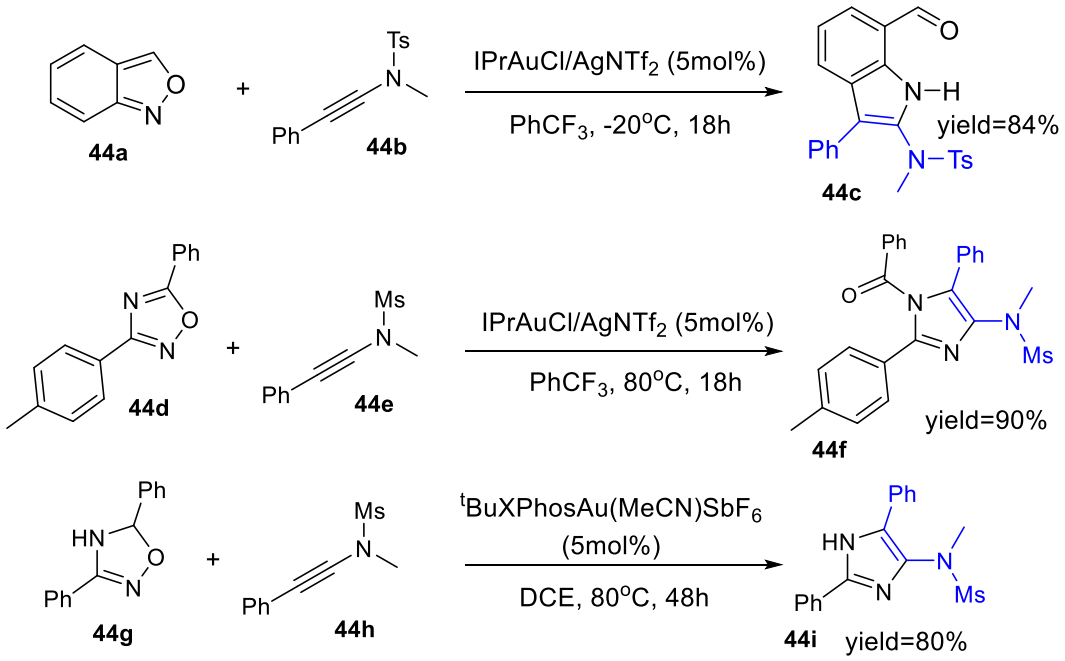


Scheme 6.44. Au(I)-catalyzed reaction of anthranil, 1,2,4-oxadiazoles or 4,5-dihydro-1,2,4-oxadiazoles with ynamides forming 2-amino-3-phenyl-7-acyl indoles, N-acyl-5-aminoimidazoles or N-alkyl-4-aminoimidazoles, respectively.

We assumed that the general mechanism for the three protocols could be analogous, according to the similarities in the structures of the three nucleophiles, and that the key feature in this reactivity is the oxime fragment embedded in the heterocyclic moiety. With that assumption at hand, and driven by our recent exploration of anthranil chemistry, [111] we anticipated a reaction pathway for the oxadiazoles involving (Scheme 6.45): 1- Au(I) activation of the alkyne, 2-nucleophilic attack by the oxime nitrogen onto the activated alkyne, 3- N-O cleavage and formation of the key α-imino gold carbene intermediate, 4- cyclization of the α-imino gold carbene intermediate via an intramolecular nucleophilic attack and 5-deauration leading to the final heterocycle.

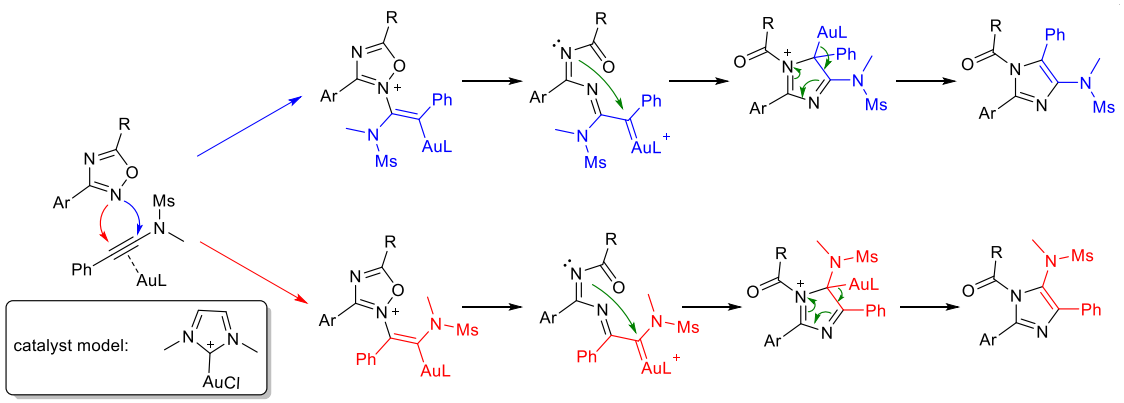


Scheme 6.45. Anticipated mechanistic steps for the Au(I) mediated reaction between ynamides and oxadiazoles by analogy to that found for anthranils.

## 6.4 Bibliography


(1) Mato, M.; Franchino, A.; García-Morales, C.; Echavarren, A. M. Gold-Catalyzed Synthesis of Small Rings. *Chem. Rev.* **2021**, *121* (14), 8613–8684. https://doi.org/10.1021/acs.chemrev.0c00697.

(2) Dominic Campeau, David F. León Rayo, Ali Mansour, Karim Muratov, and F. G. Gold-Catalyzed Reactions of Specially Activated Alkynes, Allenes, and Alkenes. *Chem. Rev.* **2021**, *121* (14), 8756−8867.

(3) Gimeno, R. P. H. and M. C. Main Avenues in Gold Coordination Chemistry. *Chem. Rev.* **2021**, *121* (14), 8311–8363. https://doi.org/10.1021/acs.chemrev.0c00930.

(4) Ronald L. Reyes, Tomohiro Iwai, and M. S. Construction of Medium-Sized Rings by Gold Catalysis. *Chem. Rev.* **2021**, *121* (14), 8926−8947.

(5) Hashmi, A. S. K. Introduction: Gold Chemistry. *Chemical Reviews*. 2021. https://doi.org/10.1021/acs.chemrev.1c00393.

(6) Luca Rocchigiani and Manfred Bochmann. Recent Advances in Gold(III) Chemistry: Structure, Bonding, Reactivity, and Role in Homogeneous Catalysis. *Chem. Rev.* **2021**, *121* (14), 8364–8451. https://doi.org/10.1021/acs.chemrev.0c00552.

(7) Hashmi, A. S. K.; Rudolph, M. Gold Catalysis in Total Synthesis. *Chem. Soc. Rev.* **2008**. https://doi.org/10.1039/b615629k.

(8) Aguilar, E.; Santamaría, J. Gold-Catalyzed Heterocyclic Syntheses through α-Imino Gold Carbene Complexes as Intermediates. *Org. Chem. Front.* **2019**, *6* (9), 1513–1540. https://doi.org/10.1039/C9QO00243J.

(9) G. Küçükgüzel and S. ŞenkardeŞ. Recent Advances in Bioactive Pyrazoles. *Eur. J. Med. Chem.* **2015**, *97*, 786–815.

(10) A. W. Schmidt, K. R. R. and H. J. K. Occurrence, Biogenesis, and Synthesis of Biologically Active Carbazole Alkaloids. *Chem. Rev.* **2012**, *112* (6), 3193–3328.

(11) Inman, M.; Moody, C. J. Indole Synthesis-Something Old, Something New. *Chem. Sci.* **2013**, *4* (1), 29–41. https://doi.org/10.1039/c2sc21185h.

(12) T. V. Sravanthi and S. L. Manju. Indoles—A Promising Scaffold for Drug Development. *Eur. J. Pharm. Sci.* **2016**, *91*, 1–10.

(13) N. Chadha and O. Silakari. Indoles as Therapeutics of Interest in Medicinal Chemistry: Bird's Eye View. *Eur. J. Med. Chem.* **2017**, *134*, 159–184.

(14) T. Takeuchi, S. Oishi, T. Watanabe, H. Ohno, J. I. S.; K. Matsuno, A. Asai, N. Asada, K. K. and N. F. Structure-Activity Relationships of Carboline and Carbazole Derivatives as a Novel Class of ATP-Competitive Kinesin Spindle Protein Inhibitors. *J. Med. Chem.* **2011**, *54* (13), 4839– 4846.

(15) Bashir, M.; Bano, A.; Ijaz, A.S.; Chaudhary, B. A. Recent Developments and Biological Activities of N-Substituted Carbazole Derivatives: A Review. *Molecules* **2015**, *20* (8), 13496–13517.

(16) Joyeeta Roy, Amit Kumar Jana, D. M. Recent Trends in the Synthesis of Carbazoles: An Update. *Tetrahedron* **2012**, *68* (31), 6099–6121.

(17) Weinreb, S. M. Some Recent Advances in the Synthesis of Polycyclic Imidazole-Containing Marine Natural Products. *Nat. Prod. Rep.* **2007**, *24*, 931–948.

(18) Bhatnagar A., Sharma P. K., K. N. A Review on "Imidazoles": Their Chemistry and Pharmacological Potentials. *Int. J. PharmTech Res.* **2011**, *3* (1), 268–282.

(19) C. M. Francini, A. L. Fallacara, R. Artusi, L. Mennuni, A. Calgani, A.

Angelucci, S. Schenone, M. B. Identification of Aminoimidazole and Aminothiazole Derivatives as Src Family Kinase Inhibitors. *ChemMedChem* **2015**, *10*, 2027.

(20) Lei Zhang, Michael A. Brodney, John Candler, Angela C. Doran, Allen J. Duplantier, Ivan V. Efremov, Edel Evrard, Kenneth Kraus, Alan H. Ganong, Jessica A. Haas, Ashley N. Hanks, Keith Jenza, John T. Lazzaro, Noha Maklad, Sheryl A. McCarthy, Weimin Qian, B, and A. Q. Z. 1-[(1-Methyl-1H-Imidazol-2-Yl)Methyl]-4-Phenylpiperidines as MGluR2 Positive Allosteric Modulators for the Treatment of Psychosis. *J. Med. Chem.* **2011**, *54* (6), 1724–1739. https://doi.org/10.1021/jm101414h.

(21) Francini, C.M.; Musumeci, F.; Fallacara, A.L.; Botta, L.; Molinari, A.; Artusi, R.; Mennuni, L.; Angelucci, A.; Schenone, S. Optimization of Aminoimidazole Derivatives as Src Family Kinase Inhibitors. *Molecules* **2018**, *23*, 2369. https://doi.org/https://doi.org/10.3390/molecules23092369.

(22) Zhongyi Zeng, Hongming Jin, Jin Xie, Bing Tian, Matthias Rudolph, Frank Rominger, and A. S. K. H. α-Imino Gold Carbenes from 1,2,4-Oxadiazoles: Atom-Economical Access to Fully Substituted 4-Aminoimidazoles. *Org. Lett.* **2017**, *19* (5), 1020–1023.

(23) Odabachian, Y.; Le Goff, X. F.; Gagosz, F. An Unusual Access to Medium Sized Cycloalkynes by a New Gold(I)-Catalysed Cycloisomerisation of Diynes. *Chem. - Eur. J.* **2009**, *15* (36), 8966–8970.

(24) Zhao, X.; Rudolph, M.; Hashmi, A. S. K. Dual Gold Catalysis -an Update. *Chem. Commun.* **2019**, No. 55, 12127–12135.

(25) Kramer, S.; Madsen, J. L. H.; Rottländer, M.; Skrydstrup, T. Access to 2,5-Diamidopyrroles and 2,5-Diamidofurans by Au(I)- Catalyzed Double Hydroamination or Hydration of 1,3-Diynes. *Org. Lett.* **2010**, *12* (12), 2758–2761.

(26) Liu, J.; Chakraborty, P.; Zhang, H.; Zhong, L.; Wang, Z.-X. .; Huang, X. Gold-Catalyzed Atom-Economic Synthesis of Sulfone- Containing Pyrrolo[2,1-a]Isoquinolines from Diynamides: Evidence for Consecutive Sulfonyl Migration. *ACS Catal.* **2019**, *9* (3), 2610–2617.

(27) Yamaguchi, A.; Inuki, S.; Tokimizu, Y.; Oishi, S.; Ohno, H. Gold(I)-Catalyzed Cascade Cyclization of Anilines with Diynes: Controllable Formation of Eight-Membered Ring-Fused Indoles and Propellane-Type Indolines. *J. Org. Chem.* **2020**, *85* (4), 2543–2559.

(28) Liu, R.; Wang, Q.; Wei, Y.; Shi, M. Synthesis of Indolizine Derivatives Containing Eight-Membered Rings via a Gold-Catalyzed Two-Fold Hydroarylation of Diynes. *Chem. Commun.* **2018**, No. 54, 1225–1228.

(29) Matsuda, Y.; Naoe, S.; Oishi, S.; Fujii, N.; Ohno, H. Formal [4+ 2] Reaction between 1,3-Diynes and Pyrroles: Gold(I)-Catalyzed Indole Synthesis by Double Hydroarylation. *Chem. - A Eur. J.* **2015**, *21* (4), 1463–1467. https://doi.org/10.1002/chem.201405903.

(30) Hamada, N.; Yoshida, Y.; Oishi, S.; Ohno, H. Gold-Catalyzed Cascade Reaction of Skipped Diynes for the Construction of a Cyclohepta[b]Pyrrole Scaffold. *Org. Lett.* **2017**, *19* (14), 3875–3878. https://doi.org/10.1021/acs.orglett.7b01759.

(31) Jack E. Baldwin. Rules for Ring Closure. *J. Chem. Soc., Chem. Commun.*, **1976**, 734–736.

(32) Fang, R.; Zhou, L.; Tu, P. C.; Kirillov, A. M.; Yang, L. Computational Study on Gold-Catalyzed Cascade Reactions of 1,4-Diynes and Pyrroles: Mechanism,

Regioselectivity, Role of Catalyst, and Effects of Substituent and Solvent. *Organometallics* **2018**, *37* (12), 1927–1936. https://doi.org/10.1021/acs.organomet.8b00201.

(33) A. Poulsen, M. Williams, H. M. Nagaraj, A. D. W.; H. Wang, C. K. Soh, Z. C. X. and B. D. Structure- Based Optimization of Morpholino-Triazines as PI3 K and MTOR Inhibitors. *Bioorg. Med. Chem. Lett.* **2012**, *22* (2), 1009–1013.

(34) Jiao, L.; Bach, T. Regioselective Direct C–H Alkylation of NH Indoles and Pyrroles by a Palladium/Norbornene-Cocatalyzed Process. *Synthesis (Stuttg).* **2014**, *46* (01), 35–41.

(35) Katsumi Maeda, Ryosuke Matsubara, and M. H. Synthesis of Substituted Anilines from Cyclohexanones Using Pd/C–Ethylene System and Its Application to Indole Synthesis. *Org. Lett.* **2021**, *23* (5), 1530–1534.

(36) Ji-Wei Ren, Meng-Nan Tong, Yu-Fen Zhao, and F. N. Synthesis of Dipeptide, Amide, and Ester without Racemization by Oxalyl Chloride and Catalytic Triphenylphosphine Oxide. *Org. Lett.* **2021**, *23* (19), 7497–7502.

(37) Michalska, M.; Grela, K. Simple and Mild Synthesis of Indoles via Hydroamination Reaction Catalysed by NHC–Gold Complexes: Looking for Optimized Conditions. *Synlett* **2016**, *27* (04), 599–603.

(38) Hyunho Chung, Jeongyun Kim, Gisela A. González-Montiel, Paul Ha-Yeon Cheong, and H. G. L. Modular Counter-Fischer–Indole Synthesis through Radical-Enolate Coupling. *Org. Lett.* **2021**, *23* (3), 1096–1102. https://doi.org/10.1021/acs.orglett.1c00003.

(39) Shuling Yu, Linjun Qi, Kun Hu, Julin Gong, Tianxing Cheng, Qingzong Wang, Jiuxi Chen, and H. W. The Development of a Palladium-Catalyzed Tandem Addition/Cyclization for the Construction of Indole Skeletons. *J. Org. Chem.* **2017**, *82* (7), 3631–3638.

(40) Zhenghui Liu, Zhenzhen Yang, Xiaoxiao Yu, Hongye Zhang, Bo Yu, Yanfei Zhao, and Z. L. Methylation of C(Sp3)–H/C(Sp2)–H Bonds with Methanol Catalyzed by Cobalt System. *Org. Lett.* **2017**, *19* (19), 5228–5231. https://doi.org/10.1021/acs.orglett.7b02462.

(41) Jannik C. Borghs, Viktoriia Zubar, Luis Miguel Azofra, Jan Sklyaruk, and M. R. Manganese-Catalyzed Regioselective Dehydrogenative C- versus N-Alkylation Enabled by a Solvent Switch: Experiment and Computation. *Org. Lett.* **2020**, *22* (11), 4222–4227. https://doi.org/10.1021/acs.orglett.0c01270.

(42) Ohmura, T.; Kaito, Y.; Takeru, T.; Michinori, S. Intramolecular Addition of a Dimethylamino C(Sp3)–H Bond across C–C Triple Bonds Using IrCl(DTBM-SEGPHOS)(Ethylene) Catalyst: Synthesis of Indoles from 2-Alkynyl-N-Methylanilines. *Synthesis (Stuttg).* **2021**, *53* (17), 3057–3064. https://doi.org/10.1055/a-1511-1025.

(43) Wu, M.; Rulong Yan. Synthesis of Indoles from 2-Vinylanilines with PIFA or TFA and Quinones. *Synlett* **2017**, *28* (06), 729–733. https://doi.org/10.1055/s-0036-1588122.

(44) Andrea Porcheddu, Manuel G. Mura, Lidia De Luca, Marianna Pizzetti, and M. T. From Alcohols to Indoles: A Tandem Ru Catalyzed Hydrogen-Transfer Fischer Indole Synthesis. *Org. Lett.* **2012**, *14* (23), 6112–6115. https://doi.org/10.1021/ol3030956.

(45) Ye Wei, Indubhusan Deb, and N. Y. Palladium-Catalyzed Aerobic Oxidative Cyclization of N-Aryl Imines: Indole Synthesis from Anilines and Ketones. *J. Am. Chem. Soc.* **2012**, *134* (22), 9098–9101. https://doi.org/10.1021/ja3030824.

(46) Anna Andries-Ulmer, Christoph Brunner, Julia Rehbein, and T. G. Fluorine as

a Traceless Directing Group for the Regiodivergent Synthesis of Indoles and Tryptophans. *J. Am. Chem. Soc.* **2018**, *140* (40), 13034–13041. https://doi.org/10.1021/jacs.8b08350.

(47) Nicolas Zeidan, Sabine Bognar, Sophia Lee, and M. L. Palladium-Catalyzed Synthesis of 2-Cyanoindoles from 2-Gem-Dihalovinylanilines. *Org. Lett.* **2017**, *19* (19), 5058–5061. https://doi.org/10.1021/acs.orglett.7b02244.

(48) Bruno Anxionnat, Domingo Gomez Pardo, Gino Ricci, Kai Rossen, and J. C. Iridium-Catalyzed Hydrogen Transfer: Synthesis of Substituted Benzofurans, Benzothiophenes, and Indoles from Benzyl Alcohols. *Org. Lett.* **2013**, *15* (15), 3876–3879. https://doi.org/10.1021/ol401610e.

(49) Laiqiang Li, Zhong-Wei Hou, Pinhua Li, and L. W. Site-Selective Electrochemical C–H Cyanation of Indoles. *Org. Lett.* **2021**, *23* (15), 5983–5987. https://doi.org/10.1021/acs.orglett.1c02063.

(50) Lu Liu, Lei Li, Xin Wang, Ran Sun, Ming-Dong Zhou, and H. W. Mn(III)-Mediated Radical Cyclization of o-Alkenyl Aromatic Isocyanides with Boronic Acids: Access to N-Unprotected 2-Aryl-3-Cyanoindoles. *Org. Lett.* **2021**, *23* (15), 5826–5830. https://doi.org/10.1021/acs.orglett.1c01979.

(51) Bin Li, Shenghai Guo, Ju Zhang, Xinying Zhang, and X. F. Selective Access to 3-Cyano-1H-Indoles, 9H-Pyrimido[4,5-b]Indoles, or 9H-Pyrido[2,3-b]Indoles through Copper-Catalyzed One-Pot Multicomponent Cascade Reactions. *he J. Org. Chem.* **2015**, *80* (11), 5444–5456. https://doi.org/10.1021/acs.joc.5b00239.

(52) Qiao Yan, Ji Luo, Daisy Zhang-Negrerie, Hui Li, Xiuxiang Qi, and K. Z. Oxidative Cyclization of 2-Aryl-3-Arylamino-2-Alkenenitriles to N-Arylindole-3-Carbonitriles Mediated by NXS/Zn(OAc)2. *J. Org. Chem.* **2011**, *76* (21), 8690–8697. https://doi.org/10.1021/jo2012187.

(53) Bolm, J. B. and C. Iron(II) Triflate as a Catalyst for the Synthesis of Indoles by Intramolecular C−H Amination. *Org. Lett.* **2011**, *13* (8), 2012–2014. https://doi.org/10.1021/ol2004066.

(54) Benjamin J. Stokes, Huijun Dong, Brooke E. Leslie, Ashley L. Pumphrey, and T. G. D. Intramolecular C−H Amination Reactions: Exploitation of the Rh2(II)-Catalyzed Decomposition of Azidoacrylates. *J. Am. Chem. Soc.* **2007**, *129* (24), 7500–7501. https://doi.org/10.1021/ja072219k.

(55) Jixiang Ni, Yong Jiang, Zhenyu An, and R. Y. Cleavage of C–C Bonds for the Synthesis of C2-Substituted Quinolines and Indoles by Catalyst-Controlled Tandem Annulation of 2-Vinylanilines and Alkynoates. *Org. Lett.* **2018**, *20* (6), 1534–1537. https://doi.org/10.1021/acs.orglett.8b00260.

(56) Dmitry I. Bugaenko, Anastasia A. Dubrovina, Marina A. Yurovskaya, and A. V. K. Synthesis of Indoles via Electron-Catalyzed Intramolecular C–N Bond Formation. *Org. Lett.* **2018**, *20* (23), 7358–7362. https://doi.org/10.1021/acs.orglett.8b02784.

(57) Patrick Levesque and Pierre-André Fournier. Synthesis of Substituted Indole from 2-Aminobenzaldehyde through [1,2]-Aryl Shift. *J. Org. Chem.* **2010**, *75* (20), 7033–7036. https://doi.org/10.1021/jo1016713.

(58) Lee, R. S. T. and Y. R. Palladium-Catalyzed Direct Oxidative C–H Activation/Annulation for Regioselective Construction of N-Acylindoles. *Org. Lett.* **2020**, *22* (9), 3397–3401. https://doi.org/10.1021/acs.orglett.0c00877.

(59) Zisong Qi, Songjie Yu, and X. L. Rh(III)-Catalyzed Synthesis of N-Unprotected Indoles from Imidamides and Diazo Ketoesters via C–H Activation and C–C/C–N Bond Cleavage. *Org. Lett.* **2016**, *18* (4), 700–703.

https://doi.org/10.1021/acs.orglett.5b03669.
(60) Yue Li, Jinsong Peng, Xin Chen, Baichuan Mo, Xue Li, Peng Sun, and C. C. Copper-Catalyzed Synthesis of Multisubstituted Indoles through Tandem Ullmann-Type C–N Formation and Cross-Dehydrogenative Coupling Reactions. *J. Org. Chem.* **2018**, *83* (9), 5288–5294. https://doi.org/10.1021/acs.joc.8b00353.
(61) Rishi G. Vaswani, Brian K. Albrecht, James E. Audia, Alexandre Côté, Les A. Dakin, Martin Duplessis, Victor S. Gehling, Jean-Christophe Harmange, Michael C. Hewitt, Yves Leblanc, Christopher G. Nasveschuk, and A. M. T. A Practical Synthesis of Indoles via a Pd-Catalyzed C–N Ring Formation. *Org. Lett.* **2014**, *16* (16), 4114–4117. https://doi.org/10.1021/ol5018118.
(62) Ju Hyun Kim and Sang-gi Lee. Palladium-Catalyzed Intramolecular Trapping of the Blaise Reaction Intermediate for Tandem One-Pot Synthesis of Indole Derivatives. *Org. Lett.* **2011**, *13* (6), 1350–1353. https://doi.org/10.1021/ol200045q.
(63) Ning Lei, Yanling Shen, Yujun Li, Pan Tao, Liquan Yang, Zhishan Su, and K. Z. Electrochemical Iodoamination of Indoles Using Unactivated Amines. *Org. Lett.* **2020**, *22* (23), 9184–9189. https://doi.org/10.1021/acs.orglett.0c03158.
(64) Yu, Q. Q. and S. Visible-Light-Promoted Redox Neutral C–H Amidation of Heteroarenes with Hydroxylamine Derivatives. *Org. Lett.* **2014**, *16* (13), 3504–3507. https://doi.org/10.1021/ol501457s.
(65) Lee, H. Y. and Y. Copper-Catalyzed Electrophilic Amination of Heteroarenes via C–H Alumination. *J. Org. Chem.* **2015**, *80* (20), 10244–10251. https://doi.org/10.1021/acs.joc.5b01863.
(66) Selvarangam E. Kiruthika and Paramasivan Thirumalai Perumal. CuI-Catalyzed Coupling of Gem-Dibromovinylanilides and Sulfonamides: An Efficient Method for the Synthesis of 2-Amidoindoles and Indolo[1,2-a]Quinazolines. *Org. Lett.* **2014**, *16* (2), 484–487. https://doi.org/10.1021/ol403365t.
(67) Chao Shu, Yong-Heng Wang, Bo Zhou, Xin-Ling Li, Yi-Fan Ping, Xin Lu, and L.-W. Y. Generation of α-Imino Gold Carbenes through Gold-Catalyzed Intermolecular Reaction of Azides with Ynamides. *J. Am. Chem. Soc.* **2015**, *137* (30), 9567–9570. https://doi.org/10.1021/jacs.5b06015.
(68) Xianhai Tian, Lina Song, Chunyu Han, Cheng Zhang, Yufeng Wu, Matthias Rudolph, Frank Rominger, and A. S. K. H. Gold(III)-Catalyzed Formal [3 + 2] Annulations of N-Acyl Sulfilimines with Ynamides for the Synthesis of 4-Aminooxazoles. *Org. Lett.* **2019**, *21* (8), 2937–2940. https://doi.org/10.1021/acs.orglett.9b01011.
(69) Xianhai Tian, Lina Song, Matthias Rudolph, Qian Wang, Xinlong Song, Frank Rominger, and A. S. K. H. N-Pyridinyl Sulfilimines as a Source for α-Imino Gold Carbenes: Access to 2-Amino-Substituted N-Fused Imidazoles. *Org. Lett.* **2019**, *21* (6), 1598–1601. https://doi.org/10.1021/acs.orglett.9b00140.
(70) Wang, Q.-D.; Zhou, B.; Yang, J.-M.; Fang, D.; Ren, J.; Zeng, B.-B. Iron-Catalyzed C3-Formylation of Indoles with Formaldehyde and Aqueous Ammonia under Air. *Synlett* **2017**, *28* (19), 2670–2674. https://doi.org/10.1055/s-0036-1589079.
(71) Prasath Kothandaraman, Srinivasa Reddy Mothe, Sharon Si Min Toh, and P. W. H. C. Gold-Catalyzed Cycloisomerizations of 1-(2-(Tosylamino)Phenyl)Prop-2-Yn-1-Ols to 1H-Indole-2-Carbaldehydes and (E)-2-(Iodomethylene)Indolin-3-Ols. *J. Org. Chem.* **2011**, *76* (19), 7633–7640.

https://doi.org/10.1021/jo201208e.

(72) Hongming Jin, Long Huang, Jin Xie, Matthias Rudolph, Frank Rominger, A. S. K. H. Gold-Catalyzed C-H Annulation of Anthranils with Alkynes: A Facile, Flexible, and Atom-Economical Synthesis of Unprotected 7-Acylindoles. *Angew. Chem. Int. Ed.* **2016**, *55* (2), 794–797.

(73) David J. Gorin, Nicole R. Davis, and F. D. T. Gold(I)-Catalyzed Intramolecular Acetylenic Schmidt Reaction. *J. Am. Chem. Soc.* **2005**, *127* (32), 11260–11261. https://doi.org/DOI: 10.1021/ja053804t.

(74) Benitez, D.; Shapiro, N. D.; Tkatchouk, E.; Wang, Y.; Goddard, W. A.; Toste, F. D. A Bonding Model for Gold(I) Carbene Complexes. *Nat. Chem.* **2009**. https://doi.org/10.1038/nchem.331.

(75) Dorel, R.; Echavarren, A. M. Gold(I)-Catalyzed Activation of Alkynes for the Construction of Molecular Complexity. *Chem. Rev.* **2015**, *115* (17), 9028–9072. https://doi.org/10.1021/cr500691k.

(76) Hong, F.-L.; Ye, L.-W. Transition Metal-Catalyzed Tandem Reactions of Ynamides for Divergent N-Heterocycle Synthesis. *Acc. Chem. Res.* **2020**, *53* (9), 2003–2019. https://doi.org/10.1021/acs.accounts.0c00417.

(77) Chen, Y. B.; Qian, P. C.; Ye, L. W. Brønsted Acid-Mediated Reactions of Ynamides. *Chemical Society Reviews*. 2020. https://doi.org/10.1039/d0cs00474j.

(78) Luo, J.; Chen, G. S.; Chen, S. J.; Yu, J. S.; Li, Z. D.; Liu, Y. L. Exploiting Remarkable Reactivities of Ynamides: Opportunities in Designing Catalytic Enantioselective Reactions. *ACS Catalysis*. 2020. https://doi.org/10.1021/acscatal.0c04180.

(79) Hu, Y. C.; Zhao, Y.; Wan, B.; Chen, Q. A. Reactivity of Ynamides in Catalytic Intermolecular Annulations. *Chemical Society Reviews*. 2021. https://doi.org/10.1039/d0cs00283f.

(80) Shandilya, S.; Protim Gogoi, M.; Dutta, S.; Sahoo, A. K. Gold-Catalyzed Transformation of Ynamides. *Chem. Rec.* **2021**, *21*, 4123–4149. https://doi.org/10.1002/tcr.202100159.

(81) M. Sc. Hongming Jin, M. Sc. Bin Tian, M. Sc. Xinlong Song, Dr. Jin Xie, Dr. Matthias Rudolph, Dr. Frank Rominger, P. D. A. S. K. H. Gold-Catalyzed Synthesis of Quinolines from Propargyl Silyl Ethers and Anthranils through the Umpolung of a Gold Carbene Carbon. *Angew. Chem. Int. Ed.* **2016**, *55* (41), 12688–12692.

(82) Lina Song, Xianhai Tian, Matthias Rudolph, F. R. and A. S. K. H. Gold(Iii)-Catalyzed Chemoselective Annulations of Anthranils with N-Allylynamides for the Synthesis of 3-Azabicyclo[3.1.0]Hexan-2-Imines. *Chem. Commun.*, **2019**, *55*, 9007–9010.

(83) Prakash D. Jadhav, Xin Lu, and R.-S. L. Gold-Catalyzed [5+2]- and [5+1]-Annulations between Ynamides and 1,2-Benzisoxazoles with Ligand-Controlled Chemoselectivity. *ACS Catal.* **2018**, *8* (10), 9697–9701. https://doi.org/10.1021/acscatal.8b03011.

(84) Wei Xu, Jidong Zhao, Xiangdong Li, and Y. L. Selective [5 + 1] and [5 + 2] Cycloaddition of Ynamides or Propargyl Esters with Benzo[d]Isoxazoles via Gold Catalysis. *J. Org. Chem.* **2018**, *83* (24), 15470–15485. https://doi.org/10.1021/acs.joc.8b02935.

(85) Wei Xu, Yulong Chen, Ali Wang, and Y. L. Benzofurazan N-Oxides as Mild Reagents for the Generation of α-Imino Gold Carbenes: Synthesis of Functionalized 7-Nitroindoles. *Org. Lett.* **2019**, *21* (18), 7613–7618.

https://doi.org/10.1021/acs.orglett.9b02893.
(86) Changlei Zhu, Luyao Kou, X. B. Au(I)-Catalyzed Annulation of Benzofurazan N-Oxides with Ynamides: From Predicting the Chemo-Selectivity to the Synthesis of 7-Nitroindole Derivatives. *Chinese J. Chem.* **2020**, *38* (1), 57–62.
(87) Zhou, A.-H.; He, Q.; Shu, C.; Yu, Y.-F.; Liu, S.; Zhao, T.; Zhang, W.; Lu, X.; Ye, L.-W. Atom-Economic Generation of Gold Carbenes: Gold-Catalyzed Formal [3 + 2] Cycloaddition between Ynamides and Isoxazoles. *Chem. Sci.* **2015**, No. 6, 1265−1271.
(88) Ai-Hua Zhou, Qiao He, Chao Shu, Yong-Fei Yu, Shuang Liu, Tian Zhao, Wei Zhang, X. L. and L.-W. Y. Atom-Economic Generation of Gold Carbenes: Gold-Catalyzed Formal [3+2] Cycloaddition between Ynamides and Isoxazoles. *Chem.Sci.* **2015**, *6*, 1265–1271.
(89) Liu, S. S. G. and R.-S. Gold-Catalyzed [4+3]- and [4+2]-Annulations of 3-En-1-Ynamides with Isoxazoles via Novel 6π-Electrocyclizations of 3-Azahepta Trienyl Cations. *Chem. Sci.* **2018**, *9*, 2991–2995. https://doi.org/10.1039/C8SC00232K.
(90) Ming Chen , Ning Sun, H. C. and Y. L. Dioxazoles, a New Mild Nitrene Transfer Reagent in Gold Catalysis: Highly Efficient Synthesis of Functionalized Oxazoles. *Chem. Commun*. **2016**, *52*, 6324–6327. https://doi.org/10.1039/C6CC02776H.
(91) Xu, W.; Wang, G.; Sun, N.; Liu, Y. Gold-Catalyzed Formal [3 + 2] Cycloaddition of Ynamides with 4,5-Dihydro-1,2,4-Oxadiazoles: Synthesis of Functionalized 4-Aminoimidazoles. *Org. Lett.* **2017**, *19* (12), 3307–3310. https://doi.org/10.1021/acs.orglett.7b01469.
(92) Julia O. Strelnikova, Nikolai V. Rostovskii, Galina L. Starova, Alexander F. Khlebnikov, and M. S. N. Rh(II)-Catalyzed Transannulation of 1,2,4-Oxadiazole Derivatives with 1-Sulfonyl-1,2,3-Triazoles: Regioselective Synthesis of 5-Sulfonamidoimidazoles. *J. Org. Chem.* **2018**, *83* (18), 11232–11244. https://doi.org/10.1021/acs.joc.8b01809.
(93) Yang Wang, Hao Shen, Z. X. Atom-Economical Synthesis of 2-Aminoimidazoles via [3+2] Annulation Catalyzed by Titanacarborane Monoamide. *Synlett* **2011**, *7*, 969–973. https://doi.org/10.1055/s-0030-1259713.
(94) Jihui Li and Luc Neuville. Copper-Catalyzed Oxidative Diamination of Terminal Alkynes by Amidines: Synthesis of 1,2,4-Trisubstituted Imidazoles. *Org. Lett.* **2013**, *15* (7), 1752–1755. https://doi.org/10.1021/ol400560m.
(95) Jun Xiong, Xiao Wei, Zi-Ming Liu, and M.-W. D. One-Pot Synthesis of Polysubstituted Imidazoles via Sequential Staudinger/Aza-Wittig/Ag(I)-Catalyzed Cyclization/Isomerization. *J. Org. Chem.* **2017**, *82* (24), 13735–13739. https://doi.org/10.1021/acs.joc.7b02606.
(96) Hendrich, C. M.; Sekine, K.; Koshikawa, T.; Tanaka, K.; Hashmi, A. S. K. Homogeneous and Heterogeneous Gold Catalysis for Materials Science. *Chem. Rev*. **2021**. https://doi.org/10.1021/acs.chemrev.0c00824.
(97) Wang, W.; Ji, C. L.; Liu, K.; Zhao, C. G.; Li, W.; Xie, J. Dinuclear Gold Catalysis. *Chem. Soc. Rev*. **2021**. https://doi.org/10.1039/d0cs00254b.
(98) Zhang, Y.; Luo, T.; Yang, Z. Strategic Innovation in the Total Synthesis of Complex Natural Products Using Gold Catalysis. *Nat. Prod. Rep*. **2014**. https://doi.org/10.1039/c3np70075e.
(99) Gorin, D. J.; Toste, F. D. Relativistic Effects in Homogeneous Gold Catalysis. *Nature*. 2007. https://doi.org/10.1038/nature05592.

(100) Rocchigiani, L.; Bochmann, M. Recent Advances in Gold(III) Chemistry: Structure, Bonding, Reactivity, and Role in Homogeneous Catalysis. *Chem. Rev.* **2021**. https://doi.org/10.1021/acs.chemrev.0c00552.

(101) Lu, Z.; Li, T.; Mudshinge, S. R.; Xu, B.; Hammond, G. B. Optimization of Catalysts and Conditions in Gold(I) Catalysis - Counterion and Additive Effects. *Chem. Rev.* **2021**, *121* (14), 8452–8477. https://doi.org/10.1021/acs.chemrev.0c00713.

(102) Chetan C. Chintawar, Amit K. Yadav, Anil Kumar, Shashank P. Sancheti, and N. T. P. Divergent Gold Catalysis: Unlocking Molecular Diversity through Catalyst Control. *Chem. Rev.* **2021**, *121* (14), 8478−8558.

(103) Reyes, R. L.; Iwai, T.; Sawamura, M. Construction of Medium-Sized Rings by Gold Catalysis. *Chem. Rev.* **2021**, *121* (14), 8926–8947. https://doi.org/10.1021/acs.chemrev.0c00793.

(104) Wang, T.; Hashmi, A. S. K. 1,2-Migrations onto Gold Carbene Centers. *Chemical Reviews*. 2021. https://doi.org/10.1021/acs.chemrev.0c00811.

(105) Zheng, Z.; Ma, X.; Cheng, X.; Zhao, K.; Gutman, K.; Li, T.; Zhang, L. Homogeneous Gold-Catalyzed Oxidation Reactions. *Chem. Rev.* **2021**. https://doi.org/10.1021/acs.chemrev.0c00774.

(106) Ximei Zhao, Matthias Rudolph, A. M. A. & A. S. K. H. Easy Access to Pharmaceutically Relevant Heterocycles by Catalytic Reactions Involving α-Imino Gold Carbene Intermediates. *Front. Chem. Sci. Eng.* **2020**, *14*, 317–349.

(107) Zeng, Z.; Jin, H.; Sekine, K.; Rudolph, M.; Rominger, F.; Hashmi, A. S. K. Gold-Catalyzed Regiospecific C−H Annulation of o -Ethynylbiaryls with Anthranils: π-Extension by Ring-Expansion En Route to N-Doped PAHs. *Angew. Chemie Int. Ed.* **2018**, *57* (23), 6935–6939. https://doi.org/10.1002/anie.201802445.

(108) Zhongyi Zeng, Hongming Jin, Matthias Rudolph, Frank Rominger, A. S. K. H. Gold(III)-Catalyzed Site-Selective and Divergent Synthesis of 2-Aminopyrroles and Quinoline-Based Polyazaheterocycles. *Angew. Chem. Int. Ed.* **2018**, *57*, 16549 –16553.

(109) González, J.; Santamaría, J.; Suárez-Sobrino, Á. L.; Ballesteros, A. One-Pot and Regioselective Gold-Catalyzed Synthesis of 2-Imidazolyl-1-Pyrazolylbenzenes from 1-Propargyl-1H-Benzotriazoles, Alkynes and Nitriles through α-Imino Gold(I) Carbene Complexes. *Adv. Synth. Catal.* **2016**. https://doi.org/10.1002/adsc.201600022.

(110) Ye, L. W.; Zhu, X. Q.; Sahani, R. L.; Xu, Y.; Qian, P. C.; Liu, R. S. Nitrene Transfer and Carbene Transfer in Gold Catalysis. *Chemical Reviews*. 2021. https://doi.org/10.1021/acs.chemrev.0c00348.

(111) Stylianakis, I.; Litinas, I.; Nieto Faza, O.; Kolocouris, A.; Silva López, C. On the Mechanism of the Au(I)-Mediated Addition of Alkynes to Anthranils to Furnish 7-Acylindoles. *J. Phys. Org. Chem.* **2022**, No. January, 1–9. https://doi.org/10.1002/poc.4333.

# Chapter 7

## The key role of protodeauration in the gold catalyzed reaction of 1,3-diynes with pyrrole and indole to form complex heterocycles

Because the indole scaffold is a significant structural motif that can be found in a large number of alkaloids, as well as several other bioactive compounds, it is worthwhile a study on the traits of a reaction for the synthesis of indole derivatives. At his former work on one pot reaction for the synthesis of 4,7-disubstituted-indole, Ohno[1] tested the possibility of intermolecular formal [4+2] reaction between 1,3-diynes and pyrroles. It is an atom economical method that provides a variety of 4,7-disubstituted-indoles and carbazoles respectively from directly available 1,3-diynes.

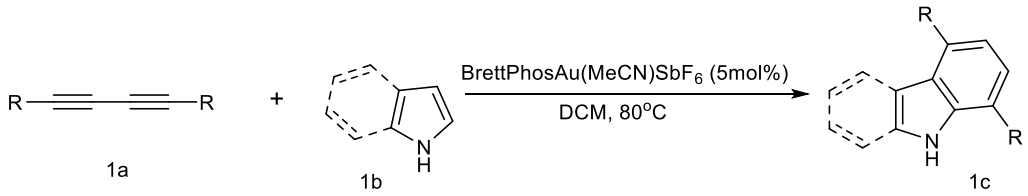


Scheme 7.1. Gold catalyzed formal [4+2] reaction between 1,3-diynes and pyrrole.

In an attempt to explore the mechanism of the reaction, discreet points of interest arise. A similar approach to Fang's work[2] was applied, by splitting the reaction to all possible obvious paths. Thus, the first part of this work is the exploration of four different paths starting from 1,3-diyne and pyrrole to regioisomeric products **P1**-**P4**. Then, a comparative study between 1,3-dines and the skipped 1,4-diynes follows, in order to reveal the role of the methylene group that interferes between the alkyne groups. That is, how the interruption of resonance among alkyne groups influence the energy profile of the reaction. Noteworthy, in the case of 1,3-diynes an enyne intermediate is isolated, while in the reaction with skipped diynes not. Next, we tried to correlate the kind of substituent of 1,3-diyne with the yield of the reaction, since there are experimental data of various substituents. Finally, based on the experimental data that the reaction proceeds not only with pyrrole, but also with indole to form carbazole, we tried to certify or to change the proposed mechanism model.

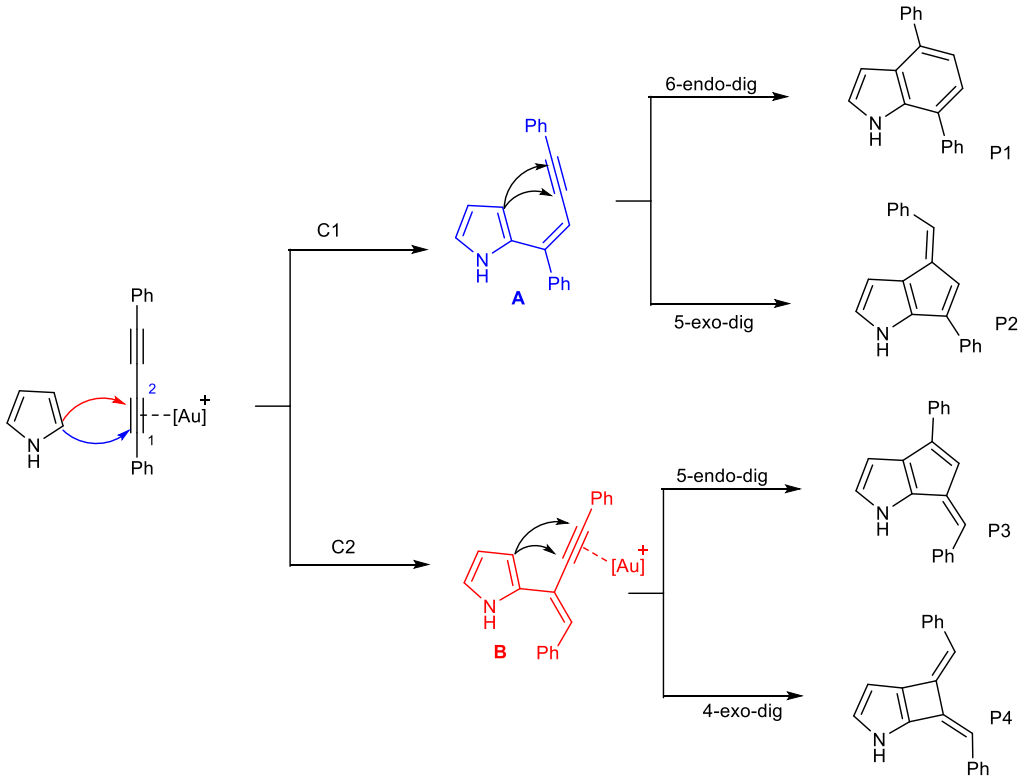


Scheme 7.2. Representation of Main Pathways in the Au(I)-Catalyzed Reaction between 1,3-Diyne and Pyrrole

The essential pattern of the mechanism of the reaction is devided to two parts, a first step of hydroarylation and a second step of cyclization. For the first step there are two possible pathways, the nucleophilic attack of C2 of pyrrole to C1 or C2 of the triple bond system of 1,3-diyne, leading to the enyne intermediates, **B** and the observable **A**. From that point, two different ways for cyclization are available for each enyne **A** and **B**. For enyne intermediate **A**, either 6-endo-dig or 5-exo-dig cyclizations are feasible, leading to products **P1** (1,4-disubstituted-indole) and **P2** (cyclopenta[b]pyrrole) respectively. Similarly, for enyne intermediate **B** either 5-endo-dig or 4-exo-dig cyclizations are feasible. Products **P3** (cyclopenta[b]pyrrole) and **P4** (cyclobuta[b]pyrrole) are formed respectively. The same model was applied with indole, instead of pyrrole, in the role of nucleophile.

### 7.1 Formal [4 + 2] reaction between pyrrole and 1,3-diynes

Based on the structures of scheme 7.2, DFT calculations realized, revealing the energy profile of the reaction as depicted at schemes 7.3a and 7.3b. The main steps of the mechanism are presented: i. the activation of triple bond of 1,3-diyne by gold catalyst, ii. nucleophilic attack by C2 of pyrrole to the activated alkyne iii migration of the gold catalyst to the unreacted distal alkyne and iv. formation of the second sigma bond by an intramolecular attack of the pyrrole ring that leads to the ring closure.

Starting from the point that only product **P1** is experimentally observed, an initial attempt was realized to clarify the mechanism analyzing step by step the traits of the reaction (Scheme 7.3a). Unexpectedly, the initial attack on the activated diyne seems to be more favourable kinetically onto the internal carbon atom ($\mathbf{TS_{2a–7a}}$ vs. $\mathbf{TS_{2a–3a}}$) by about 3 kcal mol$^{-1}$. Moreover, the terminal C–C bond formation is more stable than the internal one (0.9 vs. 4.5 kcal mol$^{-1}$ for **3a** vs. **7a**, respectively).

Then, a step of pyrrole unit re-aromatization and gold migration to the conjugated triple bond renders the reaction not only irreversible, but also offers the driving force of the overall mechanistic process due to the drop of energy (−28.3 kcal mol$^{-1}$ for **4a** and −23.6 for **8a**).

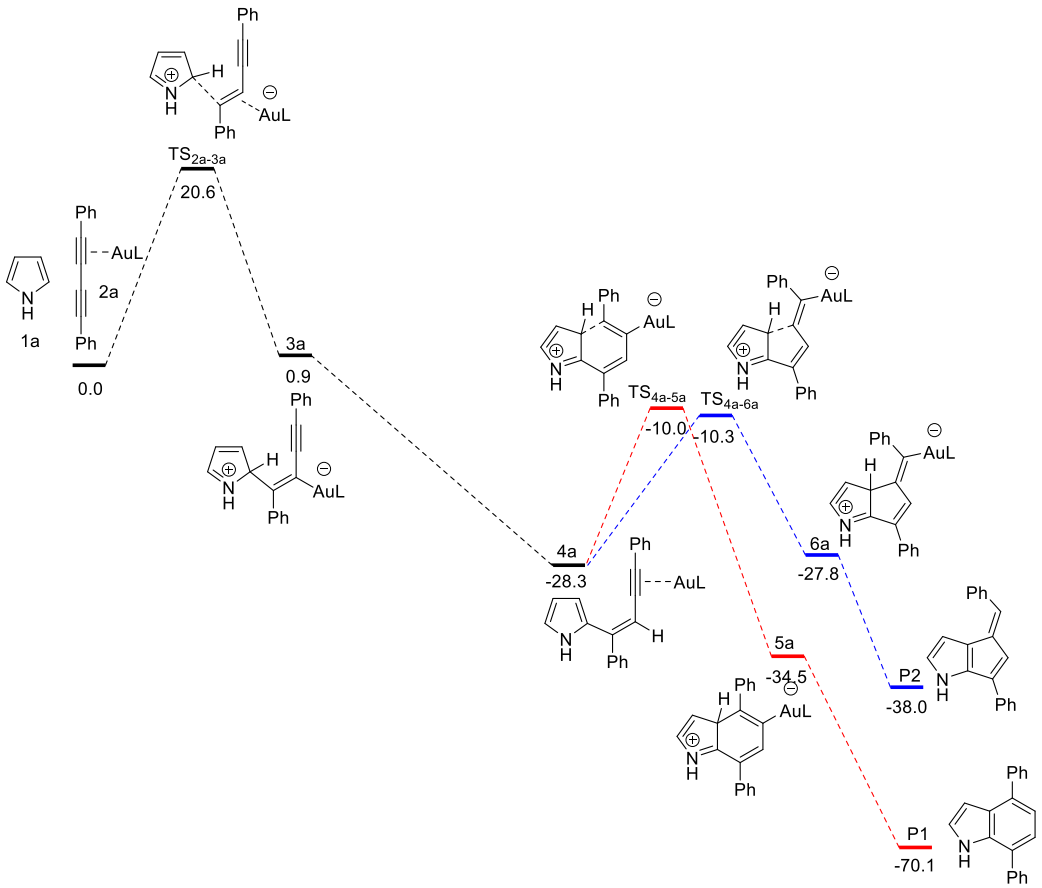

Scheme 7.3a Relative free energies (kcal/mol, 298 K and 1 atm) computed for key steps along the alternative reaction pathways in the formal [4 + 2] reaction between pyrrole and diynes (path A)

From **4a**, a cyclization step proceeds to form **6a**, a two five member ring structure, via $\mathbf{TS_{4a\_6a}}$. Alternatively, five and six member rings are fused to form the experimentally observed product via **5a**. The two paths present similar energy barriers (-10.3 kcal/mol vs -10.0kcal/mol for $\mathbf{TS_{4a\_6a}}$. vs $\mathbf{TS_{4a\_5a}}$ respectively). So, the question that arises is why the only observable product is **P1** and not **P2** since both of them present similar energy barrier (-10.3 kcal/mol vs -10.0kcal/mol for $\mathbf{TS_{4a\_6a}}$. vs $\mathbf{TS_{4a\_5a}}$ respectively).

Comparing the energy of **5a** and **6a** the conclusion is that the reverse reaction of **6a** to **4a** is easier to happen due to 17.5kcal/mol than the competitive path **5a** to **4a** that is 24.5kcal/mol. Thus, the formation of **6a** is a reversible procedure while that of **5a** an irreversible one.

For the second part of the proposed mechanism (Scheme 7.3b) the picture is even simpler. The structure **7a**, after a significant drop of energy due to a step of pyrrole unit re-aromatization and gold migration to the conjugated triple bond forms **8a** irreversibly. From the aspect of both kinetics and thermodynamics, formation of product **P3** is favoured since the difference in activation energy ($\mathbf{TS_{8a\_9a}}$ vs $\mathbf{TS_{8a\_10a}}$ is 22.8 kcal/mol vs 32.8kcal/mol respectively) leads to **9a** and consequently to a cyclopenta[b]pyrrole.

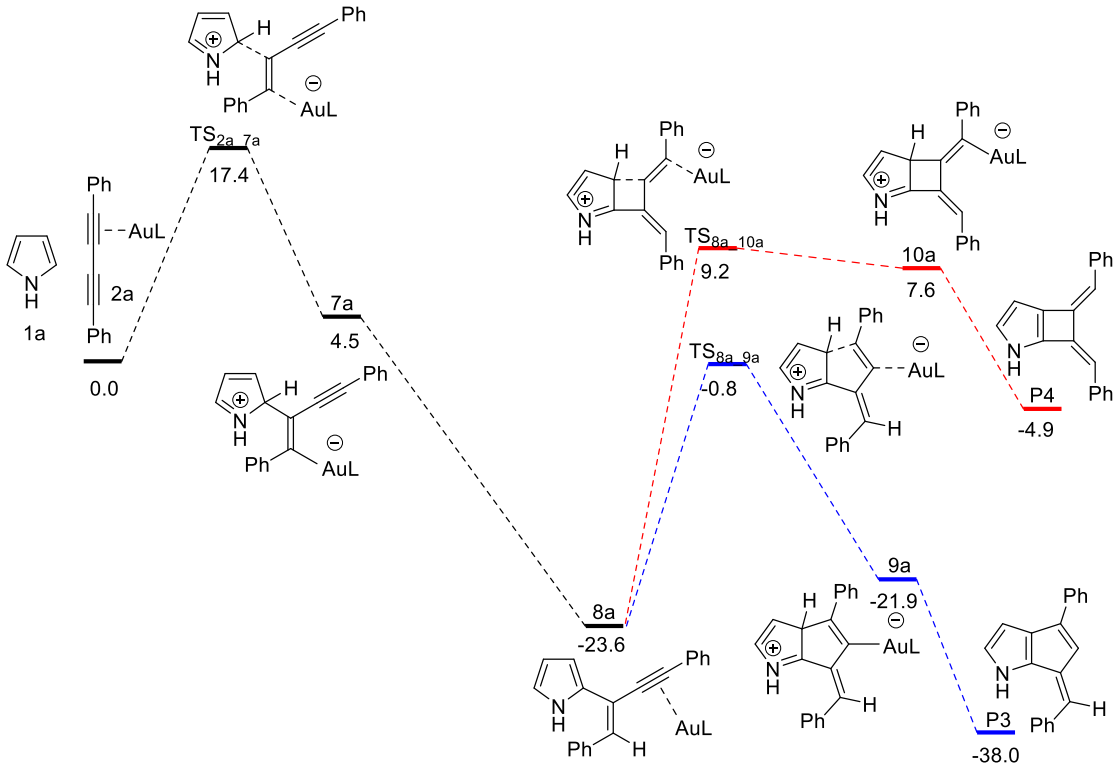


Scheme 7.3b Relative free energies (kcal/mol, 298 K and 1 atm) computed for key steps along the alternative reaction pathways in the formal [4 + 2] reaction between pyrrole and diynes (path B)

To sum up briefly, the results of the DFT calculations propose that: i. the overall product determining step is the formation of **4a** vs. **8a**, due to the drastic drop in energy after the formation of the first C–C bond. ii. the formation of product **P3** is favoured versus **P1**, since at the step of formation of the first C-C bond formation of **7a** is favoured vs **3a** ($\mathbf{TS_{2a–7a}}$ vs $\mathbf{TS_{2a–3a}}$ is 17.4 kcal $mol^{-1}$ vs. 20.6 kcal $mol^{-1}$).

Our DFT calculations are in striking contradiction not only with the observed formation of the indole products but also with the reported experimental conditions. Moreover, Ohno and coworkers[1] quenched the reaction before completion, and they only observed intermediate **4a** (not **8a**), which, when subjected again to the reaction conditions, afforded the indole product **P1**. Furthermore, the conditions of the reaction are not in compliance with the calculated findings. That is, for the favoured but unobserved product **P3**, the activation energy of the rate limiting transition state is low enough, approximately 23kcal/mol (from **8a** to $\mathbf{TS_{8a–9a}}$), while the reaction proceeds at 80°C for long reaction time.

These contradictions suggest that a key step may have been overlooked in this reaction, and that the missed step has a drastic impact on the kinetics and the reaction outcome. We therefore analyzed the reaction pathways in greater detail and found that

what may have been overlooked is the kinetic cost for the isomerizations between the pairs **3a**/**4a** and **7a**/**8a**. These isomerizations formally involve a protodeauration step and gold migration towards the remaining alkyne of the adduct.

Most computational and experimental studies in homogeneous gold catalysis deliberately skip protodeauration steps on the assumption that they are usually low cost and do not affect the overall catalytic process. A number of careful studies however have raised concerns in this regard and have found that, while in some cases these steps are indeed rapid and demand low energy inputs, for other cases, this assumption is wrong. [3,4]

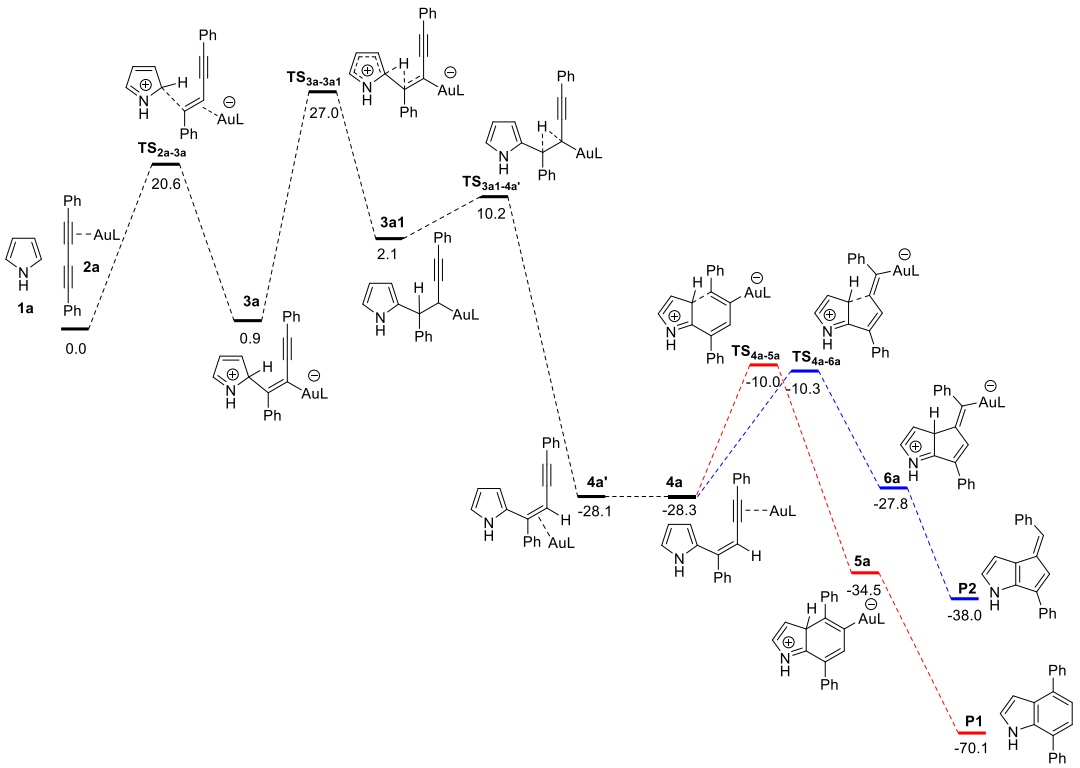


Scheme 7.4a Relative free energies (kcal/mol, 298 K and 1 atm) computed for the alternative reaction pathways in the formal [4 + 2] reaction between pyrrole and diynes including protodeauration steps of key intermediates (path A)

After the calculation of the structures for the isomerization steps of the **3a**/**4a** and **7a**/**8a** pairs we obtained the holistic view of the mechanism of the reaction. In schemes **7.4a** and **7.4b** we can find the answers to the above contradictions one by one. First, the rate determining steps for both alternatives lie within the protodeauration and migration section. To be more precise, proton migration and re-aromatization of the pyrrole ring is the most energy demanding step. Thus, the energy barrier for the first path is 26.1kcal/mol (from **3a** to $\mathbf{TS_{3a\_3a1}}$) and for the second (from **7a** to $\mathbf{TS_{7a\_7a1}}$) 30.8kcal/mol respectively. The result is consistent with the conditions

that the reaction proceeds with long reaction time at 80°C. As a consequence of the first result, we receive the response to the next contradiction. The formation of **7a1** via 1,2-H migration is more energetically demanding than that of the formation **3a1** (30.8kcal/mol vs 26.1kcal/mol). Combining that point with the low energy barrier for C-C cleavage (from **7**a to $\mathbf{TS_{2a\_7a}}$ is 12.9kcal/mol) we conclude that the reaction turns back to the reactants precluding the formation of products **P3** and **P4**. On the contrary, the path to product **P1** is consistent with the low energy barrier of the step of H-migration. Moreover, as we explain above, once **4a** is formed, the indole structure clearly has a thermodynamic advantage to become the observed product.

Checking and comparing the experimental data with our calculations we can focus on a couple of points. First, intermediate **4a** was isolated and characterized. That means that the mechanism consist of an initial step of intermolecular hydroarylation to form the enyne type intermediate **4a**, and then a second step of intramolecular 6-endo-dig hydroarylation to form indole derivative **P1**.

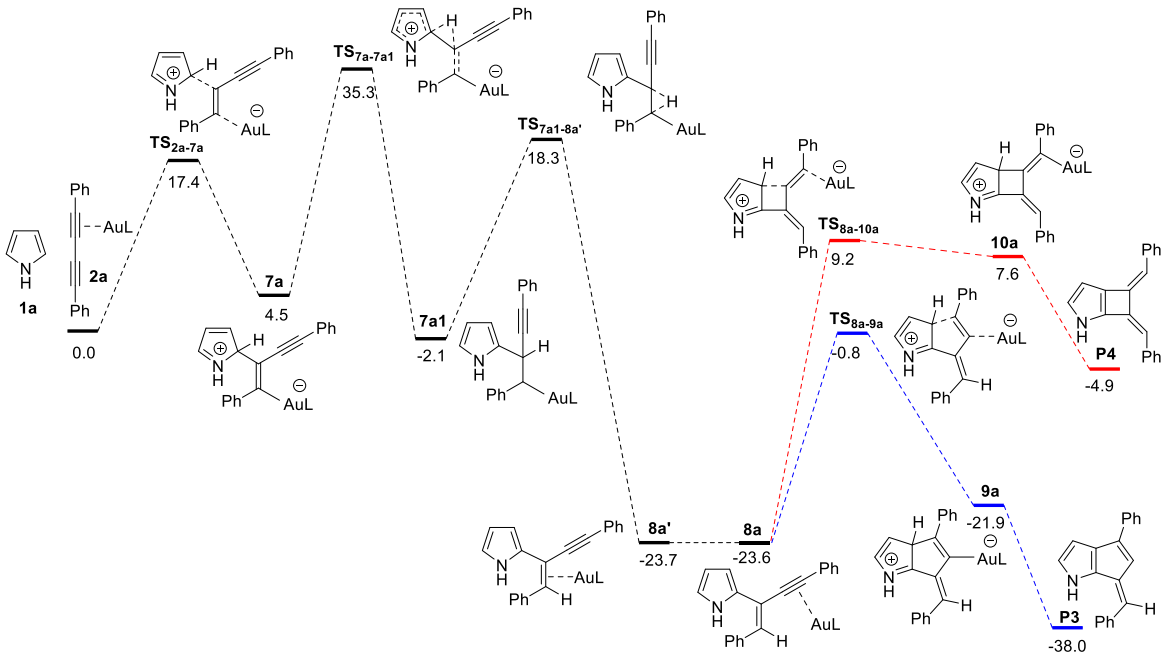


Scheme 7.4b Relative free energies (kcal/mol, 298 K and 1 atm) computed for the alternative reaction pathways in the formal [4 + 2] reaction between pyrrole and diynes including protodeauration steps of key intermediates (path B)

Comparing the two gold-catalyzed reactions of pyrrole with the conjugated 1,3-diyne and with skipped diynes or 1,4-diynes, we see similarities. The first step of the intermolecular hydroarylation, which involves the nucleophilic attack on the activated alkyne, was also defined as rate limiting. [2] Apparently, the conjugated 1,3-diyne

system is able to stabilize more efficiently the charge displacement produced upon nucleophilic attack, thus reducing the activation energy for this step.

### 7.2 Substituent effect for selectivity

Ohno and coworkers [1] applied a variety of symmetrical 1,3-diynes in the reaction receiving disparate results. They examined the role of substituent X of the diynes in relation to the yield. Most of the substituents tested were substituted phenyl ring groups so as a relation to be established between electron donating ability of the substituent and yield of the reaction. Thus, electron donating groups such as 4-MeO-phenyl group was tested, and electron withdrawing group like methoxy-carbonyl-phenyl group. Moreover, aliphatic substituents were tested also.

For our study we chose four different types of substituents (table 7.1). The first entry X=Ph is used as a control. Entry 2 is an aliphatic group with negative effect on the yield, while entry 3 is the strongest activating group with the higher value of yield. On the contrary, entry 4 bears a deactivating moiety on aryl group and presents the poorest yield.

According to the previously obtained profile, any competitive branching produces deleterious effects on the yield of the reaction. Such an effect should therefore start from **4**, where the driving force of the reaction has already been released and there are two alternative pathways not far away from each other. The alternative pathways starting at intermediate **4** include the formation of the second C–C bond towards bicyclic structures **P1** and **P2**. The calculation of the activation energies reveals a qualitative correlation between the barriers and the observed yields.

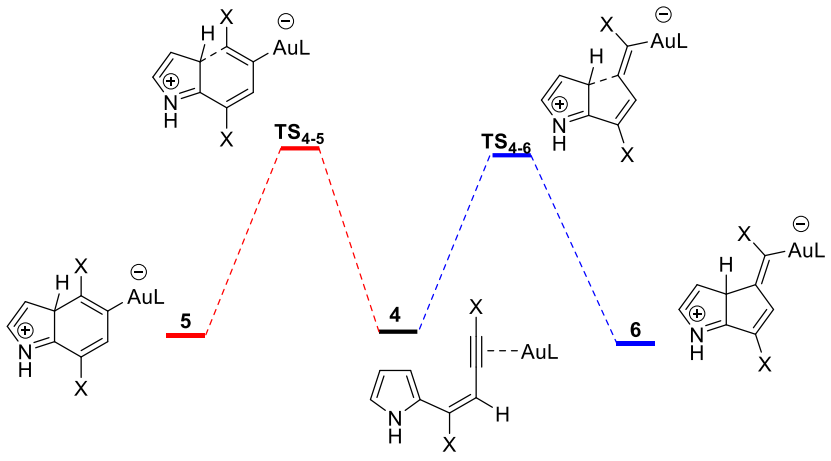


Scheme 7.5. Investigation of the impact of the substituent X on the alternative cyclization pathway starting from intermediate 4.

After the calculations of the step 4-5 and 4-6, the activation energies between the control (entry1) and the other substituents were compared and correlated to experimental data. Substitution of Ph group with Cy on 1,3-diynes alters the energy profile of the two paths. The aliphatic group increases activation energy from 18.3kcal/mol to 20.9kcal/mol at the path leading to the observable product **P1**. In parallel, it reduces the energy barrier to **P2**. Thus, the calculations explain the low yield (35% vs 66%). On the contrary, the introduction of an activating group (entry 3) reduces activation energy and turns the balance on the side of **P1**, since path 4-5 is favored versus path 4-6 ($\mathbf{TS_{4\_5}}$/$\mathbf{TS_{4\_6}}$ are 15.8kcal/mol and 16.8kcal/mol respectively) with a yield of 85%.

| Entry | X | $\Delta G^{\neq}$ $TS_{4-5}$ | $\Delta G_{4-5}$ | $\Delta G^{\neq}$ $TS_{4-6}$ | $\Delta G_{4-6}$ | % -yield / *t*(h) |
|---|---|---|---|---|---|---|
| **1** | Ph | 18.3 | -6.2 | 18.0 | 0.5 | 66 / 12 |
| **2** | Cy | 20.9 | -6.0 | 17.2 | 1.9 | 35 / 24 |
| **3** | 4-MeO-$C_6H_4$ | 15.8 | -6.6 | 16.8 | 0.4 | 85 / 4 |
| **4** | 4-COOMe- $C_6H_4$ | 18.1 | -7.6 | 15.6 | -1.0 | 26 / 24 |

Table 7.1. Activation energies calculated for the second step of the reaction between pyrrole and a symmetrical diyne.

It seems therefore that, although **6** is thermodynamically less stable than **5**, the channel leading to the formation of the former is operative, perhaps due to rapid evolution of **6** into more stable species, and it depletes **4** causing a reduction in the observed yield of the indole product **P1**.

### 7.3 Reaction of 1,3-diyne with indole

In the second part of the study we focused on the reaction of 1,3-diyne with indole. In contrast to the reaction of 1,3-diyne with pyrrole that furnished an enyne type intermediate **4a** after the nucleoplilic attack of C2 of pyrrole to the activated diyne, indole leads directly to carbazole without any isolated intermediate. So, in the case of pyrrole is relatively well known for acting as a nucleophile through its C2 position when it is not substituted and its C3 position when the former is substituted. [5]

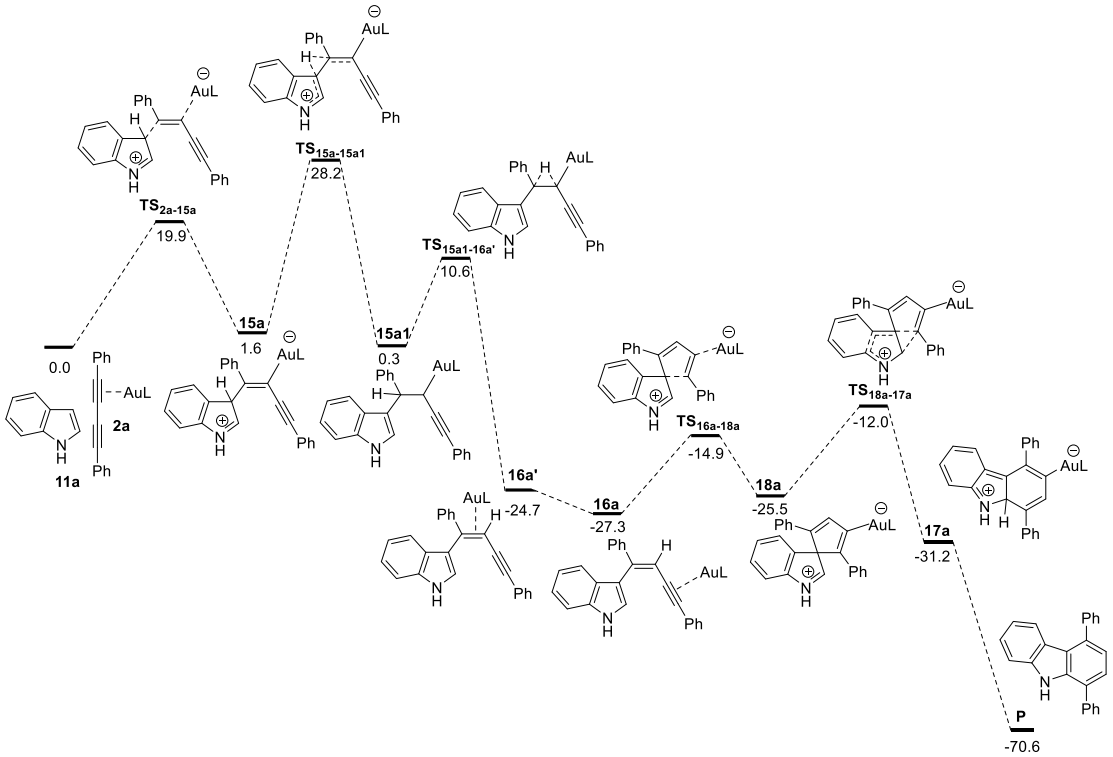


Scheme 7.6a. Reactivity profile of C3 of indole with 1,3-diyne. Relative energies used compounds **11a** and **2a** as the zero energy reference.

Additionally, the experimental evidence of C2 substituted intermediate dispels any doubt about the mechanism of the reaction. On the other hand indoles are very well known for their nucleophilic character at C3 (acting essentially as an enamine which is coincidentally attached to a by-standing benzene ring). In front of a dilemma of nucleophilic attack of indole with C2 or C3 to activated diyne we checked both options.

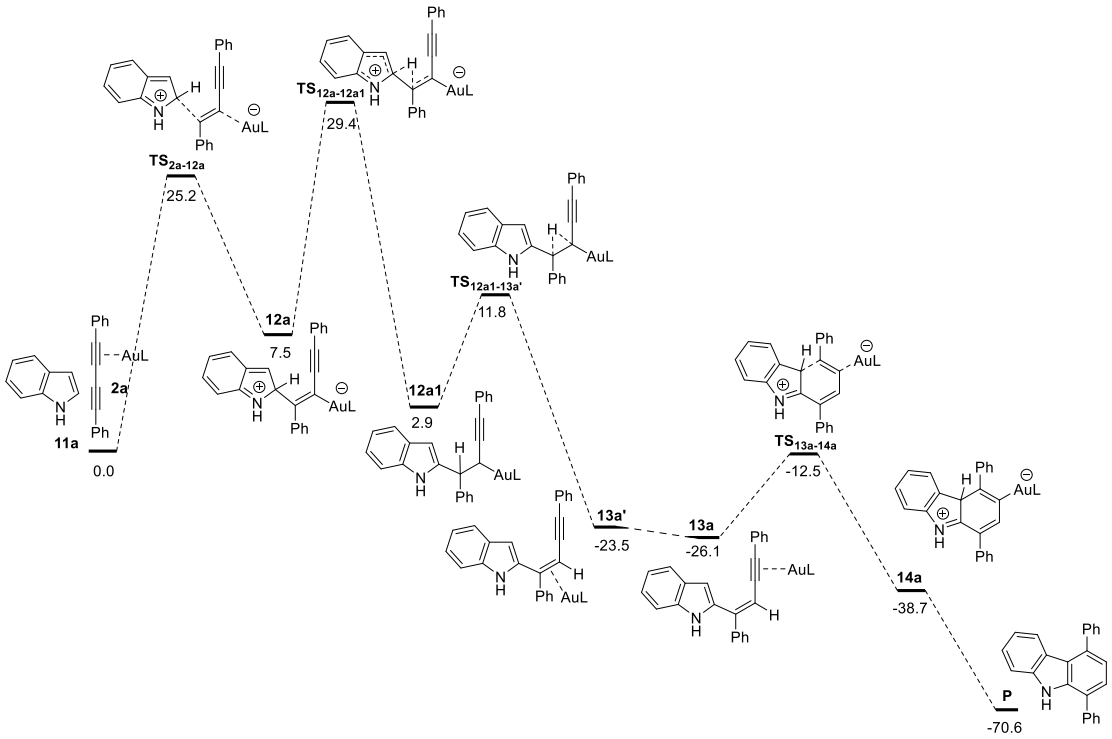


Scheme 7.6b Reactivity profile of C2 of indole with 1,3-diyne. Relative energies used compounds 11a and 2a as the zero energy reference.

Comparing two alternative paths, the nucleophilic attacks either by C2 or by C3 to activated diyne, we see that at the first attack the path of C3 is favoured by energy difference of 5.3kcal/mol (**$TS_{2a\_12a}$** vs **$TS_{2a\_15a}$** are 25.2kcal/mol vs 19.9kcal/mol respectively). However, the rate limiting step is located in the protodeauration steps following the first C–C bond formation, in agreement with what we found for pyrrole as a nucleophile. Furthermore, as illustrated in Schemes 7.6a/7.6b, all the steps associated with the attack of the indole through the C2 centre are systematically more expensive than those following the attack through C3 at least up to the point where the mechanism becomes irreversible (**13a** and **16a**, see Schemes 7.6a/7.6b). A possible explanation for the stability of C3 vs C2 attack is the complete loss of aromaticity for the intermediates involved in the C2 attack (note the o-quinone-like structure of **12a** vs. the styrene-like π-electron structure of **15a**)[6]. After the re-aromatization step, the energies of the isomers are close (1-2.5kcal/mol) up to the formation of **13a** and **16a**.

Despite that the part of the path from **13a**/**16a** to the end presents small differences in energy (−12.0 vs. −12.5 kcal $mol^{-1}$ for the highest point in that path section), the reaction profile becomes more complex for the mechanistic route that starts with the participation of C3. It was expected that carbazole could be formed by **16a** a hydroarylation at C2. Instead of that, the formation of the six-member ring proceeds

through the initial formation of the C3 spiranic intermediate **18a** (via $\mathbf{TS_{16a–18a}}$). Hence, enforcing the idea that nucleophilicity of C3 is higher even when this position is substituted rather than the C2 indole exo-dig attack on the activated triple bond. The spiro compound **18a** then rearranges to the six-member ring in carbazole **17a** through $\mathbf{TS_{18a–17a}}$ in a 1,2-alkenyl migration step. This kind of reactivity involving C3 in an indole for bond formation that ultimately occurs at C2 has been noted previously for indoles by us and other authors. [7,8,9,10,11,12]

## 7.4 Conclusions

DFT calculations were performed to investigate the mechanism of the Au-catalyzed [4 + 2]-type reaction between 1,3-diynes and pyrrole or indole leading selectively to 4,7-disubstituted indoles or 2,5-disubstituted carbazoles, respectively. After calculations for 6-endo-dig, 5-exo-dig, 5-endo-dig and 4-exo-dig cyclizations were realized, it was concluded that the experimentally observed selectivity can be explained by a two-step mechanism in which after a low energy nucleophilic attack on the C1 position of gold-activated diyne by C2 of pyrrole and by C3 of indole, a rate determining protodeauration step precedes the 6-endo-dig cyclization involving the C4 position of the remaining gold-activated triple bond leading to the indole or carbazole product. For indole, the second step proceeds via a more complicated pathway including a spiro intermediate at the C3 position which provides the carbazole through a rearrangement of C1 carbon of the diyne skeleton. The increased polarizability of the conjugated diyne substrate seems to produce a remarkable stabilizing effect facilitating the nucleophilic attack and significantly reducing the activation energy of the first step when compared to the case of a skipped diyne where a methylene group interferes between the triple bonds.

## 7.5 Bibliography


(1) Matsuda, Y.; Naoe, S.; Oishi, S.; Fujii, N.; Ohno, H. Formal [4+ 2] Reaction between 1,3-Diynes and Pyrroles: Gold(I)-Catalyzed Indole Synthesis by Double Hydroarylation. *Chem. - A Eur. J.* **2015**, *21* (4), 1463–1467. https://doi.org/10.1002/chem.201405903.

(2) Fang, R.; Zhou, L.; Tu, P. C.; Kirillov, A. M.; Yang, L. Computational Study on Gold-Catalyzed Cascade Reactions of 1,4-Diynes and Pyrroles: Mechanism, Regioselectivity, Role of Catalyst, and Effects of Substituent and Solvent. *Organometallics* **2018**, *37* (12), 1927–1936. https://doi.org/10.1021/acs.organomet.8b00201.

(3) C. A. Gaggioli, G. Ciancaleoni, D. Zuccaccia, G. B.; L. Belpassi, F. T. and P. B. Strong Electron- Donating Ligands Accelerate the Protodeauration Step in Gold(I)-Catalyzed Reactions: A Quantitative Understanding of the Ligand Effect. *Organometallics* **2016**, *35* (13), 2275–2285.

(4) R. BabaAhmadi, P. Ghanbari, N. A. Rajabi, A. S. K. H.; Ariafard, B. F. Y. and A. A Theoretical Study on the Protodeauration Step of the Gold(I)-Catalyzed Organic Reactions. *Organometallics* **2015**, *34* (13), 3186–3195.

(5) T. A. Nigst, M. Westermaier, A. R. O. and H. M. Nucleophilic Reactivities of Pyrroles. *Eur. J. Org. Chem.* **2008**, No. 14, 2369–2374.

(6) J. An, A. Parodi, M. Monari, M. C. Reis, C. S. L. and; Bandini, M. Gold-Catalyzed Dearomatization of 2-Naphthols with Alkynes. *Chem. – Eur. J.* **2017**, *23* (69), 17473– 17477.

(7) A. Suárez, S. Suárez-Pantiga, O. N.-F. and R. S. Gold-Catalyzed Synthesis of 1-(Indol-3-Yl)Carbazoles: Selective 1 2-Alkyl vs 1 2-Vinyl Migration. *Org. Lett.* **2017**, *19* (19), 5074–5077.

(8) P. L. Zhu, Z. Zhang, X. Y. Tang, I. M. and M. S. Gold and Silver-Catalyzed Intramolecular Cyclizations of Indolylcyclopropenes for the Divergent Synthesis of Azepinoindoles and Spiroindoline Piperidines. *ChemCatChem* **2015**, *7* (4), 595–600.

(9) Y. Wei and M. Shi. Divergent Synthesis of Carbo- and Heterocycles via Gold-Catalyzed Reactions. *ACS Catal.* **2016**, *6* (4), 2515–2524.

(10) C. S. López, C. Pérez-Balado, P. R.-G. and Á.; Lera, R. de. Mechanistic Insights into the Stereocontrolled Synthesis of Hexahydropyrrolo[2,3-b]Indoles by Electrophilic Activation of Tryptophan Derivatives. *Org. Lett.* **2008**, *10* (1), 77–80.

(11) S. Yaragorla, D. Bag, R. D. and K. V. J. J. Iodo- Cycloisomerization of Aryl(Indol-3-Yl)Methane-Tethered Propargyl Alcohols to 3-Iodocarbazoles via Selective 1,2- Alkyl Migration. *ACS Omega* **3AD**, *11*, 15024–15034.

(12) B. Alcaide, P. Almendros, C. Aragoncillo, E. B.; C. G. López-Calixto, M. Liras, V. A. de la P. O.; Stone, A. G.-S. and H. V. A Facile Synthesis of Blue Luminescent [7]Helicenocarbazoles Based on Gold- Catalyzed Rearrangement-Iodonium Migration and Suzuki– Miyaura Benzannulation Reactions. *Chem. – Eur. J.* **2018**, *24* (30), 7620–7625.

# Chapter 8

## On the Mechanism of the Au(I)-Mediated Addition of Alkynes to Anthranils to Furnish 7-Acylindoles

Indoles are common structural motifs not only in the alkaloid family of organic compounds, but also in a range of pharmaceuticals, aimed to treat diseases as diverse as cancer, asthma, various types of microbial infections or depression. [1,2,3,4] Regarding that 7-acyl-indoles are also a valuable building block for bioactive compounds, [5,6,7] Hashmi and coworkers developed an elegant synthetic method employing a gold(I)-catalyzed C-H annulation of anthranils with terminal alkynes, initially using ynamides with a benzyl and mesylate substituents (e.g. BnN(Ms)≡CH), but later also including non-polarized terminal alkynes or di-substituted alkynes (Scheme 8.1a). [8]

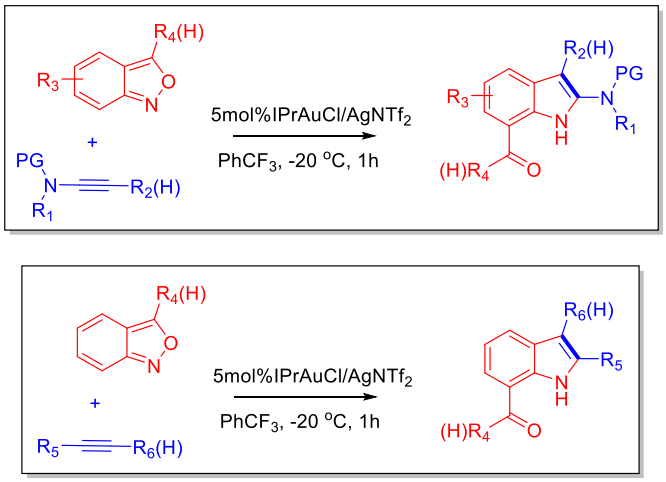


Scheme 8.1

Our interest in gold catalysis in general and gold carbene generation in particular prompted us to carry out a thorough investigation of the reaction mechanism of this promising synthetic procedure. We therefore explored the mechanism of this reaction between anthranils and a set of different alkynes to elucidate key steps in the reaction pathway. We investigated the regioselectivity with ynamides and terminal alkynes, which selectively provide the 2- compared to the 3-substituted 7-acyl-indole ring, and further expanded our analysis to the less trivial asymmetric disubstituted alkynes, for which, surprisingly, only one regioisomer is also observed in the original experimental work. [8] The results of this investigation also shed light onto the mechanistic pattern for this reaction, and they uncover details about the catalyst, the reaction conditions employed and the role of the α-imino gold carbene intermediate.

For the reaction of anthranil with the gold-activated triple bond, we anticipated a mechanism consisting of six steps. There are two alternatives for the initial nucleophilic attack onto the triple bond (Scheme 8.2), where regioselectivity is determined: The nitrogen atom of the oxazole ring can attack the gold-polarized triple bond at C-1 (Path 1) or C-2 (Path 2) to generate intermediates 3x2 or 3x1, respectively. The second step involves an interesting redistribution of π-electrons resulting in the cleavage of the N–O bond to form 4x2 (path 2) or 4x1 (path 1). Then, an electrophilic aromatic substitution reaction occurs between the electron deficient carbon of the α-imino gold carbene and the phenyl fragment resulting in intermediates 5x2 or 5x1, which can have an anti or syn relative orientation of the hydrogen atoms attached to the bond forming carbons (Scheme 8.2). The fourth and fifth steps comprise proton migrations such that ring aromaticity is recovered at the phenyl unit (6x2 or 6x1, respectively), and the sixth step includes the deauration and concomitant aromatization of the pyrrole ring to form isomeric 7-acylindoles 7x2 or 7x1, respectively. The product obtained in the experiment is 7x2 with the substituent on the reacting alkyne installed at 2- instead of the 3-carbon of the 7-acyl-indole ring.

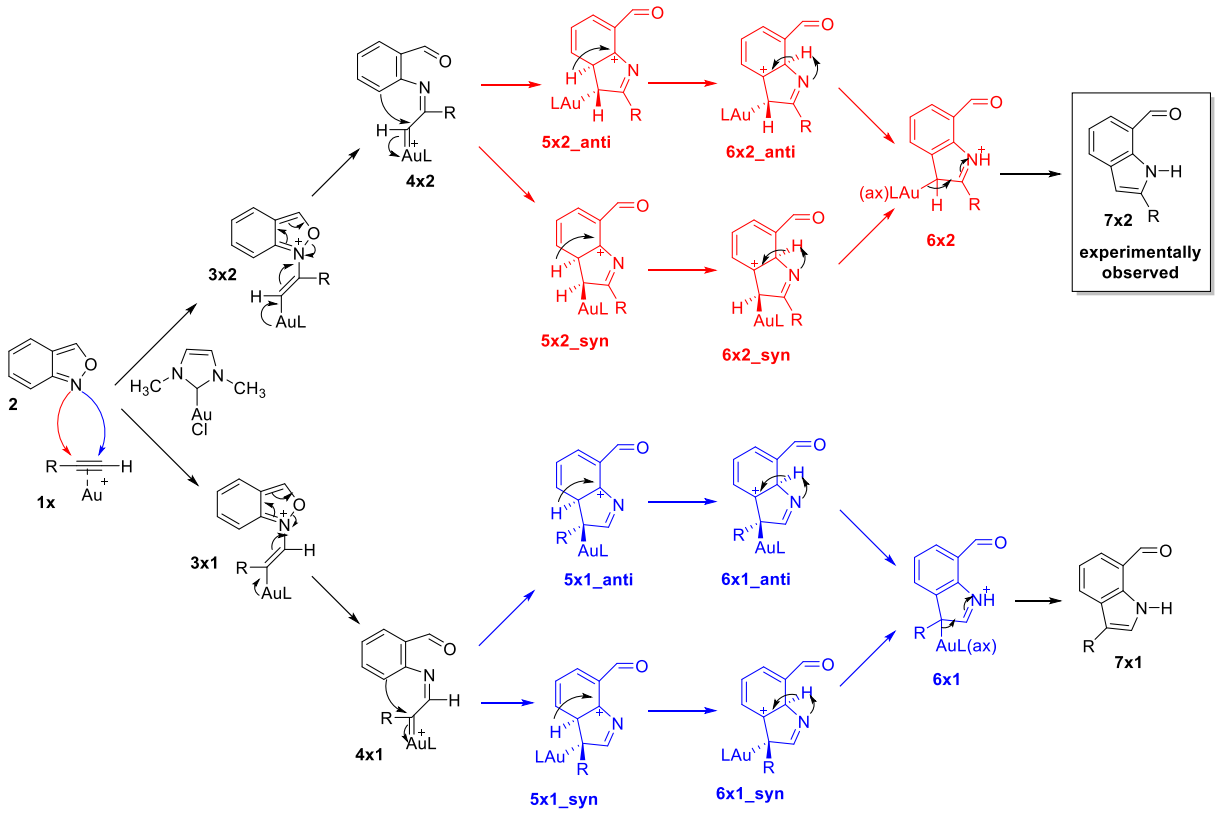


Scheme 8.2 Regioselectivity models description for the mechanism of the reaction of a terminal alkyne with anthranil. The key α-imino gold carbene intermediate is highlighted with a dashed-line frame

**8.1 Reaction between anthranil and a benzyl-substituted ynamide**

We calculated the two paths described in Scheme 8.2 for the reaction of anthranil (2a in reference [8]) with ynamide BnN(Ms)C≡CH (1a in reference [8]), in which the triple bond is polarized because of the adjacent NMs group to the triple bond carbon as described in Scheme 8.3. We used in our calculations a simpler ylide (see Scheme 8.3) as model of the catalyst IPrAuCl/$AgNTf_2$ used by Jin et al. [8]

For the nucleophilic attack of the anthranil nitrogen onto the triple bond, we calculated an energy difference of 14.9 kcal/mol between $\mathbf{TS_{3a1}}$ versus $\mathbf{TS_{3a2}}$, in favor of the attack to the internal, more polarized, alkyne carbon, which ultimately leads to **7a2**, which is the experimentally observed product. The 9.8 kcal/mol barrier for the attack at C-2 is consistent with the low thermal requirements of this process (-20°C; see Table 8.1). The structure $\mathbf{TS_{3a2}}$ may be additionally stabilized because of the cooperative π-donating character of two geminal nitrogen atoms versus one nitrogen atom at each end of the triple bond in $\mathbf{TS_{3a1}}$. This interaction has geometrical consequences at both the pair of transition states and also the subsequent intermediates **3a1** and **3a2**.

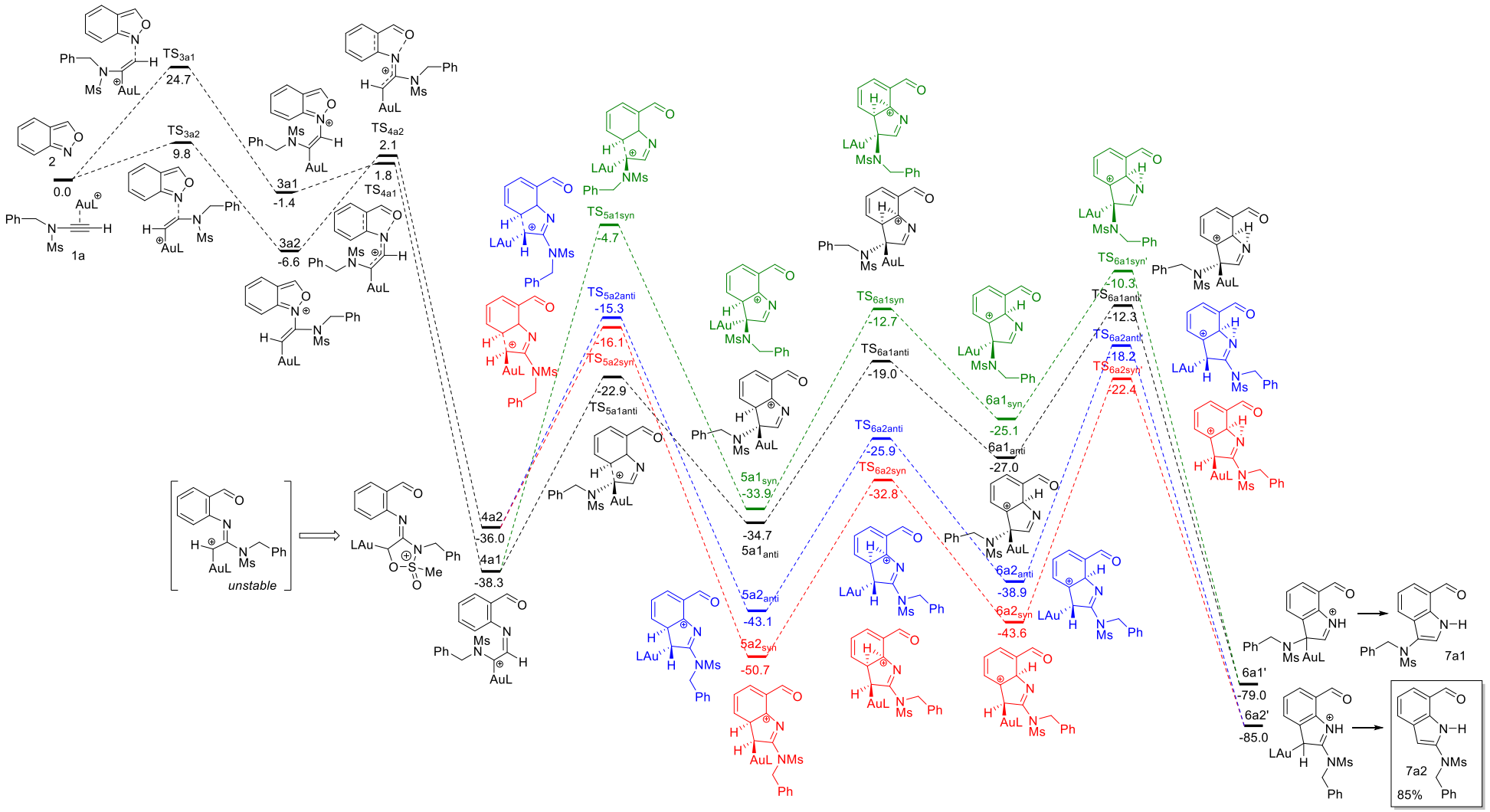


Scheme 8.3 Reaction between anthranil and the ynamide BnN(Ms)≡CH. Relative Gibbs energies (kcal/mol, 298 K and 1 atm). From the α-imino gold carbene intermediate, blue and red colours indicate the two regioselectively favorable paths whereas black and green are used for the disfavored nucleophilic attack.

| 1st step | $\Delta G^{\#}$ | 2nd step | $\Delta G^{\ddagger}$ | 3rd step | $\Delta G^{\ddagger}$ | 4th step | $\Delta G^{\ddagger}$ | 5th step | $\Delta G^{\ddagger}$ |
|---|---|---|---|---|---|---|---|---|---|
| | | | | $TS_{5a1anti}$ | 15.4 | $TS_{6a1anti}$ | 15.7 | $TS_{6a1anti'}$ | 14.7 |
| $TS_{3a1}$ | 24.7 | $TS_{4a1}$ | 3.2 | $TS_{5a1syn}$ | 33.6 | $TS_{6a1syn}$ | 21.2 | $TS_{6a1syn'}$ | 14.8 |
| | | | | $TS_{5a2anti}$ | 20.7 | $TS_{6a2anti}$ | 17.2 | $TS_{6a2anti'}$ | 20.7 |
| $TS_{3a2}$ | **9.8** | $TS_{4a2}$ | 8.7 | $TS_{5a2syn}$ | 19.9 | $TS_{6a2syn}$ | 17.9 | $TS_{6a2syn'}$ | 21.2 |
| | | | | $TS_{5b1anti}$ | 4.6 | $TS_{6b1anti}$ | 10.1 | $TS_{6b1anti'}$ | 15.4 |
| $TS_{3b1}$ | 16.2 | $TS_{4b1}$ | 4.7 | $TS_{5b1syn}$ | 12.5 | $TS_{6b1syn}$ | 16.3 | $TS_{6b1syn'}$ | 18.7 |
| | | | | $TS_{5b2anti}$ | 0.5 | $TS_{6b2anti}$ | 15.6 | $TS_{6b2anti'}$ | 18.6 |
| $TS_{3b2}$ | **10.7** | $TS_{4b2}$ | 9.6 | $TS_{5b2syn}$ | 0.0 | $TS_{6b2syn}$ | 15.3 | $TS_{6b2syn'}$ | 14.7 |
| | | | | $TS_{5canti}$ | 14.5 | $TS_{6canti}$ | 17.2 | $TS_{6canti'}$ | 16.5 |
| $TS_{3c}$ | 12.3 | $TS_{4c}$ | 6.9 | $TS_{5csyn}$ | 9.8 | $TS_{6csyn}$ | 15.8 | $TS_{6csyn'}$ | 17.9 |
| | | | | $TS_{5d1anti}$ | 14.9 | $TS_{6d1anti}$ | 18.6 | $TS_{6d1anti'}$ | 17.7 |
| $TS_{3d1}$ | 13.1 | $TS_{4d1}$ | 7.0 | $TS_{5d1syn}$ | 8.8 | $TS_{6d1syn}$ | 13.5 | $TS_{6d1syn'}$ | 15.9 |
| | | | | $TS_{5d2anti}$ | 8.7 | $TS_{6d2anti}$ | 15.2 | $TS_{6d2anti'}$ | 17.3 |
| $TS_{3d2}$ | 13.9 | $TS_{4d2}$ | 7.9 | $TS_{5d2syn}$ | **5.4** | $TS_{6d2syn}$ | 15.0 | $TS_{6d2syn'}$ | 15.3 |

Table 8.1 Calculated activation Gibbs energies (kcal/mol) for each step of the mechanism between anthranil and different alkynes, that is, BnN(Ms)C≡CH (3a series), cypC≡CH (3b series), PhC≡CPh (3c series), and PhC≡CBu (3d series)

For instance, the orientation of the amine group is drastically different in these two transition states (see Figure 8.1). In **$TS_{3a1}$**, the amine lies co-planar to the entering nucleophile and its lone pair is therefore orthogonal and non-interacting in the process. In **$TS_{3a2}$**, however, this lone pair is conjugated with the π-electrons participating in the reaction. The C-NMs bond length is diagnostic for this pi-donating interaction (1.36 vs. 1.31 Å in **$TS_{3a1}$** vs. **$TS_{3a2}$**) as well as the triple C–C bond (1.27 vs. 1.29 Å in **$TS_{3a1}$** vs. **$TS_{3a2}$**). The regioselectivity of 2- over 3-position of the final amino-substituted 7-acyl-indole ring is decided at this first transition state because the energy difference between the competing **$TS_{3a1}$** and **$TS_{3a2}$** is very large and the subsequent step involves an irreversible energy cliff. This irreversible step involves what looks like an interesting pseudopericyclic electrocyclic ring opening (vide infra).[9,10,11,12,13,14,15]

The pseudopericyclic nature of this reaction justifies the very meager energy demands in both paths (less than 10 kcal/mol). Additionally, the associated exergonicity of the process is enhanced by the recovery of aromaticity at the phenyl fragment. This conversion from an orthoquinone-like structure into an o-formyl aniline fragment is the driving force of the catalytic cycle with an energy drop of about 40 kcal/mol, leading to α-imino gold intermediates **4a1** and **4a2**. Onto these

intermediates, an electrophilic aromatic substitution takes place via the gold-activated carbon atom. Two possible approaches, anti or syn are viable for this step. In the case of the favored intermediate **4a2**, both approaches are almost equally probable, given the similarity of their energy requirements (about 22 kcal/mol). The intramolecular character of this $S_EAr$ involves the formation of isomeric fused systems **5a1** and **5a2** in their anti and syn configurations. Two sequential proton migrations allow again full recovery of the aromaticity lost in the $S_EAr$ step and furnish the final gold-activated compounds, **7a1** and **7a2**, which are released upon deauration (probably through a ligand exchange step involving the starting alkyne **1a** to reinitiate the catalytic cycle).

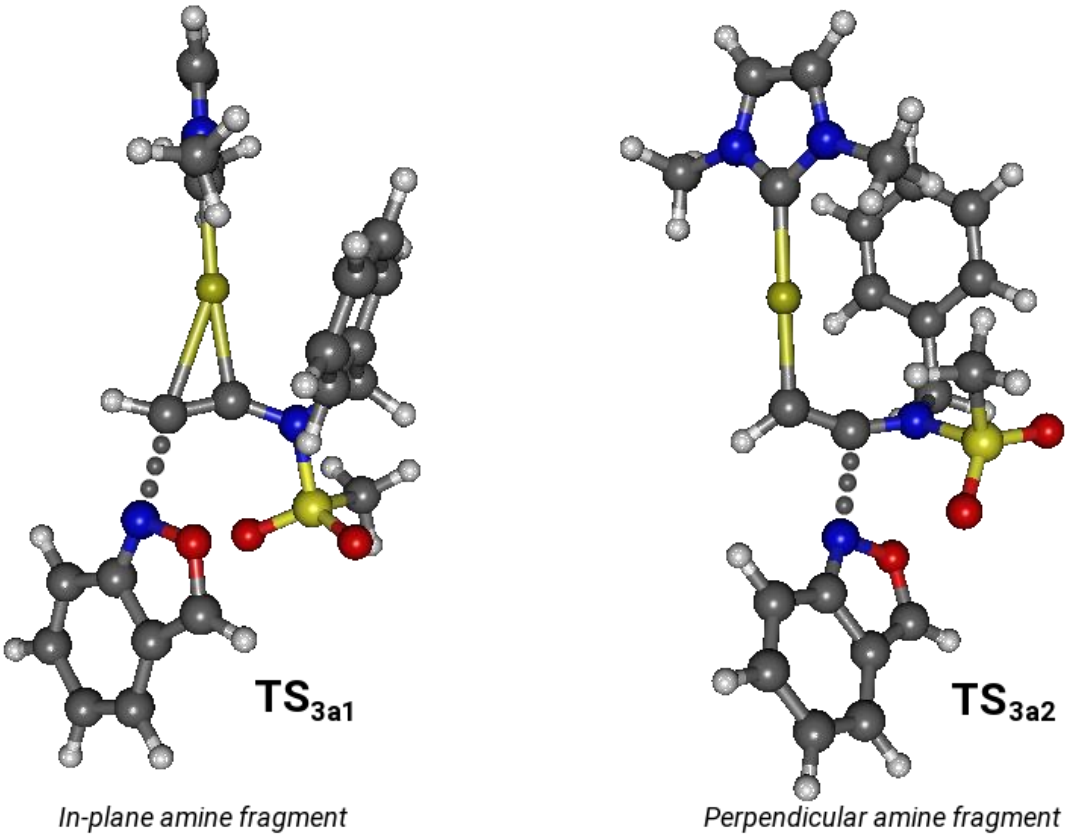


Figure 8.1. Side by side comparison of transition states $TS_{3a1}$ and $TS_{3a2}$. In the latter, geometrical evidence suggests the participation of the lone pair at the ynamide nitrogen in the stabilization of the resulting structure through conjugation to the alkyne. The Au bonding is also indicating a more advanced transition state in $TS_{3a2}$

### 8.2 Reaction between anthranil and an alkyl-substituted terminal alkyne

The barriers for the two alternative nucleophilic attacks of the anthranil nitrogen onto the gold(I)-activated triple bond are much closer than in system **1a**. The activation energies are 16.2 and 10.7 kcal/mol for terminal versus internal attack (Scheme 8.4; compared with 24.7 and 9.8 kcal/mol in system a, Scheme 8.3). These

closer values are due to the less extreme electron donating effect of the alkyl compared with the amine group. The 5.5 kcal/mol energy difference is still enough to obtain complete regioselectivity under the operating reaction conditions. In this occasion, the apparent pseudopericyclic ring opening is still showing low energy demands (less than 10 kcal/mol), but it is not nearly as exergonic (about 10 kcal/mol of product stabilization in this case vs. ~30 kcal/mol when an ynamide was the reacting counterpart). This difference is attributed to the less stabilized carbocations **4b1** and **4b2** when an alkyl group is all there is to donate charge onto the electron density depleted carbon atom. As a consequence of these unstable carbocations, the $S_EAr$ reaction becomes kinetically much faster and it also turns itself into the driving force of the catalytic process, with an associated energy drop of about 30 kcal/mol. The two steps between the initial nucleophilic attack and this energy cliff are mildly exergonic and kinetically fast, with small associated barriers. This also provides a scenario where the initial attack must be regioselectivity determining because reversion at the first two pairs of intermediates (**3b1**, **3b2** and **4b1**, **4b2**) is unlikely. Two proton migration steps, analogous to those already observed with the ynamide reaction, provide the final 7-acyl-indole isomers **7b1** and **7b2**.

For this reaction, we decided to explore in more depth the second step, for which the molecular topology suggests that a pseudopericyclic transformation may be taking place. For this, we computed nucleus-independent chemical shifts (NICS) on two axes perpendicular to the phenyl and azole fragments in the anthranil moiety (see Figure 8.2). Our results showed the obvious aromatic profile at the phenyl fragment, which is strongly conserved when going from the transition state (**$TS_{4b2}$**) into the reaction intermediate (**4b2**). On the azole ring however, aromaticity is lost in this step. Losing aromaticity is not really surprising in this step, because the azole ring is being opened, but the fact that mild aromaticity is present at the transition state is in contradiction with a fully pseudopericyclic process. The relatively mild aromaticity at this transition state and its maximum value at the molecular plane suggest that part of this aromaticity may be due to the sigma skeleton and perhaps this step lays in a gray area between peri- and pseudopericyclic mechanisms. Strongly pericyclic transition states often show NICS profiles with values much higher than those reported here and also significantly higher than values found for benzene.

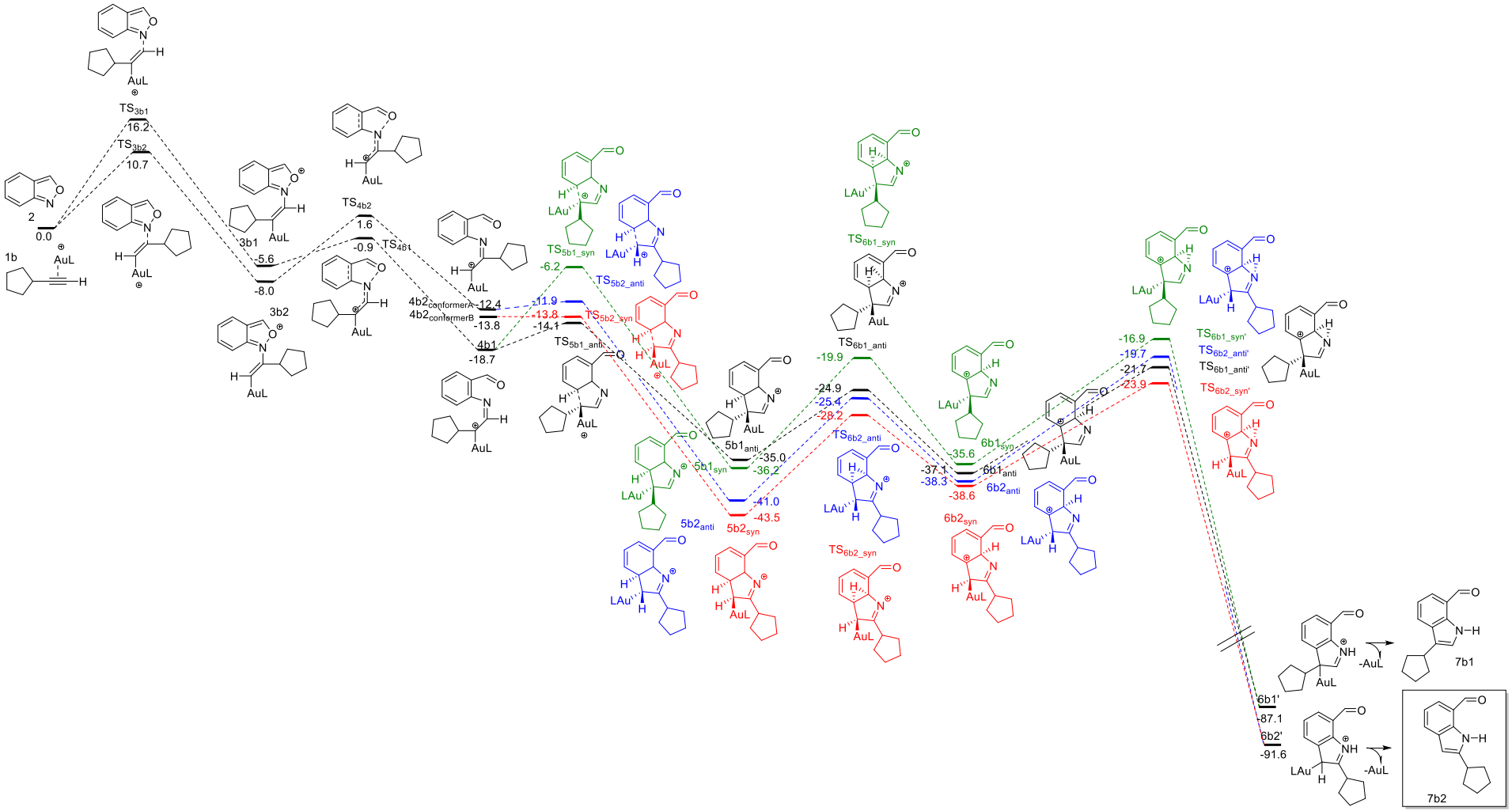


Scheme 8.4 Reaction of anthranil with an alkyl-substituted alkyne. Relative Gibbs energies (kcal/mol, 298 K and 1 atm). From the α-imino gold carbene intermediate, blue and red colours indicate the two regioselectively favourable paths whereas black and green are used for the disfavoured nucleophilic attack

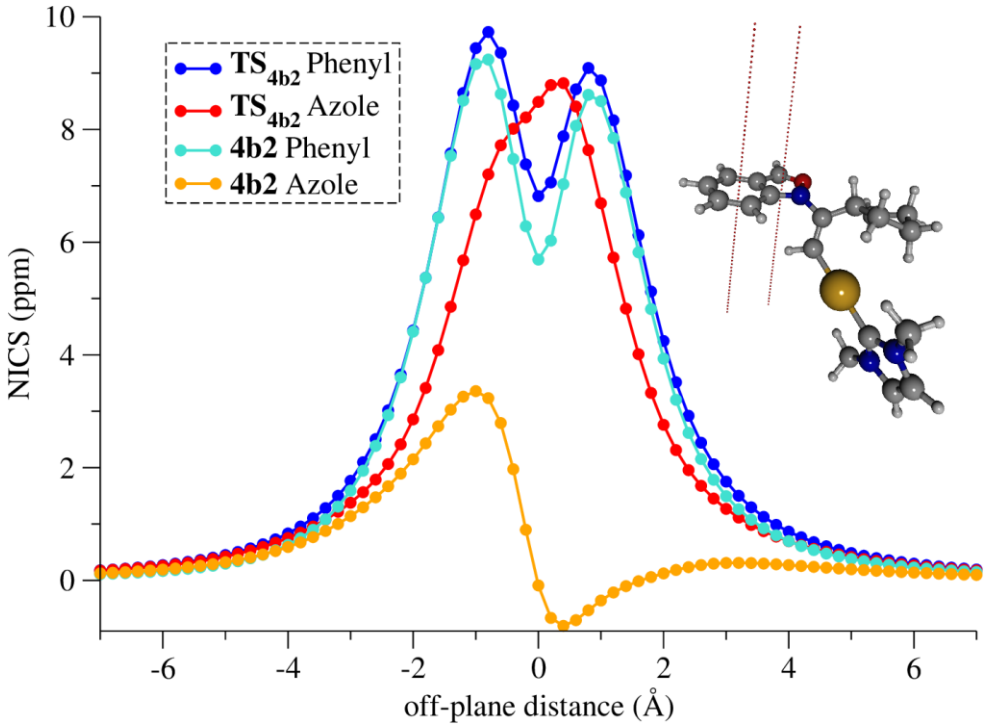


Figure 8.2. Nucleus-independent chemical shifts (NICS) computed along two axes perpendicular to the anthranil heterocycle at TS4b2 and 4b2. The axes employed are illustrated in the molecular geometry.

### 8.3 Reaction between anthranil and diphenyl acetylene

In the case of the symmetrically substituted diphenyl acetylene, our calculations show a similar profile to those discussed above. In this case, the starting barrier is 12.3 kcal/mol, again, not as low as with the ynamide due to the reduced donating capabilities of the phenyl fragment. The pseudopericyclic ring opening is also strongly exergonic (about 20 kcal/mol; Scheme 8.5) because the carbocation is stabilized by the adjacent phenyl ring. In this case, the presence of two phenyl rings at the ends of the alkyne fragment pays dividends on the reaction profile because one phenyl substituent acts in the stabilization of the initial transition state, **$TS_{3c}$**, and the other phenyl ring allows for the stabilization of the carbocation after the N–O bond cleavage (4c). The subsequent electrophilic aromatic substitution is more favorable through the syn approach and involves only a barrier of 10 kcal/mol. Then again, two proton migration steps allow for recovery of the aromaticity and the release of the experimentally observed 2,3-diphenyl 7-acylindole **7c**.

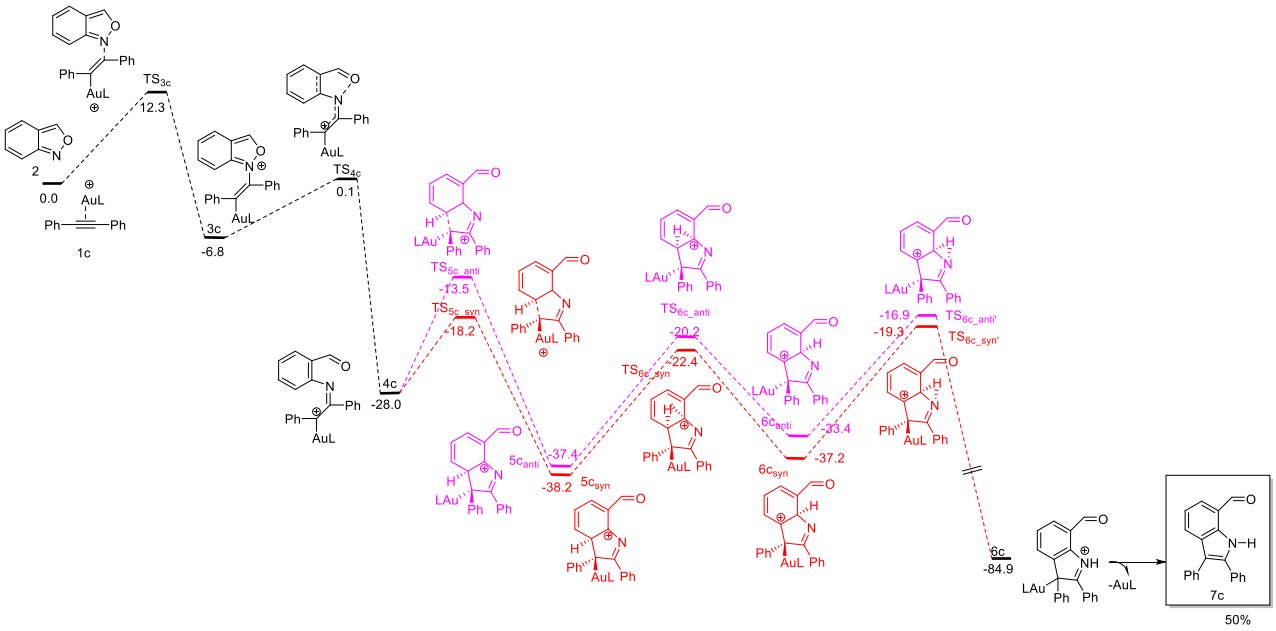

Scheme 8.5 Reaction of anthranil with diphenyl acetylene. Relative Gibbs energies (kcal/mol, 298 K and 1 atm)

## 8.4 Reaction between anthranil and non-symmetrically substituted internal alkynes

Finally, for the case of non-symmetrical alkyl/phenyl alkynes, we chose to use phenyl and n-butyl substituents to illustrate the case (Scheme 8.6). The activation energy for the initial attack at the aromatic or aliphatic sides of the triple bond is similar, differing only by 0.8 kcal/mol. The subsequent N–O bond cleavage features a small barrier and precedes a significant energy drop of about 25 kcal/mol. This situation therefore suggests that both regioisomers could be formed in this process, because the difference in energy barriers for the rate-limiting step is so shallow. Once, intermediates **4d1** and **4d2** are formed, the same sequence of events described for all the previous cases operate: cyclization via a $S_EAr$ step, two hydrogen migrations to recover aromaticity after the $S_EAr$, and gold decomplexation to furnish the final indole. Experimentally, this mode of alkyne substitution was not broadly tested, but in the few cases that it was, the reaction behaved regioselectivity by furnishing only the 2-alkyl, 3-aryl indole analogous to **7d1** in Scheme 8.6. Interestingly, however, the reaction yield is significantly lower than those observed with other kind of alkynes. Jin et al. hypothesized that perhaps the 3-aryl, 2-alkyl indole is not observed due to a competitive hydrogen migration occurring at **4d2**, which may obstruct the $S_EAr$ step. We therefore decided to explore whether such possibility may be indeed competitive and become a deleterious effect on this reaction path. Indeed, a 1,2-H migration step,

very similar to other found and described in our group in the past, could be located and found to be competitive with the cyclization via $S_EAr$ when the alkyl group is directly attached to the gold carbene. We computed the transition state for this migration lying only 1.2 kcal/mol above **$TS_{5d2syn}$**.

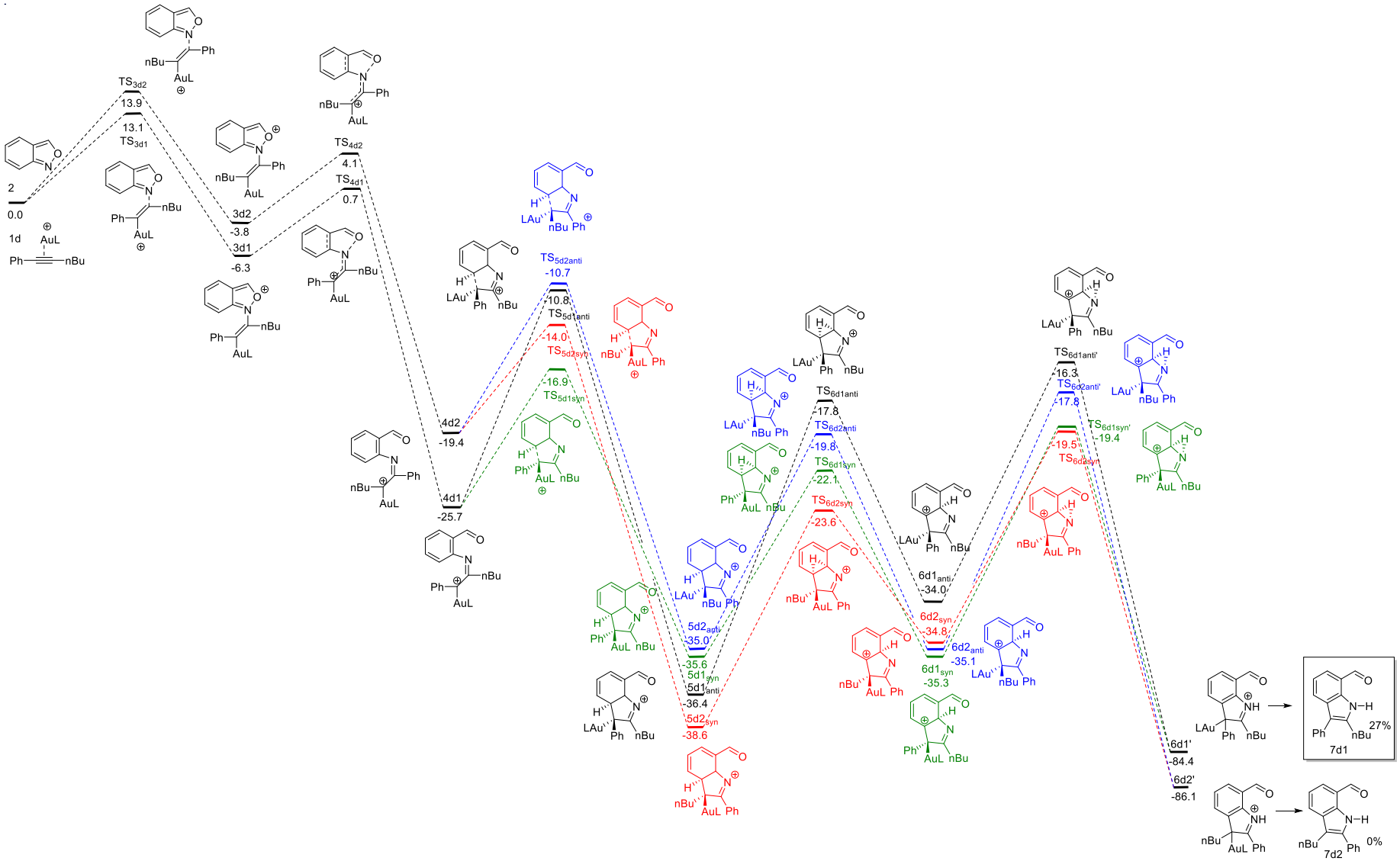


Scheme 8.6 Reaction of anthranil with an unsymmetrical disubstituted alkyne. Relative Gibbs energies (kcal/mol, 298 K and 1 atm).From the α-imino gold carbene intermediate, blue and red colors indicate the two regioselectively favorable paths whereas black and green are used for the disfavored nucleophilic attack

In general, the same main mechanistic features apply to all the alkynes considered. The reaction is initiated with a nucleophilic attack, which is also regioselectivity determining. This attack is preferentially directed onto the internal carbon atom of the alkyne, and the preference is more pronounced the more polarized the alkyne in the starting substrate. In doubly substituted triple bonds, the preference is less marked, but it seems to favour the attack onto the alkyl-substituted versus arylsubstituted carbon atoms. The N–O bond cleaves in an apparent pseudopericyclic step that is not energy demanding, but it precedes an energy drop that makes the process irreversible. The open intermediate thus obtained undergoes cyclization via a $S_EAR$ of the α-imino gold carbene onto the phenyl fragment. A hydrogen rearrangement in two steps recovers the aromaticity of the bicyclic system and furnishes the final 7-acylindole. The main differences found among the various alkynes tested are the starting barrier for the nucleophilic attack, which depends on the polarization of the triple bond and the energy drop after the N–O bond cleavage, which ranges from -35 to -13 kcal/mol, also depending on the nature of the starting alkyne and its ability to stabilize the forming α-imino gold carbene. The rate-limiting step is found at the late rearomatization stage of the mechanism of the regio-favored pathways, but in the disfavoured ones, the starting nucleophilic attack may also be rate limiting (Table 8.1).

## 8.5 Conclusions

In this work, we studied the in situ gold(I)-catalyzed generation of α-imino gold carbene intermediates en route from anthranil and a range of alkynes to 7-acyl-indoles. They are shown to be key intermediates that further evolve via a $S_EAr$ mechanism unless migrating hydrogens can be found Cα (primary or secondary alkyl substituents), in which case a 1,2-H migration becomes competitive with the electrophilic aromatic substitution. We showed that the observed regioselectivity is decided at the initial nucleophilic attack of the anthranil nitrogen onto the alkyne fragment because the formation of the α-imino gold carbene intermediate is an irreversible step. The nature of the substituents at the alkyne fragment is key to determine (1) the degree of selectivity, (2) the height of the initial and rate-limiting barrier, and (3) the energy drop associated to the formation of the α-imino gold carbene. It is worth noting that gold(III) species also catalyze a similar transformation, although the final outcome seems strongly dependent on the counterion chaperoning gold. [16,17,18]

## 8.6 Bibliography


(1) Dhuguru, J.; Skouta, R. Role of Indole Scaffolds as Pharmacophores in the Development of Anti-Lung Cancer Agents. *Molecules* **2020**, *25*, 1615. https://doi.org/https://doi.org/10.3390/molecules25071615.

(2) Navriti Chadha, O. S. Indoles as Therapeutics of Interest in Medicinal Chemistry: Bird's Eye View. *Eur. J. Med. Chem.* **2017**, *134*, 159–184.

(3) Archana Kumari, Rajesh K. Singh. Medicinal Chemistry of Indole Derivatives: Current to Future Therapeutic Prospectives. *Bioorg. Chem.* **2019**, *89*, 103021.

(4) Hazrulrizawati A. Hamid, A. N. M. R. and M. M. Y. Indole Alkaloids from Plants as Potential Leads for Antidepressant Drugs: A Mini Review. *Front. Pharmacol.* **2017**, *8*, 96.

(5) Mikel P. Moyer, John F. Shiurba, and H. R. Metal-Halogen Exchange of Bromoindoles. A Route to Substituted Indoles. *J. Org. Chem.* **1986**, *51* (26), 5106–5110. https://doi.org/10.1021/jo00376a010.

(6) Tjeerd Barf, Fredrik Lehmann, Kristin Hammer, Saba Haile, Eva Axen, Carmen Medina, Jonas Uppenberg, Stefan Svensson, Lena Rondahl, Thomas Lundbäck. N-Benzyl-Indolo Carboxylic Acids: Design and Synthesis of Potent and Selective Adipocyte Fatty-Acid Binding Protein (A-FABP) Inhibitors. *Bioorg. Med. Chem. Lett.* **2009**, *19* (6), 1745–1748.

(7) James A. Nieman, Sajiv K. Nair, Steven E. Heasley, Brenda L. Schultz, Herbert M. Zerth, Richard A. Nugent, Ke Chen, Kevin J. Stephanski, Todd A. Hopkins, Mary L. Knechtel, Nancee L. Oien, Janet L. Wieber, Michael W. Wathen. Modifications of C-2 on the Pyrroloquinoline Template Aimed at the Development of Potent Herpesvirus Antivirals with Improved Aqueous Solubility. *Bioorg. Med. Chem. Lett.* **2010**, *20* (10), 3039–3042.

(8) Jin, H.; Huang, L.; Xie, J.; Rudolph, M.; Rominger, F.; Hashmi, A. S. K. Gold-Catalyzed C□H Annulation of Anthranils with Alkynes: A Facile, Flexible, and Atom-Economical Synthesis of Unprotected 7-Acylindoles. *Angew. Chemie - Int. Ed.* **2016**, *55* (2), 794–797.

(9) Carlos Silva López, Olalla Nieto Faza, Marek Freindorf, Elfi Kraka, and D. C. Solving the Pericyclic–Pseudopericyclic Puzzle in the Ring-Closure Reactions of 1,2,4,6-Heptatetraene Derivatives. *J. Org. Chem.* **2016**, *81* (2), 404–414. https://doi.org/10.1021/acs.joc.5b01997.

(10) Roberto Villar López, Olalla Nieto Faza, E. M. and C. S. L. Cycloreversion of the CO2 Trimer: A Paradigmatic Pseudopericyclic [2 + 2 + 2] Cycloaddition Reaction. *Org. Biomol. Chem.* **2017**, *15*, 435–441.

(11) López, C.S., Faza, O.N., Cossío, F.P., York, D.M. and de Lera, A. . Ellipticity: A Convenient Tool To Characterize Electrocyclic Reactions. *Chem. – A Eur. J.* **2005**, *11*, 1734–1738. https://doi.org/https://doi.org/10.1002/chem.200401026.

(12) Walter M. F. Fabian, Vasiliy A. Bakulev, and C. O. K. Pericyclic versus Pseudopericyclic 1,5-Electrocyclization of Iminodiazomethanes. An Ab Initio and Density Functional Theory Study. *J. Org. Chem.* **1998**, *63* (17), 5801–5805. https://doi.org/10.1021/jo980238u.

(13) Birney, S. H. and D. M. Imidoylketene: An Ab Initio Study of Its Conformations and Reactions. *J. Org. Chem.* **1996**, *61* (12), 3962–3968. https://doi.org/10.1021/jo952229g.

(14) Birney, D. M. Further Pseudopericyclic Reactions: An Ab Initio Study of the Conformations and Reactions of 5-Oxo-2,4-Pentadienal and Related Molecules. *J. Org. Chem.* **1996**, *61* (1), 243–251. https://doi.org/10.1021/jo951716t.

(15) Chun Zhou and David M. Birney. A Density Functional Theory Study Clarifying the Reactions of Conjugated Ketenes with Formaldimine. A Plethora of Pericyclic and Pseudopericyclic Pathways. *J. Am. Chem. Soc.* **2002**, *124* (18), 5231–5241. https://doi.org/10.1021/ja017559z.

(16) Zeng, Z.; Jin, H.; Sekine, D. K.; Rudolph, D. M.; Rominger, F.; Hashmi, P. D. A. S. K. Gold-Catalyzed Regiospecific C−H Annulation of O-Ethynylbiaryls with Anthranils: Π-Extension by Ring-Expansion En Route to N-Doped PAHs. *Angew. Chemie - Int. Ed.* **2018**, *57* (23), 6935–6939.

(17) Kaifeng Wang, Qiao Wu, Siwei Bi, Lingjun Liu, Guang Chen, Yulin Li, T. D. J. and Y. L. Theoretical Evaluation of the Carbene-Based Site-Selectivity in Gold(Iii)-Catalyzed Annulations of Alkynes with Anthranils. *Chem. Commun.* **2021**, *57*, 1494–1497.

(18) Marta Castiñeira Reis, Marta Marín-Luna, Nenad Janković, Olalla Nieto Faza, C. S. L. Au(III) Catalyzes the Cross-Coupling between Activated Methylenes and Alkene Derivatives. *J. Catal.* **2020**, *392*, 159–164.

# Chapter 9

## Formation and Intramolecular Capture of α-Imino Gold Carbenoids in the Au(I)-Catalyzed [3+2] Reaction of Anthranils, 1,2,4-Oxadiazoles and 4,5-Dihydro-1,2,4-Oxadiazoles with Ynamides

Various novel annulation reactions have been recently developed leading to pharmaceutically relevant heterocycles. [1,2] Anthranils and isoxazoles operate as electrophilic aminating reagents in these reactions through a selective N–O bond cleavage and provide a powerful platform for C–N bond formation and N-heterocycle synthesis. [3] In the presence of gold catalysts, these species could serve as mild nucleophiles to attack the activated alkynes and to form α-imino gold carbene species.

Hashmi in 2016 published on the remarkable reactivity of the weak nucleophile anthranil with activated terminal alkynes (including ynamides) in the presence of a gold(I) catalyst (Scheme 9.1a). [16] The scope of this chemistry was extended in 2018 to non-polarized terminal alkynes and internal alkynes. [4] In these reactions, an α-imino gold carbene intermediate is formed which furnishes, after a C-H insertion step, the 7-acylindoles and the N-doped polycyclic aromatic hydrocarbons (PAHs), respectively, in an expedient and atom-economical process.

This chemistry was recently extended to oxadiazoles which allow the synthesis of *N*-acylimidazoles through the formation of an α-imino gold carbene in the Au(I) catalyzed [3+2] reaction of 1,2,4-oxadiazoles (Scheme 9.1b). [5] This reaction also occurs with total atom economy as the acyl group remains a part of oxadiazoles. The same type of reactivity takes place in the Au(I) catalyzed [3+2] reaction of dihydrooxadiazoles as nitrene transfer reagents reported by Liu in 2017 (Scheme 9.1c) which uses 4,5-dihydro-1,2,4-oxadiazoles and ynamides providing N-R-5-aminoimidazoles (R=H, alkyl, aryl). [6]

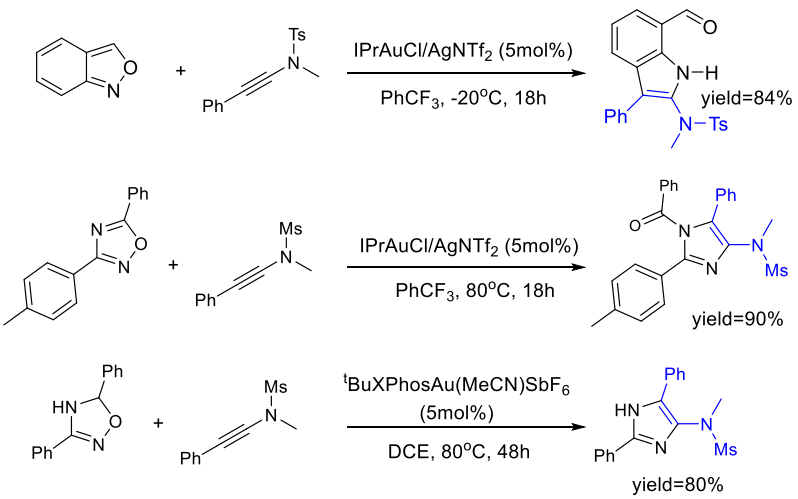


Scheme 9.1. Au(I)-catalyzed reaction of anthranil, 1,2,4-oxadiazoles or 4,5-dihydro-1,2,4-oxadiazoles with ynamides forming 2-amino-3-phenyl-7-acyl indoles, N-acyl-5-aminoimidazoles or N-alkyl-4-aminoimidazoles, respectively.

As a continuation on our efforts to gain a deeper insight in the intricacies of gold mediated transformations [7,8,9,10,11,12,13,14,15,16,17,18,19,20] and particularly reaction mechanisms including gold carbenes, [21,1,2,4,22,23,5,6,24] we carried out here a thorough investigation on the reaction mechanism of the gold(I) catalyzed [3+2] reaction of mild nitrogen nucleophiles in the anthranil, 1,2,4-oxadiazole or 4,5-dihydro-1,2,4-oxadiazole series with ynamides. We paid particular attention to the regioselectivity of these reactions which can afford 7-acylindoles substituted at 2-, or/and 3-position, and 5- or 4-aminoimidazoles, respectively, as well as to the formation of the α-imino gold carbene intermediate, and to the difference in reactivity between aromatic and non-aromatic substrates (oxadiazole vs dihydrooxadiazole).

We assumed that the general mechanism for the three protocols could be analogous, according to the similarities in the structures of the three nucleophiles, and that the key feature in this reactivity is the oxime fragment embedded in the heterocyclic moiety. With that assumption at hand, and driven by our recent exploration of anthranil chemistry, [25] we anticipated a reaction pathway for the oxadiazoles involving (Scheme 9.2): 1- Au(I) activation of the alkyne, 2- nucleophilic attack by the oxime nitrogen onto the activated alkyne, 3- N-O cleavage and formation of the key α-imino gold carbene intermediate, 4- cyclization of the α-imino gold carbene intermediate via an intramolecular nucleophilic attack and 5- deauration leading to the final heterocycle.

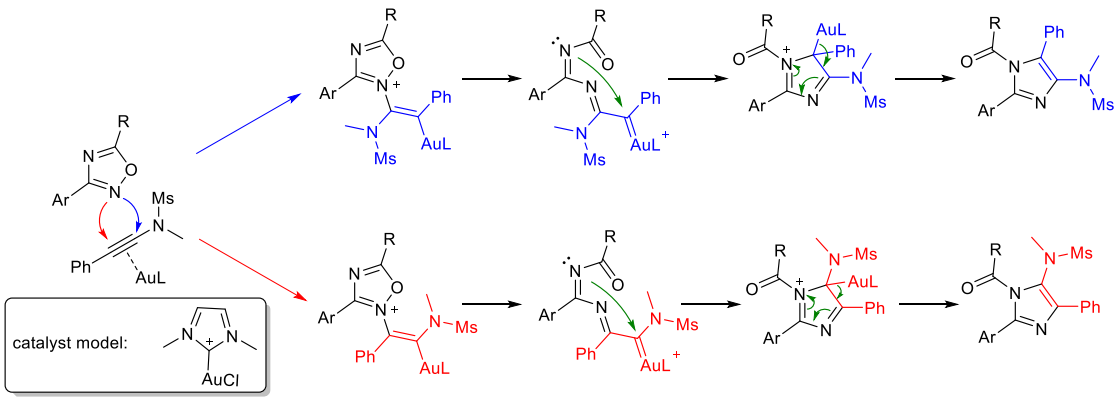


Scheme 9.2. Anticipated mechanistic steps for the Au(I) mediated reaction between ynamides and oxadiazoles by analogy to that found for anthranils.

### 9.1 Reaction of anthranil with ynamide

In our earlier approach to this chemistry we had explored in detail the reaction between anthranil and a terminal ynamide. Given the striking power and versatility of this chemistry, in an attempt to provide a generalized view to the mechanisms involved, a side by side comparison between the reactivity of terminal and substituted ynamides seems appropriate.

The full profile for the substituted ynamide can be found in Scheme 9.3 and it compares well with that obtained earlier for the terminal ynamide, [25] with regioselectively still favouring the attack onto C1 compared to C2 of the activated by gold ynamide by only 2.1 kcal/mol compared to the 14.8 kcal/mol observed for the terminal ynamide [25] (in the case the $sp^2$-N at position 4 of anthranil reacts

with the C1 the calculated barrier is 1.7 kcal/mol higher while the addition intermediate is unproductive). The key chemical steps are the same and the overall energy barriers are quite similar, and follow the general description provided above, which involves five stages (alkyne activation, nucleophillic attack, N-O bond cleavage, cyclization and deauration). Interestingly, the main difference when moving from a terminal to a substituted ynamide resides in the thermodynamics of the reaction. Whereas with the terminal ynamide the final and observed product was kinetically and thermodynamically favoured, in the substituted ynamide the observed product is only kinetically favoured (and thermodynamically less stable than the alternative regioisomer by 4.3 kcal/mol, see Scheme 9.3). This reversal in exergonicity, presumably, is due to the phenyl ring not being able to participate in extending the conjugation of the heterocycle in **7a2** vs conjugated in **7a1** (Scheme 9.3). This situation, however, applies only insofar as the gold is complexed to the substrate and it should not affect the reaction outcome since the steep energy drop in the N-O bond cleavage makes the process irreversible from that step onwards.

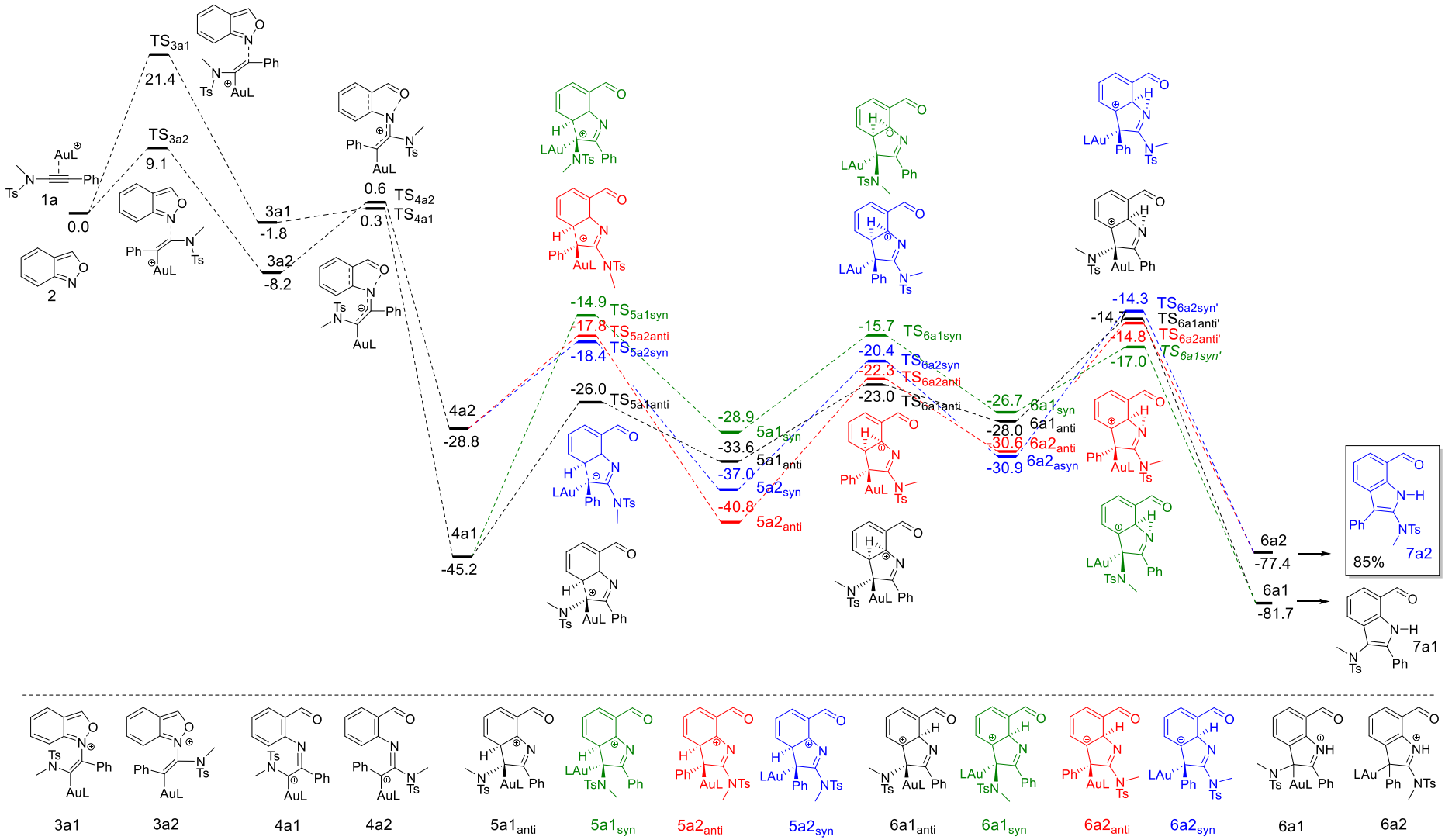


Scheme 9.3. Mechanistic pathway and relative free energies (kcal mol$^{-1}$, 298 K and 1 Atm) for the reaction between anthranil and the ynamide MeN(Ts)≡CPh.

The key activation barriers for the mechanism depicted in Scheme 9.3 are summarized below (Table 9.1) and they show why this reaction is operative even at very mild thermal conditions (-20 ºC) since the starting favoured nucleophillic attack only requires 9.1 kcal/mol and a path is available such that no step requires more than 17 kcal/mol.

| 1st step | $\Delta G^{\#}$ | 2nd step | $\Delta G^{\ddagger}$ | 3rd step | $\Delta G^{\ddagger}$ | 4th step | $\Delta G^{\ddagger}$ | 5th step | $\Delta G^{\ddagger}$ |
|---|---|---|---|---|---|---|---|---|---|
| | | | | $TS_{5a1\_anti}$ | 19.2 | $TS_{6a1\_anti}$ | 10.6 | $TS_{6a1\_anti'}$ | 13.3 |
| $TS_{3a1}$ | 21.4 | $TS_{4a1}$ | 2.1 | $TS_{5a1\ svn}$ | 30.3 | $TS_{6a1\ svn}$ | 13.2 | $TS_{6a1\ svn'}$ | *9.7* |
| | | | | $TS_{5a2\_anti}$ | 10.4 | $TS_{6a2\_anti}$ | 16.6 | $TS_{6a2\_anti'}$ | 16.6 |
| $TS_{3a2}$ | 9.1 | $TS_{4a2}$ | 8.8 | $TS_{5a2\ svn}$ | 11.0 | $TS_{6a2\ svn}$ | 18.5 | $TS_{6a2\ svn'}$ | 15.8 |

Table 9.1. Calculated transition states and Gibbs free energies of activation (kcal $mol^{-1}$) for each step of the mechanism between anthranil and ynamide MeN(Ts)C≡CPh.

### 9.2 Reaction of 1,2,4-oxadiazole with ynamide

Next, we decided to study the similarities and differences of the reaction when considering the reaction between 3-tolyl-5-diphenyl-1,2,4-oxadiazole and the internal ynamide, PhC≡C-N(Ms)Me. The first formal difference in this substrate is the presence of two nitrogen atoms within the heterocyclic structure. This could result in chemoselectivity issues, although, experimentally, a single isomer is formed.

Therefore, upon activation of the triple bond in the ynamide by gold, the nucleophilic attack of two nitrogen centers are possible. Nitrogen at position 2, directly bonded to oxygen, is expected to be a stronger nucleophile due to lone pair repulsion or alpha effect. [26] Indeed the reaction barrier is slightly more favourable for the nucleophilic attack of N2 of the oxadiazole onto the polarized alkyne (Scheme 9.4). Not only that, the formed intermediate in the case of the participation of N4 as nucleophile is unstable with respect to reactants (by almost 3 kcal/mol) contrary to the mildly stable intermediates formed when N2 is the attacking center (regardless of whether this attack occurs at the favored or disfavored site of the triple bond, ie, **3b1** and **3b2**). Nevertheless, the regioselectively of this step is still favoring the attack onto C1 compared to C2, however, the energy difference is much lower (2 kcal/mol in oxadiazole vs 12 kcal/mol when the attack was performed by anthranil) and the activation barriers lie together halfway in between those observed for anthranil.

Oxadiazole, therefore, is potentially less selective and it shows a nucleophilicity that is, as average, comparable to that of anthranil (14.9 and 16.6 kcal/mol for oxadiazole vs 9.1 and 21.4 kcal/mol for anthranil). The second step involves the N-O bond cleavage through $\mathbf{TS_{4b1}}$ or $\mathbf{TS_{4b2}}$ with low energy barriers, 5.9 and 5.6 kcal/mol, respectively. The steep energy drop associated to this bond cleavage is dampened here with respect to what we observed in

anthranil. This is mostly due to the fused benzene that is missing in this case, in anthranil part of the driving force in this step is the aromatization of this fragment from an o-quinone-like structure in the starting substrate (see **3a1** and **4a1**, for instance, in Scheme 9.3). An energy drop of 19.9 kcal/mol for the kinetically favorable **3b1** system is still enough to ensure irreversibility, as in the former mechanism. This cleavage leads to the α-imino gold carbene intermediates **4b1** and **4b2** from which we expected a 5exo-dig cyclization due to a nucleophilic attack of Bz-N onto the gold-carbene. This should readily form the desired aminoimidazole ring (**7b1** in Scheme 9.4), however, our attempts to locate this transition state for the aminoimidazole ring formation were not successful.

Unexpectedly, a four-member ring is formed through a 4-endo-trig nucleophilic attack of Bz-N onto the vicinal carbon to the gold-carbon cation with relatively high activation energies of 28.9 or 31.7 kcal/mol for $\mathbf{TS_{5b1}}$ or $\mathbf{TS_{5b2}}$, respectively (Scheme 9.4 and Table 9.2). This unexpected result brings an explanation to the striking difference in thermal requirements for this process, compared to the previous reaction with anthranil (-20 vs 80 ºC). This latter step, and its associated high activation energy due to the unfavorable 4-endo-trig requirements opens the possibility for identifying this reaction as a 4π-electron electrocyclic ring closure (vide infra).

After the formation of **5b1** and **5b2** the reaction paths form a complex manifold in which a ring expansion process occurs. Interestingly, both intermediates can ring expand via two different mechanisms: 1- The N-amide attack onto the gold carbene and 2- The N acetamide attack alternative (labelled A in Scheme 9.4) is less competitive for both intermediates and results in the concomitant cleavage of the C-N bond, furnishing the ring expanded system in a single step. The N imide attack (labelled B in Scheme 9.4) is kinetically favoured and it involves a stepwise ring expansion process through the formation of a 2.2.1 bicyclic structure, which is an actual but short lived intermediate that readily opens to furnish the final **6b2** imidazole ring. Interestingly, this complex manifold is another regioselectivity determining stage since it allows cross-linking both paths. For instance, if the concerted N acetamide attack could be made more favourable, the initial regioselectivity selected in the starting step ($\mathbf{TS_{3b1}}$ and $\mathbf{TS_{3b2}}$) would be reversed and the experimentally non-observed isomer would be formed.

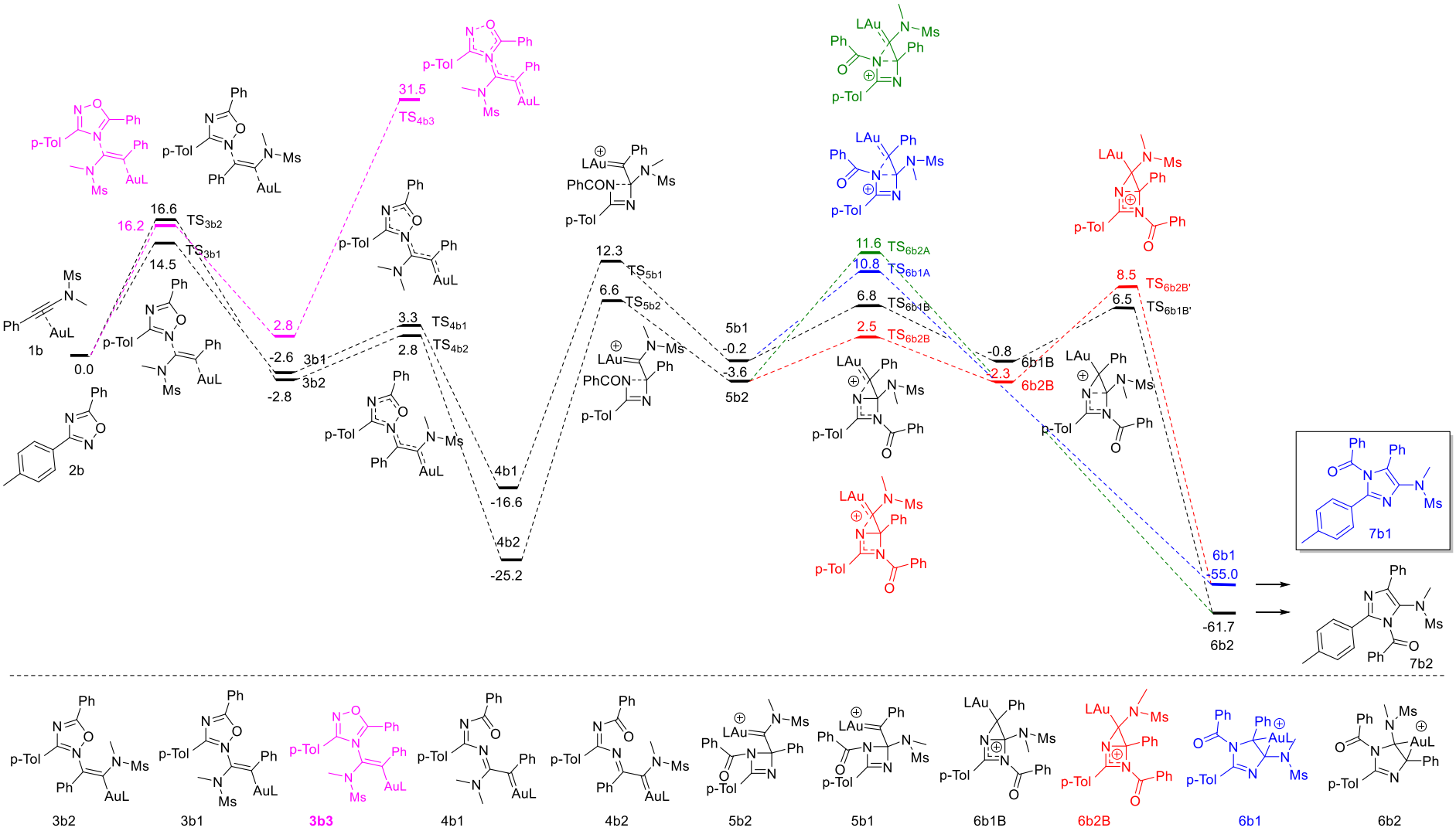


Scheme 9.4. Mechanistic pathway and relative free energies (kcal $mol^{-1}$, 298 K and 1 Atm) for the reaction between 1,2,4-oxadiazole and the ynamide MeN(Ms)≡CPh.

| 1st step | $\Delta G^{\#}$ | 2nd step | $\Delta G^{\ddagger}$ | 3rd step | $\Delta G^{\ddagger}$ | 4th step | $\Delta G^{\ddagger}$ | 5th step | $\Delta G^{\ddagger}$ |
|---|---|---|---|---|---|---|---|---|---|
| | | | | | | $TS_{6b1A}$ | 11.0 | - | |
| $TS_{3b1}$ | **14.5** | $TS_{4b1}$ | 5.9 | $TS_{5b1}$ | **28.9** | $TS_{6b1B}$ | **7.0** | $TS_{6b1B'}$ | 7.3 |
| | | | | | | $TS_{6b2A}$ | 15.2 | - | |
| $TS_{3b2}$ | 16.6 | $TS_{4b2}$ | 5.6 | $TS_{5b2}$ | 31.7 | $TS_{6b2B}$ | 6.1 | $TS_{6b2B'}$ | 10.8 |
| $TS_{3b3}$ | 16.2 | $TS_{4b3}$ | 28.7 | | | | | | |

Table 9.1. Calculated transition states and Gibbs free energies of activation (kcal $mol^{-1}$) for each step of the mechanism between 1,2,4-oxadiazoles and ynamide MeN(Ms)C≡CPh.

Due to the unexpected and rather unfavorable arrangement of the four member ring, we decided to explore whether this step features pericyclic characteristics or if it should be described as a rather unfavorable 4-endo-dig nucleophillic attack. To do that we looked for signature consequences of a pericyclic process, like aromaticity at the transition states. [27–30] Nucleus independent chemical shifts were therefore computed at the four member ring geometrical center and along an axis perpendicular to the ring. Pericyclic transition states show a bell our double bell shape profile for this aromaticity magnetic parameter, with maximum value(s) near the center of the ring. As it can see in Figure 9.1 this is hardly the case of the four member ring formation. Chemical shift values are very low in the equatorial region of the ring being formed, and they only increase when moving away from the ring due to the accidental encounter with electron density from other fragments of the molecule. With these results in hand, we can safely assume that this is not reaction of pericyclic nature, but a fairly unfavorable nucleophillic attack.

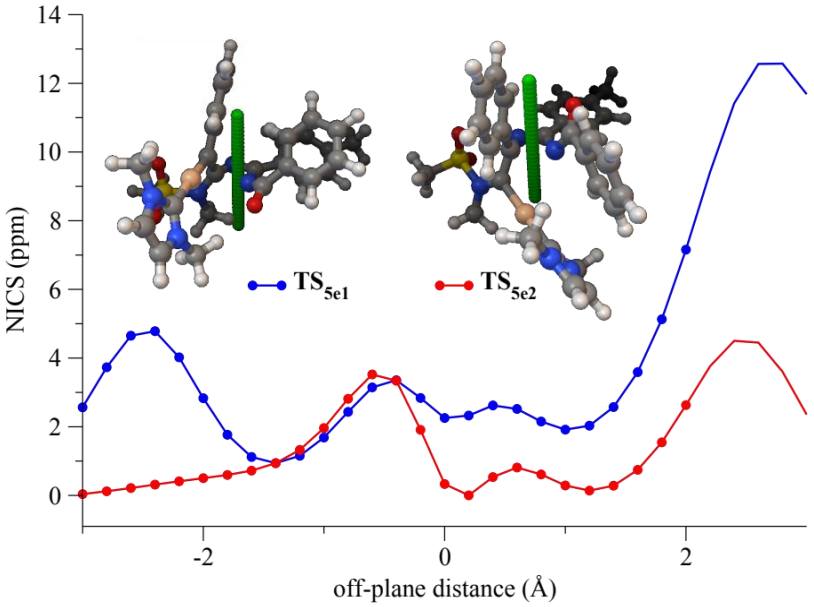


Figure 9.1. Nucleus independent chemical shifts computed at the M06/Def2SVPP level for **TS$_{5b1}$** and **TS$_{5b2}$**.

### 9.3 Reaction of 4,5-dihydro-1,2,4-oxadiazole with ynamide

Finally, we considered the pathway for the reaction between 3,5-diphenyl-4,5-dihydro-1,2,4-oxadiazole and ynamide PhC≡C-N(Ms)Me (Scheme 9.5) to study how the saturation of the 4,5 N-C bond affects the reactivity. With this substrate, the starting nucleophilic attack of oxadiazole onto the activated ynamide triple bond shows improved selectivity traits, comparable to that of anthranil (10.2 vs 18.2 kcal/mol). The favoured attacks for these two species show remarkably similar barriers since the nucleophilic attack of anthranil onto the C1 of an activated terminal ynamide required only 9.1 kcal/mol (the $sp^3$ nitrogen attack was also explored and it is uncompetitive by more than 7 kcal/mol with respect to **TS$_{3c1}$**). Then a low activation barrier allows for N-O bond cleavage, leading to α-imino gold carbene intermediates **4c1** and **4c2**. In this occasion the sole N-O cleavage does not produce a remarkable energy drop, however, it is tightly associated to the loss of benzaldehyde (in a barrierless manner for **3c2** and through a short lived intermediate for **3c2**). Both steps combined do provide a remarkable steep drop of more than 30 kcal/mol to yield the α-imino gold carbene intermediates **4c1** and **4c2** and ensuring again irreversibility. The open substrate undergoes again a costly 4-endo-trig cyclization, which requires about 30 kcal/mol for the favoured regioisomer **4c1**. This high energy barrier explains why the dehydrogenated substrate needs not only harsh temperatures, but also extended

reaction times (Scheme 9.1). In this occasion, the four member cyclic intermediate proceeds to the ring expansion only through a stepwise process and via the formation of a short lived 2.1.0 bicyclic intermediate. The difference in energy of activation for the imine (favoured) and the amine (unfavoured) attack in both paths is enough (5-6 kcal/mol, approximately) to ensure maintaining the regioselectivity obtained in the starting step although, again, reversal of this trend would also revert the regioselectivity of the process. A summary of the cost of each reaction step in this catalytic process can be found in Table 9.2.

| 1st step | $\Delta G^{\#}$ | 2nd step | $\Delta G^{\ddagger}$ | 3rd step | $\Delta G^{\ddagger}$ | 4th step | $\Delta G^{\ddagger}$ | 5th step | $\Delta G^{\ddagger}$ | 6th step | $\Delta G^{\ddagger}$ |
|---|---|---|---|---|---|---|---|---|---|---|---|
| | | | | | | | | $TS_{6c1A}$ | 6.9 | $TS_{7c1A}$ | 1.2 |
| $TS_{3c1}$ | 10.2 | $TS_{4c1A}$ | 13.3 | $TS_{4c1B}$ | 1.6 | $TS_{5c1A}$ | 29.3 | $TS_{6c1B}$ | 1.1 | $TS_{7c1B}$ | 7.1 |
| | | | | | | | | $TS_{6c2A}$ | 14.9 | $TS_{7c2A}$ | 1.5 |
| $TS_{3c2}$ | 18.2 | $TS_{4c2A}$ | 9.9 | $TS_{4c2B}$ | -- | $TS_{5c2A}$ | 32.4 | $TS_{6c2B}$ | 10.2 | $TS_{7c2B}$ | 11.4 |
| $TS_{3c3}$ | 18.0 | | | | | | | | | | |

Table 9.2. Calculated transition states and Gibbs free energies of activation (kcal $mol^{-1}$) for each step of the mechanism between 1,5-dihydro-1,2,4-oxadiazole and the ynamide MeN(Ms)≡CPh.

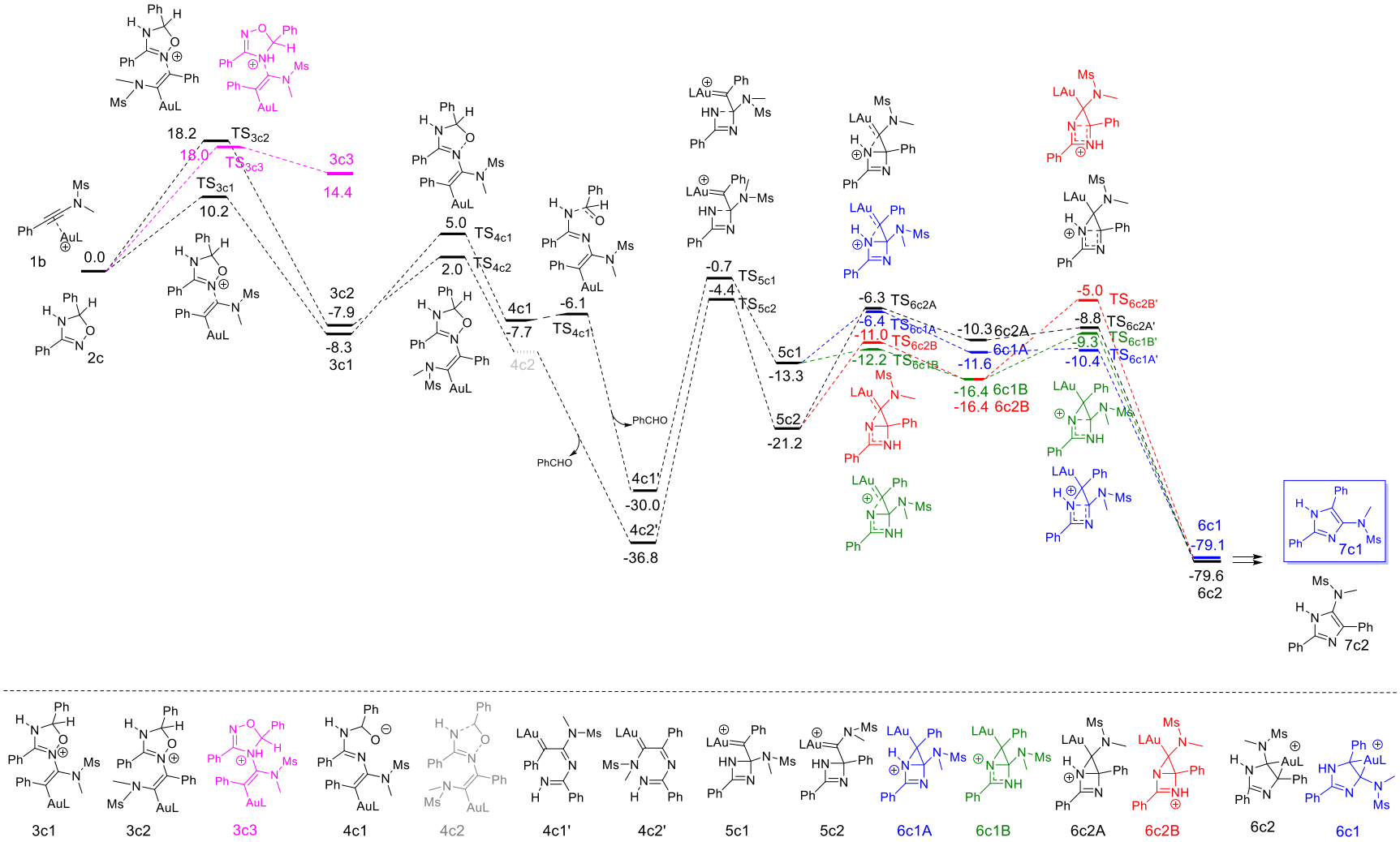


Scheme 9.5. Mechanistic pathway and relative free energies (kcal $mol^{-1}$, 298 K and 1 Atm) for the reaction between 1,5-dihydro-1,2,4-oxadiazole and the ynamide MsN(Ms)≡CPh.

## 9.4 Conclusions

We investigated the similarities and differences in the mechanism of Au(I) catalyzed [3+2] reaction between the mild nucleophiles anthranil, 3-tolyl-1,2,4-oxadiazole and 3-phenyl-4,5-dihydro-1,2,4-oxadiazole and the highly polarized alkyne, i.e. the ynamide PhC≡C-N(Ms)Me. These reactions regioselectively afford 2-amino-3-phenyl-7-acyl indoles, N-acyl-5-aminoimidazoles or N-H-5-phenyl-4-aminoimidazoles, respectively. In the proposed mechanisms, the vinyl gold intermediate evolves by the oxazole or oxadiazole ring opening to a key α-imino gold carbene complex. In all cases the regioselectivity is decided early in the reaction coordinate, at the initial nucleophilic attack of N in anthranil or N2 in oxadiazole onto the C1 carbon the gold(I)-activated ynamide in combination with an energy drop during α-imino gold carbene formation. In the five member rings, however, a late stage reaction path manifold opens the door for regioselectivity reversal, although this is not the case in the reactions considered and tested experimentally. Such possibility is opened through an unexpected four member ring formation which necessitates a posterior ring expansion stage during which the C-N bond formed in the starting step may be conserved or it may be broken. This late stage mechanism manifold could therefore be exploited to steer regioselectivity towards the, so far, non-observed product.

## 9.5 Bibliography

(1) Aguilar, E.; Santamaría, J. Gold-Catalyzed Heterocyclic Syntheses through α-Imino Gold Carbene Complexes as Intermediates. *Org. Chem. Front.* **2019**, *6* (9), 1513–1540. https://doi.org/10.1039/C9QO00243J.

(2) Ximei Zhao, Matthias Rudolph, A. M. A. & A. S. K. H. Easy Access to Pharmaceutically Relevant Heterocycles by Catalytic Reactions Involving α-Imino Gold Carbene Intermediates. *Front. Chem. Sci. Eng.* **2020**, *14*, 317–349.

(3) Gao, Y.; Nie, J.; Huo, Y.; Hu, X. Q. Anthranils: Versatile Building Blocks in the Construction of C-N Bonds and N-Heterocycles. *Organic Chemistry Frontiers*. 2020. https://doi.org/10.1039/d0qo00163e.

(4) Zeng, Z.; Jin, H.; Sekine, K.; Rudolph, M.; Rominger, F.; Hashmi, A. S. K. Gold-Catalyzed Regiospecific C−H Annulation of o -Ethynylbiaryls with Anthranils: π-Extension by Ring-Expansion En Route to N-Doped PAHs. *Angew. Chemie Int. Ed.* **2018**, *57* (23), 6935–6939. https://doi.org/10.1002/anie.201802445.

(5) Zhongyi Zeng, Hongming Jin, Jin Xie, Bing Tian, Matthias Rudolph, Frank Rominger, and A. S. K. H. α-Imino Gold Carbenes from 1,2,4-Oxadiazoles:

Atom-Economical Access to Fully Substituted 4-Aminoimidazoles. *Org. Lett.* **2017**, *19* (5), 1020–1023.

(6) Xu, W.; Wang, G.; Sun, N.; Liu, Y. Gold-Catalyzed Formal [3 + 2] Cycloaddition of Ynamides with 4,5-Dihydro-1,2,4-Oxadiazoles: Synthesis of Functionalized 4-Aminoimidazoles. *Org. Lett.* **2017**, *19* (12), 3307–3310. https://doi.org/10.1021/acs.orglett.7b01469.

(7) Gorin, D., Toste, F. Relativistic Effects in Homogeneous Gold Catalysis. *Nature* **2007**, No. 446, 395–403.

(8) Hashmi, A. S. K. Introduction: Gold Chemistry. *Chemical Reviews*. 2021. https://doi.org/10.1021/acs.chemrev.1c00393.

(9) Mato, M.; Franchino, A.; García-Morales, C.; Echavarren, A. M. Gold-Catalyzed Synthesis of Small Rings. *Chem. Rev.* **2021**, *121* (14), 8613–8684. https://doi.org/10.1021/acs.chemrev.0c00697.

(10) Ronald L. Reyes, Tomohiro Iwai, and M. S. Construction of Medium-Sized Rings by Gold Catalysis. *Chem. Rev.* **2021**, *121* (14), 8926−8947.

(11) Wang, T.; Hashmi, A. S. K. 1,2-Migrations onto Gold Carbene Centers. *Chemical Reviews*. 2021. https://doi.org/10.1021/acs.chemrev.0c00811.

(12) Zheng, Z.; Ma, X.; Cheng, X.; Zhao, K.; Gutman, K.; Li, T.; Zhang, L. Homogeneous Gold-Catalyzed Oxidation Reactions. *Chem. Rev.* **2021**. https://doi.org/10.1021/acs.chemrev.0c00774.

(13) Hendrich, C. M.; Sekine, K.; Koshikawa, T.; Tanaka, K.; Hashmi, A. S. K. Homogeneous and Heterogeneous Gold Catalysis for Materials Science. *Chem. Rev.* **2021**. https://doi.org/10.1021/acs.chemrev.0c00824.

(14) Wang, W.; Ji, C. L.; Liu, K.; Zhao, C. G.; Li, W.; Xie, J. Dinuclear Gold Catalysis. *Chem. Soc. Rev.* **2021**. https://doi.org/10.1039/d0cs00254b.

(15) Ai-Hua Zhou, Qiao He, Chao Shu, Yong-Fei Yu, Shuang Liu, Tian Zhao, Wei Zhang, X. L. and L.-W. Y. Atom-Economic Generation of Gold Carbenes: Gold-Catalyzed Formal [3+2] Cycloaddition between Ynamides and Isoxazoles. *Chem.Sci.* **2015**, *6*, 1265–1271.

(16) Zhang, Y.; Luo, T.; Yang, Z. Strategic Innovation in the Total Synthesis of Complex Natural Products Using Gold Catalysis. *Nat. Prod. Rep.* **2014**. https://doi.org/10.1039/c3np70075e.

(17) Dominic Campeau, David F. León Rayo, Ali Mansour, Karim Muratov, and F. G. Gold-Catalyzed Reactions of Specially Activated Alkynes, Allenes, and Alkenes. *Chem. Rev.* **2021**, *121* (14), 8756−8867.

(18) Rocchigiani, L.; Bochmann, M. Recent Advances in Gold(III) Chemistry: Structure, Bonding, Reactivity, and Role in Homogeneous Catalysis. *Chem. Rev.* **2021**. https://doi.org/10.1021/acs.chemrev.0c00552.

(19) Zhichao Lu, Tingting Li, Sagar R. Mudshinge, Bo Xu, G. B. H. Optimization of Catalysts and Conditions in Gold(I) Catalysis-Counterion and Additive Effects. *Chem. Rev.* **2021**, *121* (14), 8452−8477.

(20) Chetan C. Chintawar, Amit K. Yadav, Anil Kumar, Shashank P. Sancheti, and N. T. P. Divergent Gold Catalysis: Unlocking Molecular Diversity through Catalyst Control. *Chem. Rev.* **2021**, *121* (14), 8478−8558.

(21) Shandilya, S.; Protim Gogoi, M.; Dutta, S.; Sahoo, A. K. Gold-Catalyzed Transformation of Ynamides. *Chem. Rec.* **2021**, *21*, 4123–4149. https://doi.org/10.1002/tcr.202100159.

(22) Zhongyi Zeng, Hongming Jin, Matthias Rudolph, Frank Rominger, A. S. K. H. Gold(III)-Catalyzed Site-Selective and Divergent Synthesis of 2-Aminopyrroles and Quinoline-Based Polyazaheterocycles. *Angew. Chem. Int. Ed.* **2018**, *57*, 16549 –16553.

(23) González, J.; Santamaría, J.; Suárez-Sobrino, Á. L.; Ballesteros, A. One-Pot and Regioselective Gold-Catalyzed Synthesis of 2-Imidazolyl-1-Pyrazolylbenzenes from 1-Propargyl-1H-Benzotriazoles, Alkynes and Nitriles through α-Imino Gold(I) Carbene Complexes. *Adv. Synth. Catal.* **2016**. https://doi.org/10.1002/adsc.201600022.

(24) Ye, L. W.; Zhu, X. Q.; Sahani, R. L.; Xu, Y.; Qian, P. C.; Liu, R. S. Nitrene Transfer and Carbene Transfer in Gold Catalysis. *Chemical Reviews*. 2021. https://doi.org/10.1021/acs.chemrev.0c00348.

(25) Stylianakis, I.; Litinas, I.; Nieto Faza, O.; Kolocouris, A.; Silva López, C. On the Mechanism of the Au(I)-Mediated Addition of Alkynes to Anthranils to Furnish 7-Acylindoles. *J. Phys. Org. Chem.* **2022**, No. January, 1–9. https://doi.org/10.1002/poc.4333.

(26) Hansen, T.; Vermeeren, P.; Bickelhaupt, F. M.; Hamlin, T. A. Origin of the A-Effect in S N 2 Reactions. *Angew. Chemie Int. Ed.* **2021**, *60* (38), 20840–20848. https://doi.org/10.1002/anie.202106053.

(27) Schleyer, P. V. R.; Maerker, C.; Dransfeld, A.; Jiao, H.; Van Eikema Hommes, N. J. R. Nucleus-Independent Chemical Shifts: A Simple and Efficient Aromaticity Probe. *J. Am. Chem. Soc.* **1996**. https://doi.org/10.1021/ja960582d.

(28) Moll, J. F.; Pemberton, R. P.; Gutierrez, M. G.; Castro, C.; Karney, W. L. Configuration Change in [14]Annulene Requires Möbius Antiaromatic Bond Shifting. *J. Am. Chem. Soc.* **2007**. https://doi.org/10.1021/ja0678469.

(29) Fallah-Bagher-Shaidaei, H.; Wannere, C. S.; Corminboeuf, C.; Puchta, R.; Schleyer, P. V. R. Which NICS Aromaticity Index for Planar π Rings Is Best? *Org. Lett.* **2006**. https://doi.org/10.1021/ol0529546.

(30) Chen, Z.; Wannere, C. S.; Corminboeuf, C.; Puchta, R.; Schleyer, P. von R. Nucleus-Independent Chemical Shifts (NICS) as an Aromaticity Criterion. *Chem. Rev.* **2005**, *105* (10), 3842–3888. https://doi.org/10.1021/cr030088+.

# PUBLICATIONS

1. Stylianakis, I.; Nieto Faza, O., Silva López, C., Kolocouris, A. The key role of protodeauration in the gold-catalyzed reaction of 1,3-diynes with pyrrole and indole to form complex heterocycles. *Org. Chem. Front* **2020**, *7*, 997. **DOI:** 10.1039/C9QO01544B

2. Stylianakis, I., Litinas, I., Nieto Faza, O., Kolocouris, A., Silva López, C. On the mechanism of the Au(I)-mediated addition of alkynes to anthranils to furnish 7-acylindoles. *J Phys Org Chem* **2022**, *35*( 11), e4333. https://doi.org/10.1002/poc.4333

3. Stylianakis, I.; Litinas, I.; Kolocouris, A.; Silva López, C. Formation and Intramolecular Capture of α-Imino Gold Carbenoids in the Au(I)-Catalyzed [3 + 2] Reaction of Anthranils, 1,2,4-Oxadiazoles, and 4,5-Dihydro-1,2,4-Oxadiazoles with Ynamides. *Catalysts* **2022**, *12*, 915. https://doi.org/10.3390/catal12080915